

STRUCTURE PROPERTY RELATIONSHIPS IN DISCOTIC MESOGENS

by

Earl Johan Foster
Bachelor of Science, Simon Fraser University, 2002

THESIS
SUBMITTED IN PARTIAL FULFILLMENT OF
THE REQUIREMENTS FOR THE DEGREE OF
DOCTOR OF PHILOSOPHY

In the
Department
of
Chemistry

© E. Johan Foster 2006

SIMON FRASER UNIVERSITY

Fall 2006

All rights reserved. This work may not be
reproduced in whole or in part, by photocopy
or other means, without permission of the author.

APPROVAL

Name: Earl Johan Foster

Degree: Doctor of Philosophy

Title of Thesis: Structure Property Relationships in Discotic Mesogens

Examining Committee: **Dr. George R. Agnes**
Chair
Associate Professor, Department of Chemistry

Dr. Vance E. Williams
Senior Supervisor
Assistant Professor, Department of Chemistry

Dr. Neil R. Branda
Supervisor
Professor, Department of Chemistry

Dr. Peter D. Wilson
Supervisor
Associate Professor, Department of Chemistry

Dr. David J. Vocadlo
Internal Examiner
Assistant Professor, Department of Chemistry

Dr. Michael O. Wolf
External Examiner
Professor, Department of Chemistry

Date Defended/Approved: November 24, 2006



SIMON FRASER
UNIVERSITY library

DECLARATION OF PARTIAL COPYRIGHT LICENCE

The author, whose copyright is declared on the title page of this work, has granted to Simon Fraser University the right to lend this thesis, project or extended essay to users of the Simon Fraser University Library, and to make partial or single copies only for such users or in response to a request from the library of any other university, or other educational institution, on its own behalf or for one of its users.

The author has further granted permission to Simon Fraser University to keep or make a digital copy for use in its circulating collection (currently available to the public at the "Institutional Repository" link of the SFU Library website <www.lib.sfu.ca> at: <<http://ir.lib.sfu.ca/handle/1892/112>>) and, without changing the content, to translate the thesis/project or extended essays, if technically possible, to any medium or format for the purpose of preservation of the digital work.

The author has further agreed that permission for multiple copying of this work for scholarly purposes may be granted by either the author or the Dean of Graduate Studies.

It is understood that copying or publication of this work for financial gain shall not be allowed without the author's written permission.

Permission for public performance, or limited permission for private scholarly use, of any multimedia materials forming part of this work, may have been granted by the author. This information may be found on the separately catalogued multimedia material and in the signed Partial Copyright Licence.

The original Partial Copyright Licence attesting to these terms, and signed by this author, may be found in the original bound copy of this work, retained in the Simon Fraser University Archive.

Simon Fraser University Library
Burnaby, BC, Canada

ABSTRACT

Columnar liquid crystals have emerged as a promising class of materials for light emitting diodes, photovoltaic devices and field effect transistors. In addition to their practical importance, the ability of disc-shaped molecules to spontaneously form columnar nanostructures represents a striking example of self-assembly driven largely by π - π interactions. Any factor that alters the strength of π -stacking between neighbouring molecules should therefore have a dramatic impact on the propensity of these molecules to form columnar mesophases. Studying the relationship between a molecule's structure and its tendency to self-assemble into columns can thus provide valuable insight into the nature and strength of noncovalent interactions between discotic mesogens in addition to facilitating the design of new liquid crystalline materials.

A series of disc-shaped molecules was produced by the condensation of 1,2-diamines with 2,3,6,7-tetraalkoxy-phenanthrene-9,10-diones in order to systematically investigate the relationship between changes in molecular structure and the self-assembly of columnar liquid crystalline phases. Functional groups were found to have a pronounced effect on the tendency of these molecules to self-assemble. Moreover, the thermal stability of these columnar phases was very sensitive to the position of the substituents and their electron withdrawing ability, with the columnar-to-isotropic transition temperature strongly related to Hammett σ -parameters of the functional groups. The effect of core size were also investigated through the preparation of molecules containing 4-, 5-

and 6-membered fused aromatic rings. The effects of heteroatoms in the aromatic core were also explored. Phase behaviour had a striking dependence on both the number and position of heteroatoms in the core. Furthermore, substituting hexaalkoxy-[a,c]dibenzophenazine with different lengths of pendant chains showed that changing molecular symmetry and shape had an effect on the phase behaviour of discotic mesogens.

To my parents. For always being there. Knowing you are always there,
regardless, is the best gift someone can give.

ACKNOWLEDGEMENTS

I would like to thank Dr. Vance Williams, my senior supervisor, for his guidance and mentorship through my doctoral studies. For the skills and training in his group I am extremely grateful. I would also like to thank the members of my supervisory committee, Dr. Neil Branda and Dr. Peter Wilson, for their helpful suggestions and time.

My past and present laboratory colleagues, Ms. Christine Lavigueur, Ms. Muriel Rakotomalala, Ms. Emilie Voisin, Mr. David Bailey, Mr. Kevin Hon Lau, Mr. Jarrett Babuin, are all thanked for the help with my projects, fun times in lab, keeping me sane and 'keeping it real'.

Dr. Andrew Cammidge and Mr. Hemant Gopee (University of East Anglia) for their help in the synthesis and characterization of compound **3.6**. Ms. Christine Lavigueur for her help with the characterization of compounds **3.7**, **3.8** and **3.9**. Mr. Jarrett Babuin and Natalie Nyugen for the preliminary research into phenantherene quinone. Ms. Muriel Rakotomalala for the synthesis and characterization of compounds **2.8e**, **2.8f**, **2.9e** and **2.9f**.

The technical assistance of Mrs. Marcy Tracey (NMR), Mr. Greg Owen (MS), Mr. Simon Wong (MS), Mr. Philip Ferreira (MS) and Mr. Mikki Yang (CHN microanalysis) is gratefully acknowledged.

Finally, Simon Fraser University and the Natural Sciences and Engineering Research Council of Canada are thanked for their financial support.

TABLE OF CONTENTS

Approval	ii
Abstract	iii
Dedication.....	v
Acknowledgements	vi
Table of Contents.....	vii
List of Figures	ix
List of Schemes.....	xii
List of Tables	xiv
List of Abbreviations	xv
1 GENERAL INTRODUCTION.....	1
1.1 Self-Assembly	1
1.2 Liquid Crystals.....	4
1.2.1 Discovery and History	4
1.2.2 Liquid Crystal Phases	5
1.2.3 Phases Formed by Discotic Mesogens.....	10
1.2.4 Applications.....	14
1.3 Liquid Crystal Characterization Techniques	15
1.3.1 Differential Scanning Calorimetry.....	16
1.3.2 Polarized Optical Microscopy.....	17
1.3.3 Variable Temperature X-Ray Diffraction	19
1.4 Structure-Property Relationships in Discotic Liquid Crystals.....	22
1.4.1 Heteroatoms	26
1.4.2 Substituent effect	29
1.4.3 Core-Size	30
1.5 Molecular Design and Evolution.....	33
2 Symmetry and Shape Effects on Self-Assembly	37
2.1 Introduction.....	37
2.1.1 Previous Studies.....	38
2.1.2 Benzil Derivatives as Precursors	41
2.2 Synthesis of Divergent Precursors	43
2.3 Tetraalkoxy-Dicyanodibenzoquinoline	46
2.4 Hexaalkoxy-Dibenzo[a,c]phenazine Derivatives.....	51
2.4.1 Preparation of 4,5-Alkoxy-1,2-phenylenediamines.....	52
2.5 ‘Sore-Thumb’ Effect.....	65
2.6 Summary.....	67
2.7 Experimental	68

2.7.1	General Experimental	68
2.7.2	Experimental	69
3	Effects of Core-Size and Heteroatoms on Self-Assembly.....	97
3.1	Introduction.....	97
3.2	Core-Size and Phase Behaviour Relationships.....	98
3.2.1	Core-Size Results and Discussion.....	102
3.3	Heteroatoms in the Core	105
3.3.1	Heteroatom Results and Discussion	109
3.4	Summary.....	116
3.5	Experimental	117
4	Substituent Effects on Self-Assembly.....	123
4.1	Introduction.....	123
4.2	Synthesis.....	125
4.3	Results	128
4.4	Discussion.....	133
4.5	Summary.....	144
4.6	Experimental	145
5	'Side'-Substituent Effects on Self Assembly	154
5.1	Introduction.....	154
5.2	Dibrominated 2,3,6,7-Tetrakis(hexyloxy)-dibenzo[a,c]phenazine Derivatives	155
5.2.1	Synthesis of Differentially Substituted 1,2-Phenylenediamines.....	155
5.2.2	Synthesis of Functionalized Dibenzophenazine Derivatives	156
5.2.3	Dibrominated compounds results and discussion	157
5.3	'Side'-Substituted 2,3,6,7-Tetrakis(hexyloxy)-dibenzo[a,c]phenazine.....	159
5.3.1	Synthesis	159
5.3.2	Results.....	161
5.3.3	Discussion.....	163
5.4	Summary.....	167
5.5	Experimental	168
6	Conclusion and Future Work.....	175
6.1	Conclusion.....	175
6.2	Future work	176
7	References	180

LIST OF FIGURES

Figure 1.1: Self-assembly of a lipid bi-layer.	3
Figure 1.2: Structure and phase characteristics of cholesteryl benzoate.	4
Figure 1.3: States of matter for a thermotropic mesogen.	6
Figure 1.4: An example of a monotropic liquid crystal.	6
Figure 1.5: Examples of typical calamitic mesogens.	7
Figure 1.6: Different phases of rod shaped molecules.	9
Figure 1.7: Examples of typical discotic mesogens.	10
Figure 1.8: Columnar order and disorder.	12
Figure 1.9: Liquid crystal phases formed by discotic mesogens.	13
Figure 1.10: Two-dimensional lattices of common columnar phases.	14
Figure 1.11: Typical DSC endotherm and exotherm.	17
Figure 1.12: Schematic representations of a polarized optical microscopy experiment.	18
Figure 1.13: Typical optical textures observed for discotic mesogens.	19
Figure 1.14: Variable temperature X-ray diffraction setup.	20
Figure 1.15: Typical X-ray diffraction pattern of a columnar hexagonal ordered phase.	21
Figure 1.16: Planes in 2D hexagonal and rectangular lattices.	22
Figure 1.17: α - and β - positions of triphenylenes.	29
Figure 1.18: Target molecules discussed in Chapter 2.	35
Figure 1.19: Target molecules discussed in Chapter 3.	36
Figure 1.20: Target molecules discussed in Chapter 4.	36
Figure 1.21 Target molecules discussed in Chapter 5.	36
Figure 2.1: Representative polarized optical micrographs of compounds (2.7b-f).	49
Figure 2.2: Phase ranges of mesogenic compounds (2.7b-f).	51
Figure 2.3: 2,3,6,7,11,12-Hexalkoxy-dibenzo[a,c]phenazine derivatives.	52
Figure 2.4: Comparison of dibenzo[a,c]phenazine compounds (2.11) and previously reported 2,3,6,7,10,11-hexaalkoxytriphenylenes.	57
Figure 2.5: Notation for dibenzo[a,c]phenazine derivatives.	58
Figure 2.6: Dibenzo[a,c]phenazine with $p+m+n = 22$	59
Figure 2.7: Dibenzo[a,c]phenazine with $p+m+n = 24$	59
Figure 2.8: Dibenzo[a,c]phenazine with $p+m+n = 26$	59
Figure 2.9: Dibenzo[a,c]phenazine isomers of the same symmetry.	60

Figure 2.10: Structure and notation for hexaalkoxytriphenylene series HAT(p.n.m).....	61
Figure 2.11: HAT with p+m+n = 18.....	62
Figure 2.12: HAT with p+m+n = 22.....	62
Figure 2.13: HAT with p+m+n = 24.....	62
Figure 2.14: HAT with p+m+n = 26.....	63
Figure 2.15: HAT with p+m+n = 28.....	63
Figure 2.16: HAT with p+m+n = 30.....	63
Figure 2.17: Structure and notation for hexaalkoxytriphenylene series HATb.....	64
Figure 2.18: Triphenylene series HATb.....	65
Figure 2.19: Phase behaviour from altering one alkoxy-chain.....	66
Figure 2.20: Hexaalkoxytriphenylenes differing at one position.....	67
Figure 3.1: Previously reported molecular structures of macrocycles forming the cores of discotic materials.....	99
Figure 3.2: Structures of previously reported hexa- <i>peri</i> - hexabenzocoronene based disc shaped molecules.....	101
Figure 3.3: Polarized optical photomicrograph of compound (3.3) at 167 °C.....	104
Figure 3.4: Structure and phase behaviour of compounds (3.4) and (3.5).....	110
Figure 3.5: Polarized optical micrograph of compound (3.5) at 137 °C.....	111
Figure 3.6: Structure and phase behaviour of compounds (2.7d) and (3.6).....	112
Figure 3.7: Synthesis and phase behaviour of compounds (3.7-3.9).....	113
Figure 3.8: Polarized optical micrograph of compound 3.9 at 177 °C.....	114
Figure 4.1: Polarized optical micrograph of monotropic phase of compound (4.2b) at 158 °C.....	129
Figure 4.2: Polarized optical photomicrograph of compounds (4.2j) at 235°C (left) and (4.2d) at 190°C (right).....	133
Figure 4.3: Plot of Hammett σ_p versus clearing temperature (T_c).....	135
Figure 4.4: Plot of Hammett σ_m versus clearing temperature (T_c).....	136
Figure 4.5: Schematic representation of antiferroelectric ordering in columnar phases.....	137
Figure 4.6: Phase behaviour of previously reported 10,11-substituted 2,3,6,7-tetrahexyloxytriphenylenes.....	141
Figure 4.7: Previously reported monofunctionalized pentapentoxytriphenylene.....	143
Figure 4.8: Phase behaviour of previously reported α -substituted triphenylene hexahexyl ether.....	144
Figure 5.1: Positions on tetraalkoxydibenzophenazine.....	154

Figure 5.2: Positions on 2,1,3-benzothiadiazole and 1,2-phenylenediamine.....	155
Figure 5.3: Dibrominated derivatives.....	157
Figure 5.4: Polarized optical micrograph of compounds (5.3a) and (5.3b).....	158
Figure 5.5: Polarized optical micrograph of compounds (5.3c) (top) and (5.3e) (bottom).....	163
Figure 5.6: Hammett σ_p versus clearing temperature (T_c) for compounds (5.3c-f) and (4.2c-g).....	164
Figure 5.7: Hammett σ_m versus clearing temperature (T_c) for compounds (5.3c-f) and (4.2c-g).....	165
Figure 5.8: Graphical representation of molecular dipoles for (4.2c-g) and (5.3c-g).....	166
Figure 5.9: Anti-parallel alignment of adjacent molecules.....	167
Figure 6.1: Hexaalkoxydibenzophenazine derivatives.....	176
Figure 6.2: 2,3,6,7-Tetraalkoxy-10-nitrodibenzo[a,c]phenazines.....	179

LIST OF SCHEMES

Scheme 1.1: Synthesis of previously published hexa-alkoxytriphenylenes.....	23
Scheme 1.2: Statistical route to unsymmetrical triphenylenes.....	25
Scheme 1.3: Oxidative coupling synthesis of triphenylenes.....	25
Scheme 1.4: Cyclization of <i>o</i> -terphenyl synthesis of triphenylene.....	26
Scheme 1.5: Synthesis of truxene, oxatruxene and thiatruxene derivatives.....	27
Scheme 1.6: Synthesis and phase behaviour of 'pocket-substituted' hexaalkoxytriphenylenes.....	30
Scheme 1.7: Octaalkoxyphthalocyanines.....	31
Scheme 1.8: Synthesis of hexaalkoxybenzo[<i>b</i>]triphenylene.....	33
Scheme 1.9: Proposed modular synthetic approach to disc-shaped molecules.....	34
Scheme 2.1: Previously reported statistical synthetic route to unsymmetrical triphenylenes.....	39
Scheme 2.2: Previously reported rational unsymmetrical triphenylene synthesis.....	40
Scheme 2.3: Previously reported rational synthesis of triphenylene from tetraalkoxybenzil.....	42
Scheme 2.4: Synthesis of symmetrical benzil compounds (2.1a-d).....	43
Scheme 2.5: Unsymmetrical synthesis of benzil compounds (2.5a-c).....	44
Scheme 2.6: Oxidative cyclization of benzils to phenanthrene quinone compounds (2.6a-g).....	46
Scheme 2.7: Synthesis of dicyanodibenzoquinoxaline derivatives (2.7a-f).....	47
Scheme 2.8: Synthesis of 1,2-dialkoxy-4,5-diaminobenzenes.....	53
Scheme 2.9: Condensation synthesis of compounds (2.11a-q).....	54
Scheme 3.1: Synthetic route to core-size series.....	103
Scheme 4.1: Synthesis of substituent series (4.2a-m) from 2,3,6,7-tetra(hexyloxy)phenanthrene-9,10-dione.....	125
Scheme 4.2: Synthesis of 4-bromo-1,2-diaminobenzene.....	126
Scheme 4.3: Synthesis of compound 4.2d via a Sandmeyer reaction.....	127
Scheme 4.4: Attempted synthesis of 1,2-diamino-4,5-dibromobenzene.....	128
Scheme 4.5: Synthesis of 1,2-diamino-4,5-dibromobenzene.....	128
Scheme 5.1: Routes to functionalized <i>o</i> -phenylenediamines.....	155
Scheme 5.2: Synthesis of dibrominated 1,2-phenylenediamines.....	156
Scheme 5.3: Substitution of 2,1,3-benzothiadiazole.....	160

Scheme 5.4: 10-Substituted-2,3,6,7-tetrakis(hexyloxy)dibenzo[a,c]phenazines.	161
Scheme 6.1: Synthesis of sulphur containing core – type I.....	177
Scheme 6.2: Synthesis of sulphur containing core – type II.....	178

LIST OF TABLES

Table 1.1: Phase behaviour of hexaesters reported by Chandrasekhar in 1977.....	11
Table 1.2: Phase behaviour of previously published hexaalkoxytriphenylenes.....	24
Table 1.3: Phase behaviour of truxene, oxatruxene and thiatruxene derivatives.....	28
Table 2.1: Examples of Carnelley's rule for crystalline solids.....	38
Table 2.2: Oxidation of diphenylacetylene to benzil.....	45
Table 2.3: Phase behaviour of 6,7,10,11-tetraalkoxy-dibenzo[f,h]quinoxaline-2,3-dicarbonitrile derivatives (2.7a-f).....	48
Table 2.4: Phase behaviour of dibenzo[a,c]phenazine derivatives (2.11a-q).....	56
Table 3.1: Average phase transitions for core-size series reported by van de Craats and Warman.....	100
Table 3.2: Average phase transitions for mesogenic molecules in hexa-peri-hexabenzocoronene core series reported by Müllen and co-workers.....	102
Table 3.3: Phase behaviour of compounds 3.1 , 3.2 and 3.3	104
Table 3.4: Phase behaviour of previously reported thioethers of triphenylene and hexaazatriphenylene.....	106
Table 3.5: Phase behaviour of previously reported triphenylenes and hexaazatriphenylenes.....	107
Table 3.6: Phase behaviour of previously reported phthalocyanine and tetrapyrazinophyrazine.....	108
Table 4.1: Phase behaviour of tetraalkoxy-diazatriphenylenes.....	124
Table 4.2: Phase behaviour of compounds (4.2a-m).....	131
Table 4.3: X-Ray diffraction data for liquid crystalline derivatives of (4.2).....	132
Table 5.1: 10-Substituted-2,3,6,7-tetrakis(hexyloxy)dibenzo[a,c]phenazines phase behaviour.....	162

LIST OF ABBREVIATIONS

ΔH	change in enthalpy
AcOH	acetic acid
Col	columnar phase
Col _d	columnar disordered
Col _h	columnar hexagonal
Col _{hd}	disordered columnar hexagonal
Col _{ho}	ordered columnar hexagonal
Col _o	columnar ordered
Col _{ob}	columnar oblique
Col _r	columnar rectangular
Col _{rd}	disordered columnar rectangular
Col _{ro}	ordered columnar rectangular
Cr	crystalline
d	doublet
DMAP	<i>N,N</i> -4-dimethylaminopyridine
DME	1,2-dimethoxyethane
DMF	<i>N,N</i> -dimethylformamide
DBA	dibenzylidene acetone

DMSO	dimethylsulfoxide
DNA	deoxyribonucleic acid
DSC	differential scanning calorimetry
HAT	2,3,6,7,10,11 hexaalkoxy triphenylene
I	isotropic
IR	infrared spectroscopy
<i>J</i>	coupling constant
LC	liquid crystal
LCD	liquid crystal display
m	multiplet
MeOH	methanol
N	nematic
NBS	<i>n</i> -bromosuccinimide
NMR	nuclear magnetic resonance
<i>n</i> -BuLi	<i>n</i> -butyl lithium
N _D	nematic discotic
POM	polarized optical microscopy
RBr	alkyl bromide
RNA	ribose nucleic acid

s	singlet
S _a	smectic A
S _c	smectic C
t	triplet
T	phase transition
T _c	clearing point
THF	tetrahydrofuran
T _m	melting point
TMS	tetramethylsilane (or trimethylsilyl)
TsCl	<i>p</i> -toluenesulfonic chloride
TsOH	<i>p</i> -toluenesulfonic acid
T _t	transition temperature
XRD	X-ray diffraction
σ _{<i>m</i>}	Hammett value (<i>meta</i>)
σ _{<i>p</i>}	Hammett value (<i>para</i>)

1 GENERAL INTRODUCTION

1.1 Self-Assembly

Self-assembly is the process by which complex structures spontaneously form from simple parts. Examples of self-assembly are seen at virtually every length scale throughout nature, from sub-nanoscale objects (e.g. molecules)^{1,2} to macroscopic entities (e.g. galaxies).³ Molecular self-assembly is the process by which molecules spontaneously organize into larger structures. Research in this area has been largely directed towards the molecular components that will assemble into desired supramolecular architectures.⁴⁻¹⁵

Research into self-assembly has far reaching consequences and offers one of the few processes by which molecule-sized parts can be organized into nano-sized 'devices',¹⁶⁻¹⁹ making nanotechnology and nanostructures much more accessible. In the broader sense, research into the patterns of self-assembly bridges the study of distinct components and the study of systems with many interacting components.²⁰

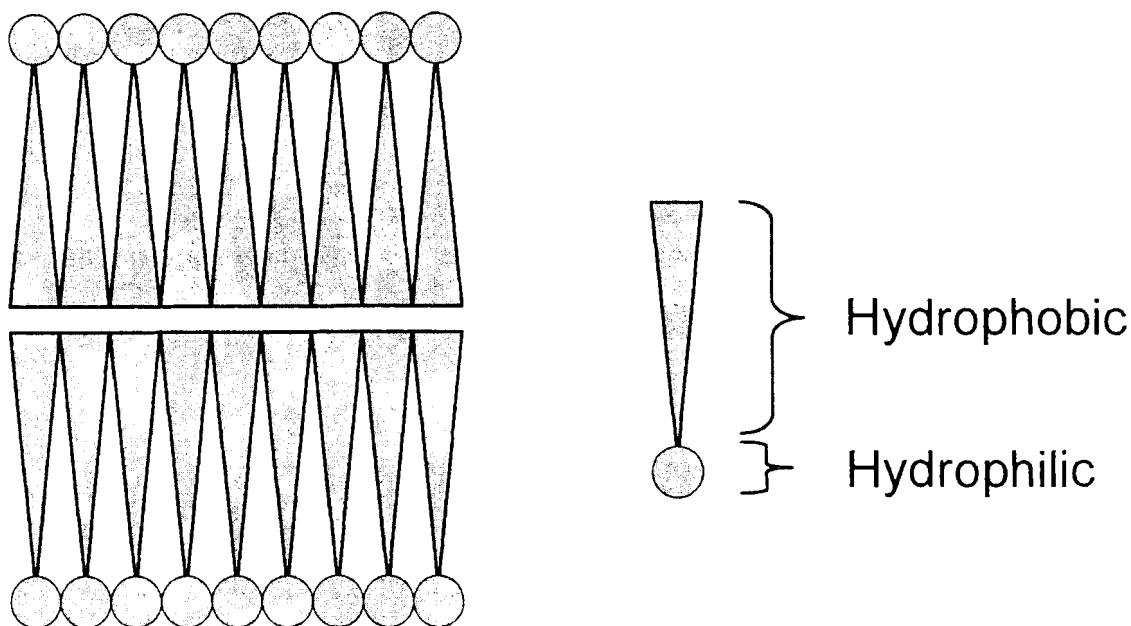
In the simplest sense, molecular self-assembly depends on two factors: movement and stickiness. Movement refers to the random motion that molecules experience due to thermal energy. Molecules must align in the right orientation to assemble; given enough thermal energy, motion will eventually result in the desired orientation. Stickiness refers to intermolecular attractions, varying in strength that make molecules 'stick' to one another. In the molecular

realm, self-assembly is driven by non-covalent forces, such as van der Waals, electrostatic, hydrophobic interactions, hydrogen bonds and ionic bonds. While these forces are weak individually, the cumulative effect of many such interactions can result in a strong attraction between sets of molecules.

With self-assembly, there exists a thermodynamic barrier to the breaking and reforming of the assembled macrostructure. The barrier must be sufficiently high so that the assembly is stable, but low enough to allow a reversible breaking and reformation of the structure. Such reversibility is crucial since the components must be able to “find” the thermodynamically favoured assemblies, rather than being trapped irreversibly in less favourable kinetic constructs.

An example of self-assembly is a lipid bi-layer of a cell membrane. A lipid has two important structural features: a hydrophilic part and a hydrophobic region. The hydrophilic portion, usually called the polar head, is miscible with aqueous solution, while the hydrophobic portion, called the non-polar tail, is immiscible with water. The lipid bi-layer assembles so that the non-polar tails face one another and the polar heads face the aqueous solution on each side of the membrane (see Figure 1.1).

Figure 1.1: Self-assembly of a lipid bi-layer.



Although definitions for self-assembly are many and varied, for the purpose of this thesis the definition proposed by Whitesides and Grzybowski will be used:²⁰

"Self-assembly" is not a formalized subject, and definitions of the term "self-assembly" seem to be limitlessly elastic. As a result, the term has been overused to the point of cliché. Processes ranging from the non-covalent association of organic molecules in solution to the growth of semiconductor quantum dots on solid substrates have been called self-assembly. Here, we limit the term to processes that involve pre-existing components (separate or distinct parts of a disordered structure), are reversible, and can be controlled by proper design of the components. "Self-assembly" is thus not synonymous with "formation."

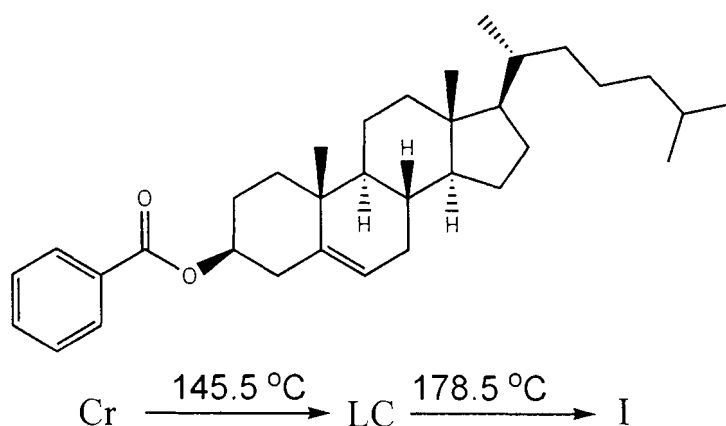
Liquid crystals, are ordered fluids that form 2D and 3D structures and as such are a fundamental example of self-assembly that allow the probing of how self-assembly works. In this thesis, we will attempt to address how molecular structural features, such as symmetry, size and electronic properties guide the self-assembly of one class of liquid crystalline materials.

1.2 Liquid Crystals

1.2.1 Discovery and History

In 1888 the Austrian chemist Friedrich Reinitzer observed that cholesteryl benzoate formed a cloudy liquid upon melting and that a clear liquid was produced upon further heating (Figure 1.2). At first Reinitzer thought that this might be a sign of impurities in the material, but further purification did not bring any changes to this behaviour. Reinitzer consulted the German physicist Otto Lehmann, an expert in crystal optics. Lehmann surmised that the optical anisotropy which gave rise to the cloudy appearance of the liquid initially formed upon melting might be due to the elongated molecules oriented in a parallel manner. Eventually the two concluded that the cloudy liquid was a new state of matter and coined the terms "fluid crystal" and "liquid crystal" (LC), to indicate that it was something between a liquid and a crystalline solid, sharing important properties of both.²¹

Figure 1.2: Structure and phase characteristics of cholesteryl benzoate.



Cholesteryl benzoate melts from a solid (Cr) to a cloudy liquid (LC) at 145.5 °C and to a clear liquid (I) at 178.5 °C.²² Further research revealed this liquid crystal to be a nematic phase (see text).

1.2.2 Liquid Crystal Phases

An isotropic liquid is, by definition, identical irrespective of direction and the molecules which make up that matter have no orientational order. A phase of matter that is anisotropic (i.e. ordered) yet still exhibits some degree of fluidity is described as "liquid-crystalline" or "mesomorphic." The properties and intermolecular packing arrangements of these phases are intermediate between those of an isotropic liquid and those of a crystalline solid. Like a crystalline solid, the molecules in a liquid crystal possess orientational and/or positional ordering, albeit generally to a lesser extent than crystalline solids. Thus, while solid crystals are ordered in 3-dimensions, liquid crystals often possess order in one or two dimensions. Their lower degree of ordering permits the molecules some degree of movement, which allows them to flow like liquids. There are two broad categories of liquid crystals, distinguished by the forces that drive their self-organization: lyotropic and thermotropic.²³ Lyotropic liquid crystals exhibit a mesophase (a phase intermediate between an isotropic liquid and crystalline solid) only when mixed with a solvent, and the phase behaviour is dependent upon both the concentration and the temperature of the solution. Liquid crystals that do not require the presence of a solvent and exhibit temperature dependent phase behaviour are termed thermotropic liquid crystals. Since only thermotropic liquid crystals were examined in the course of this thesis, we will limit our discussion to these types of mesophases.

Thermotropic mesomorphism is an intrinsic property of a material, and phase transitions to and from the liquid crystalline state occur as a function of

temperature (Figure 1.3). Liquid crystals that exhibit a mesophase above their melting point upon heating are referred to as enantiotropic and are thermodynamically stable states within a definite temperature range. Cholesteryl benzoate (Figure 1.2) melts from a crystalline solid at 145.5 °C into a liquid crystal; upon further heating, the liquid crystal phase “clears” into an isotropic liquid at 178.5 °C. Thermotropic mesophases that form only on cooling below the clearing point (the point above which an isotropic liquid is observed) are thermodynamically unstable and are called monotropic phases. For example, the diphenylacetylene derivative shown melts from a crystalline solid directly to an isotropic liquid at 49 °C; upon cooling, a liquid crystalline phase is observed below 37 °C (Figure 1.4).²⁴

Figure 1.3: States of matter for a thermotropic mesogen.

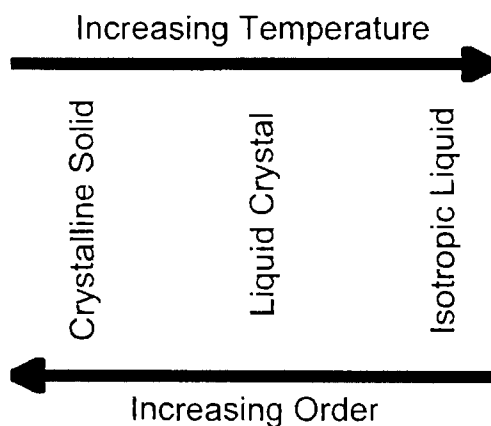
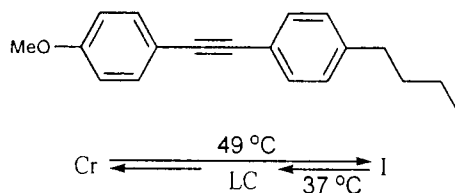
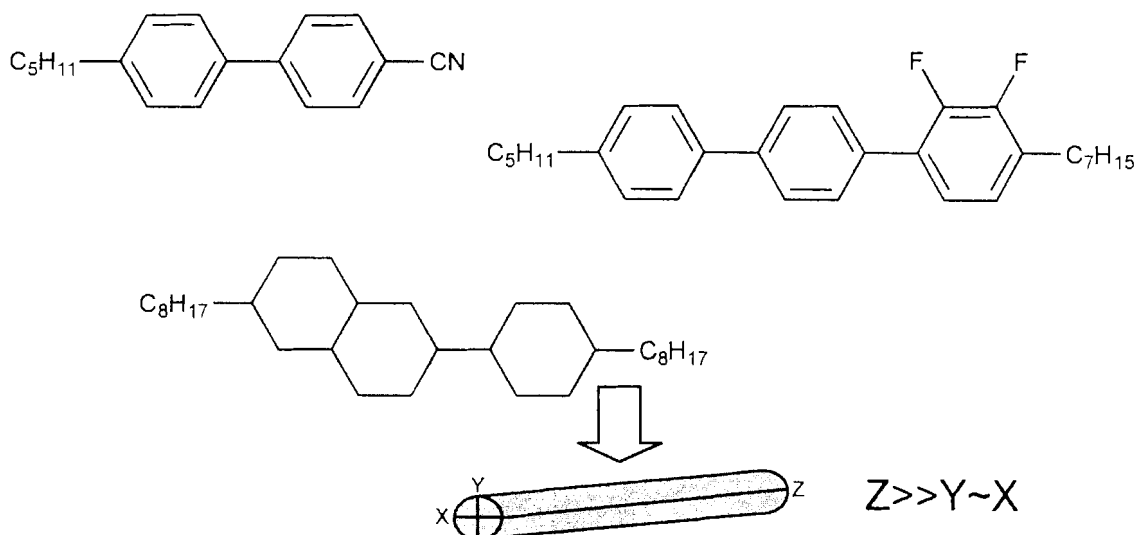


Figure 1.4: An example of a monotropic liquid crystal.



The anisotropic ordering within a liquid crystal can in most cases be attributed at least in part to the anisotropic shape of the molecules that form the phase. Often, the molecule is either much larger or much smaller in one dimension than in another. Many different classifications of mesogens (i.e. molecules that form a mesophase) have been proposed, but two broad groups are most common: calamitic (rod-like) and discotic (disc-like). Calamitic mesogens have an elongated shape, and prefer to form phases in which molecules align in one direction. A rod is defined as having one dimension much larger than the other two ($z \gg x \approx y$) (Figure 1.5). While not the focus of this thesis, calamitic mesogens are by far the largest and technologically most important class of mesogens and therefore will be briefly discussed.

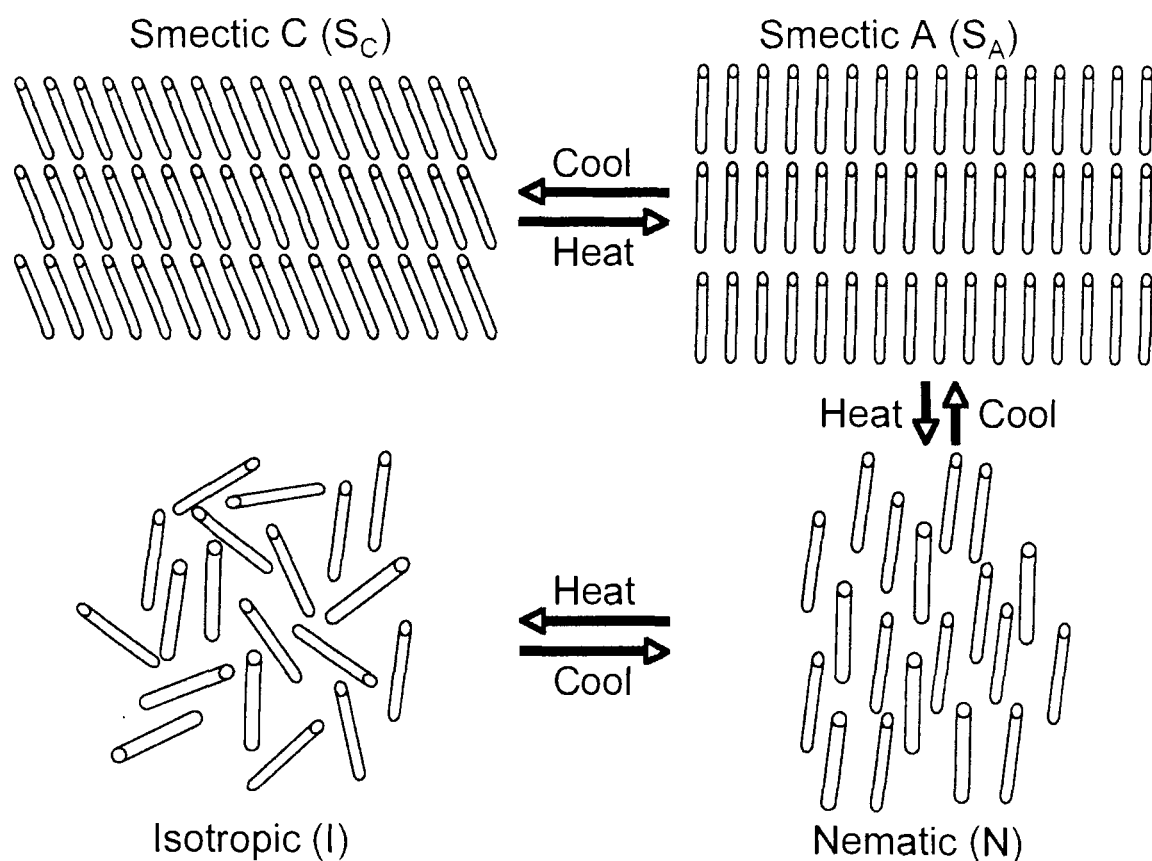
Figure 1.5: Examples of typical calamitic mesogens.



Calamitic mesogens form a variety of liquid crystalline phases that are differentiated based on the ordering of their component molecules. The simplest liquid crystal is the nematic phase (N). The molecules in these phases have no positional order, but are orientationally ordered, i.e. the molecules tend to point in one direction (Figure 1.6).

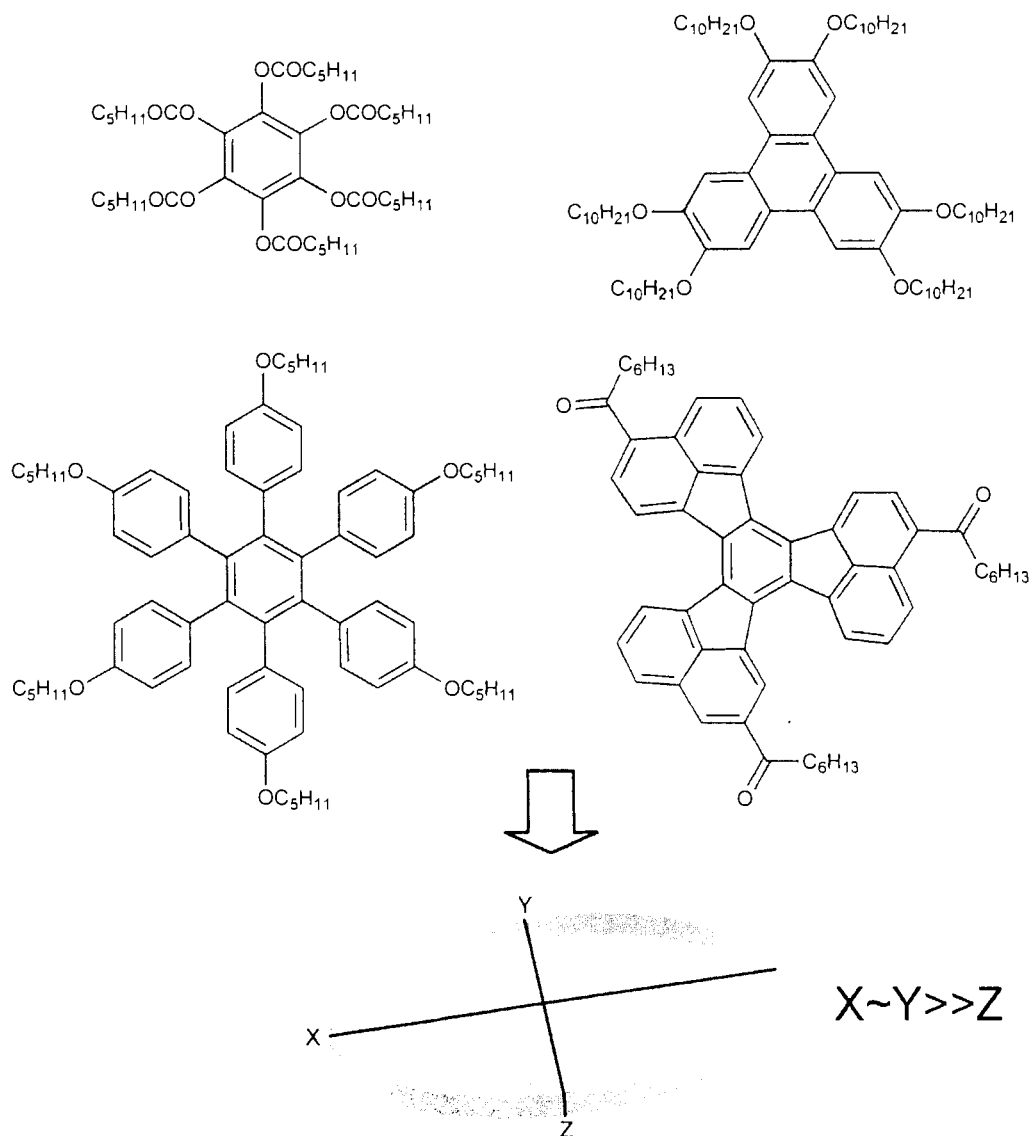
The molecules in smectic phases (S) possess orientational order, but also order into layers. This lamellar ordering has the macroscopic effect of making smectic liquid crystals much more viscous than nematic phases. Although many different types of smectic phases have been identified, two are most prevalent. If the molecules in the smectic layer align themselves perpendicular to the plane of the layer, the phase is designated by convention as smectic A (S_A) phase. If the molecules are tilted with respect to the layer normal (i.e. the vector perpendicular to the plane of the layers), the phase is referred to as smectic C (S_C) (Figure 1.6).²¹ Some molecules form just a single liquid crystal phase, while others form several. If a molecule forms multiple liquid crystal phases, the more ordered phase occurs at lower temperatures.

Figure 1.6: Different phases of rod shaped molecules.



Discotic mesogens are flat disc-like molecules that usually consist of a core of fused aromatic rings substituted with flexible chains. These molecules tend to stack into columns, giving rise to columnar liquid crystal phases (Col) (Figure 1.7). Generally, disc-shaped mesogens form only columnar phases, although occasionally they form nematic phases. The flexible side chains serve to lower melting temperatures as well as to act as a buffer between one column and another, giving the resultant packed columns an added degree of mobility. This thesis will focus on discotic mesogens and we will discuss the phases formed by these molecules in more detail in the following section.

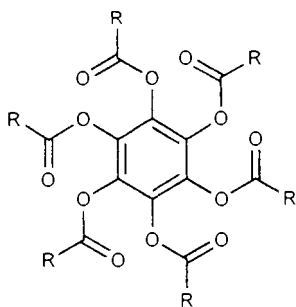
Figure 1.7: Examples of typical discotic mesogens.



1.2.3 Phases Formed by Discotic Mesogens

The first liquid crystal formed from a disc-shaped molecule was reported in 1977 by Sivaramakrishna Chandrasekhar (Table 1.1).²⁵ These molecules were alkylated benzene hexaesters, which were later determined to form columnar phases.

Table 1.1: Phase behaviour of hexaesters reported by Chandrasekhar in 1977.



	Phase	$T_{ij}/^{\circ}\text{C}$	Phase
R=C ₅ H ₁₁	Cr	106.0	I
R=C ₆ H ₁₃	Cr	68.3	Col _h
		86.0	I
		83.3	
R=C ₇ H ₁₅	Cr	80.2	Col _h
		86.2	I
		83.6	
R=C ₈ H ₁₇	Cr	79.4	Col _h
		83.6	I
		81.5	
R=C ₉ H ₁₉	Cr	79.6	Col _h
		74.7	I
R=C ₁₀ H ₂₁	Cr	85.4	I

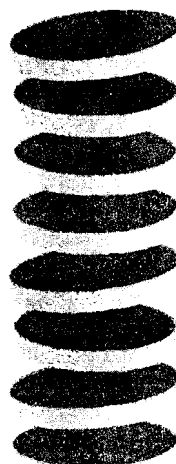
Adapted from Chandrasekhar.²⁵

In general, columnar phases are classified according to two main factors: the packing of the two-dimensional array of columns and the degree of order within the column. Columnar liquid crystals (Col) have a variable order within the column; if periodic long range order between molecules within the column is observed, the phase is termed as 'ordered' (subscript o). Phases that lack this periodicity are termed 'disordered' (subscript d) (Figure 1.8).

Figure 1.8: Columnar order and disorder.



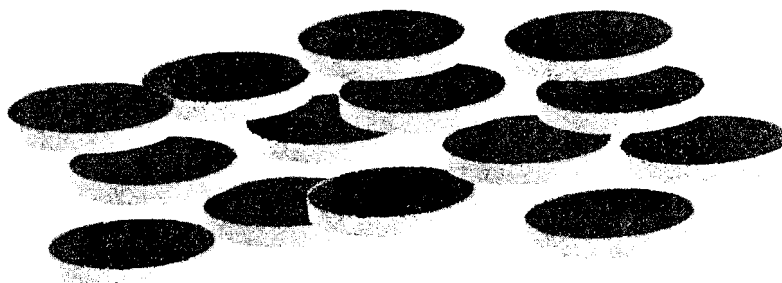
Columnar Disordered (Col_d)



Columnar Ordered (Col_o)

The columns of these mesophases can pack in a variety of two dimensional lattices, depending on the arrangement of molecules within the columns. Several such geometries are shown in Figure 1.9 and Figure 1.10, such as hexagonal (Col_h), rectangular (Col_r) and oblique (Col_{ob}).

Figure 1.9: Liquid crystal phases formed by discotic mesogens.



Discotic Nematic (N_D)

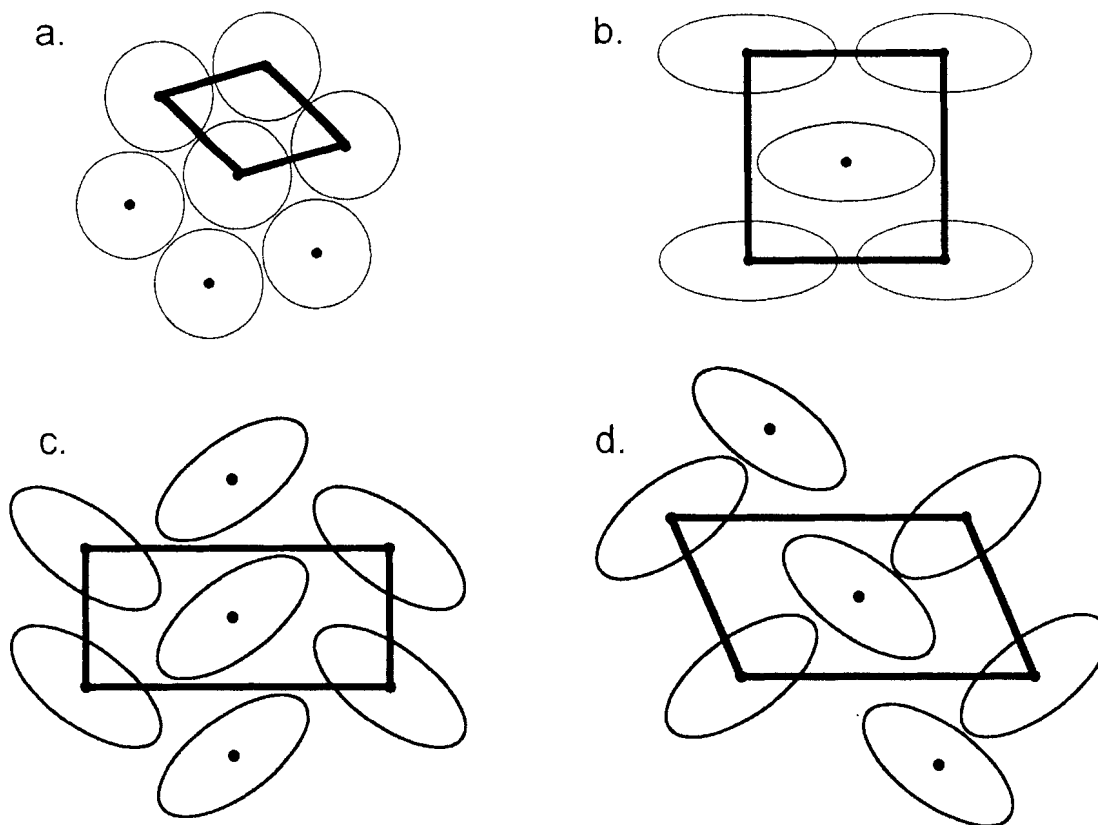


Columnar Hexagonal Ordered (Col_{HO})



Columnar Rectangular Ordered (Col_{RO})

Figure 1.10: Two-dimensional lattices of common columnar phases.



Adapted from Levelut et al.²⁶ Ellipses denote discs that are tilted with respect to the column axis: a) hexagonal, b) rectangular face-centred, c) rectangular, d) oblique

Although most discotic mesogens form columnar phases, there are a few examples in which disc-like molecules form a nematic phase (N_D), denoted with a subscript D to avoid confusion with the analogous phase formed by rod-like molecules.

1.2.4 Applications

1.2.4.1 Applications of Calamitic Mesogens

Liquid crystal technology has had a major effect in many areas of science and engineering, especially in the area of device technology. The most common application of calamitic liquid crystal technology is in liquid crystal displays

(LCDs), which rely on the optical properties of nematic liquid crystals in the presence or absence of an electric field.

1.2.4.2 Applications of Discotic Mesogens

Columnar liquid crystals have emerged as a promising class of materials for light emitting diodes,^{27,28} photovoltaic devices²⁹ and field effect transistors.³⁰ These liquid crystals exhibit a host of attractive properties, including high charge carrier mobilities, a lack of grain boundaries and the potential to be uniformly aligned.³¹⁻³⁴ Although many applications have been suggested for liquid crystal systems formed by discotic mesogens, the only commercially successful application to date has been the production of optical compensating films using nematic discotics, which are used to improve the viewing angle on most modern LCDs.³⁵⁻³⁷

One of the important limitations of columnar liquid crystal phases is the lack of understanding of the factors that determine their thermal stability. Understanding the factors that effect the formation of a mesophase will make the modification and syntheses of discotic liquid crystals with different physical and electronic properties possible and enable the molecules to be tailored for specific applications. Elucidating these factors is the primary goal of the research described in this thesis.

1.3 Liquid Crystal Characterization Techniques

The phase properties of potential liquid crystalline materials are most commonly analyzed using a combination of differential scanning calorimetry

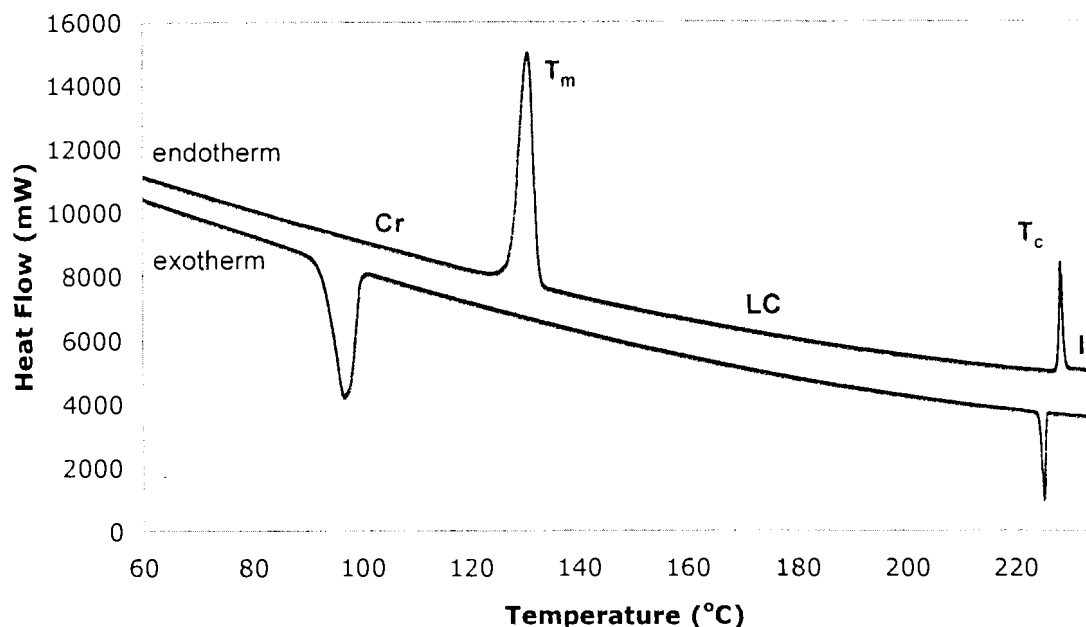
(DSC), polarized optical microscopy (POM) and variable temperature X-ray diffraction (XRD). These complementary techniques together provide considerable information regarding the liquid crystalline phases. Each will be briefly described below.

1.3.1 Differential Scanning Calorimetry

Differential scanning calorimetry, or DSC, is a technique used to measure the phase transitions of a material. In this method, two pans are simultaneously heated in separate holders. The first pan contains 5-10 mg of the material to be analyzed, while the second (empty) pan is used as a reference. The temperature of the two pans is changed at a constant rate and the difference in heat flow required to maintain both at the same temperature is measured. At a phase transition (T), excess heat is absorbed (on heating) or released (on cooling) by the sample, which results in the appearance of a peak on a plot of temperature versus heat flow. These plots are referred to as endotherms when the sample is heated and exotherms when it is cooled (Figure 1.11). These plots produce two very useful pieces of information regarding phase information: the temperature at which phase transitions occur and the enthalpy of those transitions. The temperature at which a transition occurs is useful in relating how stable a phase is. A higher transition equates to a phase being more thermally stable. The magnitude of the enthalpy of transition reveals how large the change in molecular order is between the two phases. Crystal-to-liquid crystal transitions (T_m) tend to have large enthalpies of transitions (~ 20 -100 kJ/mol), whereas the enthalpy of

liquid crystal-to-isotropic (T_c) or liquid crystal-to-liquid crystal transitions tend to be smaller ($\sim 1-10$ kJ/mol).³⁸

Figure 1.11: Typical DSC endotherm and exotherm.



Cr = crystalline solid, LC = liquid crystal, I = isotropic liquid, T_m = melting temperature, T_c = clearing temperature.

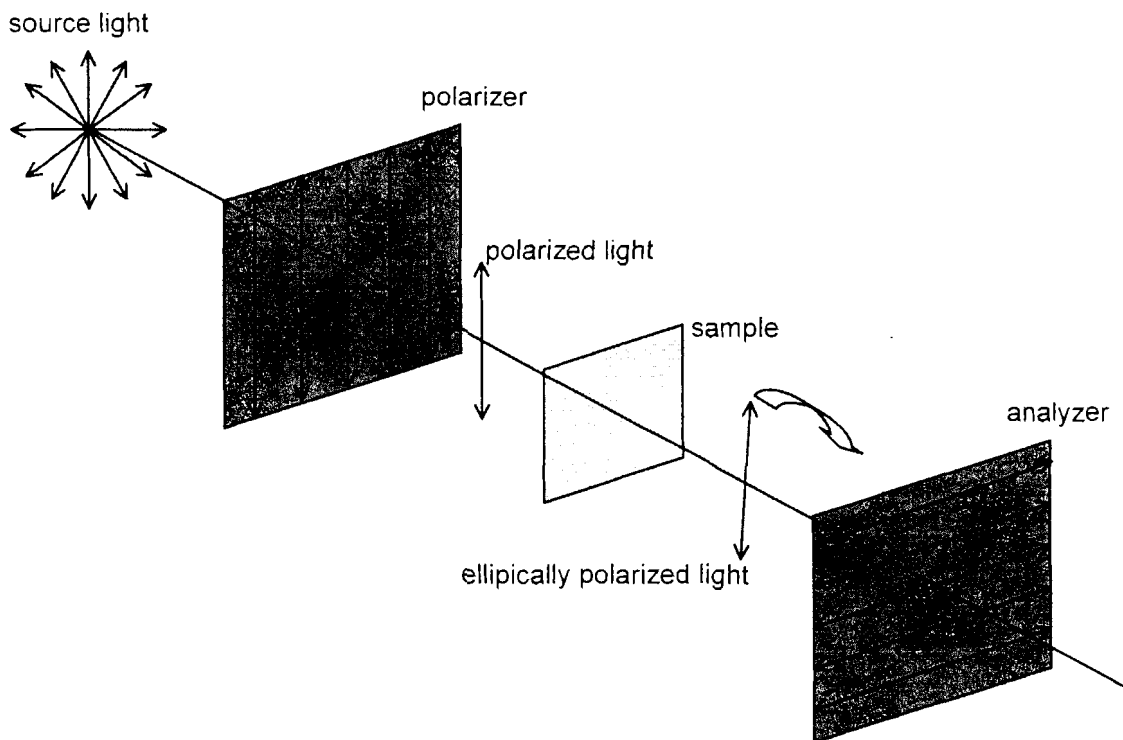
1.3.2 Polarized Optical Microscopy

Polarized optical microscopy (POM) provides a great deal of information not available with other techniques. The polarized light microscope is designed to observe material characteristics that are visible primarily due to their optically anisotropic nature.

Isotropic materials have the same refractive index in all directions. Many anisotropic materials have optical properties that vary with the orientation of incident light with respect to the axes of the crystal (or liquid crystal) and light will propagate at different rates in different directions through the material. Such

materials are said to have two different indices of refraction and are termed birefringent. One of the features of birefringent materials is that they can (depending on its orientation) change the direction of plane polarized light passing through it.^{21,38,39}

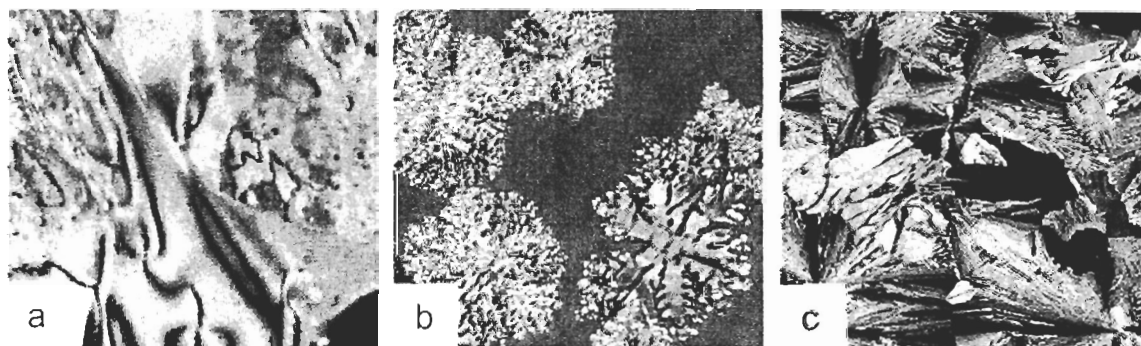
Figure 1.12: Schematic representations of a polarized optical microscopy experiment.



In POM, the sample is placed between two crossed polarizers, i.e. two polarizers that are rotated 90° with respect to one another (Figure 1.12). One polarizer is between the light source and the sample, while the other is between the sample and the observer. Changes in the image viewed relative to that of a regular microscope arises from the interaction of linearly-polarized light with a birefringent material. Optical textures arise because the liquid crystals are not perfectly homogenous and defects and deformations occur as the liquid crystal

patterns grow from an isotropic phase. A nematic phase will usually show 'brush-like' Schlieren textures (Figure 1.13). Columnar phases are often identified by characteristic dendritic patterns, which have the appearance of a tree or snowflake. Observation of angles close to 60° between branches of these dendritic patterns usually indicates the formation of a hexagonal phase, while 90° angles indicate a rectangular phase. As a material is heated on the microscope, the clearing temperature (T_c) can be observed as the textures disappear and the material becomes non-birefringent. Although a very useful tool, characterization of liquid crystals via polarized optical microscopy is somewhat subjective in nature and must be used in conjunction with other techniques such as X-ray diffraction and differential scanning calorimetry.

Figure 1.13: Typical optical textures observed for discotic mesogens.



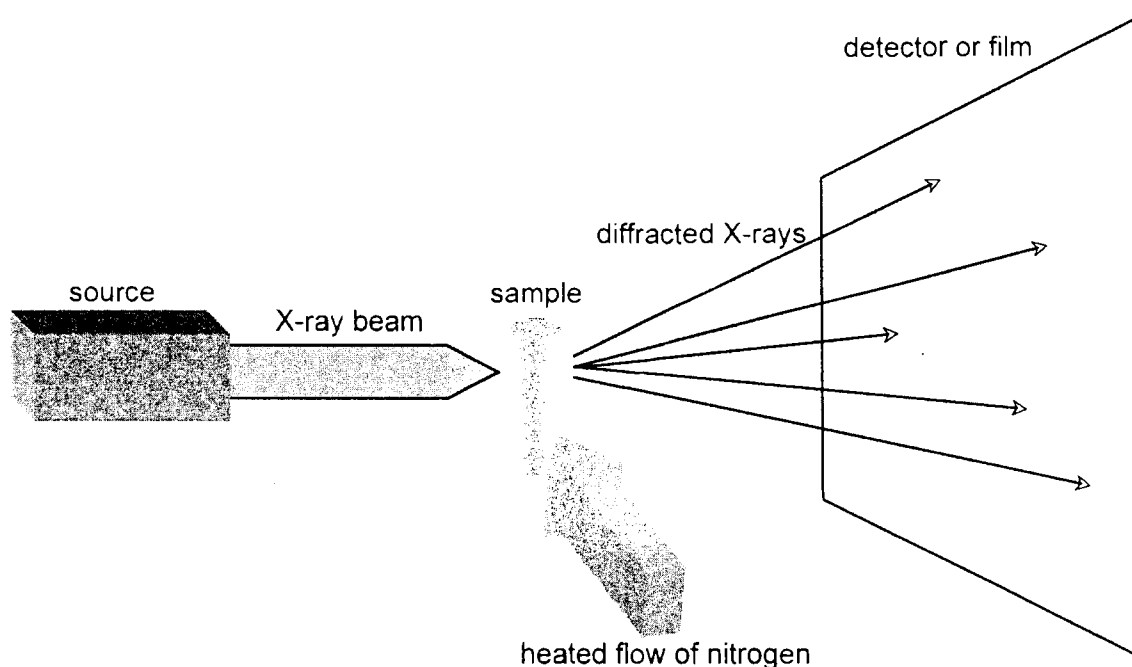
Polarized optical micrographs. a) discotic nematic, b) hexagonal columnar, c) rectangular columnar.

1.3.3 Variable Temperature X-Ray Diffraction

Liquid crystals are often characterized by X-ray diffraction at several temperatures to identify the phase in question. Most X-ray diffractometers do not come equipped with a heating device suitable for fluid (or semi-fluid) materials.

For our experiments, a heated stream of nitrogen was used to warm samples that were loaded into a glass capillary (Figure 1.14). Here, the temperature is maintained and measured by a thermocouple located next to the sample as well as a thermocouple within the heating unit.

Figure 1.14: Variable temperature X-ray diffraction setup.



Once the diffraction patterns are integrated through 2θ versus intensity, the plot shows a pattern that can be related to distance using the Bragg equation ($n\lambda = 2d \sin\theta$). X-Ray diffraction patterns of columnar liquid crystals show a peak at approximately 4.5 \AA , usually called the alkyl chain halo, that is due to the periodic spacing between the flexible side chains (Figure 1.15). Hexagonal columnar mesophases give rise to two diffractions at low angles, one that is usually very strong and the other less intense, corresponding to the (100) and (110) Bragg peaks, respectively (Figure 1.16). Rectangular columnar phases

show two nearly equally high intensity peaks corresponding to the (110) and (200) peaks as well as several lower intensity peaks, associated with higher order refractions. Both rectangular and hexagonal columnar phases can also be ordered or disordered. The observation of a broad peak at ~ 3.5 Å, which corresponds to the average distance between the stacked cores within the column, is commonly used to determine whether a system is ordered or disordered within the column. In disordered columnar phases, this peak is generally too broad to observe.

Figure 1.15: Typical X-ray diffraction pattern of a columnar hexagonal ordered phase.

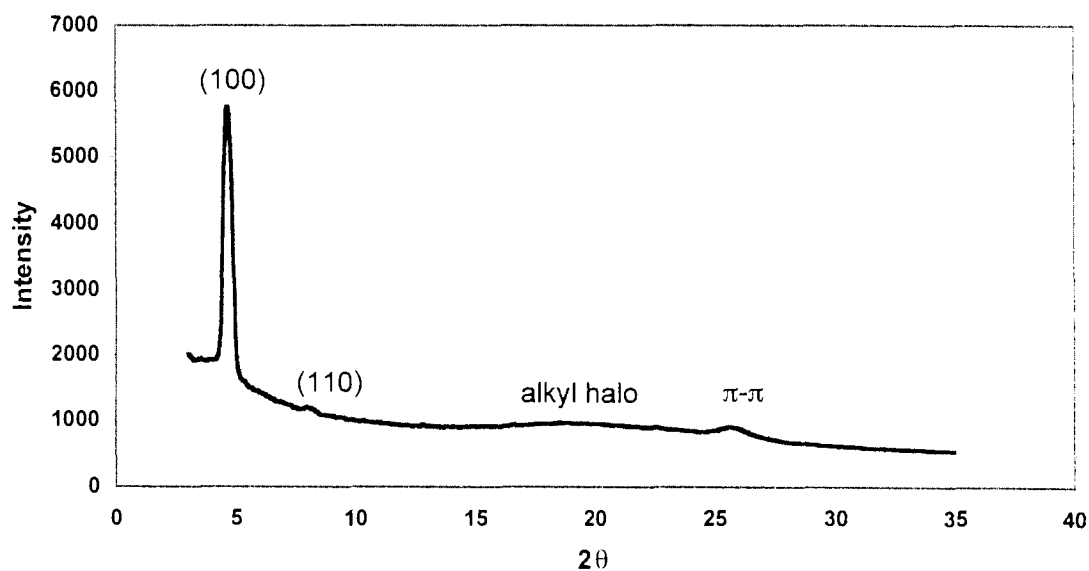
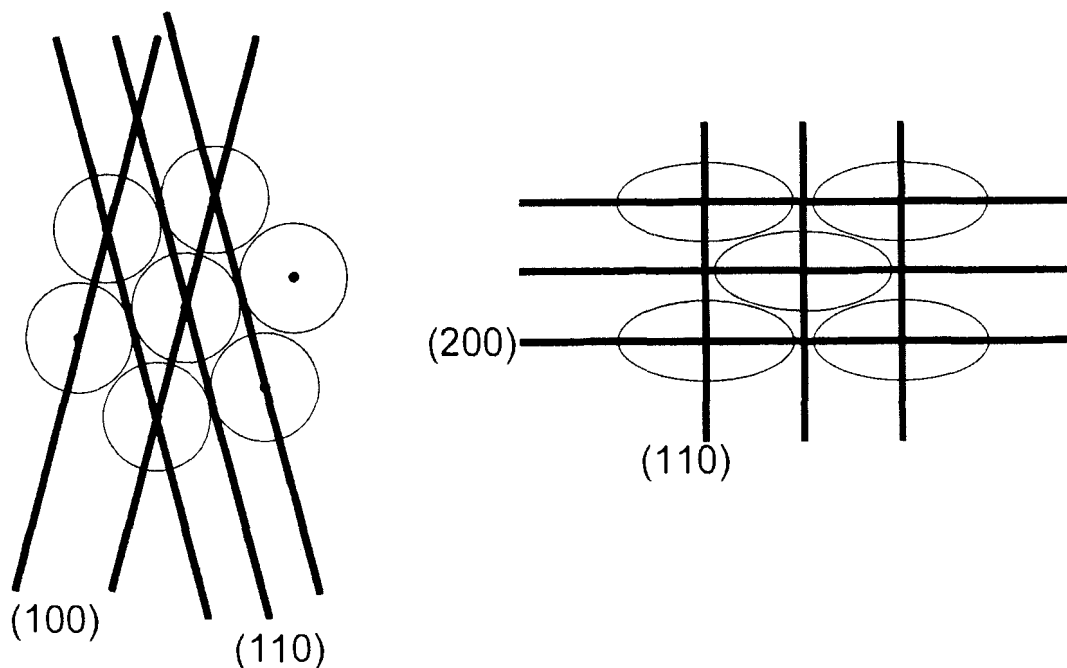


Figure 1.16: Planes in 2D hexagonal and rectangular lattices.



The planes of 2D hexagonal (left) and rectangular (right) lattices.

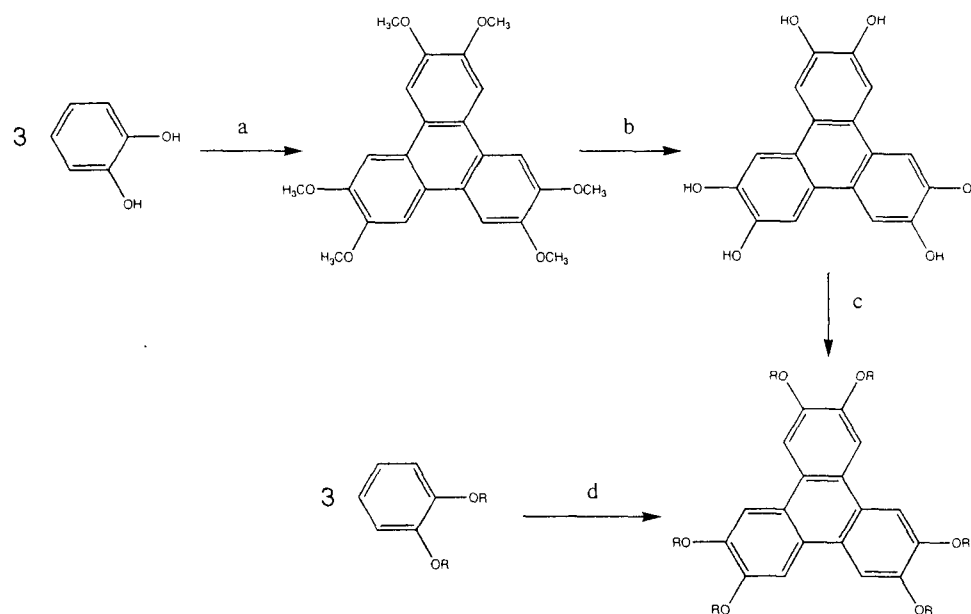
1.4 Structure-Property Relationships in Discotic Liquid Crystals

Despite the fact that research into the structure-property relationships of liquid crystals has been ongoing for more than 100 years, our understanding of how changes in molecular structure effect material properties remains poor. This is especially true for discotic mesogens, since they were discovered in 1977, and as such, there are far fewer examples of these types of molecules as compared to calamitic mesogens.

Research into the structure-property relationships of discotic mesogens has focused mainly on triphenylene derivatives. Triphenylenes were one of the first classes of discotic mesogens discovered and quickly became favoured

relative to the original discotic hexaesterbenzenes²⁵ due to their broader phase ranges. Triphenylenes can be synthesized in many different ways and the general simplicity of triphenylene syntheses has made them attractive for study and for commercial applications.

Scheme 1.1: Synthesis of previously published hexa-alkoxytriphenylenes.



Synthesis of ethers of triphenylene, adapted from Destrade et al.⁴⁰ a) chloroanil, H₂SO₄, b) HBr, AcOH, c) RBr, Base, d) FeCl₃, CH₂Cl₂.

The synthetic route shown above makes use of oxidative coupling of dimethoxybenzene to create a triphenylene (Scheme 1.1). The relative ease of this route has facilitated the preparation and study of a large number of triphenylenes of this type. In general, increasing the alkoxy chain length has the effect of lowering both the melting and clearing temperatures (Table 1.2). This general trend has been observed for the ethers, thioethers and selenoethers of triphenylene.^{41,42}

Table 1.2: Phase behaviour of previously published hexaalkoxytriphenylenes.

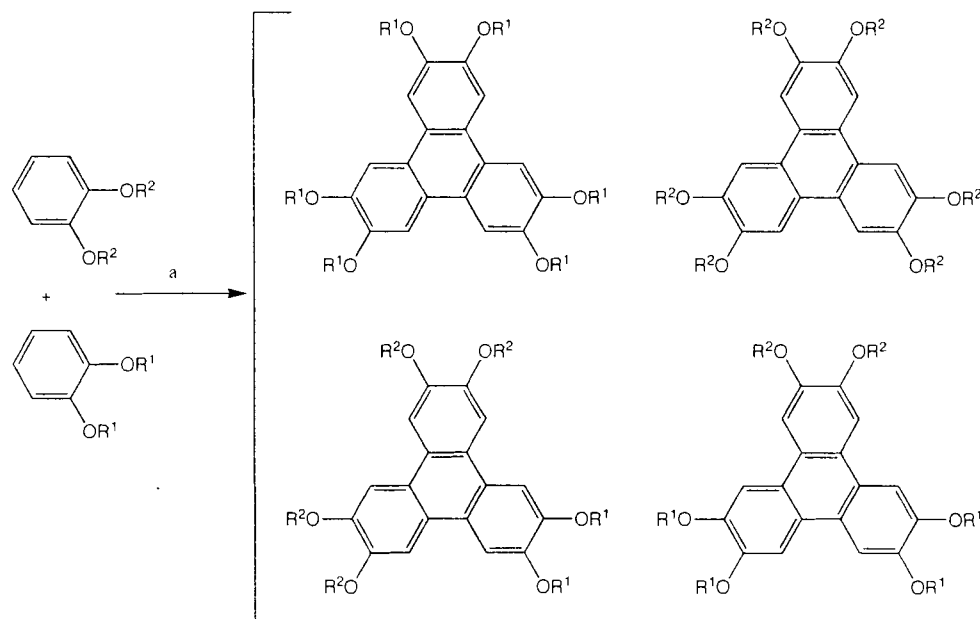
	Phase $\xrightarrow{T_l/^\circ\text{C}}$ Phase	
C ₃ H ₇	Cr $\xrightleftharpoons{177}$ I	
C ₄ H ₉	Cr $\xrightleftharpoons{89}$ Col _{ho} $\xrightleftharpoons{146}$ I	
C ₅ H ₁₁	Cr $\xrightleftharpoons{69}$ Col _{ho} $\xrightleftharpoons{122}$ I	
C ₆ H ₁₃	Cr $\xrightleftharpoons{68}$ Col _{ho} $\xrightleftharpoons{97}$ I	
C ₇ H ₁₅	Cr $\xrightleftharpoons{69}$ Col _{ho} $\xrightleftharpoons{93}$ I	
C ₈ H ₁₇	Cr $\xrightleftharpoons{67}$ Col _{ho} $\xrightleftharpoons{86}$ I	
C ₉ H ₁₉	Cr $\xrightleftharpoons{57}$ Col _{ho} $\xrightleftharpoons{78}$ I	
C ₁₀ H ₂₁	Cr $\xrightleftharpoons{58}$ Col _{ho} $\xrightleftharpoons{69}$ I	

Adapted from Destrade et al⁴⁰

In order to access derivatives in which the pendant alkyl groups surrounding the triphenylene core are non-identical, different synthetic techniques must be used. In statistical routes, reaction of two different 1,2-dialkoxybenzenes via oxidation results in a mixture of products, which are usually exceedingly difficult to separate from one another (see Scheme 1.2).²¹ Rational syntheses of unsymmetrical triphenylenes have been carried out using a variety of approaches, including oxidative coupling of biphenyls and benzenes (Scheme

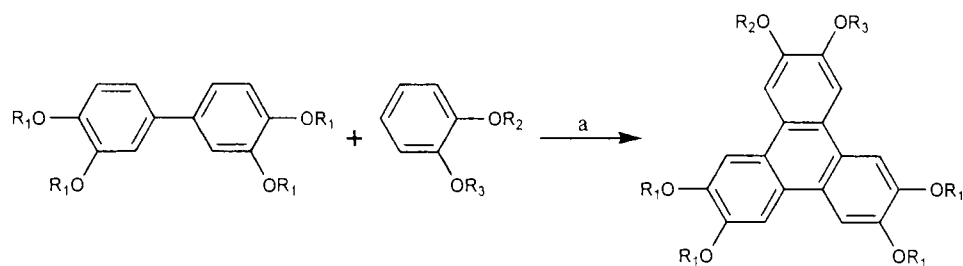
1.3), or cyclization of *o*-terphenyls (Scheme 1.4).²¹ These synthetic approaches will be discussed in greater length in Chapter 2.

Scheme 1.2: Statistical route to unsymmetrical triphenylenes.



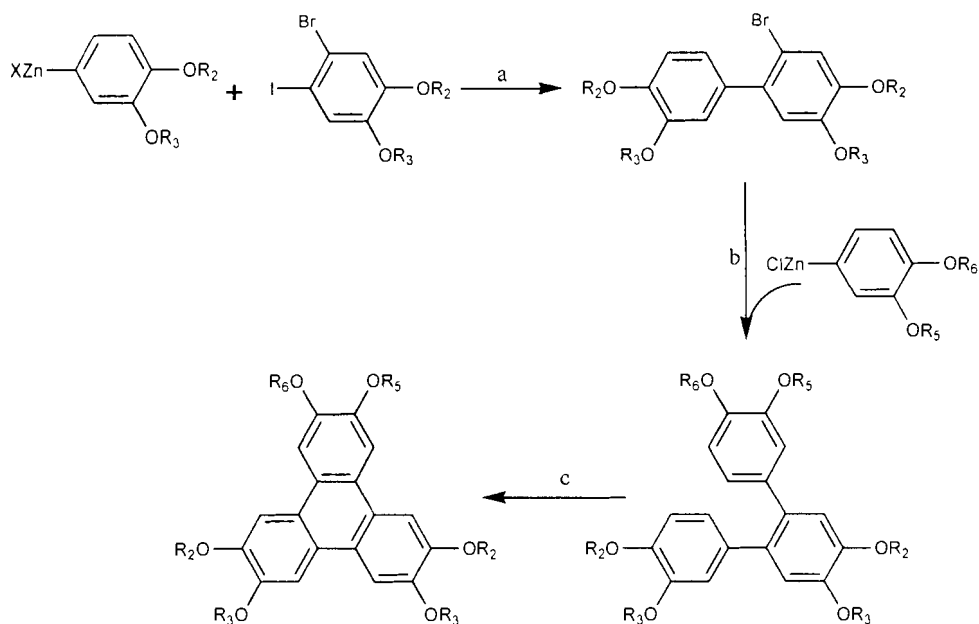
Reagents and conditions. a) FeCl₃/CH₂Cl₂.

Scheme 1.3: Oxidative coupling synthesis of triphenylenes.



Reagents and conditions. a) FeCl₃/CH₂Cl₂, then MeOH.

Scheme 1.4: Cyclization of o-terphenyl synthesis of triphenylene.



Reagents a) $\text{Pd}_2(\text{dba})_3/\text{Ph}_3\text{P}/\text{THF}/\text{reflux}$ b) $\text{Pd}_2(\text{dba})_3/\text{Ph}_3\text{P}/\text{THF}/\text{reflux}$, c) $\text{FeCl}_3/\text{CH}_2\text{Cl}_2$ then MeOH .⁴³ (dba = dibenzylidene acetone)

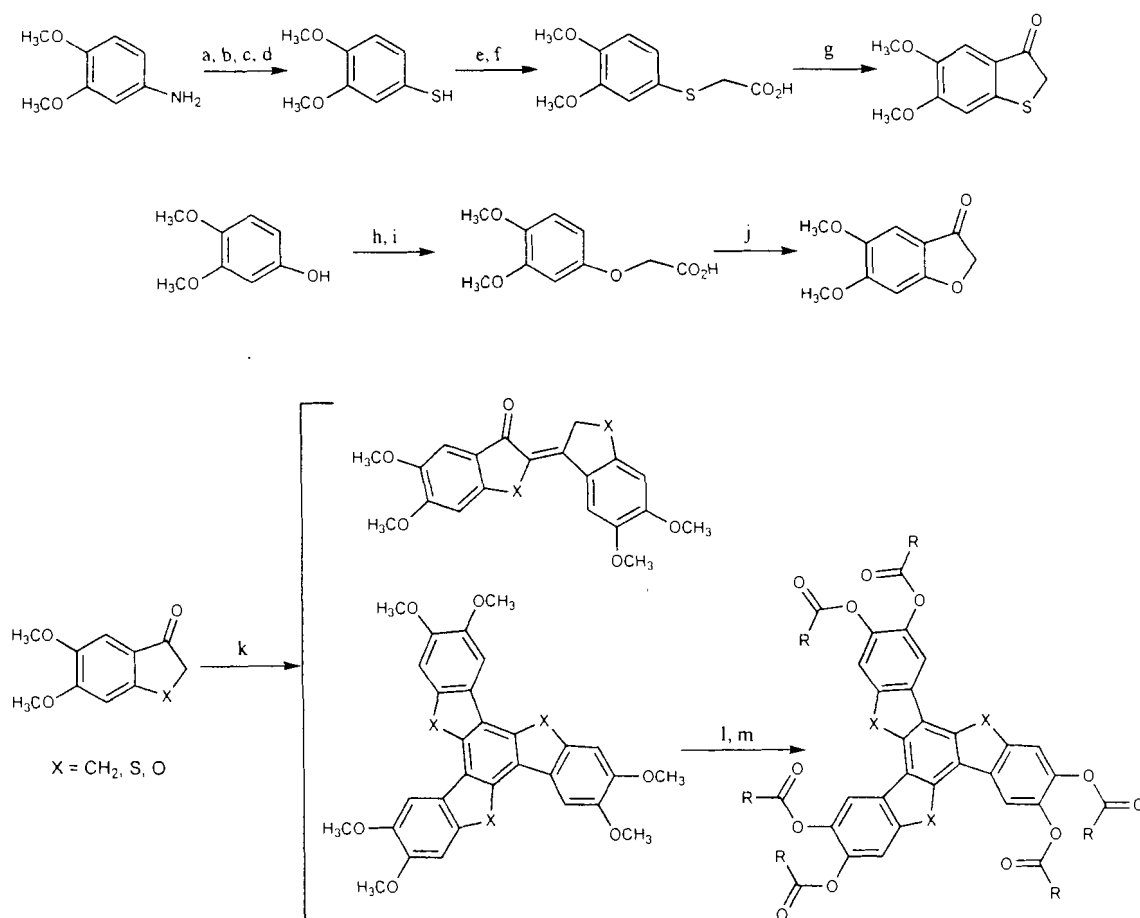
Unfortunately, the syntheses developed for triphenylenes do not lend themselves to the preparation of discotic mesogens with different aromatic cores. Since core-size, substituents and heteroatoms in the core all can potentially alter the propensity of molecules to self-assemble into columnar structures, these are precisely the type of structural factors that need to be studied. Representative examples of molecules that have in the past been used to probe these effects are described below.

1.4.1 Heteroatoms

Few studies have examined the effect of heteroatoms in the core of aromatic discotic mesogens. The synthesis of a series of potential discotic mesogens, differing only in the number and position of heteroatoms present, generally requires lengthy multistep routes. Below are shown three different

derivatives of truxene, each of which required a different synthetic approach (Scheme 1.5). The parent compounds, where $X=CH_2$, have a commercially available starting material,⁴⁴ while the oxa-^{45,46} and thia-^{47,48} analogues required lengthy syntheses to form the 'common' indanone precursors.

Scheme 1.5: Synthesis of truxene, oxatruxene and thiatruxene derivatives.

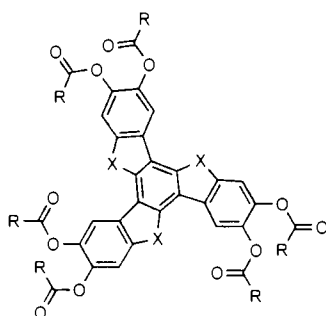


Reagents and conditions. a) $NaNO_2/HCl$, b) $KSCSOEt$, c) $KOH/EtOH$, d) HCl , e) $BrCH_2CO_2Et/base$. f) $KOH/EtOH$, g) H_2SO_4 , h) $BrCH_2CO_2Et/K_2CO_3$, i) $KOH/EtOH$, j) P_2O_5/H_3PO_4 , k) $PPE/CHCl_3, EtOH$, l) $BBr_3/Me_2S/ClCH_2CH_2Cl/reflux$, m) $RCOCl/pyridine, DMAP$.

The series of derivatives of truxene suggests that the introduction of a sulphur or oxygen depresses the clearing temperature relative to the methylene analogue (Table 1.3). Furthermore, with the presence of an oxygen atom

appears to form a single type of liquid crystalline phase (Col_r), whereas all of the methylene and sulphur analogues form two or more types of phase (Col_r , Col_h , N_D). These systems are controlled by a complex mixture of effects, as the introduction of a sulphur or oxygen is accompanied with a change in orientation of the outer rings relative to the central benzene ring.^{21,45}

Table 1.3: Phase behaviour of truxene, oxatruxene and thiatruxene derivatives.



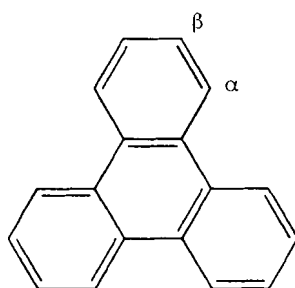
Compound		Phase	T_f /°C	Phase		Phase		Phase
Trx.CH ₂ .7	R = OC ₇ H ₁₅ X = CH ₂	Cr	98	Col _r	140	Col _h	280	I
Trx.S.7	R = OC ₇ H ₁₅ X = S	Cr	103	Col _{rd}	212	Col _{hd}	236	I
Trx.O.7	R = OC ₇ H ₁₅ X = O	Cr	95	Col _{rd}	194	I		
Trx.CH ₂ .8	R = OC ₈ H ₁₇ X = CH ₂	Cr	88	Col _r	141	Col _h	280	I
Trx.S.8	R = OC ₈ H ₁₇ X = S	Cr	90	Col _{rd}	191	Col _{hd}	229	I
Trx.O.8	R = OC ₈ H ₁₇ X = O	Cr	90	Col _{rd}	197	I		
Trx.CH ₂ .10	R = OC ₁₀ H ₂₁ X = CH ₂	Cr	62	N _D	89	Col _r	118	Col _h 250 I
Trx.S.10	R = OC ₁₀ H ₂₁ X = S	Cr	62	N _D	98	Col _{rd}	155	Col _{hd} 193 I
Trx.O.10	R = OC ₁₀ H ₂₁ X = O	Cr	76	Col _{rd}	194	I		

Adapted from: Trx.CH₂⁴⁴, Trx.O^{45,46}, Trx.S^{47,48}

1.4.2 Substituent effect

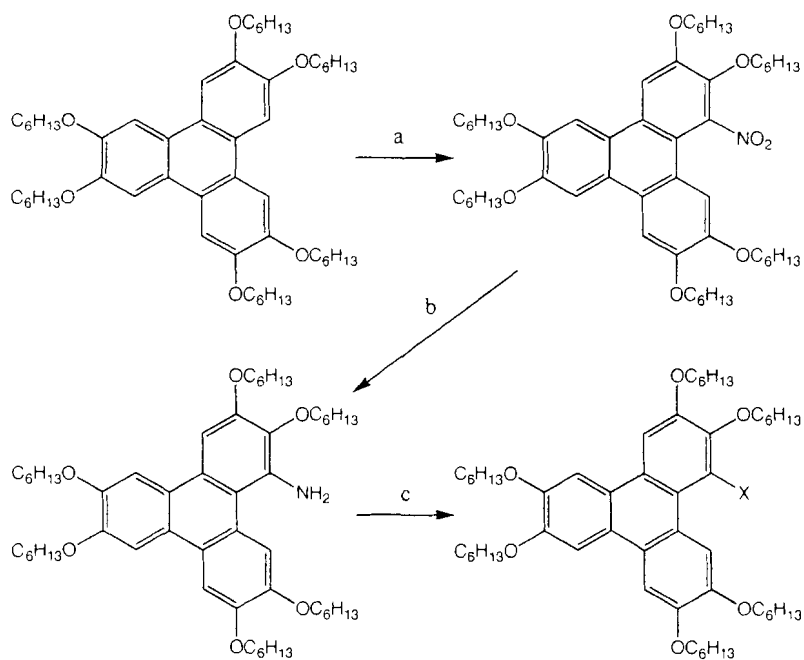
Direct substitution of groups onto the triphenylene core is governed by a conflict between electronic effects that favour attack at the α -position and steric factors (involving mainly the interaction with the *peri*-hydrogen atoms) that favour β attack (Figure 1.17). Normally, reaction at the β -position predominates.

Figure 1.17: α - and β - positions of triphenylenes.



The effect of placing different functional groups on a triphenylene core has typically required post-modification of the triphenylene. For example, in the case of Boden and Bushby's preparation of 'pocket-substituted' triphenylenes, electrophilic substitution was used to functionalize the hexalkoxytriphenylene in the α -position (Scheme 1.6). This α -position is in this case functionalized because the favoured β -sites are occupied by alkoxy groups. The authors noted that addition of a functional group at the α -position resulted in stabilization of the mesophase relative to the unsubstituted analogue, although twisting of the aromatic core often occurs due to steric crowding. There have been other syntheses of substituted triphenylenes that will be discussed in greater length in this thesis (Chapter 4).

Scheme 1.6: Synthesis and phase behaviour of 'pocket-substituted' hexaalkoxytriphenylenes.



	Phase	T_i /°C	Phase
X = H	Cr	68	Col _{h0} 97 I
X = NO ₂	Cr	<25	Col 136 I
X = NH ₂	Cr	35	Col 77 I
X = Cl	Cr	37	Col 98 I
X = NHCOCH ₃	Cr	99	Col 162 I
X = NHCOC ₆ H ₁₃	Cr	90	Col 191 I

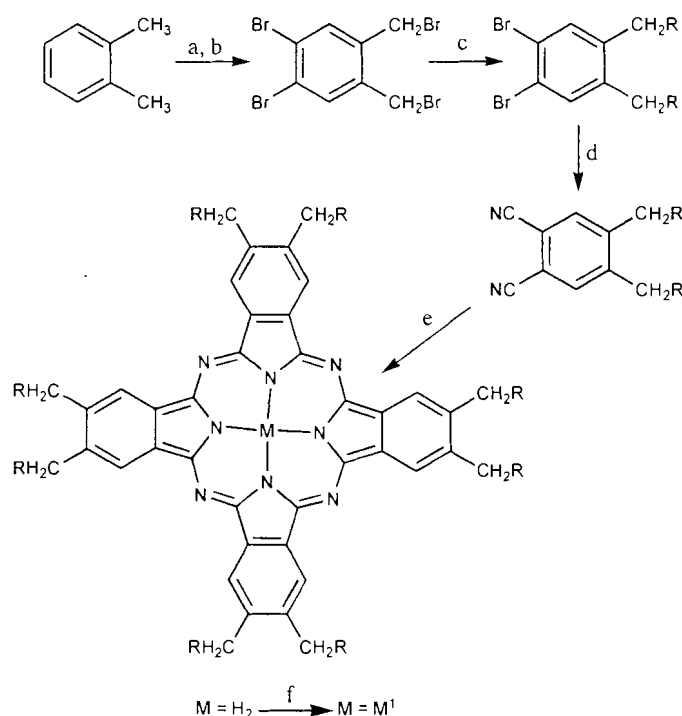
Reagents and conditions. ⁴⁹⁻⁵⁰ a) HNO₃/Et₂O/AcOH, b) Sn/AcOH/reflux, c) NaNO₂, HCl, CuCl, RCOCl/K₂CO₃/CH₂Cl₂

1.4.3 Core-Size

Another important class of discotic mesogens are the phthalocyanines. The presence of the four isoindole nitrogen atoms allows the molecule to coordinate hydrogen or metal cations in the centre. A large number of

mesogenic phthalocyanine complexes have been prepared, as there are many substituents and many metals that can be combined to induce mesogenic behaviour (Scheme 1.7). As with other discotic mesogens, between 6 and 8 pendant chains are required to inhibit crystallization and promote liquid crystallinity.

Scheme 1.7: Octaalkoxyphthalocyanines.

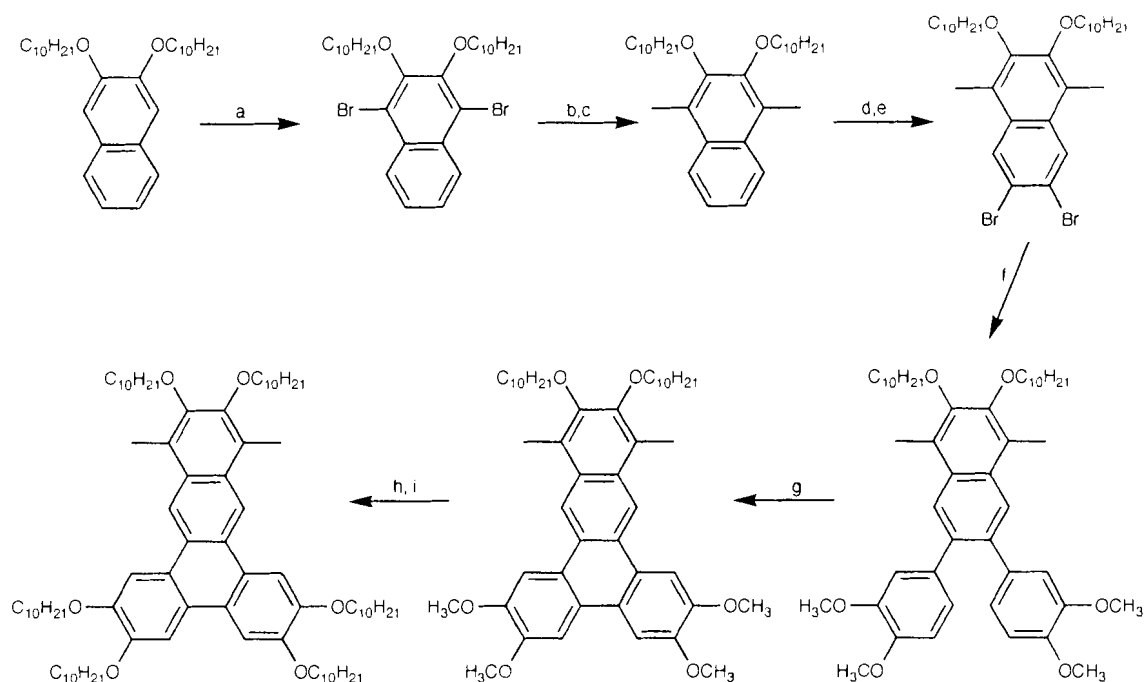


Compound	Phase	$T_f / ^\circ C$		Phase
		→	→	
R = OC ₈ H ₁₇ M = Ni	Cr	68	→	Col
			→	I _{Decomp}
R = OC ₈ H ₁₇ M = Co	Cr	72	→	Col
			→	I _{Decomp}
R = OC ₈ H ₁₇ M = Pb	Cr	45	→	Col _n
			→	158
			→	I
R = OC ₁₂ H ₂₅ M = H ₂	Cr	78	→	Col _n
			→	264
			→	I
R = OC ₁₂ H ₂₅ M = Cu	Cr	53	→	Col
			→	>300
			→	I
R = OC ₁₂ H ₂₅ M = Zn	Cr	78	→	Col
			→	>300
			→	I

Reagents and conditions.⁵¹⁻⁵⁴ a) Br₂, b) NBS, c) RO⁻, d) CuCN/DMF, e) *N,N*-dimethylethanolamine, f) M¹OAc.

When a disc-shaped molecule is significantly larger than triphenylene, it is usually termed "macrodiscotic", i.e. a disc-shaped molecules with a large core. This class of molecules has been well studied, chiefly by Müllen and co-workers.⁵⁵⁻⁵⁸ Comparatively little work has been carried out on discotic mesogens with core sizes intermediate between that of triphenylene and the macrodiscotic mesogens.^{59,60} The hexaalkoxybenzo[b]triphenylene derivative prepared in the Williams group was designed to probe the effect of an aromatic core slightly larger than triphenylene (Scheme 1.8).⁶¹ Although this molecule was found to be liquid crystalline over a broader range than the corresponding hexaalkoxytriphenylene, the cumbersome length of synthesis, the lower symmetry of the molecule and the presence of two methyl groups makes this compound unsuitable for core-size comparisons to triphenylene. Further discussion of research into core-size effects will be discussed later in Chapter 3.

Scheme 1.8: Synthesis of hexaalkoxybenzo[*b*]triphenylene.



Reagents and conditions.⁶¹ a) Br₂, AcOH, 85%, b) *n*-BuLi, Et₂O, -78 °C, c) CH₃I, 93%, d) Br₂, CH₂Cl₂, e) NaBH₄, DMSO, 50 °C, 3 days, 75%, f) 3,4-dimethoxyphenylboronic acid, Pd(PPh₃)₄, Na₂CO₃, DME, H₂O, 70 °C, 40%, g) FeCl₃, CH₂Cl₂, 44%, h) BBr₃, CH₂Cl₂, i) 1-bromodecane, K₂CO₃, DMF, 110 °C, 5 days, 42%.

1.5 Molecular Design and Evolution

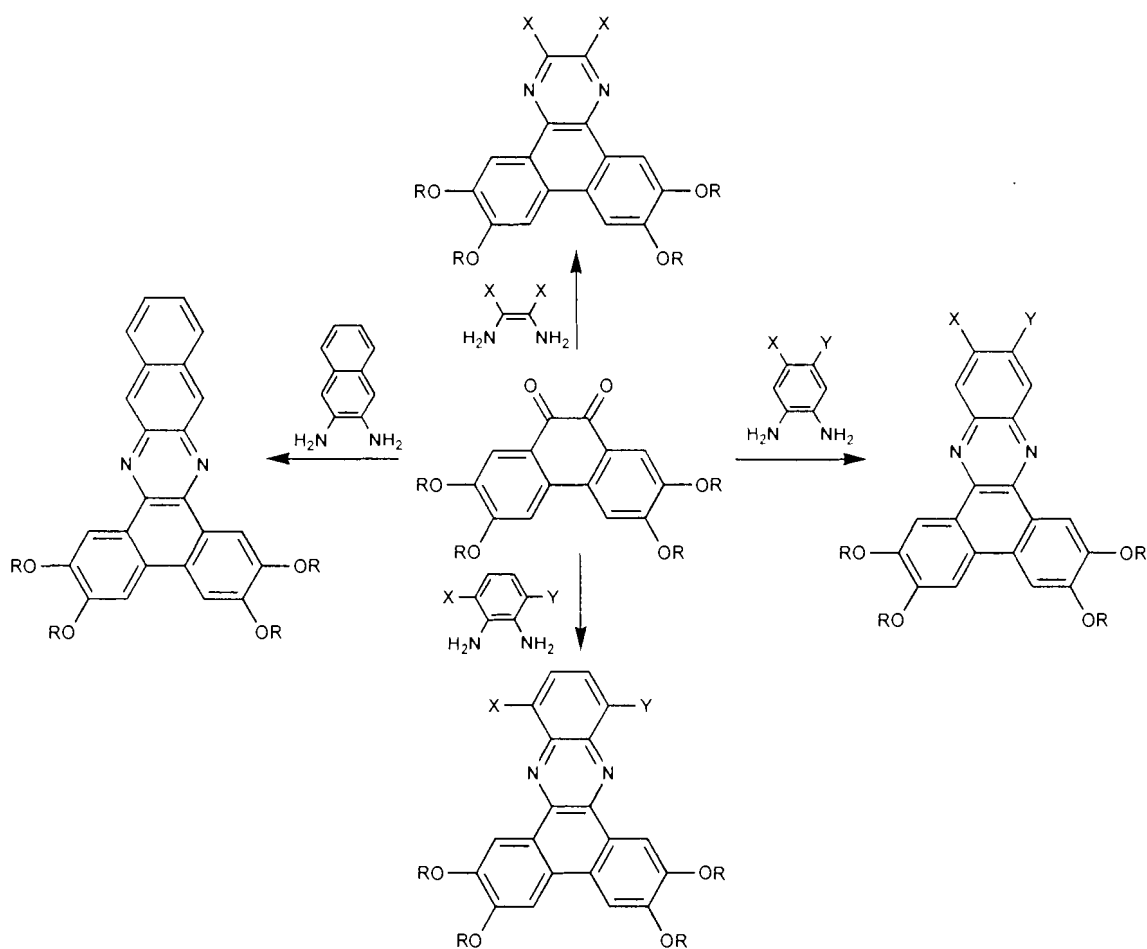
In principle, the relationship between molecular structure and macroscopic properties can be investigated through the synthesis of a series of similar mesogenic compounds. Towards this end, several series of disc-shaped molecules for systematically investigating structure-property relationships are reported in this thesis.

We envisioned that a wide variety of molecules could be synthesized based on a modular approach (Scheme 1.9). Using a common synthetic precursor, such as the tetraalkoxyphenanthrene quinones **2.6a-g**, together with the large number of *ortho*-diamines synthetically available as starting materials greatly facilitates the preparation of a broad family of potential mesogens. Using

these large series of molecules, trends in structure-property relationships will be investigated.

During the discussion of previously reported molecules, any molecule not synthesized or characterized within our laboratory will be reported with letters (e.g. HAT-6 or TH-HH). All compounds prepared in the course of this thesis will be represented as numbers (e.g. 2.11a).

Scheme 1.9: Proposed modular synthetic approach to disc-shaped molecules.



These synthetic routes should enable us to systematically investigate the effects of functional groups, core-size, heteroatoms in the core and molecular

symmetry on columnar self-assembly. Shown below are the target molecules that will be discussed in the subsequent chapters (Figure 1.18 – 1.21).

Figure 1.18: Target molecules discussed in Chapter 2.

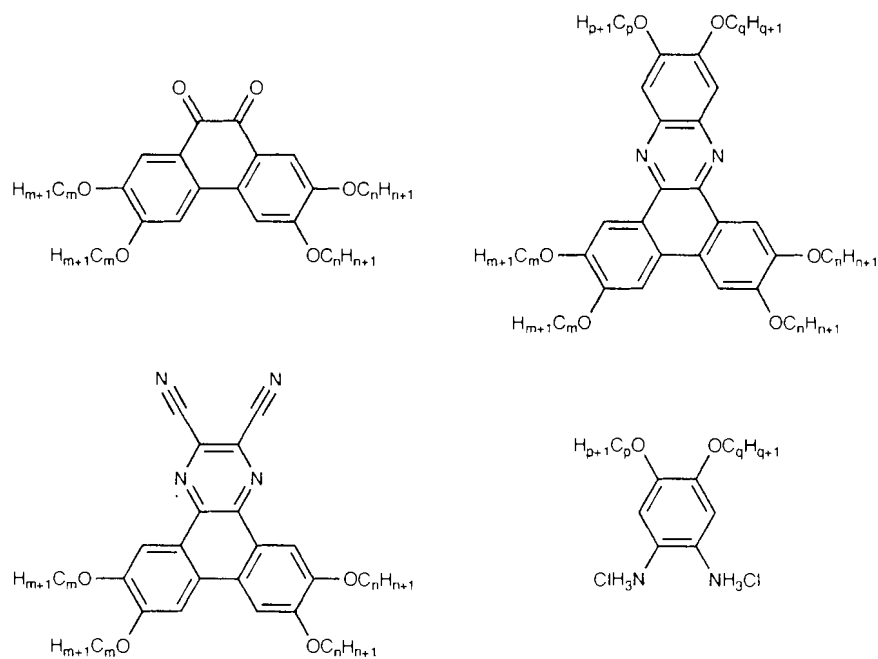


Figure 1.19: Target molecules discussed in Chapter 3.

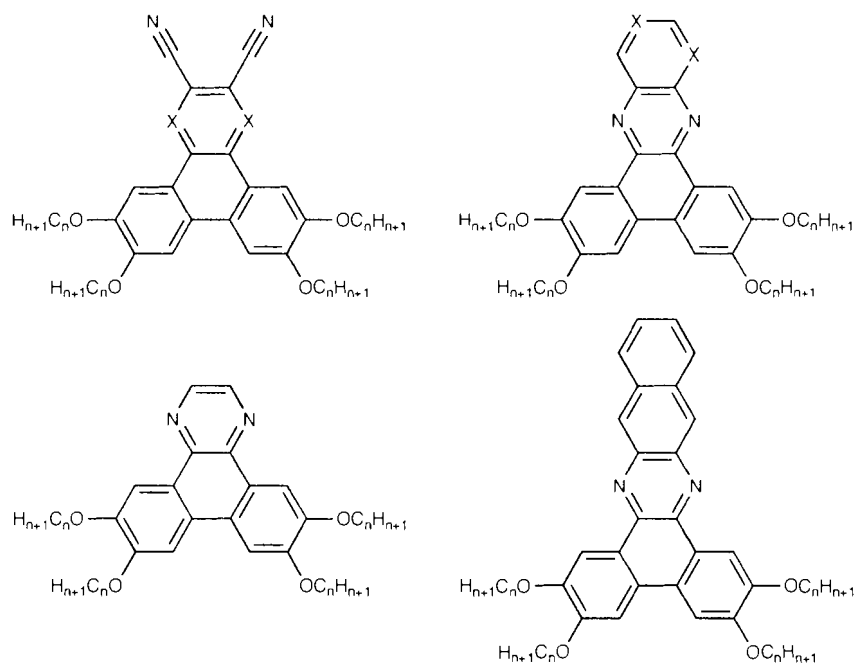


Figure 1.20: Target molecules discussed in Chapter 4.

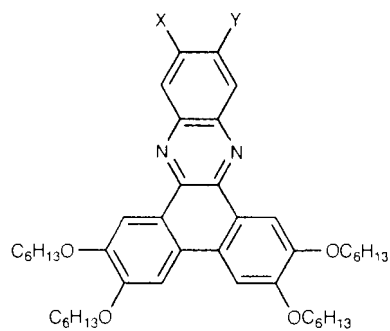
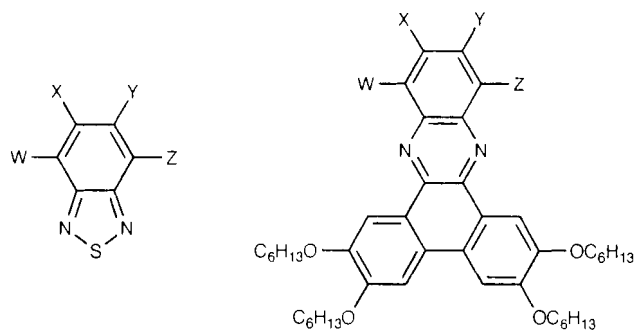


Figure 1.21 Target molecules discussed in Chapter 5.



2 SYMMETRY AND SHAPE EFFECTS ON SELF-ASSEMBLY

2.1 Introduction*

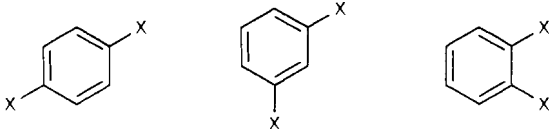
Understanding the relationship between molecular structure and the tendency of molecules to self-assemble into columnar structures remains an important and difficult challenge. Many factors can influence the self-organization of molecules into ordered structures, including π -stacking, dipole-dipole interactions and molecular symmetry. In this chapter we will attempt to address the last of these effects.

It has been suggested that, as a general rule, "...of two or more isomeric compounds, those whose atoms are the more symmetrically and more compactly arranged melt higher than those in which the atomic arrangement is unsymmetrical or in the form of long chains." This rule was originally suggested by Thomas Carnelley in 1882.⁶² Simple put, 'Carnelley's rule' states that crystals of symmetrical molecules have higher melting temperatures and are less soluble than the crystals of less symmetrical isomeric molecules.⁶³ The origin of this effect is most likely the greater entropy of crystalline phases formed by more symmetric molecules. Hence, these crystals gain less entropy upon melting, and therefore persist to higher temperatures. Several examples of this effect are

* Portions of this chapter were previously reported, see: a) E.J. Foster, J. Babuin, N. Nyugen and V. E. Williams *Chem. Commun.*, **2004**, 2052–2053 b) J. Babuin, J. Foster and V. E. Williams *Tet. Lett.* **2003**, 7003-7005.

listed below (Table 2.1). This rule has been found to be remarkably general, although some exceptions do exist. What is unknown is whether Carnelley's rule also applies to crystal-to-liquid crystal and liquid crystal-to-isotropic transitions. If so, symmetry could be used to tune phase ranges of liquid crystals.

Table 2.1: Examples of Carnelley's rule for crystalline solids.



X	Melting Point (°C)		
CH ₃	13.2	-47.8	-25.2
Cl	52.7	-24.8	-16.7
Br	87.3	-7.0	7.1
OH	172.3	111.0	105.0
NO ₂	174.0	90.0	118.5
OCH ₃	59.0	-52.0	22.5
OCH ₂ CH ₃	72.0	12.4	44.0

From CRC Handbook, 76ed. 1996

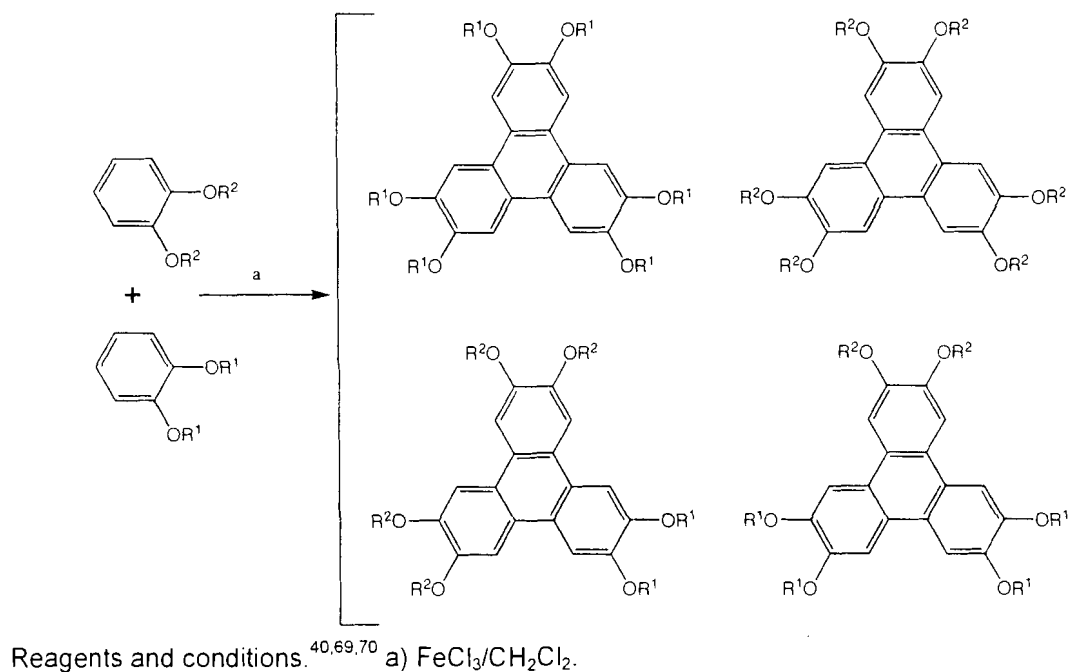
2.1.1 Previous Studies

Investigations of symmetry effects on the phase behaviour of liquid crystals invariably require the synthesis of unsymmetrical molecules that can be compared to symmetrical analogues. In the case of discotic mesogens, the examinations of this type have been carried out on 'mixed tail' triphenylenes, in which the alkoxy-chain lengths differ around the core.⁶⁴⁻⁶⁷ These unsymmetrical

triphenylenes can be synthesized in a number of ways (Figure 2.2 – 2.4). In general, these synthetic routes are more difficult than those of symmetrical molecules.^{21,38,68}

One of the earliest approaches to lower symmetry triphenylenes made use of a statistical synthesis (Scheme 2.1) that yielded a mixture of different products. Separation of the resulting four isomers was extremely difficult, if not impossible, when the pendant chains were similar.^{40,69,70} Chapuzet and co-workers did show it was possible to favour one isomer over another in a statistical synthesis of triphenylenes by altering the ratios of starting materials.^{71,72}

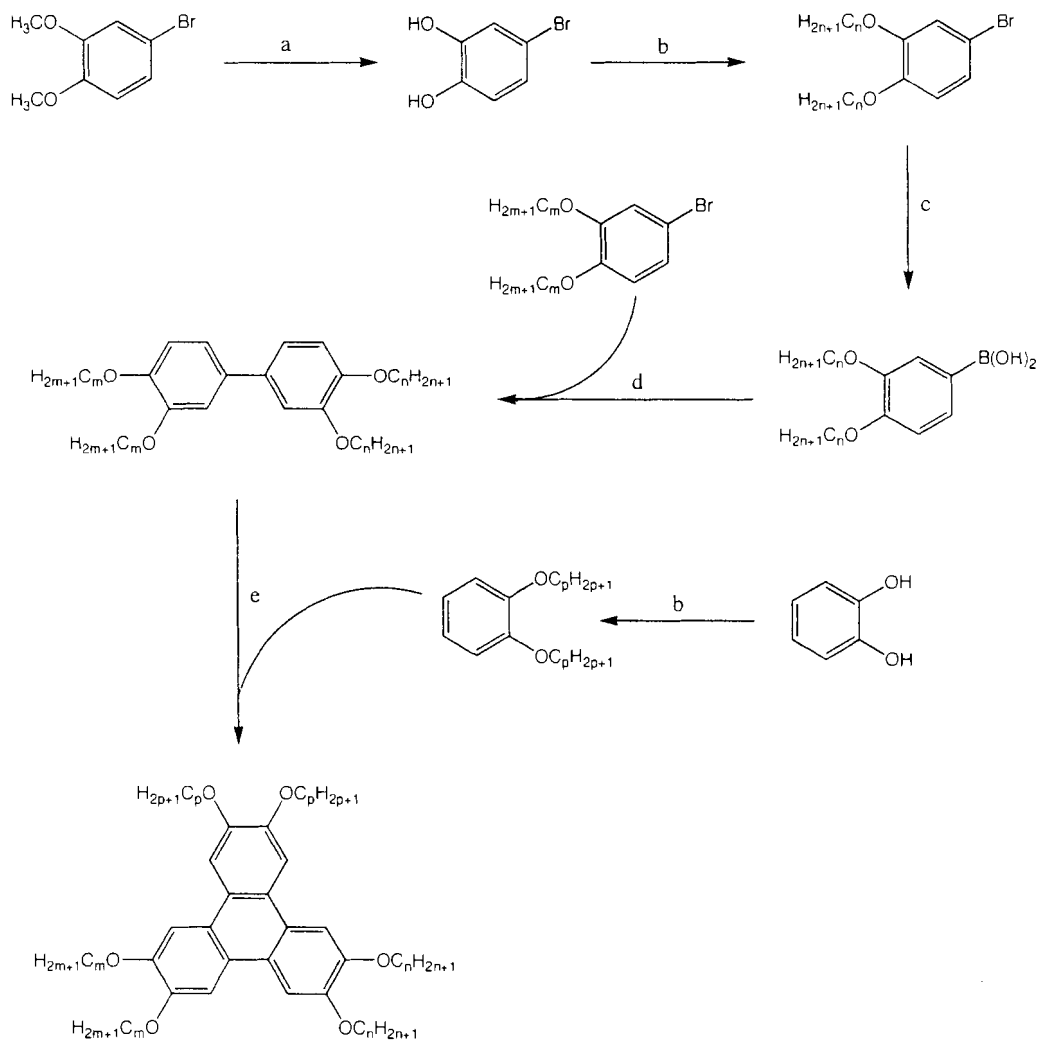
Scheme 2.1: Previously reported statistical synthetic route to unsymmetrical triphenylenes.



Cross and co-workers carried out a more systematic synthesis of triphenylenes to create a series of symmetrical and unsymmetrical molecules

capable of forming mesophases.⁷³ As shown below, a Suzuki coupling reaction was used to create tetra-substituted biphenyl, followed by oxidative coupling of another dialkoxybenzene to create the triphenylene core (Scheme 2.2).

Scheme 2.2: Previously reported rational unsymmetrical triphenylene synthesis.



Reagents and conditions.⁷³ a) BBr_3 , CH_2Cl_2 , b) $\text{C}_n\text{H}_{2n+1}\text{Br}$, K_2CO_3 , butanone, c) $n\text{-BuLi}$ then $(\text{MeO})_3\text{B}$, iii) 10% HCl , d) $\text{Pd}(\text{PPh}_3)_4$, DME, 10% Na_2CO_3 , e) FeCl_3 , H_2SO_4 , CH_2Cl_2 .

Zuilhof and co-workers used a nearly identical synthesis to assemble a series of hexaalkoxytriphenylenes in which one chain is different from the other five.⁷⁴ This convergent synthesis, wherein the last step entailed oxidative

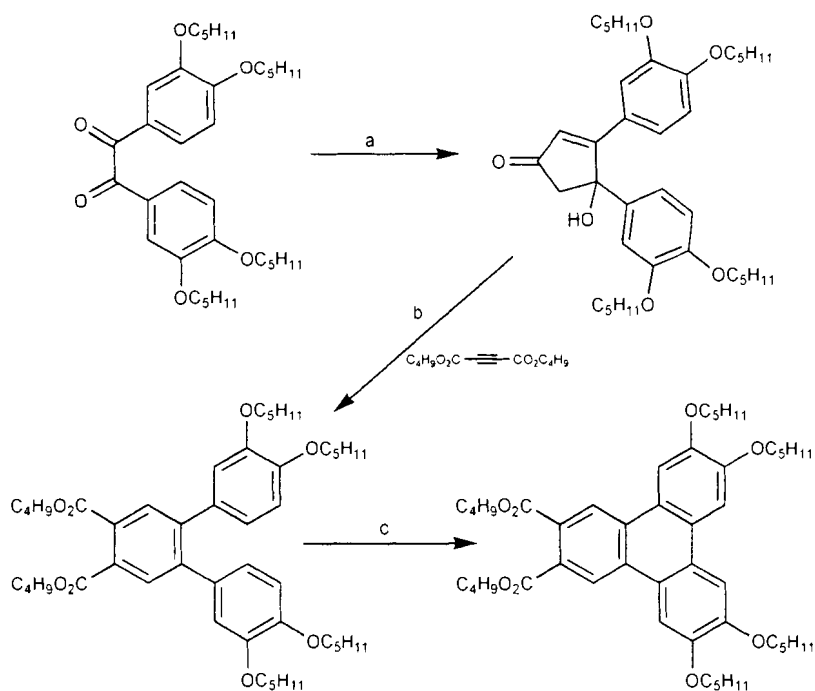
coupling of a biphenyl and a benzene has been used extensively for the synthesis of triphenylene cores.^{21,38,40,75} The phase behaviour of these materials will be discussed in detail later in the chapter.

The previous investigations into triphenylenes illustrates that there are many different routes to triphenylenes, although triphenylenes are sometimes disadvantageous due to the relatively small phase ranges. This chapter will discuss the synthesis and characterization of molecules with different shape and symmetry while focusing on differences between constitutional isomers.

2.1.2 Benzil Derivatives as Precursors

Triphenylenes have also been prepared from 3,3',4,4'-tetraalkoxybenzils (Scheme 2.3).^{76,77} Wenz, and later Josefowicz, used tetraalkoxybenzils to make substituted triphenylenes that were used to investigate self-organizing behaviour at interfaces.^{76,78-80} In addition, these benzil derivatives have been used to explore the effects of discogens incorporated into the main chains of polymers.^{77,81-83} These benzil derivatives have also been exploited as precursors to a variety of mesogens, including diazatriphenylenes,⁸⁴ phthalocyanines,⁸⁵ metallomesogens⁸⁶ and macrodiscotic species.⁸⁷

Scheme 2.3: Previously reported rational synthesis of triphenylene from tetraalkoxybenzil.

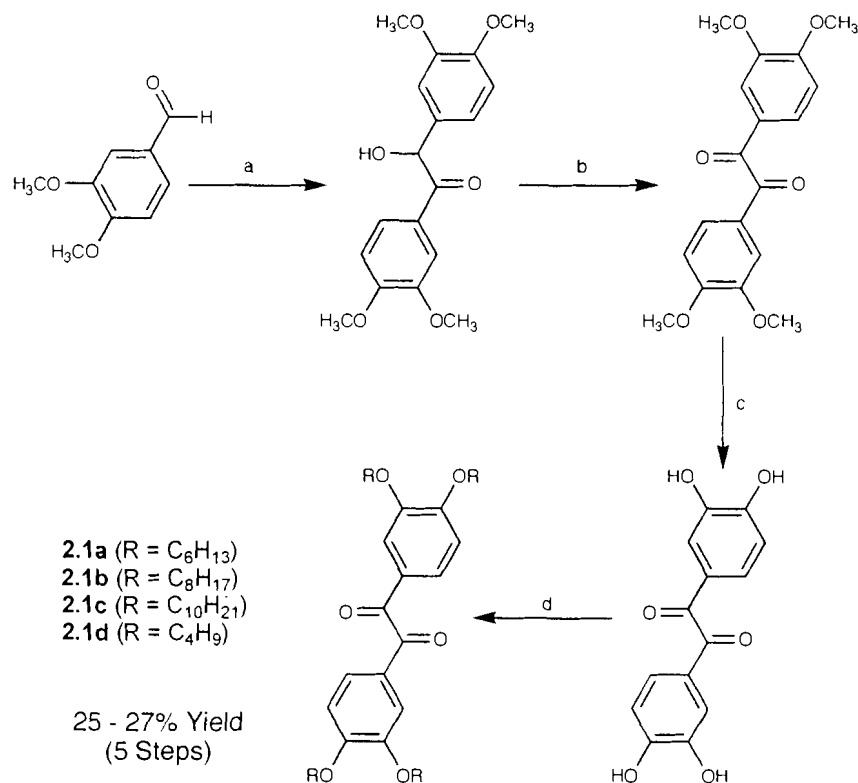


Reagents and conditions. a) CH_3COCH_3 , $^t\text{BuOK}$, EtOH, reflux, b) TsOH, H_2O , $\text{C}_6\text{H}_5\text{Cl}$, c) I_2/light .

Given their remarkable versatility as building blocks, the benzil derivative shown above represent an inviting entry point into the synthesis of low-symmetry discotic molecules. Symmetrical benzils ($\text{R}^1 = \text{R}^2$) can be prepared using a variety of methods, including the benzoin condensation route reported by Wenz (Scheme 2.4).⁷⁷ We therefore decided to use these precursors to construct a variety of discogens in order to investigate the effect of molecular symmetry and shape on liquid crystalline behaviour.

2.2 Synthesis of Divergent Precursors

Scheme 2.4: Synthesis of symmetrical benzil compounds (2.1a-d).



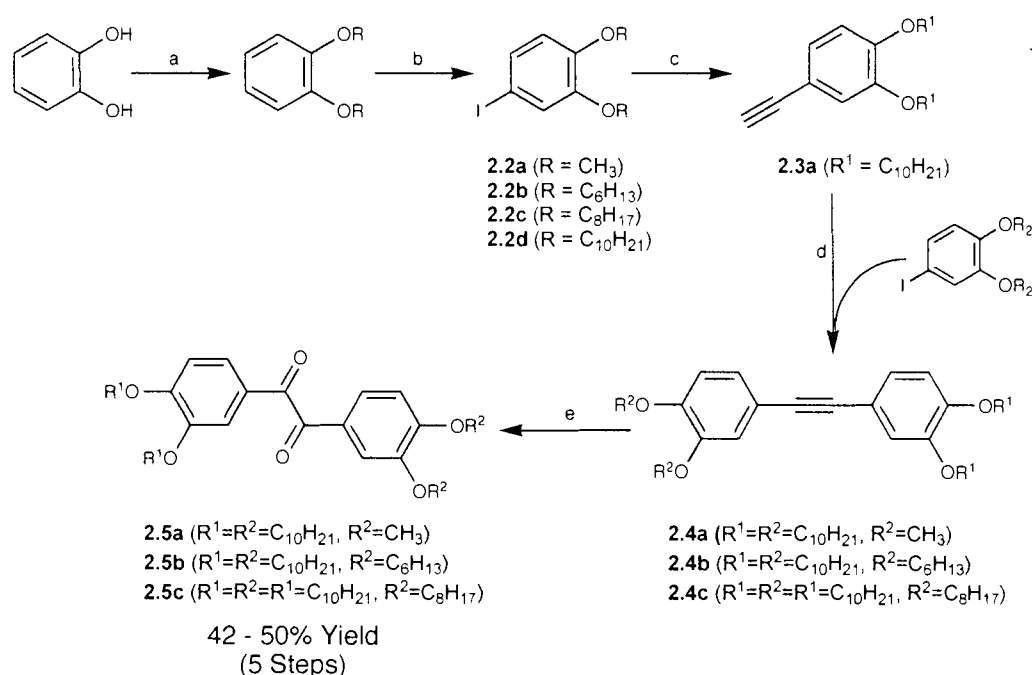
Reagents and conditions. a) KCN, H₂O, EtOH, reflux, b) CuSO₄, pyridine, reflux, c) AcOH, HBr, reflux, d) BrC_nH_{2n+1}, K₂CO₃, DMF.

We used Wenz's route to assemble benzil derivatives **2.1a-d** in four steps from veratraldehyde in an overall yield of 27-29%. Unfortunately, while the benzoin condensation has been used to cross-couple electronically disparate aldehydes, it cannot be viably applied to the assembly of benzil derivatives that have similar functional groups on both rings because of the resulting statistical mixture of products.^{88,89}

Unsymmetrical benzil derivatives with electronically similar groups can be synthesized from the corresponding tetraalkoxydiphenylacetylenes **2.4a-c**, which in turn were prepared in four steps from 1,2-dialkoxybenzenes (Scheme 2.5).

Iodination of 1,2-dialkoxybenzenes with iodine and iododic acid in acetic acid afforded the corresponding iodo-derivatives **2.2a-d**, in a yield of 65-72%. Compound **2.2a** was converted to compound **2.3a** by treatment with trimethylsilyl-acetylene under standard Hagihara-Sonogashira conditions, followed by base-promoted cleavage of the TMS group. A subsequent Hagihara-Sonogashira cross-coupling of this terminal alkyne with an appropriate iodobenzene derivative **2.2b-d** afforded the unsymmetrically tetra-substituted diphenylacetylene adducts **2.4a-c** in excellent overall yields.

Scheme 2.5: Unsymmetrical synthesis of benzil compounds (2.5a-c).

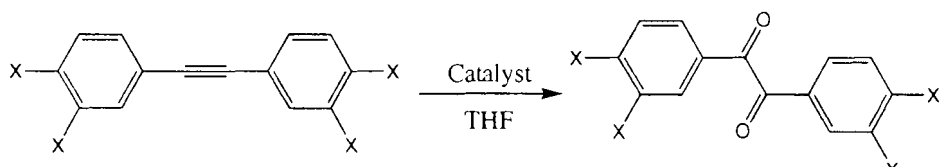


Reagents and conditions. a) BrC_nH_{2n+1}, K₂CO₃, DMF, b) I₂, HIO₃, AcOH, H₂SO₄, H₂O, c) TMS-C₂H, PdCl₂(PPh₃)₂, CuI, (ⁱPr)₂NH, THF, d) K₂CO₃, MeOH, THF, e) Pd(PPh₃)₄, CuI, (ⁱPr)₂NH, THF, f) I₂, DMSO, 145 °C.

A number of methods for the oxidation of diphenylacetylene to benzil have been reported and were examined in an effort to convert the alkynes **2.4a-c**

to their corresponding 1,2-diones **2.5a-c** (Table 2.2). Attempts to carry out this transformation using potassium permanganate were largely unsuccessful, yielding only trace quantities of the desired products.⁹⁰⁻⁹² Considerably better results were obtained by employing dimethylsulphoxide as the oxidant in the presence of 5 mol% palladium (II) chloride.⁹³ Equally satisfactory results were obtained using stoichiometric amounts of iodine in dimethylsulphoxide, which affords the diones in nearly quantitative yields.⁹⁴ Since almost identical results are obtained using either iodine or palladium (II) chloride, the former less expensive reagent was employed.

Table 2.2: Oxidation of diphenylacetylene to benzil.

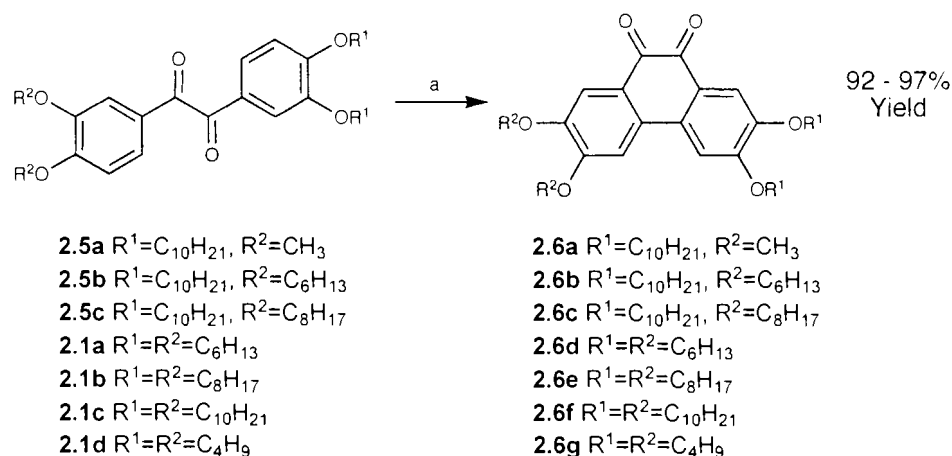


X	Catalyst (mol ratio)	Temp. (°C)	Time (Hours)	Yield (%)
H	-	140	24	0
H	PdCl ₂ (0.05)	140	4	12
H	PdCl ₂ (0.05)	140	24	43
H	PdCl ₂ (0.10)	140	24	85
OCH ₃	PdCl ₂ (0.05)	140	3	72
OCH ₃	PdCl ₂ (0.05)	80	4	54
OCH ₃	PdCl ₂ (0.05)	103	4	74
OC ₁₀ H ₂₁	PdCl ₂ (0.10)	140	24	84
H	I ₂ (1.0)	145	24	44
OCH ₃	I ₂ (1.0)	145	24	93
OC ₁₀ H ₂₁	I ₂ (1.0)	145	24	92

The overall yields obtained for the preparation the unsymmetrical benzil **2.5a-c** derivatives from the iodinated precursors **2.2a-c** via the diphenylacetylene route ranged from 45-53%. This compares favourably with the yields obtained by

the benzoin condensation route of the symmetrical derivatives **2.1a-d**. However, the scalable nature and fewer steps of the benzoin route makes it a better method for the large scale synthesis of symmetrical derivatives. Oxidative cyclization of the benzil derivatives (**2.5a-c** and **2.1a-d**) to the phenanthrene-9,10-diones, **2.6a-g** was carried out using vanadium oxytrifluoride (Scheme 2.6). Attempts were made to cyclize benzil derivatives using iron trichloride or vanadium oxytrichloride, but only starting materials were recovered.

Scheme 2.6: Oxidative cyclization of benzils to phenanthrene quinone compounds (2.6a-g).



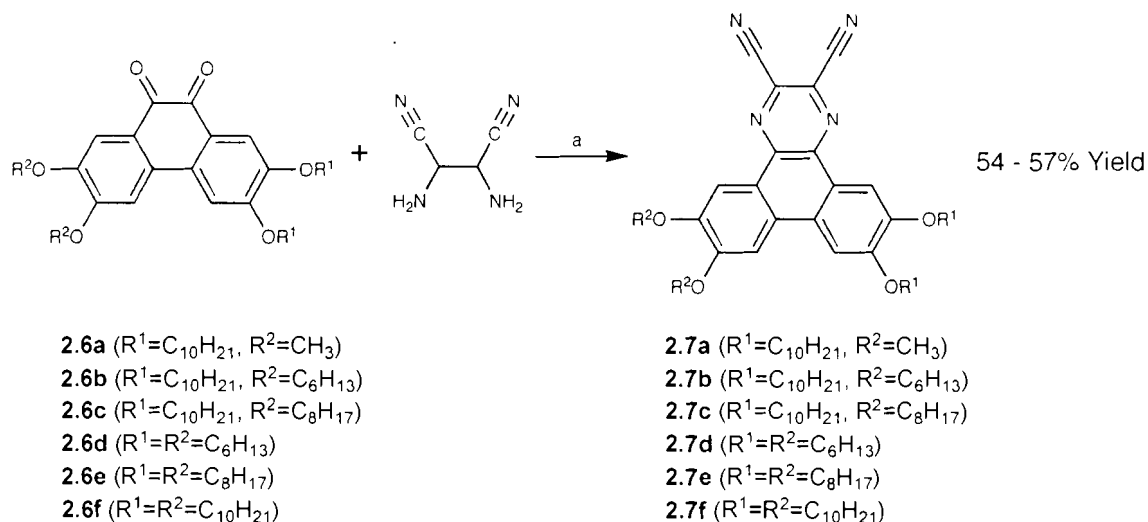
Reagents and conditions. a) VOF_3 , $BF_3 \cdot Et_2O$, CH_2Cl_2 .

2.3 Tetraalkoxy-Dicyanodibenzoquinoxaline

Previously, Mohr and Ohta have reported that the columnar phase of the dicyanodibenzoquinoxaline derivative (**2.7f**) had a remarkably broad temperature range (72 - 256 °C), making analogues of this compounds attractive candidates for device applications.⁸⁴ However, for technological applications, lower melting and clearing temperatures are generally required. Room temperature liquid crystals are clearly desirable, which requires a lower melting point. Moreover, a

high clearing temperature makes device construction difficult, as liquid crystals are often processed from their isotropic states.⁹⁵ A high clearing temperature is often incompatible with device components that may decompose above 200 °C. Lowering the symmetry is one potential method that could be used to alter the temperatures. To this end, we examined a series of new dicyanodibenzoquinoxaline derivatives, (**2.7a-e**) that were accessible via a coupling reaction of the phenanthrene-9,10-diones **2.6a-f** with diaminomaleonitrile (Scheme 2.7).

Scheme 2.7: Synthesis of dicyanodibenzoquinoxaline derivatives (2.7a-f).



Reagents and conditions. a) AcOH, reflux. Compound **2.7f** was previously reported.⁸⁴

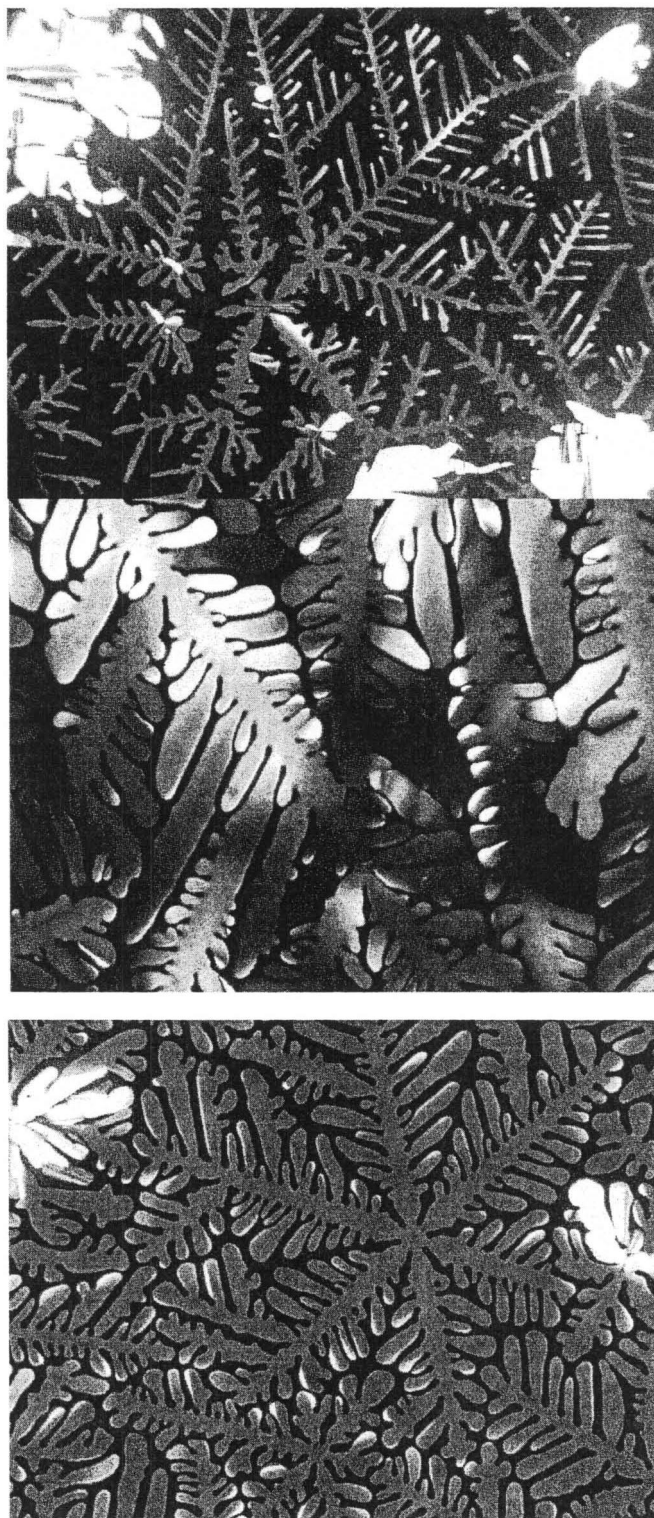
The phase behaviour of the coupled compounds **2.7a-f** was examined using polarized optical microscopy (POM), X-ray diffraction (XRD) and differential scanning calorimetry (DSC). With the exception of the nonmesogenic derivative **2.7a**, all members are liquid crystalline over broad temperatures ranges (Table 2.3). These liquid crystals exhibit the characteristic dendritic textures of

columnar hexagonal phases when viewed by POM (Figure 2.1). The XRD patterns of these mesophases exhibit peaks that index to the (100) and (110) spacing of a two dimensional hexagonal lattice and a broad peak at approximately 3.5 Å, corresponding to the π - π stacking distance within a column. On the basis of these observations, the liquid crystals **7b-f** were identified as ordered columnar hexagonal phases (Col_{ho}).

Table 2.3: Phase behaviour of 6,7,10,11-tetraalkoxy-dibenzo[f,h]quinoxaline-2,3-dicarbonitrile derivatives (2.7a-f).

Compound	Phase	$T_i/^\circ\text{C}$ ($\Delta H/J\text{ g}^{-1}$)	Phase	Lattice Const.
2.7a $R^1=C_{10}H_{21}, R^2=CH_3$	Cr	265.1 (4.8)	I	
2.7b $R^1=C_{10}H_{21}, R^2=C_6H_{13}$	Cr	37.8 (56.0)	Col _{ho}	a = 22.1 Å
2.7c $C_{10}H_{21}, R^2=C_8H_{17}$	Cr	56.2 (62.2)	Col _{ho}	a = 23.3 Å
2.7d $R^1=R^2=C_6H_{13}$	Cr	72.4 (75.3)	Col _{ho}	a = 20.2 Å
2.7e $R^1=R^2=C_8H_{17}$	Cr	85.7 (38.2)	Col _{ho}	a = 21.5 Å
2.7f $R^1=R^2=C_{10}H_{21}$	Cr	71.6 (10.5)	Col _{ho}	a = 22.7 Å

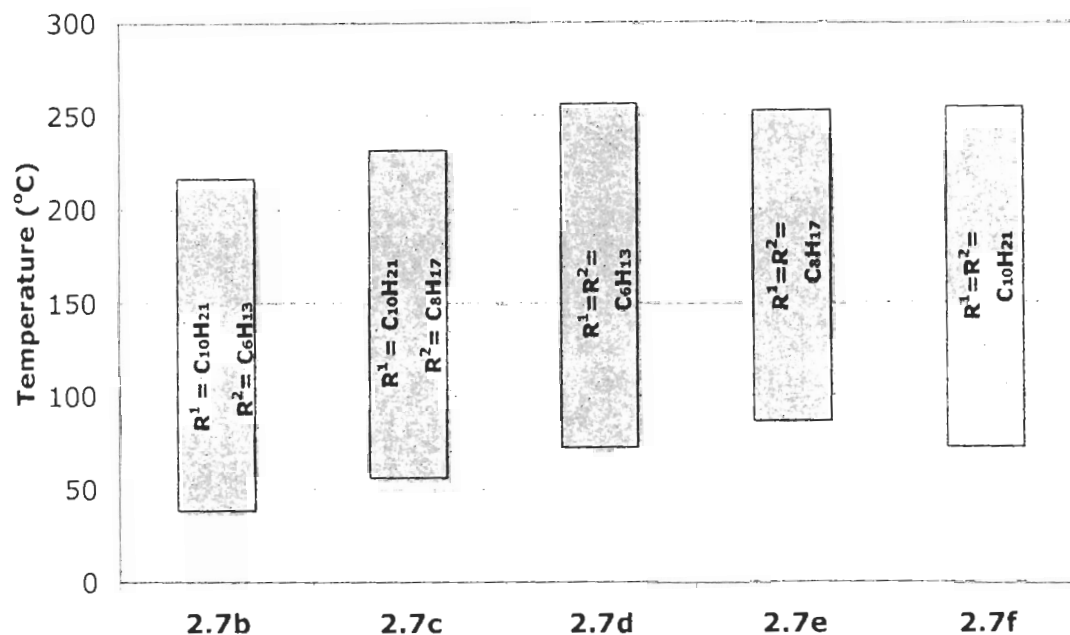
Figure 2.1: Representative polarized optical micrographs of compounds (2.7b-f).



Compound **2.7b** at 210 °C (top), **2.7c** at 230 °C (middle), **2.7e** at 250 °C (bottom). 200x magnification

Breaking the symmetry in this class of mesogens appears to have a dramatic effect on their observed mesophase stabilities. While the symmetrical dicyanodibenzoquinoline derivatives **2.7d-f** exhibit columnar phases over similar temperature ranges, both the melting and clearing temperatures of the unsymmetrical mesogens **2.7b** and **2.7c** are appreciably lowered. This results in phase ranges that are of similar breadth to those of the parent compounds, but that are shifted to lower temperatures by 20-40 °C depending on the chain lengths. This effect becomes more pronounced as the disparity between the chain lengths, R^1 and R^2 , increases. It should be noted that compounds **2.7b** and **2.7e** are constitutional isomers, yet both the melting and clearing temperatures are depressed for the unsymmetrical analogue (Figure 2.2). Depression of the phase transitions is consistent with less efficient packing of the columnar structures in the case of the unsymmetrical derivatives and also with Carnelley's rule.

Figure 2.2: Phase ranges of mesogenic compounds (2.7b-f).



In the case of the dimethoxy compound **2.7a**, mesophase formation is not observed, which appears to indicate that more than two alkoxy chains greater than a single carbon are needed to allow liquid crystalline self-assembly.

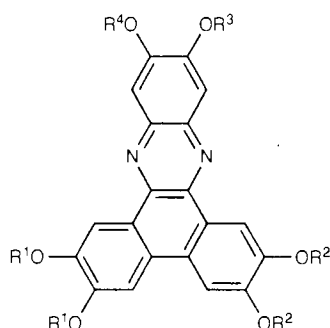
2.4 Hexaalkoxy-Dibenzo[a,c]phenazine Derivatives

Although the dicyano-dibenzoquinoxalines (**2.7a-f**) have wide liquid crystal phase ranges, they are not typical mesogenic systems, since they have alkoxy chains on only two sides of the molecule and most likely adopt an antiparallel (antiferroelectric) ordering, as will be discussed in greater detail later in this thesis (Chapter 4). 2,3,6,7,11,12-Hexaalkoxy-dibenzo[a,c]phenazine derivatives in contrast, have structures that are more similar to hexaalkoxytriphenylenes and a broad array of such derivatives can be examined (Figure 2.3). These

derivatives were prepared from the condensation of 3,4-dialkoxy-1,2-phenylenediamines and provide an opportunity for altering the position of chains present, and therefore the molecular symmetry.

The sheer number of mesogens that can be readily prepared in this series is enormous, since m diamines and n diones could afford $m \cdot n$ derivatives. Excluding the combination of unsymmetrical diones with unsymmetrical diamines, which would yield multiple regioisomers, there are 34 compounds available theoretically from the 6 diones and 7 diamines that were prepared. 17 derivatives were prepared, in order to specifically probe the effects of chain lengths and molecular symmetry. In many cases, we targeted sets of isomeric derivatives, i.e. two or more compounds with the same total number of carbons in the flexible alkyl chains, but which differed in their overall molecular symmetry.

Figure 2.3: 2,3,6,7,11,12-Hexalkoxy-dibenzo[a,c]phenazine derivatives.

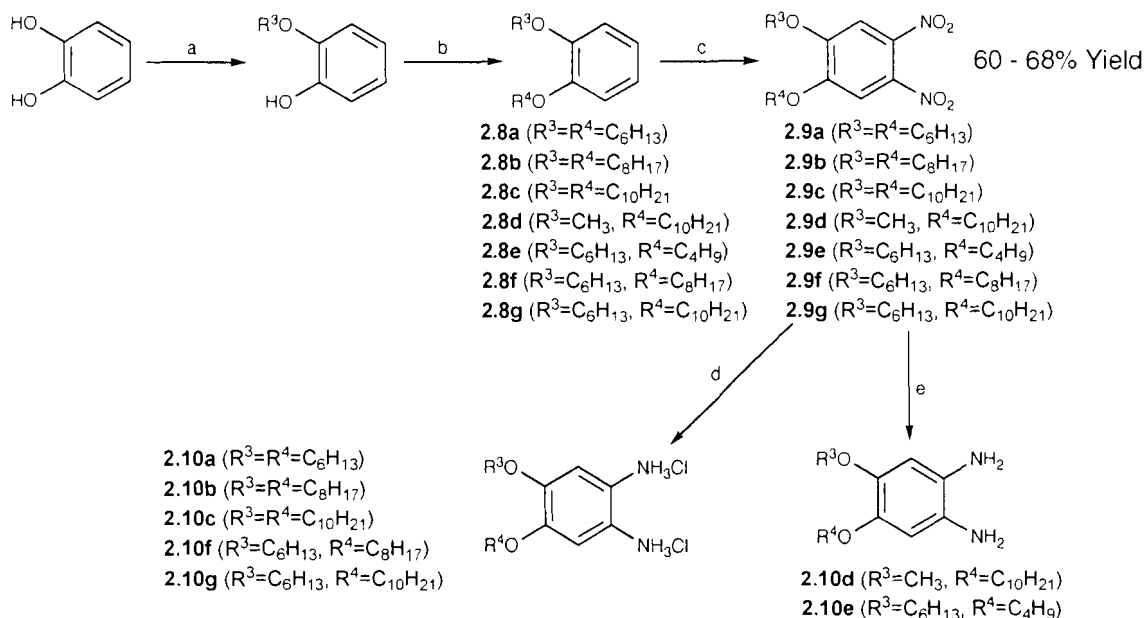


2.4.1 Preparation of 4,5-Alkoxy-1,2-phenylenediamines

4,5-Alkoxy-1,2-phenylenediamines were prepared using the route shown below (Scheme 2.8). Catechol was first alkylated with the appropriate alkyl-bromide. The resulting dialkoxy benzenes (**2.8a-g**) were then dinitrated in concentrated nitric acid (**2.9a-g**). Initial attempts to reduce compounds **2.9a-c**

and **2.9f-g** using palladium on carbon and hydrazine produced white solids that quickly decomposed. Efforts to characterize these solids, or to immediately use these materials in a coupling reaction were unsuccessful. Reduction using stannous chloride in ethanol produced the same result. It was finally found that after reduction using stannous chloride and addition of excess concentrated HCl caused the salt of the diamine to precipitate, stabilizing this compound towards oxidation. For compounds with chains shorter than six carbons, (**2.9d-e**), addition of HCl does not precipitate a salt, so reduction using palladium on carbon and hydrazine must be used. Great pains had to be taken to use the unstable diamine as quickly as possible, keeping them away from oxygen and using them directly in the next step.

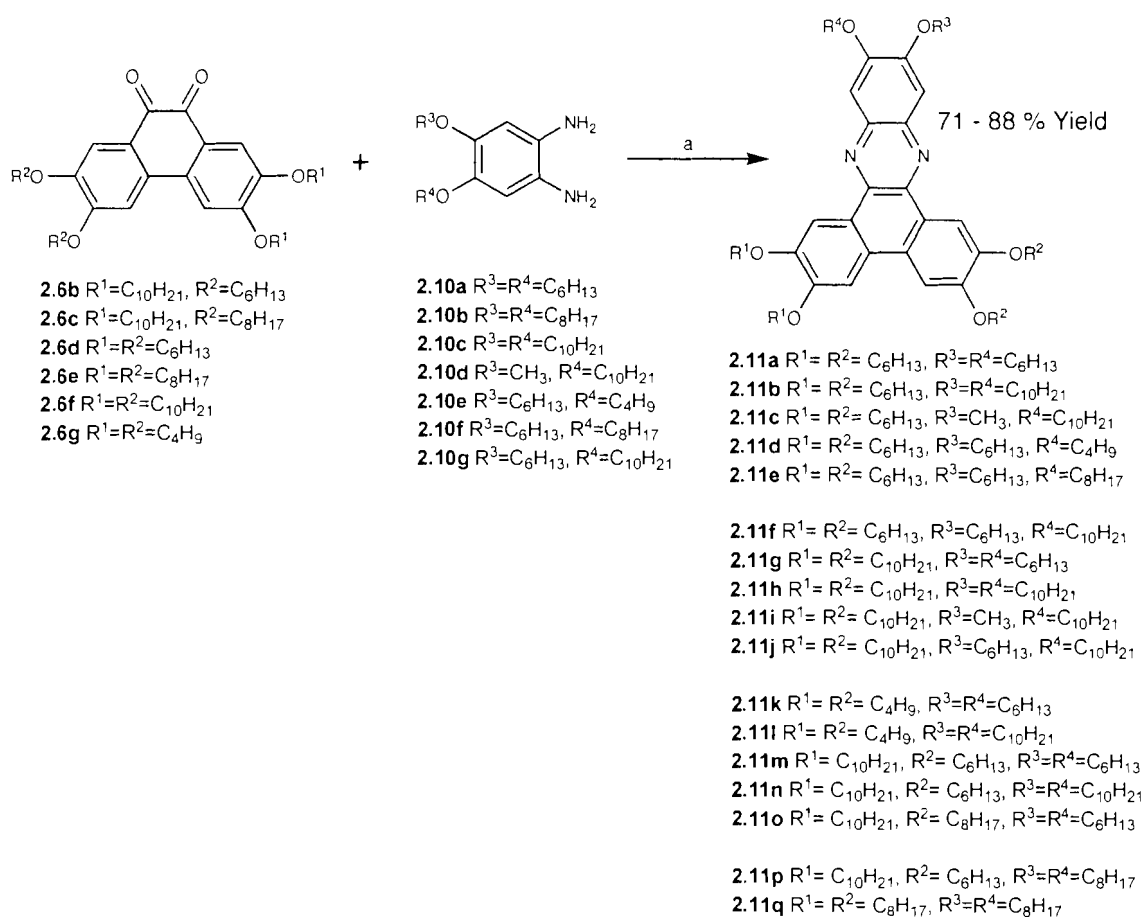
Scheme 2.8: Synthesis of 1,2-dialkoxy-4-5-diaminobenzenes.



Reagents and conditions. a) BrC_nH_{2n+1} , K_2CO_3 , DMF, b) BrC_nH_{2n+1} , K_2CO_3 , DMF, c) HNO_3 , d) $SnCl_2$, HCl, EtOH, e) EtOH, Pd/C, N_2H_4 .

The hydrochloride salts (**2.10a-c** and **2.10f-g**) and free amines (**2.10d-e**), **2.10a-g** were condensed with phenanthrene quinones **2.6a-g** to afford phenazine derivatives **2.11a-q** (Scheme 2.9). The salts were condensed in the presence of sodium acetate and the free amines were condensed in the presence of acetic acid.

Scheme 2.9: Condensation synthesis of compounds (2.11a-q).



Reagents and conditions. a) EtOH and AcOH or CH₃COONa.

The phase behaviours of the products **2.11a-q** were examined by polarized optical microscopy (POM), differential scanning calorimetry (DSC) and variable temperature X-ray diffraction (XRD) experiments, the results of which

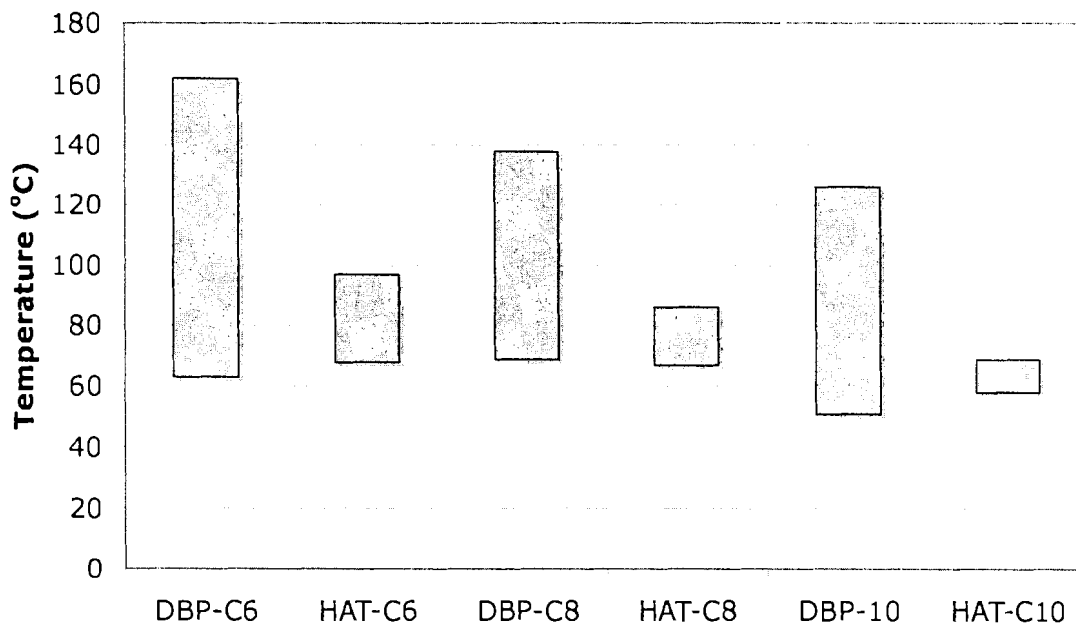
are summarized below (Table 2.4). Compounds **2.11c**, **i** and **I** failed to exhibit any liquid crystalline phases, but instead melted directly from crystalline solids to isotropic liquids. Derivative **2.11b** formed a liquid crystal phase upon cooling from the isotropic state. On the basis of the dendritic texture observed by POM, this phase was identified as a rectangular columnar phase (Col_r). XRD experiments confirmed this assignment, showing two intense peaks in the low angle region. All of the other compounds in series **2.11** formed hexagonal columnar phases.

Table 2.4: Phase behaviour of dibenzo[a,c]phenazine derivatives (2.11a-q).

Compound	Phase	$T_i/^{\circ}\text{C}$ ($\Delta H/\text{J g}^{-1}$)	Phase	Lattice Const.
2.11a	Cr $\xrightleftharpoons[23.5 (-22.1)]{62.9 (38.2)}$	Col _{ho} $\xrightleftharpoons[145.7 (-3.1)]{161.5 (3.2)}$	I	a = 22.7 Å
2.11b	Cr $\xrightleftharpoons[82.7 (27.1)]{82.7 (27.1)}$	Col _{ho} $\xrightleftharpoons[105.4 (-2.4)]{112.6 (2.5)}$	I	a = 51.2 Å b = 20.9 Å
2.11c	Cr $\xrightleftharpoons[87.2 (-55.5)]{119.3 (55.2)}$	I		
2.11d	Cr $\xrightleftharpoons[28.1 (-31.9)]{76.2 (53.3)}$	Col _{ho} $\xrightleftharpoons[142.8 (-3.8)]{165.2 (3.1)}$	I	a = 21.4 Å
2.11e	Cr $\xrightleftharpoons[88.1 (-39.3)]{146.2 (29.3)}$	Col _{ho} $\xrightleftharpoons[158.9 (-3.2)]{172.8 (2.1)}$	I	a = 21.5 Å
2.11f	Cr $\xrightleftharpoons[32.2 (-38.4)]{34.5 (44.3)}$	Col _{ho} $\xrightleftharpoons[122.0 (-4.8)]{129.1 (5.2)}$	I	a = 21.8 Å
2.11g	Cr $\xrightleftharpoons[17.2 (-39.7)]{72.8 (55.2)}$	Col _{ho} $\xrightleftharpoons[123.9 (-2.0)]{128.8 (2.4)}$	I	a = 25.9 Å
2.11h	Cr $\xrightleftharpoons[14.3 (-38.2)]{50.6 (44.1)}$	Col _{ho} $\xrightleftharpoons[114.1 (-3.9)]{126.3 (4.2)}$	I	a = 27.6 Å
2.11i	Cr ₁ $\xrightleftharpoons[73.5 (-69.3)]{89.7 (0.7)}$	Cr ₂ $\xrightleftharpoons[115.6 (6.24)]{115.6 (6.24)}$	Cr ₃ $\xrightleftharpoons[121.3 (37.7)]{121.3 (37.7)}$	I
2.11j	Cr $\xrightleftharpoons[49.9 (39.4)]{49.9 (39.4)}$	Col _{ho} $\xrightleftharpoons[120.8 (-3.0)]{124.2 (3.3)}$	I	a = 23.7 Å
2.11k	Cr $\xrightleftharpoons[48.0 (-49.2)]{91.4 (51.1)}$	Col _{ho} $\xrightleftharpoons[154.5 (-5.7)]{162.1 (5.6)}$	I	a = 19.9 Å
2.11l	Cr $\xrightleftharpoons[72.1 (-76.3)]{97.2 (78.2)}$	I		
2.11m	Cr $\xrightleftharpoons[46.7 (37.6)]{46.7 (37.6)}$	Col _{ho} $\xrightleftharpoons[134.2 (-3.5)]{137.2 (3.4)}$	I	a = 23.9 Å
2.11n	Cr $\xrightleftharpoons[24.1 (-47.1)]{50.2 (78.3)}$	Col _{ho} $\xrightleftharpoons[120.1 (-3.1)]{124.1 (3.4)}$	I	a = 25.2 Å
2.11o	Cr $\xrightleftharpoons[72.0 (65.7)]{72.0 (65.7)}$	Col _{ho} $\xrightleftharpoons[132.2 (-2.8)]{135.2 (3.2)}$	I	a = 23.6 Å
2.11p	Cr $\xrightleftharpoons[62.7 (49.7)]{62.7 (49.7)}$	Col _{ho} $\xrightleftharpoons[122.3 (-2.0)]{169.4 (2.2)}$	I	a = 23.5 Å
2.11q	Cr $\xrightleftharpoons[28.8 (-40.1)]{68.2 (42.1)}$	Col _{ho} $\xrightleftharpoons[126.4 (-3.4)]{138.3 (4.2)}$	I	a = 23.5 Å

Analysis of the phase data of this series of compounds showed some remarkable trends. Compounds **2.11a**, **h** and **q** represent derivatives in which all six alkoxy chains are identical. As noted for other discotic mesogens, increasing the length of chains leads to a depression of clearing temperature. A similar trend is commonly observed for a variety of discotic mesogens, including previously published data on triphenylene derivatives of similar size.²¹ When this series is directly compared to that of analogous triphenylenes, it was shown that like-substituted dibenzophenazines have a much broader phase range (Figure 2.4). This trend could be due to the increase in core size, as will be discussed later in Chapter 3.

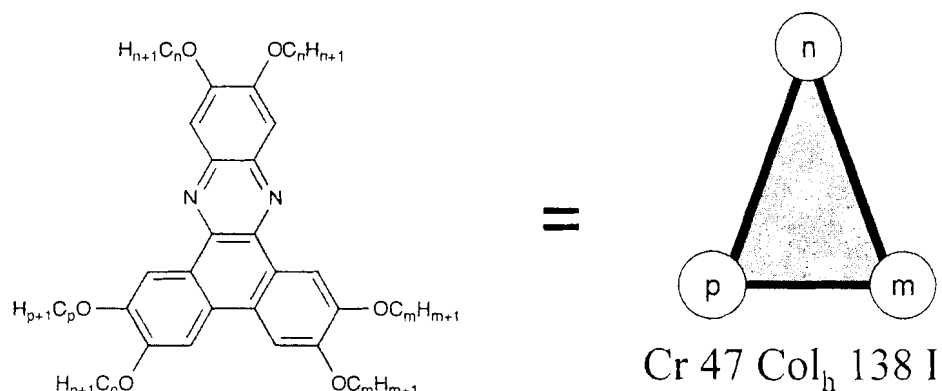
Figure 2.4: Comparison of dibenzo[a,c]phenazine compounds (2.11) and previously reported 2,3,6,7,10,11-hexaalkoxytriphenylenes.



DBP is the dibenzo[a,c]phenazine compound from series **2.11** (DBP-C6 = **2.11a**, DBP-C8 = **2.11q**, DBP-C10 = **2.11h**). HAT is the 2,3,6,7,10,11-hexaalkoxytriphenylene⁹⁶, substituted symmetrically, bearing C₆H₁₃ (HAT-C6), C₈H₁₇ (HAT-C8) or C₁₀H₂₁ (HAT-10) chains.

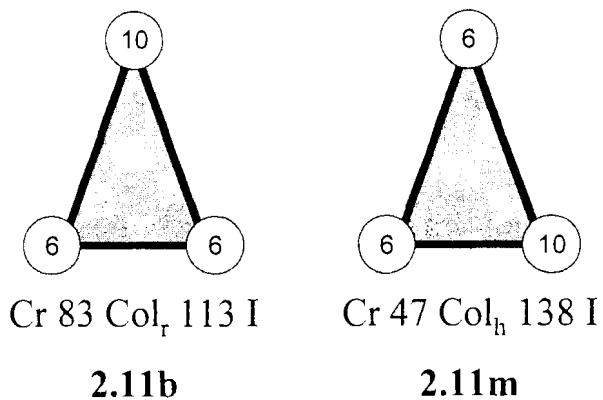
In previous papers, researchers have suggested that unsymmetrical molecular shape is disadvantageous for columnar mesophase formation.^{64,73,74} Following Carnelley's rule, we decided to analyze differentially substituted hexaalkoxy discotic mesogens by comparing constitutional isomers. For these reasons, the derivatives are grouped according to the total number of carbon atoms in the pendant chains (Figure 2.6 - Figure 2.8) using the graphical notation shown below (Figure 2.5).

Figure 2.5: Notation for dibenzo[a,c]phenazine derivatives.



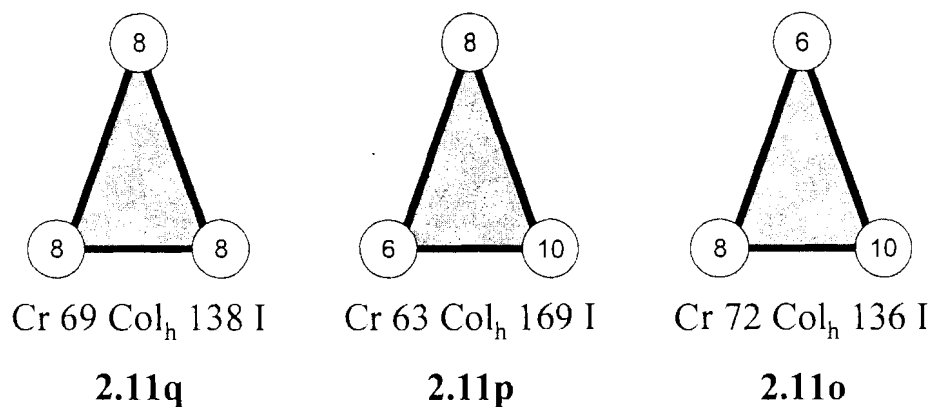
The notation shown on the lower right denotes a mesogen that is a crystalline solid until 47 °C, a columnar hexagonal liquid crystal until 138 °C and an isotropic liquid above that temperature. The values n , p and m denote the number of carbons in the side chains. Note that due to lower symmetry of the core, a derivative in which $p=m \neq n$ is higher symmetry than in which $p=n \neq m$.

Figure 2.6: Dibenzo[a,c]phenazine with $p+m+n = 22$.



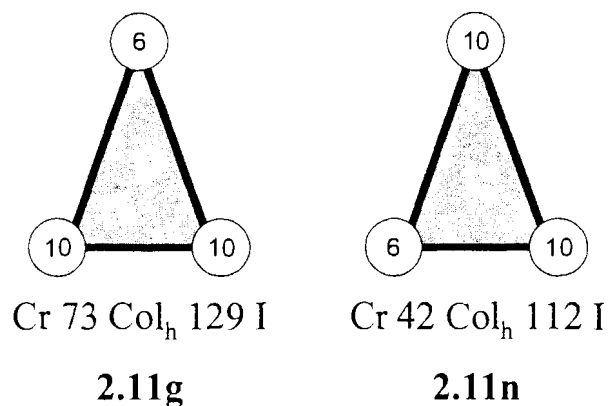
$2(n + m + p) = 44$. **2.11b** has the molecular symmetry C_{2V} , **2.11m** is C_s

Figure 2.7: Dibenzo[a,c]phenazine with $p+m+n = 24$.



$2(n + m + p) = 48$. **2.11q** has the molecular symmetry C_{2V} , **2.11p** and **2.11o** have the symmetry C_s

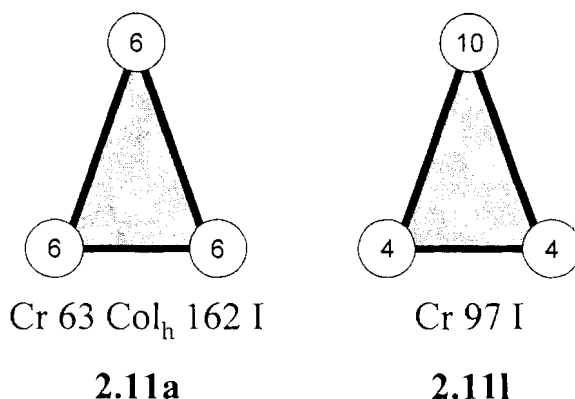
Figure 2.8: Dibenzo[a,c]phenazine with $p+m+n = 26$.



$2(n + m + p) = 52$. **2.11g** has the molecular symmetry C_{2V} , **2.11n** is C_s

As shown in the series with $p+m+n = 24$, there are three comparable isomers, with **2.11q** ($m = n = p = 8$) having the highest symmetry, **2.11p** (6.8.10) has a depressed T_m , but not T_c . For **2.11o** (8.10.6), the molecule has a depressed T_c but not T_m (Figure 2.7). Notably, there is a larger difference between the phase behaviour of **2.11p** and **2.11o**, which have the same symmetry than between **2.11q** and **2.11o**, which have different symmetry. This suggests that factors other than symmetry, such as shape, play a predominant role, at least in the case of T_c . A similar observation can be made in the case of the series shown in Figure 2.9, compounds **2.11a** and **2.11l**, both have the same symmetry but have dramatically different phase behaviour.

Figure 2.9: Dibenzo[a,c]phenazine isomers of the same symmetry.



Both of the above molecules have the point symmetry C_{2v}

In the four cases where isomers of different symmetry could be compared, the melting point was always lower for the lower symmetry analogues, whereas the clearing temperature of the lower symmetry derivative was only depressed in two out of four cases. These trends would seem to indicate that symmetry has

only a small role in determining phase transitions between liquid phases, although this is a limited data set that needs to be expanded. A stronger relationship appears to exist for solid to liquid crystal transitions.

Since only a weak relationship between symmetry of the dibenzo[a,c]phenazine and the mesophase stability in series **2.11**, it was decided to re-examine the trends obtained by other researchers working with symmetric and unsymmetrical triphenylenes.

The data for the compounds previously reported by Cross and co-workers were re-examined using the same approach described above, with the constitutional isomers grouped together below (Figure 2.11 - Figure 2.16)⁷³ using the notation shown in Figure 2.10.

Figure 2.10: Structure and notation for hexaalkoxytriphenylene series HAT(p.n.m).

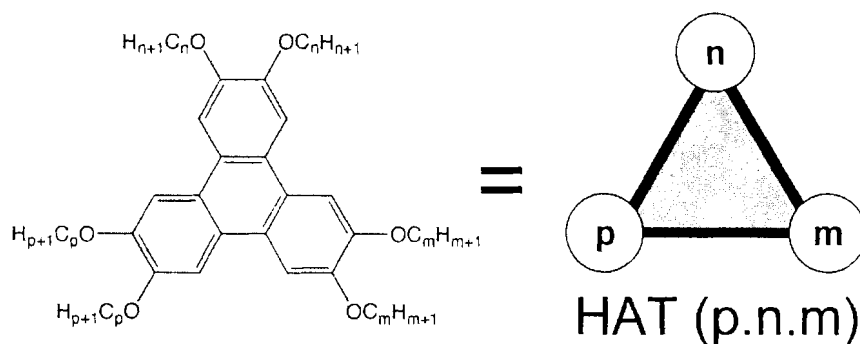


Figure 2.11: HAT with $p+m+n = 18$.

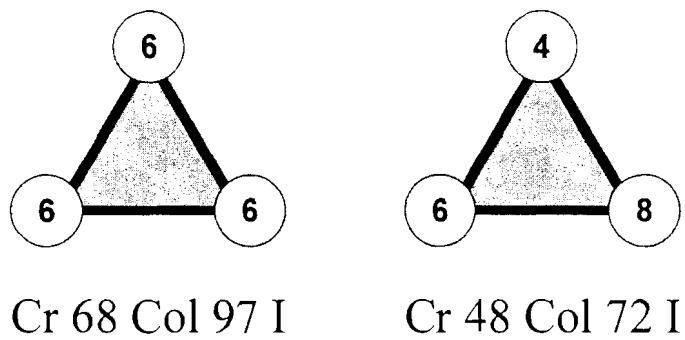


Figure 2.12: HAT with $p+m+n = 22$.

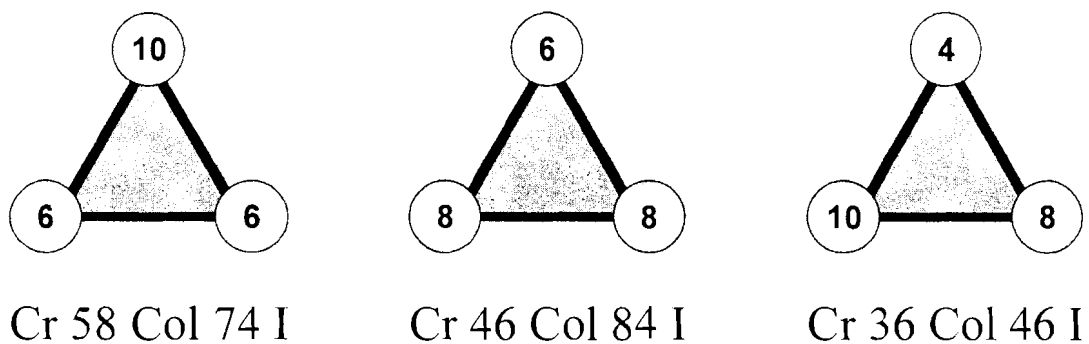


Figure 2.13: HAT with $p+m+n = 24$.

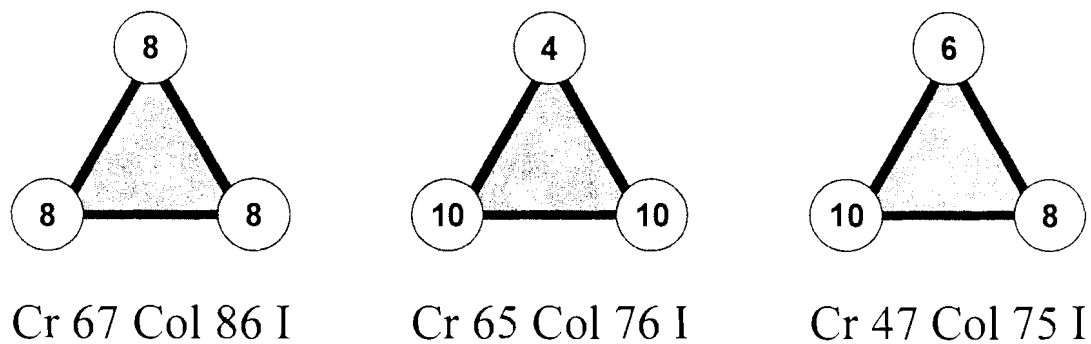
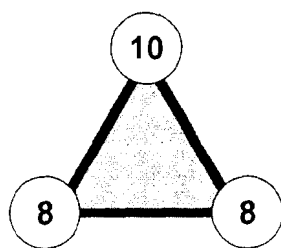
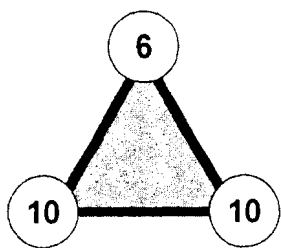


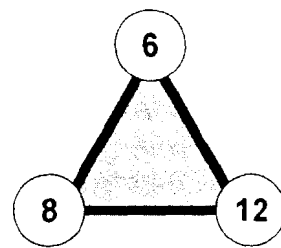
Figure 2.14: HAT with $p+m+n = 26$.



Cr 48 Col 73 I

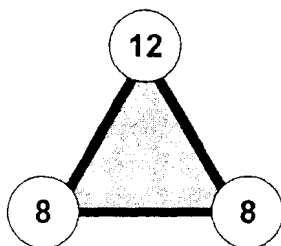


Cr 44 Col 72 I

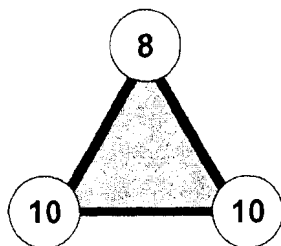


Cr 39 Col 75 I

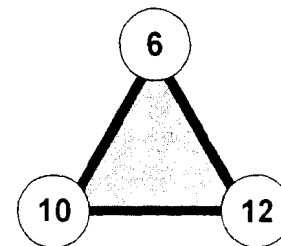
Figure 2.15: HAT with $p+m+n = 28$.



Cr 51 Col 61 I

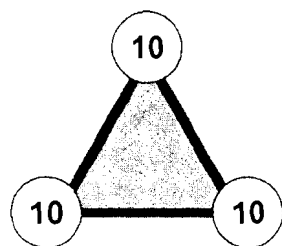


Cr 60 Col 86 I

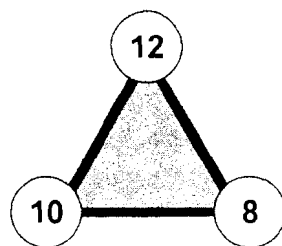


Cr 43 Col 51 I

Figure 2.16: HAT with $p+m+n = 30$.



Cr 58 Col 69 I



Cr 47 Col 65 I

With the exception of the isomers with $p+m+n = 26$ (Figure 2.14), these HAT comparisons appear to show that the lower symmetry analogues have a depressed T_c and T_m , relative to the symmetrical isomers. In the series $p+m+n = 26$, there are two exceptions, since the lowest symmetry derivative (8.6.12) actually has a higher T_c than either of the more symmetrical compounds. It is

unclear why this one set of compounds does follow the trend. However, the melting point for this compound was significantly lower.

It is also possible to synthesize triphenylenes with alternating pendant chains, as shown in series **HATb** (Figure 2.17 and Figure 2.18). When constitutional isomers, prepared previously by Sakashita⁹⁶ are compared to the alternating chain analogues, all of the lower symmetry isomers were found to have depressed T_c and T_m values.⁶⁴

Figure 2.17: Structure and notation for hexaalkoxytriphenylene series HATb.

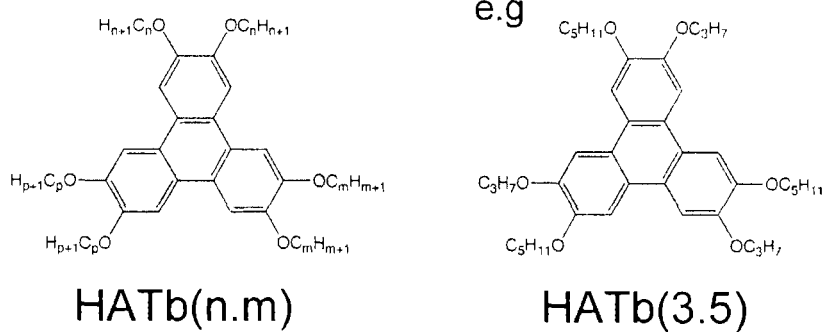
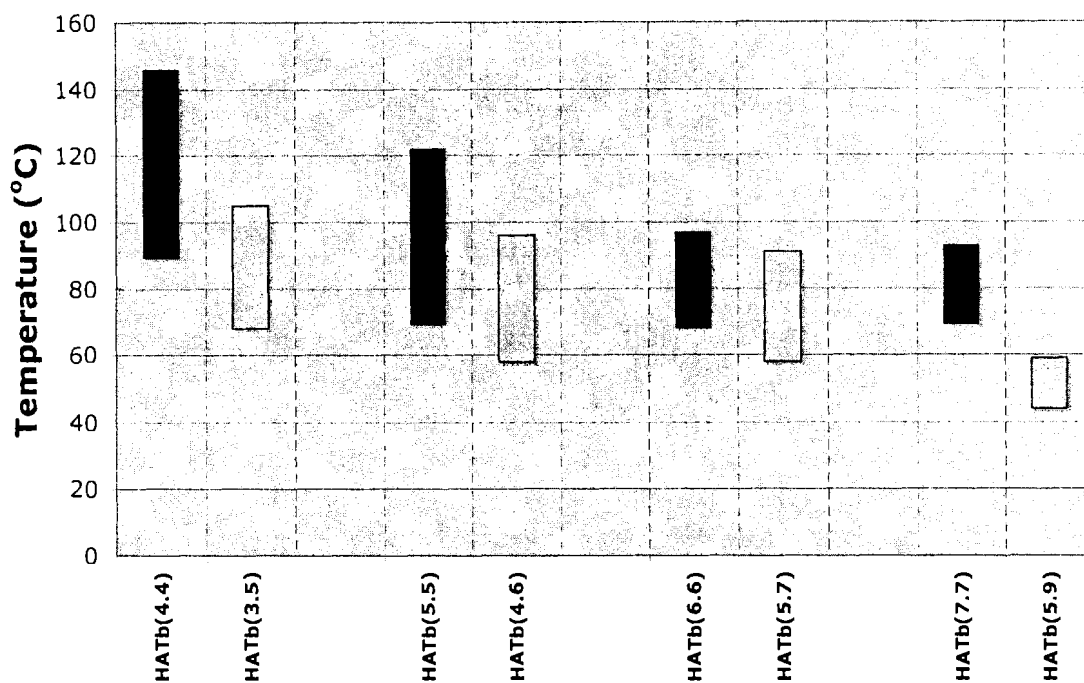


Figure 2.18: Triphenylene series HATb.



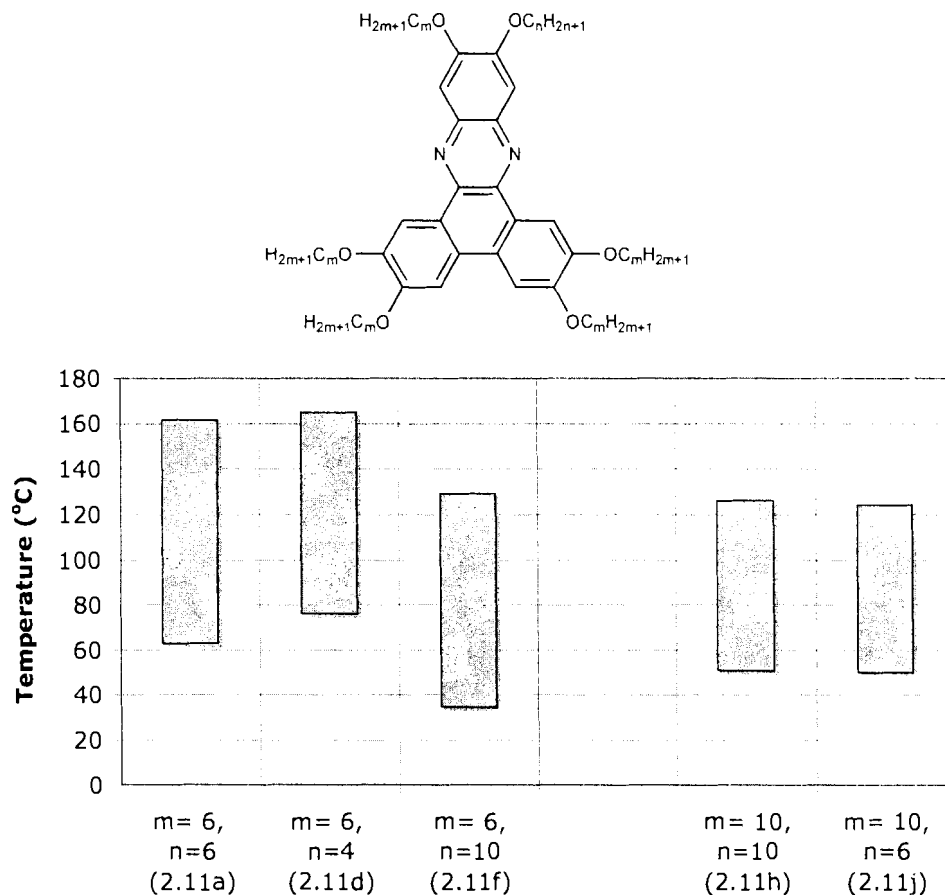
Comparison of Hexaalkoxytriphenylene compounds, adapted from Allen *et al.* and Sakashita *et al.*^{64,96}

2.5 'Sore-Thumb' Effect

It was also possible to prepare diamines with two different alkoxy chains, permitting us to assemble mesogens in which five chains are identical and the sixth is different (Figure 2.19). Two subsequent alkylations of 1,2-dihydroxybenzene, followed by dinitration and reduction afforded diamines that are suitable for coupling with a phenanthrene quinone. In this manner, three such derivatives were prepared (**2.11d,f** and **j**). These were compared to the corresponding compounds in which all six chains were of equal length (**2.11a** and **h**). The results, shown below suggest that reducing the number of carbons on the sixth alkoxy chain has little effect on phase transitions, since both **2.11a** and **2.11d** have fairly similar T_c values and **2.11h** and **2.11j** have almost identical

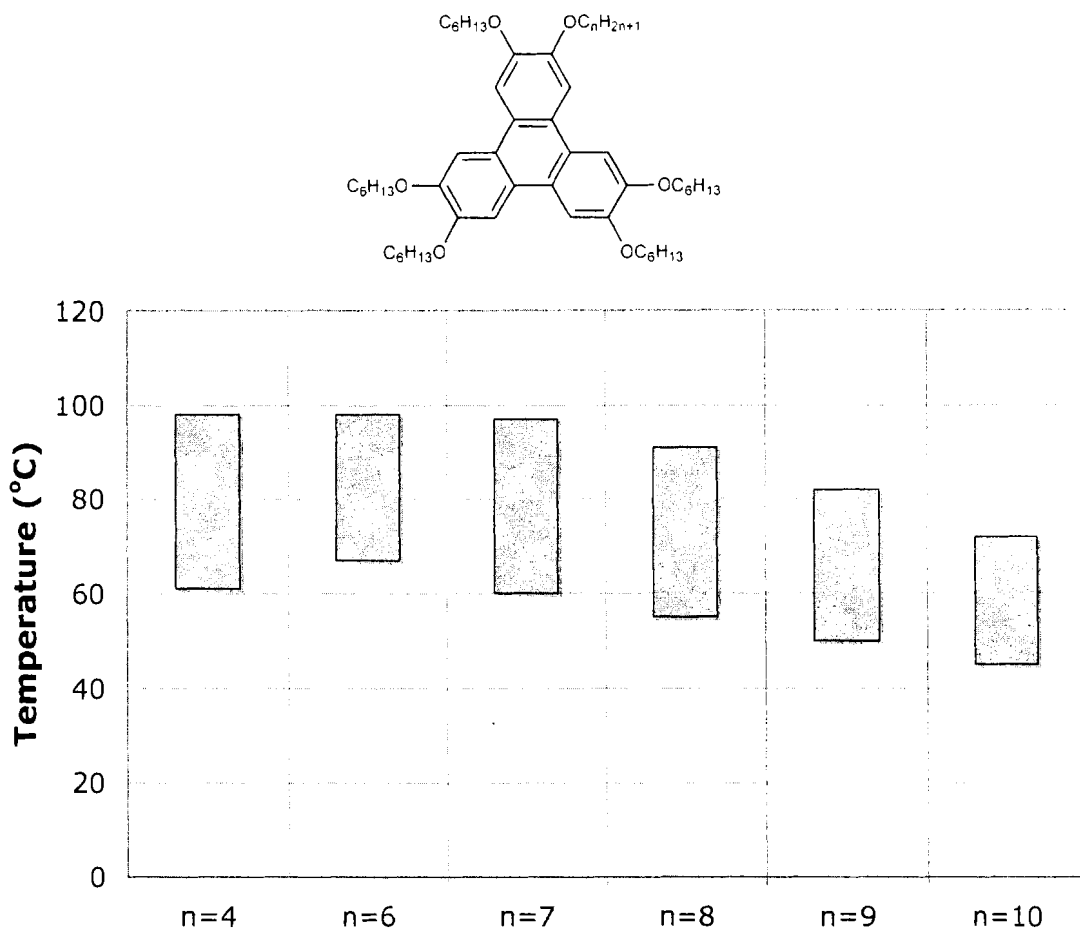
T_m and T_c values (Figure 2.19). In contrast, when one of the chains is longer than the other five (**2.11f**) both the T_c and T_m are appreciably depressed (32 °C for T_c , 28 °C for T_m) relative to the values for **2.11a**.

Figure 2.19: Phase behaviour from altering one alkoxy-chain.



A similar trend has been observed by Zuilhof and co-workers, who synthesized and characterized hexaalkoxytriphenylene compounds, in which one chain differed from the others (Figure 2.20).⁷⁴ A single shorter chain leads to an increase in phase breadth and only a slight depression of clearing temperatures. Increasing a single chain beyond that of the other alkoxy chains causes subsequent depression of the T_c and T_m .

Figure 2.20: Hexaalkoxytriphenylenes differing at one position.



Phase ranges reported by Zuilhof.⁷⁴

We have dubbed this the ‘sore-thumb effect.’ Increasing the sixth chain beyond that of the other five causes it to stick out ‘like a sore-thumb’, which presumably disrupts the crystalline and liquid crystalline packing, leading to lower phase transition temperatures. When the sixth chain is shorter than the other five chains, packing is less disrupted, resulting in smaller perturbation of T_m and T_c .

2.6 Summary

We have developed a convenient synthesis of unsymmetrical benzil and phenanthrene quinone derivatives that provides access to a broad array of

potential mesogens. Our preliminary investigations indicate that reducing the symmetry of the mesogen provides a practical method for shifting the phase transitions to lower temperatures, and as such is complementary to other strategies that have been developed for the modification of columnar phase behaviour.

Transitions from crystalline solids to columnar liquid crystal phases generally do appear to obey Carnelley's rule. In the systems we studied, only one example of the lower symmetry isomer exhibiting the higher melting point was found. Carnelley's rule does not appear to be as general for clearing temperatures. More than 20% of the isomer pairs that were investigated violated this rule. For this reason, Carnelley's rule may be termed better as a 'guide' with respect to liquid crystals.

2.7 Experimental^{*}

2.7.1 General Experimental

Compounds were characterized by 400 MHz ¹H-NMR and 100 MHz ¹³C-NMR (Bruker AMX-400 400 MHz spectrometer) or 500 MHz ¹H-NMR and 125 MHz ¹³C-NMR (Varian 500). Integrations of alkyl chain regions (0.9 – 2.5 ppm) are reported as approximate values. Mass spectrometry was carried out using a Perseptive Voyager-DE STR from PE Applied Biosystems with a nitrogen laser (337 nm) to desorb the ions from the source using 2,5-dihydroxybenzoic acid as the matrix (MALDI-TOF) or EI (70 eV) using a Hewlett Packard 5985 mass

^{*} Preliminary research into the synthesis of phenantherene quinone **2.6a-f** was performed by J. Babuin and N. Nyugen. Compounds **2.8e**, **2.8f**, **2.9e** and **2.9f** were synthesized and characterized by M. Rakotomalala.

spectrometer). Melting points of intermediates were determined using a Fisher Johns Melting Point Apparatus, and are uncorrected. Phase transition temperatures and enthalpies were investigated using differential scanning calorimetry (Perkins Elmer DSC 7, heating and cooling rate was $5^{\circ}\text{C min}^{-1}$). Texture analysis was carried out using polarised optical microscopy (Olympus BX50 microscope with crossed polarizers using a Linkam LTS350 heating stage). Compounds were heated at 10°C per minute, until an isotropic liquid was observed, and then cooled at 0.5°C per minute until textures formed. X-ray scattering experiments were conducted using a Rigaku R-Axis Rapid diffractometer equipped with a temperature controller. Microanalyses (C, H, N) were performed at Simon Fraser University by Mr. Miki Yang.

2.7.2 Experimental

3,3',4,4'-Tetrakis-decyloxy-benzil (2.1c)⁸⁶ A solution of 3,3',4,4' tetrakis-hydroxybenzil (1.633 g, 5.96 mmol) and 1-bromodecane (5.27 g, 23.8 mmol) in DMF (300 mL) was stirred for 15 minutes while being purged with N_2 . K_2CO_3 was added (3.29 g, 23.8 mmol) and the solution purged with N_2 for a further 15 minutes before stirring overnight at 70°C . The solution was allowed to cool, poured over 1000 mL ice, and vacuum filtered. The resultant solid was purified by column chromatography (silica gel, 10% ethyl acetate in hexanes) to yield **2.1c** (4.593 g, 92%), an off-white solid. $^1\text{H-NMR}$ (400 MHz) (CDCl_3) δ (ppm), 7.58 (d, 2H $J = 2$ Hz), 7.42 (dd, 2H $J = 2.0, 8$ Hz), 6.84 (d, 2H 8 Hz), 4.05 (t, 8H $J = 7$ Hz), 1.20-2.00 (m, ~64H), 0.80-1.00 (m, ~12H). $^{13}\text{C-NMR}$ (100 MHz) (CDCl_3) 194.1, 194.1, 155.2, 149.5, 146.3, 146.2, 126.3, 124.6, 115.1, 112.4, 112.3,

111.7, 111.1, 111.0, 69.5, 69.4, 69.3, 64.1, 63.2, 51.5, 33.0, 32.1, 32.0, 31.1, 29.8, 29.8, 29.7, 29.6, 29.6, 29.5, 29.5, 29.4, 29.4, 29.3, 29.1, 26.4, 26.2, 26.1, 26.0, 23.0, 22.9, 14.3. Mpt. (lit) 91-92°C (93 °C).⁸⁶ MALDI-TOF. calc. (found) 835 (835).

3,3',4,4'-Tetrakis-hexyloxybenzil (2.1a)⁹⁷ Synthesized from 3,3',4,4'-tetrakis-hydroxybenzil (2.32 g, 8.46 mmol) and 1-bromohexane (5.73 g, 34.7 mmol) in the manner described above to afford **2.1a** (4.60 g, 89%), an off-white solid. ¹H-NMR (400 MHz) (CDCl₃) δ(ppm), 7.56 (d, 2H *J* = 2 Hz), 7.43 (dd, 2H *J* = 2, 9 Hz), 6.87 (d, 2H *J* = 9 Hz), 4.05 (t, 8H *J* = 7 Hz), 1.20-2.00 (m, ~32H), 0.80-1.00 (m, ~12H). ¹³C-NMR (100 MHz) (CDCl₃) 194.2, 194.2, 194.0, 155.1, 155.1, 152.4, 149.4, 147.3, 126.9, 126.3, 126.2, 124.0, 115.2, 112.4, 112.3, 111.7, 111.2, 111.0, 77.5, 77.2, 77.0, 69.4, 69.3, 32.0, 31.8, 31.1, 29.5, 29.5, 29.4, 29.2, 29.1, 26.2, 26.1, 22.8, 14.3. Mpt. (lit) 97-99°C (97°C).⁹⁷ MALDI-TOF. calc. (found) 610 (610).

3,3',4,4'-Tetrakis-octyloxybenzil (2.1b)⁹⁷ Synthesized from 3,3',4,4'-tetrakis-hydroxybenzil (1.51 g, 5.51 mmol) and 1-bromooctane (4.99 g, 22.6 mmol) in the manner described above to afford **2.1b** (3.61 g, 91%), an off-white solid. ¹H-NMR (400 MHz) (CDCl₃) δ(ppm), 7.56 (d, 2H *J* = 2 Hz), 7.42 (dd, 2H *J* = 2.0, 8 Hz), 6.87 (d, 2H *J* = 9 Hz), 4.06 (t, 8H *J* = 7 Hz), 1.20-2.00 (m, ~48H), 0.80-1.00 (m, ~12H). ¹³C-NMR (100 MHz) (CDCl₃) 194.2, 194.2, 194.0, 155.1,

155.1, 152.4, 149.2, 147.0, 126.9, 126.3, 126.2, 124.0, 115.2, 112.4, 112.1, 111.6, 111.0, 111.0, 69.2, 31.9, 31.8, 31.1, 29.5, 29.4, 29.2, 26.2, 26.0, 22.2, 14.3. Mpt. (lit) 91-93°C (95°C).⁹⁷ MALDI-TOF. calc. (found) 723 (723).

3,3',4,4'-Tetrakis-butoxybenzil (2.1d)⁹⁷ Synthesized from 3,3',4,4' tetrakis-hydroxybenzil (1.11 g, 4.05 mmol) and 1-bromobutane (2.89 g, 16.6 mmol) in the manner described above to afford **2.1d** (1.78 g, 88%), an off-white solid. ¹H-NMR (400 MHz) (CDCl₃) δ(ppm), 7.57 (d, 2H *J* = 2 Hz), 7.44 (dd, 2H *J* = 2, 8 Hz), 6.86 (d, 2H *J* = 9 Hz), 4.05 (t, 8H *J* = 7 Hz), 1.88-0.96 (m, ~28H). ¹³C-NMR (100 MHz) (CDCl₃) δ(ppm). 155.2, 149.5, 149.5, 149.4, 126.4, 126.3, 126.3, 126.3, 126.3, 112.5, 111.8, 77.4, 77.2, 76.9, 69.1, 69.0, 31.3, 31.1, 29.9, 19.4, 19.3, 14.0, 14.0. Elemental analysis (%): calc. (found) for C₃₀H₄₂O₆. C, 72.26(72.36); H, 8.49(8.62). Maldi-TOF. calc. (found) 498.30 (500).

1,2-Didecyloxy-4-iodobenzene (2.2d) A solution of 1,2-didecyloxybenzene (0.50 g, 1.28 mmol) and iodine (0.17 g, 0.67 mmol) in glacial acetic acid (15 mL), water (5 mL) and sulphuric acid (0.4 mL) was heated to 40°C and iodic acid (0.025 g, 0.14 mmol) was added. The solution was stirred at 40°C for 1 hour at which time a second portion of iodic acid (0.025 g, 0.14 mmol) was added. After another hour, a third portion of 0.025 g iodic acid was added. The solution was then allowed to stir a further 1.5 hours at 40°C. Upon cooling the solution was added to water (30 mL) and extracted with diethyl ether (3 x 25 mL).

The combined ether extracts were washed with aqueous 50 mL Na₂CO₃, 50 mL brine, dried (MgSO₄) and the solvent removed under reduced pressure. The resultant product was recrystallized from ethanol to afford 2.2d (0.23 g, 68%), an off-white solid. ¹H-NMR (400 MHz) (CDCl₃) δ(ppm), 7.19 (dd, 1H *J* = 2, 9 Hz), 7.13 (d, 1H *J* = 2 Hz), 6.58 (d, 1H *J* = 9 Hz), 3.97 (t, 4H *J* = 7 Hz), 1.20-2.00 (m, ~32H), 0.80-1.03 (m, 6H). Elemental analysis (%): calc. (found) for C₂₆H₄₅I₂O₂. C, 60.46 (60.58); H, 8.78 (8.65). Mpt. 38-39°C

4-Iodo-1,2-dimethoxybenzene (2.2a)⁹⁸ Synthesized from 1,2-dimethoxybenzene (4.00 g, 29.3 mmol) in the manner described above to afford **2.2a** (5.01 g, 65%) as a red liquid product. ¹H-NMR (400 MHz) (CDCl₃) δ(ppm), 7.19 (dd, 1H *J* = 2, 9 Hz), 7.14 (d, 1H *J* = 2 Hz), 6.65 (d, 1H *J* = 9 Hz), 3.84 (s, 6H). EI-MS calc. (found) 264 (264).

1,2-Dihexyloxy-4-iodobenzene (2.2b)²⁸ was synthesized from 1,2-dihexyloxybenzene (2.00 g, 7.18 mmol) in the manner described above to afford **2.2b** (1.95 g, 67%), as a red liquid. ¹H-NMR (400 MHz) (CDCl₃) δ(ppm) 7.20 (dd, 1H *J* = 2, 9 Hz), 7.13 (d, 1H *J* = 2 Hz), 6.58 (d, 1H *J* = 9 Hz), 4.03 (t, 4H *J* = 7 Hz), 1.20-2.01 (m, 16H), 0.83-1.05 (m, 6H). EI-MS calc. (found) 404 (404).

4-Iodo-1,2-dioctyloxybenzene (2.2c)²⁸ Synthesized from 1,2-dioctyloxybenzene (2.00 g, 5.98 mmol) in the manner described above to afford a white

solid product (1.98 g, 72%). ¹H-NMR (400 MHz) (CDCl₃) δ(ppm), 7.19 (dd, 1H *J* = 2, 9 Hz), 7.13 (d, 1H *J* = 2 Hz), 6.62 (d, 1H *J* = 9 Hz), 3.98 (t, 4H *J* = 7 Hz), 1.20-2.00 (m, 24H), 0.80-1.01 (m, 6H). EI-MS calc. (found) 460 (460). Mpt. 36-38°C.

1,2-Didecyloxy-4-ethynylbenzene (2.3a)⁹⁹ To a solution of 1,2-didecyloxy-4-iodobenzene (1.30 g, 2.52 mmol), copper(I)iodide, (0.16 g, 0.86 mmol), and PdCl₂(PPh₃)₂ (0.047 g, 0.067 mmol) in anhydrous THF (40mL) was added trimethylsilylacetylene (4.3 mL, 0.030 mmol) and *N,N*-diisopropylamine (1 mL) under N₂. The solution was heated at 60°C for 24 hours under a nitrogen atmosphere. Upon cooling the solution was passed through a short column of silica and the solvent evaporated. The resultant brown oil was subjected to column chromatography (silica gel, 10% ethyl acetate in hexanes).

A solution of (3,4-didecyloxy-phenylethynyl)trimethylsilane (1.38 g, 2.84 mmol) and potassium carbonate (1.02 g, 7.39 mmol) in a 1:1 MeOH:THF (60 mL) mixture and stirred for 24 hours. The solution was passed through a column (silica gel, CH₂Cl₂), the solvent evaporated to yield a brown solid. The solid was subjected to further column chromatography (silica gel, 10% ethyl acetate in hexanes) to yield a yellow-white solid (2.10 g, 74% over two steps). ¹H-NMR (400 MHz) (CDCl₃) δ(ppm), 7.19 (d, 1H *J* = 2 Hz), 7.12 (dd, 1H *J* = 2, 9 Hz), 6.83 (d, 1H *J* = 9 Hz), 3.99 (t, 4H *J* = 6 Hz), 3.05 (s, 1H), 1.20-2.01 (m, ~32H), 0.83-1.04 (m, ~6H). Maldi-TOF. calc. (found) 414 (414).

3,4-Didecyloxy-3'4'-dioctyloxy-diphenylacetylene (2.4c) To a stirred solution of 1,2-didecyloxy-4-ethynylbenzene (0.94 g, 2.27 mmol), 4-iodo-1,2-dioctyloxybenzene (1.05 g, 2.29 mmol), copper(I)iodide, (0.13 g, 0.69 mmol), and Pd(PPh₃)₄ (0.045 g, 0.39 mmol) in anhydrous THF (100 mL) was added *N,N*-diisopropylamine (8 mL). The solution was heated at 60°C for 19 hours. Upon cooling, the solution was passed through a short plug of silica gel and the resultant solid was subjected to column chromatography (silica gel, 10% ethyl acetate in hexanes) to yield a pale yellow solid (1.493 g, 88%). ¹H-NMR (400 MHz) (CDCl₃) δ(ppm), 7.03 (dd, 2H *J* = 2, 9 Hz), 7.00 (d, 2H *J* = 2 Hz), 6.82 (d, 2H *J* = 9 Hz), 3.98 (m, 8H), 1.20-1.81 (m, ~56H), 0.84-0.90 (m, ~12H). ¹³C-NMR (100 MHz) (CDCl₃) 145.6; 144.8; 123.9; 123.7; 116.7; 115.8; 114.4; 88.1; 88.0; 69.3; 69.3; 32.0; 31.5; 30.1; 30.0; 30.0; 29.9; 29.8; 29.7; 29.6; 29.5; 29.3; 29.2; 26.2; 25.8; 22.9; 22.8; 14.1; 14.0; 14.0; 14.0. Elemental analysis (%): calc. (found) for C₅₀H₈₂O₄. C, 80.37 (80.24); H, 11.06 (11.13). Mpt. 76-77 °C. MALDI-TOF. calc. (found) 747 (770 M + Na).

3,4-Didecyloxy-3'4'-dimethoxy-diphenylacetylene (2.4a) Synthesized from 1,2-didecyloxy-4-ethynylbenzene (0.50 g, 1.21 mmol) and 4-iodo-1,2-dimethoxy-benzene (0.32 g, 1.21 mmol) in the manner described above to afford **2.4a** (0.49 g, 74%) a white solid. ¹H-NMR (400 MHz) (CDCl₃) δ(ppm), 7.04 (dd, 2H *J* = 2, 9 Hz), 7.01 (d, 2H *J* = 2 Hz), 6.81 (d, 2H *J* = 9 Hz), 4.01 (t, 4H *J* = 7 Hz), 3.90 (s, 6H), 1.23-1.80 (m, ~32H), 0.82-0.99 (m, ~6H). ¹³C-NMR (100 MHz)

(CDCl₃)) 147.3, 147.1, 144.1, 144.0, 124.4, 124.3, 119.7, 118.4, 115.0, 114.6, 114.5, 91.0, 72.6, 72.6, 56.3, 56.3, 32.5, 32.5, 30.6, 30.6, 30.3, 30.3, 30.3, 30.3, 30.1, 30.0, 26.6, 26.6, 24.2, 23.1, 14.1, 14.0. Elemental analysis (%): calc. (found) for C₃₆H₅₄O₄. C, 78.50 (78.61); H, 9.88 (9.92). Mpt. 88-89 °C. MALDI-TOF. calc. (found) 551 (551).

3,4-Didecyloxy-3'4'-dihexyloxy-diphenylacetylene (2.4b) Synthesized from 1,2-didecyloxy-4-ethynylbenzene (1.12 g, 2.70 mmol) and 1,2-dihexyloxy-4-iodo-benzene (1.10 g, 2.73 mmol) in the manner described above to afford **2.4b** (1.66 g, 89%) a white solid. ¹H-NMR (400 MHz) (CDCl₃) δ(ppm), 7.04 (dd, 2H J = 2, 9 Hz), 7.01 (d, 2H J = 2 Hz), 6.81 (d, 2H J = 9 Hz), 4.00 (m, 8H), 1.26-1.83 (m, ~48H), 0.86-0.91 (m, ~12H). ¹³C-NMR (100 MHz) (CDCl₃) 149.6; 148.8; 124.9; 116.7; 115.8; 113.4; 88.1; 69.4; 69.3; 32.1; 31.8; 30.1; 29.8; 29.8; 29.6; 29.5; 29.3; 29.2; 26.2; 25.8; 22.9; 22.8; 14.3; 14.2. Elemental analysis (%): calc. (found) for C₄₆H₇₄O₄. C, 79.95 (80.13); H, 10.79 (10.68). Mpt. 73-75°C. MALDI-TOF. calc. (found) 691 (691).

3,4-Didecyloxy-3'4'-dioctyloxybenzil (2.5c) A solution of 3,4-didecyloxy-3'4'-dioctyloxy-diphenylacetylene (0.95 g, 1.27 mmol) and iodine (0.35 g, 1.39 mmol) in DMSO (70 mL) was heated at 145°C for 3 hours. Upon cooling the solution was poured into an aqueous 1% sodium thiosulfate pentahydrate solution (200 mL). The resulting solution was collected by vacuum filtration and

then purified by column chromatography (silica gel, 5:1 toluene:hexanes) to yield a beige solid (0.81 g, 82%). $^1\text{H-NMR}$ (400 MHz) (CDCl_3) δ (ppm), 7.56 (d, 2H J = 2 Hz), 7.43 (dd, 2H J = 2, 8 Hz), 6.84 (d, 2H J = 8 Hz), 4.05 (m, 8H), 1.20-2.00 (m, ~56H), 0.80-1.00 (m, 12H). $^{13}\text{C-NMR}$ (100 MHz) (CDCl_3) 193.8, 154.9, 149.3, 126.2, 126.1, 112.3, 111.6, 69.2, 69.1, 31.9, 31.8, 29.6, 29.5, 29.3, 29.3, 29.1, 28.9, 25.9, 25.9, 22.6, 14.1. Elemental analysis (%): calc. (found) for $\text{C}_{50}\text{H}_{82}\text{O}_6$. C, 77.07 (77.41); H, 10.61 (10.55). Mpt. 109-111 °C. MALDI-TOF. calc. (found) 779 (779).

3,4-Didecyloxy-3'4'-dimethoxybenzil (2.5a) Synthesised from 3,4-didecyloxy-3'4'-dimethoxy-diphenylacetylene (0.30 g, 0.55 mmol) and iodine (0.14 g, 0.545 mmol) in the manner described above to afford **2.5a** (0.29 g, 82%) an off-white solid. $^1\text{H-NMR}$ (400 MHz) (CDCl_3) δ (ppm), 7.58 (d, 2H J = 2 Hz), 7.48 (dd, 1H J = 2, 8 Hz), 7.43 (dd, J = 1H 2, 8 Hz), 6.87 (d, 1H J = 8 Hz), 6.86 (d, 1H 8.3 Hz), 4.05 (t, 4H J = 7 Hz), 3.95 (s, 6H), 1.20-2.00 (m, ~32H), 0.80-1.00 (m, ~6H). $^{13}\text{C-NMR}$ (100 MHz) (CDCl_3) 193.7, 193.6, 155.0, 154.7, 151.9, 151.6, 149.5, 128.5, 127.9, 127.6, 126.5, 114.5, 110.9, 110.3, 69.3, 69.2, 69.1, 31.9, 29.6, 29.5, 29.4, 29.3, 29.4, 29.0, 28.9, 26.0, 25.9, 25.9, 22.65, 14.1. Elemental analysis (%): calc. (found) for $\text{C}_{36}\text{H}_{54}\text{O}_6$. C, 74.19 (74.29); H, 9.34 (9.45). Mpt. 78-79 °C. MALDI-TOF. calc. (found) 583 (583).

3,4-Didecyloxy-3'4'-dihexyloxybenzil (2.5b) Synthesized from 3,4-didecyloxy-3'4'-dihexyloxy-diphenylacetylene (0.11 g, 0.15 mmol) and iodine (0.039 g, 0.15 mmol) in the manner described above to afford **2.5b** (0.074 g, 68%) as an off-white solid. ¹H-NMR (400 MHz) (CDCl₃) δ(ppm), 7.55 (d, 2H *J* = 2 Hz), 7.43 (dd, 2H *J* = 2, 9 Hz), 6.83 (d, 2H *J* = 9), 4.05 (m, 8H), 1.20-2.00 (m, ~48H), 0.80-1.00 (m, ~12H). ¹³C-NMR (100 MHz) (CDCl₃) 187.7, 185.5, 182.9, 155.1, 147.6, 138.6, 138.1, 137.9, 137.5, 135.3, 114.2, 101.8, 89.4, 78.0, 75.3, 74.9, 43.7, 42.6, 38.7, 37.4, 36.6, 35.5, 33.5, 33.5, 32.1, 32.1, 32.1, 31.8, 30.4, 30.4, 30.1, 30.1, 29.9, 29.9, 29.6, 29.5, 29.4, 29.4, 29.2, 29.2, 29.1, 29.1, 29.0, 26.2, 26.2, 26.2, 26.1, 25.8, 25.7, 23.1, 14.3, 14.2, 14.1, 14.0. Elemental analysis (%): calc. (found) for C₄₆H₇₄O₆. C, 76.41 (76.40); H, 10.32 (10.42). Mpt. 84-86 °C. MALDI-TOF. calc. (found) 723 (746 M + Na).

2,3-Didecyloxy-6,7-dioctyloxy-phenanthrene-9,10-dione (2.6c) To a stirred solution of 3,4-didecyloxy-3'4'-dioctyloxybenzil (0.50 g, 0.64 mmol) and boron trifluoride etherate (0.27 mL) in anhydrous dichloromethane (80 mL) was added vanadium (V) oxytrifluoride (0.17 g, 1.41 mmol). This mixture stirred at room temperature for 30 min and then was poured into 10% aqueous citric acid (200 mL). The organic layer was separated and the aqueous layer was extracted with CH₂Cl₂ (3 x 40 mL). The organic layers were combined, washed with water, dried (MgSO₄), filtered, and rotary evaporated. The resulting product was passed through a column (silica gel, CH₂Cl₂) under vacuum to yield a deep red solid (0.47 g, 95%). ¹H-NMR (400 MHz) (CDCl₃) δ(ppm), 7.56 (s, 2H), 6.65 (s, 2H),

3.95-4.35 (m, ~8H), 1.20-2.00 (m, ~56H), 0.80-1.00 (m, ~12H). ^{13}C -NMR (100 MHz) (CDCl_3) 179.7; 156.1; 148.8; 132.2; 124.6; 114.8; 106.8; 69.8; 69.5; 32.2; 30.7; 29.8; 29.6; 29.6; 29.5; 29.3; 29.2; 29.2; 26.2; 26.1; 25.7; 25.6; 22.8; 22.4; 14.3. Elemental analysis (%): calc. (found) for $\text{C}_{50}\text{H}_{80}\text{O}_6$. C, 77.27 (77.34); H, 10.38 (10.17). Mpt. 68-70 °C. MALDI-TOF. calc. (found) 777 (790 M + Na).

2,3-Didecyloxy-6,7-dimethoxy-phenanthrene-9,10-dione (2.6a)

Synthesized from 3,4-didecyloxy-3'4'-dimethoxybenzil (0.30 g, 0.52 mmol) in the manner described above to afford **2.6a** (0.29 g, 96%) as a deep red solid. ^1H -NMR (400 MHz) (CDCl_3) δ (ppm), 7.62 (s, 2H), 7.02 (s, 2H), 3.95-4.35 (m, 4H), 3.77 (s, 6H), 1.20-2.00 (m, ~32H), 0.80-1.00 (m, ~6H). ^{13}C -NMR (100 MHz) (CDCl_3). 173.5, 155.0, 154.4, 151.6, 149.4, 128.6, 128.5, 123.4, 123.4, 114.5, 113.4, 112.6, 110.2, 69.2, 69.2, 69.1, 56.1, 56.0, 55.9, 55.8, 31.8, 29.5, 29.5, 29.3, 29.3, 29.30, 29.0, 29.8, 25.9, 25.9, 25.8, 22.7. Elemental analysis (%): calc. (found) for $\text{C}_{36}\text{H}_{52}\text{O}_6$. C, 74.45 (74.77); H, 9.02 (8.87). Mpt. 114-117 °C. MALDI-TOF. calc. (found) 549 (572 = M + Na).

2,3-Didecyloxy-6,7-dihexyloxy-phenanthrene-9,10-dione (2.6b)

Synthesized from 3,4-didecyloxy-3'4'-dihexyloxybenzil (1.06 g, 1.47 mmol) in the manner described above to afford **2.6b** (1.03 g, 97%) as a deep red solid. ^1H -NMR (400 MHz) (CDCl_3) δ (ppm), 7.49 (s, 2H), 7.08 (s, 2H), 4.04-4.19 (m, 8H), 1.20-2.00 (m, ~48H), 0.80-1.00 (m ~12H). ^{13}C -NMR (100 MHz) (CDCl_3) 179.4;

155.7; 149.6; 131.3; 124.6; 113.1; 107.3; 69.7; 69.3; 32.1; 31.7; 29.8; 29.8; 29.6;
29.5; 29.3; 29.3; 29.2; 29.2; 26.2; 26.1; 25.8; 25.8; 22.9; 22.8; 14.3; 14.2.
Elemental analysis (%): calc. (found) for C₄₆H₇₂O₆. C, 76.62 (76.31); H, 10.06
(10.26). Mpt. 59-92 °C. MALDI-TOF. calc. (found) 721 (721).

2,3,6,7-Tetrakis-hexyloxyphenanthrene-9,10-dione (2.6d)⁸⁶

Synthesized from 3,3',4,4' tetrakis-hexyloxybenzil (3.00 g, 4.91 mmol) in the manner described above to afford **2.6d** (2.87 g, 96%) as a deep red solid. ¹H-NMR (400 MHz) (CDCl₃) δ(ppm), 7.49 (s, 2H), 7.07 (s, 2H), 4.18 (t, 4 H J = 7 Hz), 4.05 (t, 4H J = 7 Hz), 1.20-2.00 (m, ~32H), 0.80-1.00 (m, ~12H). ¹³C-NMR (100 MHz) (CDCl₃) 179.3, 155.8, 149.5, 131.2, 124.6, 113.1, 107.2, 69.7, 69.4, 69.3, 69.0, 31.7, 31.6, 29.3, 29.2, 29.1, 25.8, 25.8, 22.8, 14.2. Mpt. 104-106 °C. MALDI-TOF. calc. (found) 608 (609 M+1).

2,3,6,7-Tetrakis-octyloxy-phenanthrene-9,10-dione (2.6e) was

synthesized from 3,3',4,4' tetrakis-octyloxybenzil (1.03 g, 1.42 mmol) in the manner described above to afford **2.6e** (0.97 g, 94%), a deep red solid. ¹H-NMR (400 MHz) (CDCl₃) δ(ppm), 7.48 (s, 2H), 7.07 (s, 2H), 4.18 (t, 4H J = 6.4 Hz), 4.05 (t, 4H J = 6 Hz), 1.20-2.00 (m, ~48H), 0.80-1.00 (m, ~12H). ¹³C-NMR (100 MHz) (CDCl₃) 179.4, 155.7, 131.3, 124.6, 113.1, 107.3, 100.9, 86.0, 69.7, 69.4, 69.3, 69.0, 31.7, 31.6, 29.3, 29.2, 29.1, 25.8, 25.8, 22.8, 14.2. Mpt. 98-100 °C.

Elemental analysis (%): calc. (found) for C₄₆H₇₂O₆. C, 76.62 (76.73); H, 10.06 (9.96). MALDI-TOF. calc. (found) 721 (721).

2,3,6,7-Tetrakis-decyloxyphenanthrene-9,10-dione (2.6f)⁸⁶ Synthesized from 3,3',4,4' tetrakis-decyloxybenzil (3.01 g, 3.59 mmol) in the manner described above to afford **2.6f** (2.86 g, 95%), as a deep red solid. ¹H-NMR (400 MHz) (CDCl₃) δ(ppm), 7.47 (s, 2H), 7.06 (s, 2H), 4.17 (t, 4H *J* = 6 Hz), 4.02-4.05 (t, 4H *J* = 6 Hz), 1.20-2.00 (m, 64H), 0.80-1.00 (m, 12H). ¹³C-NMR (100 MHz) (CDCl₃) 179.4, 155.7, 149.6, 131.3, 126.3, 113.1, 107.2, 69.7, 69.4, 69.4, 69.3, 32.1, 32.0, 29.8, 29.8, 29.6, 29.6, 29.3, 29.3, 29.1, 26.2, 26.2, 26.1, 25.9, 22.9, 22.8, 22.7, 14.3, 14.2, 14.1. Melting Point 101-103 °C. MALDI-TOF. calc. (found) 833 (833).

2,3,6,7-Tetrakis-butoxyphenanthrene-9,10-dione (2.6g) Synthesized from 3,3',4,4' tetrakis-butoxybenzil (1.78 g, 3.54 mmol) in the manner described above to afford **2.6g** (1.63 g, 92%) as a deep red solid. ¹H-NMR (400 MHz) (CDCl₃) (400) δ(ppm), 7.53 (s, 2H), 7.10 (s, 2H), 4.19 (t, 4H *J* = 7 Hz), 4.07 (t, 4H *J* = 7 Hz), 1.92-0.97 (m, ~28H). ¹³C-NMR (100 MHz) (CDCl₃) (125) δ(ppm). 179.3, 155.7, 149.5, 131.2, 124.5, 113.0, 107.1, 77.5, 77.2, 77.0, 69.3, 69.0, 31.3, 31.2, 19.4, 19.4, 14.1. Elemental analysis (%): calc. (found) for C₃₀H₄₀O₆. C, 72.55 (72.27); H, 8.12 (7.98). Maldi-TOF. calc. (found) 496.28 (497).

6,7-Didecyloxy-10,11-dioctyloxy-dibenzo[f,h]quinoxaline-2,3-

dicarbonitrile (2.7c) A solution of 2,3-didecyloxy-6,7-dioctyloxy-phenanthrene-9,10-dione (0.11 g, 0.14 mmol), diaminomaleonitrile (0.22 g, 2.1 mmol) and AcOH (20mL) were heated at reflux for 2 days. Upon cooling, water (50 mL) added and was extracted with CHCl₃ (3 x 40 mL). The organic layers were combined, washed with water, dried (MgSO₄), filtered, and evaporated under reduced pressure. The resultant brown solid was passed through a short column (silica gel, CH₂Cl₂), and then passed through a longer column (silica gel, 5:1 toluene:hexanes) to yield a yellow solid (0.063 g, 54%). ¹H-NMR (400 MHz) (CDCl₃) δ(ppm), 8.35 (s, 2H), 7.64 (s, 2H), 4.17-4.35(m, ~8H), 1.17-2.24 (m, ~56H), 0.78-1.10 (m, ~12H). ¹³C-NMR (100 MHz) (CDCl₃). 142.3, 142.3, 142.1, 142.0, 128.2, 126.4, 124.1, 122.3, 122.2, 108.7, 108.6, 72.4, 72.4, 72.3, 32.4, 32.1, 32.0, 30.6, 30.6, 30.5, 30.3, 30.3, 30.2, 30.0, 30.0, 29.9, 29.4, 26.6, 26.5, 26.5, 26.5, 23.1, 23.1, 23.0, 14.1, 14.1, 14.1. Elemental analysis (%): calc. (found) for C₅₄H₈₀N₄O₄. C, 76.37 (76.21); H, 9.50 (9.70); N, 6.60 (6.21). MALDI-TOF. calc. (found) 829 (829).

6,7-Didecyloxy-10,11-dimethoxy-dibenzo[f,h]quinoxaline-2,3-

dicarbonitrile (2.7a) Synthesized from 2,3-didecyloxy-6,7-dimethoxy-phenanthrene-9,10-dione (0.12 g, 0.16 mmol) in the manner described above to afford **2.7a** (0.071 g, 61%) as a yellow solid. ¹H-NMR (400 MHz) (CDCl₃) δ(ppm), 8.39 (s, 2H), 7.62 (s, 2H), 4.15-4.35 (m, 4H), 3.76 (s 6H), 1.20-2.20 (m, ~32H), 0.80-1.13 (m, ~6H). ¹³C-NMR (100 MHz) (CDCl₃). 145.3, 145.3, 142.3,

142.1, 128.1, 126.3, 126.2, 125.1, 124.0, 123.1, 114.7, 114.6, 108.9, 108.6, 72.5, 56.1, 56.0, 32.1, 32.1, 30.6, 30.5, 30.2, 30.1, 30.1, 30.1, 30.0, 30.0, 26.8, 26.8, 23.1, 23.0, 14.1, 14.1. Elemental analysis (%): calc. (found) for C₅₀H₇₂N₄O₄. C, 73.59 (73.38); H, 8.03 (8.35); N, 8.58 (8.51). Melting point: 264 ° C. MALDI-TOF. calc. (found) 653 (676 M + Na).

6,7-Didecyloxy-10,11-dihexyloxy-dibenzo[f,h]quinoxaline-2,3-dicarbonitrile (2.7b) Synthesised from 2,3-didecyloxy-6,7-dihexyloxy-phenanthrene-9,10-dione (0.11 g, 0.16 mmol) in the manner described above to afford **2.7b** (0.067 g, 57%) a yellow solid. ¹H-NMR (400 MHz) (CDCl₃) δ(ppm), 8.46 (s, 2H), 7.63 (s, 2H), 4.15-4.35 (m, 8H), 1.20-2.21 (m, ~48H), 0.80-1.13 (m, ~12H). ¹³C-NMR (100 MHz) (CDCl₃). 142.6, 142.6, 142.5, 128.2, 126.4, 126.3, 124.1, 122.2, 114.4, 114.2, 108.6, 73.1, 73.0, 32.5, 32.4, 32.4, 30.6, 30.5, 30.5, 30.2, 30.1, 30.0, 30.0, 30.0, 26.6, 23.2, 23.1, 23.0, 14.1, 14.1, 14.1. Elemental analysis (%): calc. (found) for C₅₀H₇₂N₄O₄. C, 75.72 (75.78); H, 9.15 (9.08); N, 7.06 (7.35). MALDI-TOF. calc. (found) 793 (793).

6,7,10,11-Tetrakis-hexyloxy-dibenzo[f,h]quinoxaline-2,3-dicarbonitrile (2.7d) Synthesized from 2,3,6,7-tetrakis-hexyloxyphenanthrene-9,10-dione (0.20 g, 0.33 mmol) in the manner described above to afford **2.7d** (0.128 g, 57%), a yellow solid. ¹H-NMR (400 MHz) (CDCl₃) δ(ppm), 8.37 (s, 2H), 7.55 (s, 2H), 4.17-4.37 (m, ~8H), 1.20-2.21 (m, ~48H), 0.83-1.10 (m, ~12H). ¹³C-NMR (100 MHz) (CDCl₃) 154.1, 151.0, 141.2, 127.1, 127.1, 120.6, 114.3, 114.2, 107.6, 104.4,

76.9, 69.7, 69.4, 31.8, 31.7, 29.9, 29.3, 29.3, 29.1, 25.9, 25.8, 25.8, 22.8, 22.8, 22.7, 14.2, 14.1. Elemental analysis (%): calc. (found) for C₄₂H₅₆N₄O₄. C, 74.08 (74.43); H, 8.29 (8.53); N, 8.23 (8.18). MALDI-TOF. calc. (found) 681 (681).

6,7,10,11-Tetrakis-octyloxy-dibenzo[f,h]quinoxaline-2,3-dicarbonitrile

(2.7e) Synthesized from 2,3,6,7-tetrakis-octyloxyphenanthrene-9,10-dione (0.45 g, 0.62 mmol) in the manner described above to afford **2.7e** (0.269 g, 55%) a yellow solid. ¹H-NMR (400 MHz) (CDCl₃) δ(ppm), 8.31 (s, 2H), 7.56 (s, 2H), 4.09-4.31 (m, 8H), 1.20-2.21 (m, ~48H), 0.85-1.08 (m, ~12H). ¹³C-NMR (100 MHz) (CDCl₃) 153.8, 150.0, 140.9, 128.1, 128.0, 120.8, 114.6, 107.8, 104.9, 76.9, 69.6, 69.4, 32.2, 32.0, 30.0, 29.9, 29.8, 29.7, 29.5, 29.4, 26.4, 26.3, 23.0, 22.9, 14.3. Elemental analysis (%): calc. (found) for C₅₀H₇₂N₄O₄. C, 75.72 (75.47); H, 9.15 (9.12); N, 7.06 (7.21). MALDI-TOF. calc. (found) 793 (793).

6,7,10,11-Tetrakis-decyloxy-dibenzo[f,h]quinoxaline-2,3-dicarbonitrile

(2.7f)¹⁰⁰ Synthesized from 2,3,6,7-tetrakis-decyloxyphenanthrene-9,10-dione (0.201 g, 0.240 mmol) in the manner described above to afford **2.7f** as a yellow solid (0.122 g, 56%). ¹H-NMR (400 MHz) (CDCl₃) δ(ppm), 8.51 (s, 2H), 7.72 (s, 2H), 4.10-4.32 (m, 8H), 1.21-2.22 (m, ~64H), 0.81-1.11 (m, ~12H). ¹³C-NMR (100 MHz) (CDCl₃). 155.7, 149.6, 131.3, 124.6, 113.1, 113.1, 107.3, 32.1, 31.7, 29.8, 29.8, 29.6, 29.6, 29.5, 29.3, 29.3, 29.2, 29.2, 26.2, 26.2, 25.8, 25.8, 22.9, 22.8, 14.3, 14.2. Elemental analysis (%): calc. (found) for C₅₅H₈₈N₄O₄. C, 76.95 (76.84); H, 9.80 (10.12); N, 6.19 (5.89). MALDI-TOF. calc. (found) 905 (905).

General procedure for the synthesis of 1,2-dialkoxybenzenes **2.8a-c**

A stirred solution of 1,2-dihydroxybenzene (20.0 g, 182 mmol) and 1-bromohexane (60.0 g, 364 mmol) in DMF (300 mL) was stirred for 15 minutes while being purged with N₂. Potassium carbonate (126.0 g, 908 mmol) was added and the solution purged with N₂ for a further 15 minutes before stirring overnight at 80°C. The solution was allowed to cool, poured over ice (1000 mL) and vacuum filtered. The resultant solid was purified by column chromatography (silica gel, 100 % hexanes gradient to 10% ethyl acetate in hexanes) to yield a clear liquid **2.8a**, (92%).

General procedure for the synthesis of 1,2-dialkoxybenzenes **2.8d-g**

A stirred solution of 1,2-dihydroxybenzene (20.0 g, 182 mmol) and 1-bromohexane (30.0 g, 182 mmol) in DMF (300 mL) was stirred for 15 minutes while being purged with N₂. Potassium carbonate (126.0 g, 908 mmol) was added and the solution purged with N₂ for a further 15 minutes before stirring overnight at 70°C. The solution was allowed to cool, poured over ice (1000 mL), and vacuum filtered. The resulting solid was purified by column chromatography (silica gel, 100 % hexanes gradient to 10% ethyl acetate in hexanes) to yield a clear liquid (2-hexyloxyphenol). This liquid was alkylated as above with 1-bromodecane (40.0 g, 182 mmol), and then purified by column chromatography

(silica gel, 100 % hexanes gradient to 10% ethyl acetate in hexanes) to yield **2.8g** (50 g, 149 mmol) (85% over two steps)

General procedure for the synthesis of 1,2-Bis-alkoxy-4,5-dinitro-benzene (**2.9a-g**)

HNO₃ (50 mL) was slowly added to a neat solution of the appropriate 1,2-bis-alkoxy-benzene (10 mmol) while stirring in an ice bath. The solution was allowed to warm to room temperature and then was heated to 85°C in an oil bath and stirred for a further 2 hours. The mixture was poured into a mixture of H₂O (200 mL), saturated aqueous NaHCO₃ (200 mL) and the precipitate was collected by vacuum filtration. The resulting solid was passed through a silica gel column (10% ethyl acetate, 90% hexanes) to yield a bright yellow solid. The product was recrystallized in anhydrous EtOH, yielding the corresponding 1,2-dialkoxy-4,5-dinitro-benzene derivative.

1,2-Bis-hexyloxy-4,5-dinitro-benzene (2.9a)¹⁰¹ Synthesized and purified as described above, from **2.8a**. ¹H-NMR (400 MHz) (CDCl₃) δ(ppm) 7.29 (s, 2H), 4.09 (t, 4H J = 6 Hz), 1.91-0.86 (m, ~22H). CI - MS. calc. (found) 368 (M+ 368).

1,2-Dinitro-4,5-bis-octyloxy-benzene (2.9b)¹⁰² Synthesized and purified as described above, from **2.8b**. ¹H-NMR (400 MHz) (CDCl₃) δ(ppm) 7.29 (s, 2H),

4.09 (t, 4H $J = 6$ Hz), 1.91-0.86 (m, ~30H). Maldi-TOF. calc. (found) 424 (424).
Mpt. lit. (found). 83-96 (82-83)

1,2-Bis-decyloxy-4,5-dinitro-benzene (2.9c) Synthesized and purified as described above, from **2.8c**. $^1\text{H-NMR}$ (400 MHz) (CDCl_3) $\delta(\text{ppm})$ 7.29 (s, 2H), 4.09 (t, 4H $J = 6$ Hz), 1.91-0.86 (m, ~38H). Maldi-TOF. calc. (found): 480 (480).
Mpt. Lit. (found): 84 (82-83)

1-Decyloxy-2-methoxy-4,5-dinitro-benzene (2.9d) Synthesized and purified as described above, from **2.8d**. $^1\text{H-NMR}$ (400 MHz) (CDCl_3) $\delta(\text{ppm})$ 7.33 (s, 1H), 7.30 (s, 1H), 4.11 (t, 2H $J = 7$ Hz), 3.99 (s, 3H), 1.91-0.86 (m, 19H). $^{13}\text{C-NMR}$ (100 MHz) (CDCl_3) $\delta(\text{ppm})$. 152.1, 151.8, 107.8, 107.2, 77.5, 77.2, 76.9, 70.5, 57.2, 32.1, 29.7, 29.7, 29.7, 29.5, 29.4, 28.8, 25.9, 22.9, 14.3. CI-MS. calc. (found) 354 (354)

1-Butoxy-2-hexyloxy-4,5-dinitro-benzene (2.9e) Synthesized and purified as described above, from **2.8e**. $^1\text{H-NMR}$ (400 MHz) (CDCl_3) $\delta(\text{ppm})$. 7.28 (s, 2H), 4.10 (m, 4H), 1.90-0.90 (m, ~18H). $^{13}\text{C-NMR}$ (100 MHz) (CDCl_3) $\delta(\text{ppm})$ 151.4, 137.0, 109.2, 76.6, 71.2, 32.0, 29.6, 28.9, 28.7, 26.0, 26.1, 22.7, 22.7, 14.3, 14.1.

1-Hexyloxy-2-octyloxy-4,5-dinitro-benzene (2.9f) Synthesized and purified as described above, from **2.8f**. $^1\text{H-NMR}$ (400 MHz) (CDCl_3) δ (ppm). 7.29 (s, 2H), 4.09 (m, 4H), 1.89-0.87 (m, ~30H). $^{13}\text{C-NMR}$ (100 MHz) (CDCl_3) δ (ppm) 152.0, 136.5, 107.6, 76.5, 71.1, 32.1, 31.5, 30.6, 29.5, 29.2, 28.9, 28.7, 26.1, 25.5, 22.9, 22.7, 14.3, 14.1.

1-Decyloxy-2-hexyloxy-4,5-dinitro-benzene (2.9g) Synthesized as described above, from **2.8g**. $^1\text{H-NMR}$ (400 MHz) (CDCl_3) δ (ppm). 7.29 (s, 2H), 4.11-4.07 (t, 4H $J = 7$ Hz), 1.91-0.86 (m, 30H). $^{13}\text{C-NMR}$ (100 MHz) (CDCl_3) δ (ppm) 151.9, 136.6, 108.0, 77.4, 77.2, 77.1, 76.9, 70.3, 32.1, 31.5, 29.7, 29.5, 29.4, 28.9, 28.8, 26.0, 25.6, 22.9, 22.7, 14.3, 14.2. Maldi-TOF. calc. (found) 424 (424).

General procedure for the synthesis of 4,5-bisalkoxy-1,2-phenylenediamine hydrochlorides (**2.10a-c**, **2.10f-g**)

The 1,2-bis-alkoxy-4,5-dinitro-benzene (0.5 mmol) was dissolved in anhydrous EtOH (15 mL) while heating at 75°C. SnCl_2 (0.76 g, 4.0 mmol) was dissolved in concentrated HCl (3 mL) and added slowly at 75°C. The solution was stirred for 2 hours then removed from the heat and concentrated HCl (50 mL) was added, causing a white precipitate to form. The white precipitate was filtered off under vacuum and washed with H_2O (3 x 30 mL), yielding the

hydrochloride salt of the 4,5-Bis-alkoxy-benzene-1,2-diamine. This compound is extremely unstable and was used immediately without further purification.

General procedure for the synthesis of 4,5-bisalkoxy-1,2-phenylenediamine hydrochlorides (**2.10d-e**)

1,2-bis-alkoxy-4,5-dinitro-benzene (0.5 mmol) was dissolved in anhydrous ethanol (10 mL) and 10% palladium on activated carbon (0.050 g) was added. Hydrazine hydrate (0.15 ml, 3.0 mmol) was added dropwise and the mixture was then refluxed for 3 hours. The resultant solution was filtered hot through a plug of silica. This plug was washed with ethanol (50 mL), and the solvent evaporated under reduced pressure. The resulting solid was used immediately without further purification.

General procedure for the synthesis of dibenzo[a,c]phenazine derivatives (**2.11a-b, e-h, j-q**)

A solution of 2,3,6,7-tetrakis-dealkoxy-phenanthrene-9,10-dione and sodium acetate (20 eq.) was stirred in anhydrous ethanol (20 mL). The hydrochloride salt of the appropriate 4,5-bis-alkoxy-benzene-1,2-diamine was added, and the solution heated at reflux overnight. Upon cooling, water (150 mL) was added and then extracted with CHCl_3 (3 x 15 mL). The organic layers were combined, washed with water, dried (MgSO_4), filtered, and the solvent removed under reduced pressure. The resultant orange solid was passed eluted through

a short plug of silica (CH₂Cl₂), and then passed through a longer column (silica gel, 1:1 CH₂Cl₂:hexanes gradient to 100% CH₂Cl₂). The solid was recrystallized in EtOH (95%) and 5-6 drops of acetone, giving a yellow solid, the corresponding dibenzo[a,c]phenazine derivative.

2,3,6,7,11,12-Hexakis-hexyloxy-dibenzo[a,c]phenazine (2.11a)

Synthesized as above, from **2.6d** and **2.8a** (84%). ¹H-NMR (400 MHz) (CDCl₃) δ(ppm), 8.78 (s, 2H), 7.76 (s, 2H), 7.53 (s, 2H), 4.35 (t, 4H *J* = 6 Hz) , 4.26 (t, 8H *J* = 6 Hz), 2.21-0.91 (m, ~66H). ¹³C-NMR (100 MHz) (CDCl₃) δ(ppm). 152.8, 151.0, 149.3, 125.7, 108.0, 106.6, 106.4, 96.5, 77.2, 77.0, 76.7, 69.6, 69.0, 31.6, 31.5, 29.6, 29.3, 29.3, 28.8, 25.8, 22.6, 14.0. Elemental analysis (%): calc. (found) for C₅₆H₈₄N₂O₆. C, 76.32 (76.10); H, 9.31 (9.47); N, 3.18 (3.02). Maldi-TOF. calc. (found) 881 (881).

11,12-Bis-decyloxy-2,3,6,7-tetrakis-hexyloxy-dibenzo[a,c]phenazine

(2.11b) Synthesized as above, from **2.6d** and **2.8c** (78%). ¹H-NMR (400 MHz) (CDCl₃) δ(ppm), 8.75 (s, 2H), 7.75 (s, 2H), 7.53 (s, 2H), 4.35 (t, 4H *J* = 7 Hz) , 4.26 (t, 8H *J* = 7 Hz), 2.21-0.91 (m, ~82H). ¹³C-NMR (100 MHz) (CDCl₃) δ(ppm). 149.59, 108.18, 106.63, 77.5, 77.26, 77.00, 69.86, 69.40, 69.32, 32.17, 31.93, 31.92, 29.89, 29.84, 29.67, 29.62, 29.59, 29.53, 29.19, 26.36, 26.09, 26.06, 22.95, 22.92, 22.90, 14.38, 14.33, 14.31. Elemental analysis (%): calc. (found)

for $C_{64}H_{100}N_2O_6$. C, 77.37 (77.14); H, 10.15 (10.05); N, 2.82 (2.90). Maldi-TOF. calc. (found) 993 (994 M+1).

11-Decyloxy-2,3,6,7-tetrakis-hexyloxy-12-methoxy-dibenzo[a,c]phenazine (2.11c) Synthesized as above, from **2.6d** and **2.8d** (81%). 1H -NMR (400 MHz) ($CDCl_3$) δ (ppm), 8.74 (s, 2H), 7.74 (s, 2H), 7.54 (s, 2H), 4.34 (t, 4H J = 7 Hz), 4.29-4.24 (m, 6H), 4.12 (s, 3H), 2.21-0.91 (m, ~63H). ^{13}C -NMR (100 MHz) ($CDCl_3$) δ (ppm) 149.6, 106.4, 77.4, 77.2, 76.9, 76.8, 69.8, 69.4, 56.7, 32.1, 31.9, 29.8, 29.6, 29.5, 29.1, 26.2, 26.0, 22.8, 14.3. Elemental analysis (%): calc. (found) for $C_{55}H_{82}N_2O_6$. C, 76.17 (75.97); H, 9.53 (9.28); N, 3.23 (3.27). Maldi-TOF. calc. (found) 867 (867).

11-Butoxy-2,3,6,7,12-pentakis-hexyloxy-dibenzo[a,c]phenazine (2.11d) Synthesized as above, from **2.6d** and **2.8e** (83%). 1H -NMR (400 MHz) ($CDCl_3$) δ (ppm), 8.76 (s, 2H), 7.76 (s, 2H), 7.52 (s, 2H), 4.34 (t, 4H J = 6 Hz), 4.29-4.25 (m, 6H), 1.99 -0.91 (m, ~64H). ^{13}C -NMR (100 MHz) ($CDCl_3$) δ (ppm) 151.1, 107.4, 106.3, 104.5, 76.5, 70.1, 69.3, 56.5, 32.1, 31.9, 29.8, 29.6, 29.4, 29.0, 26.1, 26.0, 22.6, 14.3, 14.2. Elemental analysis (%): calc. (found) for $C_{54}H_{80}N_2O_6$. C, 76.02 (75.99); H, 9.45 (9.58); N, 3.28 (3.25). Maldi-TOF. calc. (found) 853 (853).

2,3,6,7,11-pentakis-hexyloxy--12-octyloxy-dibenzo[a,c]phenazine

(2.11e) Synthesized as above, from **2.6d** and **2.8f** (76%). ¹H-NMR (400 MHz) (CDCl₃) δ(ppm), 8.76 (s, 2H), 7.76 (s, 2H), 7.53 (s, 2H), 4.35 (t, 4H *J* = 7 Hz), 4.29-4.26 (m, 6H), 2.21-0.91 (m, ~72H). ¹³C-NMR (100 MHz) (CDCl₃) δ(ppm) 149.6, 148.1, 110.1, 108.1, 106.4, 76.5, 69.8, 69.3, 32.1, 32.0, 31.9, 29.9, 29.5, 29.5, 29.1, 26.1, 26.0, 14.3, 14.2. Elemental analysis (%): calc. (found) for C₅₈H₈₈N₂O₆. C, 76.61 (76.64); H, 9.75 (9.52); N, 3.08 (3.23). Maldi-TOF. calc. (found) 909 (910 M+1).

11-Decyloxy-2,3,6,7,12-pentakis-hexyloxy-dibenzo[a,c]phenazine

(2.11f) Synthesized as above, from **2.6d** and **2.8g** (81%). ¹H-NMR (400 MHz) (CDCl₃) δ(ppm), 8.76 (s, 2H), 7.76 (s, 2H), 7.53 (s, 2H), 4.35 (t, 4H *J* = 7 Hz), 4.27 (t, 8H *J* = 6.83), 2.21-0.84 (m, ~74H). ¹³C-NMR (100 MHz) (CDCl₃) δ(ppm) 151.2, 149.2, 106.5, 77.8, 77.8, 77.7, 77.6, 77.4, 77.2, 76.9, 76.7, 69.8, 32.1, 31.9, 31.8, 29.8, 29.8, 29.6, 29.5, 29.5, 29.5, 29.1, 29.0, 26.3, 26.0, 25.9, 22.8, 14.3, 14.3, 14.3, 14.2. Elemental analysis (%): calc. (found) for C₆₀H₉₂N₂O₆. C, 76.88 (76.54); H, 9.89 (9.66); N, 2.99 (2.66). Maldi-TOF. calc. (found) 937 (937).

2,3,6,7-Tetrakis-decyloxy-11,12-bis-hexyloxy-dibenzo[a,c]phenazine

(2.11g) Synthesized as above, from **2.6f** and **2.8a** (83%). ¹H-NMR (400 MHz) (CDCl₃) δ(ppm), 8.76 (s, 2H), 7.76 (s, 2H), 7.53 (s, 2H), 4.35 (t, 4H *J* = 6 Hz), 4.27 (m, 8H), 2.21-0.91 (m, ~98H). ¹³C-NMR (100 MHz) (CDCl₃) δ(ppm) 151.1,

151.0, 149.4, 125.7, 108.0, 106.5, 96.5, 77.2, 77.0, 76.7, 69.6, 69.1, 31.9, 31.5, 29.6, 29.6, 29.5, 29.3, 28.8, 26.1, 25.7, 22.6, 22.6, 14.0. Elemental analysis (%): calc. (found) for $C_{72}H_{116}N_2O_6$. C, 78.21 (78.49); H, 10.57 (10.35); N, 2.53 (2.61). Maldi-TOF. calc. (found) 1105 (1106 M+1).

2,3,6,7,11,12-Hexakis-decyloxy-dibenzo[a,c]phenazine (2.11h)

Synthesized as above, from **2.6f** and **2.8c** (85%). 1H -NMR (400 MHz) ($CDCl_3$) δ (ppm), 8.76 (s, 2H), 7.76 (s, 2H), 7.54 (s, 2H), 4.35 (t, 4H J = 6 Hz), 4.26 (t, 8H J = 6 Hz), 2.21-0.91 (m, ~114H). ^{13}C -NMR (100 MHz) ($CDCl_3$) δ (ppm) 151.4, 151.3, 149.6, 126.0, 108.3, 106.8, 77.6, 77.4, 77.2, 76.9, 76.7, 69.9, 69.3, 32.1, 29.9, 29.8, 29.7, 29.6, 29.6, 29.1, 26.4, 26.3, 22.9, 14.3. Elemental analysis (%): calc. (found) for $C_{80}H_{132}N_2O_6$. C, 78.89 (78.60); H, 10.92 (10.68); N, 2.30 (2.04). Maldi-TOF. calc. (found) 1217 (1219 M+2).

2,3,6,7,11-Pentakis-decyloxy-12-methoxy-dibenzo[a,c]phenazine

(2.11i) Synthesized as above, from **2.6f** and **2.8d** (86%). 1H -NMR (400 MHz) ($CDCl_3$) δ (ppm), 8.77 (s, 2H), 7.75 (s, 2H), 7.58 (s, 2H), 4.35 (t, 4H J = 6 Hz), 4.32-4.24 (m, 6H), 4.12 (s, 3H), 2.21-0.91 (m, ~95H). ^{13}C -NMR (100 MHz) ($CDCl_3$) δ (ppm) 149.4, 125.8, 108.1, 106.4, 96.5, 77.2, 77.0, 76.7, 69.6, 69.2, 31.9, 29.6, 29.6, 29.5, 29.3, 28.8, 26.1, 26.0, 22.6, 14.0, 56.4, 125.8. Elemental analysis (%): calc. (found) for $C_{71}H_{114}N_2O_6$. C, 78.11 (77.99); H, 10.53 (10.24); N, 2.57 (2.22). Maldi-TOF. calc. (found) 1091 (1092 M+1).

2,3,6,7,11-Pentakis-decyloxy-12-hexyloxy-dibenzo[a,c]phenazine

(**2.11j**) Synthesized as above, from **2.6f** and **2.8b** (76%). ¹H-NMR (400 MHz) (CDCl₃) δ(ppm), 8.77 (s, 2H), 7.75 (s, 2H), 7.54 (s, 2H), 4.38 (t, 4H *J* = 7 Hz), 4.27 (t, 8H *J* = 7), 2.21-0.84 (m, ~106H). ¹³C-NMR (100 MHz) (CDCl₃) δ(ppm) 149.7, 124.7, 106.6, 77.4, 77.2, 76.9, 76.9, 76.9, 76.8, 76.8, 76.8, 76.8, 76.8, 76.8, 76.8, 76.8, 76.8, 76.7, 76.7, 76.7, 69.8, 32.1, 29.9, 29.8, 29.7, 29.6, 26.4, 26.3, 22.9, 22.8, 14.3, 14.2. Elemental analysis (%): calc. (found) for C₇₆H₁₂₄N₂O₆. C, 78.57 (78.29); H, 10.76 (10.88); N, 2.41 (2.34). Maldi-TOF. calc. (found) 1161 (1161).

2,3,6,7-Tetrabutoxy-11,12-bis-hexyloxy-dibenzo[a,c]phenazine (2.11k)

Synthesized as above, from **2.6g** and **2.8a** (83%). ¹H-NMR (400 MHz) (CDCl₃) δ(ppm), 8.76 (s, 2H), 7.75 (s, 2H), 7.56 (s, 2H), 4.36 (t, 4H *J* = 7 Hz), 4.30-4.25 (m, ~8H), 2.21-0.91 (m, ~50H). ¹³C-NMR (100 MHz) (CDCl₃) δ(ppm) 151.3, 149.6, 125.9, 108.2, 106.5, 77.5, 77.2, 76.9, 69.6, 69.4, 69.0, 31.8, 31.6, 29.9, 29.1, 26.0, 22.8, 19.6, 14.2. Elemental analysis (%): calc. (found) for C₄₈H₆₈N₂O₆. C, 74.96 (74.59); H, 8.91 (8.61); N, 3.64 (3.31). Maldi-TOF. calc. (found) 768 (768 M+1).

2,3,6,7-Tetrabutoxy-11,12-bis-decyloxy-dibenzo[a,c]phenazine (2.11l)

Synthesized as above, from **2.6g** and **2.8c** (81%). ¹H-NMR (400 MHz) (CDCl₃)

δ (ppm), 8.74 (s, 2H), 7.72 (s, 2H), 7.55 (s, 2H), 4.36 (t, 4H $J = 7$ Hz), 4.29-4.24 (m, 8H), 2.21-0.91 (m, ~66H). ^{13}C -NMR (100 MHz) (CDCl_3) δ (ppm) 149.3, 147.8, 106.5, 77.8, 77.8, 77.7, 77.4, 77.2, 76.9, 69.5, 32.1, 32.1, 31.5, 29.8, 29.8, 29.6, 29.6, 29.1, 26.3, 22.9, 19.6, 19.6, 19.5, 14.3, 14.2. Elemental analysis (%): calc. (found) for $\text{C}_{56}\text{H}_{84}\text{N}_2\text{O}_6$. C, 76.36 (76.22); H, 9.61 (9.34); N, 3.18 (2.89). Maldi-TOF. calc. (found) 881 (881).

2,3-Bis-decyloxy-6,7,11,12-tetrakis-hexyloxy-dibenzo[a,c]phenazine

(2.11m) Synthesized as above, from **2.6b** and **2.8a** (88%). ^1H -NMR (400 MHz) (CDCl_3) δ (ppm), 8.77 (s, 2H), 7.76 (s, 2H), 7.56 (s, 2H), 4.35 (t, 4H $J = 6$ Hz), 4.27 (t, 8H $J = 6$ Hz), 2.21-0.91 (m, ~82H). ^{13}C -NMR (100 MHz) (CDCl_3) δ (ppm) 149.4, 148.0, 145.9, 108.1, 106.4, 96.5, 77.2, 77.0, 76.7, 69.6, 69.2, 31.9, 31.6, 31.5, 29.6, 29.6, 29.5, 29.3, 28.8, 26.1, 25.8, 25.7, 22.6, 14.1, 14.0. Elemental analysis (%): calc. (found) for $\text{C}_{64}\text{H}_{100}\text{N}_2\text{O}_6$. C, 77.37 (77.68); H, 10.15 (10.23); N, 2.82 (2.57). Maldi-TOF. calc. (found) 993 (993).

2,3,11,12-Tetrakis-decyloxy-6,7-bis-hexyloxy-dibenzo[a,c]phenazine

(2.11n) Synthesized as above, from **2.6b** and **2.8c** (76%). ^1H -NMR (400 MHz) (CDCl_3) δ (ppm), 8.76 (s, 2H), 7.75 (s, 2H), 7.55 (s, 2H), 4.35 (t, 4H $J = 6$ Hz), 4.27 (t, 8H $J = 6$ Hz), 2.21-0.91 (m, ~98H). ^{13}C -NMR (100 MHz) (CDCl_3) δ (ppm) 149.6, 131.1, 129.0, 106.4, 77.5, 77.2, 76.9, 69.8, 69.4, 69.4, 38.9, 32.1, 31.9, 30.5, 29.9, 29.8, 29.8, 29.7, 29.6, 29.5, 29.5, 29.1, 29.1, 26.4, 26.3, 26.0, 23.2,

22.9, 14.3, 14.3. Elemental analysis (%): calc. (found) for $C_{72}H_{116}N_2O_6$. C, 78.21 (77.99); H, 10.57 (10.68); N, 2.53 (2.67). Maldi-TOF. calc. (found) 1105 (1105).

2,3-Bis-decyloxy-11,12-bis-hexyloxy-6,7-bis-octyloxy-

dibenzo[a,c]phenazine (2.11o) Synthesized as above, from **2.6c** and **2.8a** (79%). 1H -NMR (400 MHz) ($CDCl_3$) δ (ppm), 8.77 (s, 2H), 7.77 (s, 2H), 7.55 (s, 2H), 4.35 (t, 4H $J = 6$ Hz), 4.27 (t, 8H $J = 6$ Hz), 2.21-0.91 (m, ~90H). ^{13}C -NMR (100 MHz) ($CDCl_3$) δ (ppm) 150.1, 132.0, 129.0, 107.4, 69.7, 69.5, 69.5, 37.9, 32.1, 29.2, 29.6, 29.6, 29.6, 29.4, 29.3, 29.2, 26.4, 26.2, 26.1, 24.2, 22.9, 14.2, 14.2. Elemental analysis (%): calc. (found) for $C_{68}H_{108}N_2O_6$. C, 77.81 (77.98); H, 10.37 (10.35); N, 2.67 (3.01). Maldi-TOF. calc. (found) 1049 (1049).

2,3-Bis-decyloxy-6,7-bis-hexyloxy-11,12-bis-octyloxy-

dibenzo[a,c]phenazine (2.11p) Synthesized as above, from **2.6b** and **2.8b** (80%). 1H -NMR (400 MHz) ($CDCl_3$) δ (ppm), 8.77 (s, 2H), 7.77 (s, 2H), 7.55 (s, 2H), 4.35 (t, 4H $J = 6$ Hz), 4.27 (t, 8H $J = 6$ Hz), 2.21-0.91 (m, ~90H). ^{13}C -NMR (100 MHz) ($CDCl_3$) δ (ppm) 152.1, 138.2, 106.5, 77.6, 77.4, 77.2, 76.9, 69.8, 32.1, 32.0, 31.9, 29.9, 29.8, 29.7, 29.6, 29.5, 29.5, 29.1, 26.3, 26.3, 26.0, 22.9, 22.9, 14.3, 14.3. Elemental analysis (%): calc. (found) for $C_{68}H_{108}N_2O_6$. C, 77.81 (78.02); H, 10.37 (10.08); N, 2.67 (2.60). Maldi-TOF. calc. (found) 1049 (1050 M+1).

2,3,6,7,11,12-Hexakis-octyloxy-dibenzo[a,c]phenazine (2.11q)

Synthesized as above, from **2.6e** and **2.8b** (71%). ¹H-NMR (400 MHz) (CDCl₃) δ(ppm), 8.77 (s, 2H), 7.77 (s, 2H), 7.55 (s, 2H), 4.35 (t, 4H *J* = 6 Hz), 4.27 (t, 8H *J* = 6 Hz), 2.21-0.91 (m, ~90H). ¹³C-NMR (100 MHz) (CDCl₃) δ(ppm) 149.6, 139.5, 108.2, 106.7, 106.6, 77.7, 77.6, 77.4, 77.2, 76.9, 69.8, 69.4, 69.4, 69.367, 32.0, 32.0, 29.7, 29.7, 29.6, 29.5, 29.5, 29.4, 29.1, 26.4, 26.3, 26.3, 22.9, 14.3
Elemental analysis (%): calc. (found) for C₆₈H₁₀₈N₂O₆. C, 77.81 (77.67); H, 10.37 (10.43); N, 2.67 (2.48). Maldi-TOF. calc. (found) 1049 (1049).

3 EFFECTS OF CORE-SIZE AND HETEROATOMS ON SELF-ASSEMBLY

3.1 Introduction*

In the previous chapter we described the effect of molecular symmetry on the phase behaviour of discotic mesogens. In this chapter, the effects of core-size and the presence of heteroatom on macroscopic properties will be discussed. Both of these factors are of immediate interest in the context of using discotic mesogens as electronic materials.

The preparation of large-core mesogens has been pursued on the assumption that increased core-size will lead to superior electronic properties^{59,60,103-105} while other groups have prepared nitrogen-containing discotic mesogens in order to create liquid crystals that can act as better electron-carrier materials.¹⁰⁶⁻¹¹⁵ Previous synthetic approaches have not been amenable to the preparation of a series of molecules in which small, systematic changes in core structure are introduced. Not being able to introduce such incremental changes makes studying effects such as this difficult. The coupling of a series of 1,2-diamines with a versatile precursor molecule, 2,3,6,7-tetra(hexyloxy)phenanthrene-9,10-dione provides a highly efficient and modular approach that facilitates the preparation of a broad family of potential mesogens

* Portions of this chapter have been previously reported, see: a) E. J. Foster, R. B. Jones, C. Lavigueur and V. E. Williams *J. Am. Chem. Soc.*, **2006**, 128: 8569-8574 b) E. J. Foster, J. Babuin, N. Nyugen and V. E. Williams *Chem. Commun.*, **2004** 2052-2053

that are structurally similar, allowing us to systematically probe both the effects of core-size and heteroatoms on columnar self-assembly.

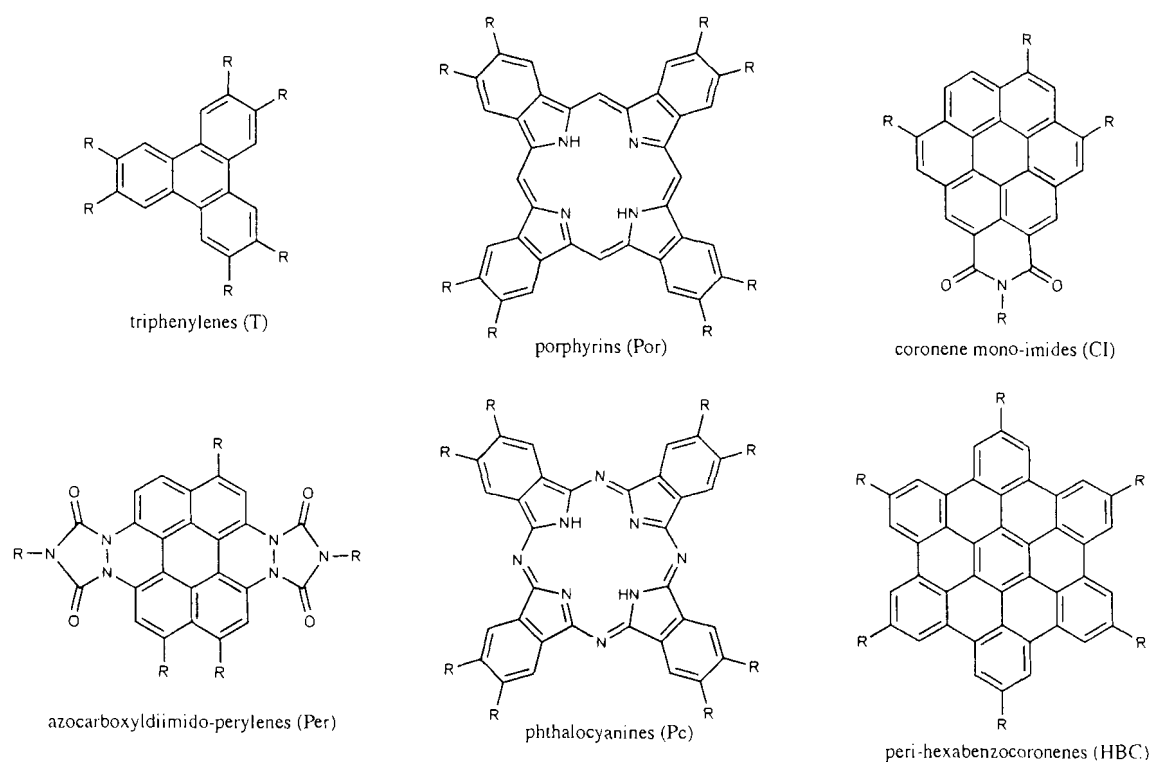
3.2 Core-Size and Phase Behaviour Relationships

In general, the columnar phases formed by discotic mesogens with large aromatic cores tend to exhibit both greater ordering and broader temperature ranges over which they are stable.^{59,60} As the charge-carrier mobility has been shown to be related to the size of the aromatic core, larger cores are desirable for many semiconducting applications.⁶⁰ Photovoltaic applications require a high extinction coefficient over a broad range of the visible spectrum, which can also be achieved by enlarging the aromatic core.^{60,114} Larger disks are expected to exhibit an improved self-ordering due to the extended π -area, which promotes π -stacking and higher order. Higher order has been used extensively to improve performances in organic semiconductors.¹¹⁶⁻¹²¹

Two recent papers have attempted to relate core-size to phase behaviour. Van de Craats and colleagues investigated phase behaviour and charge mobility as it relates to increasing core-size.⁶⁰ The core sizes studied ranged from triphenylenes up to peri-hexabenzocoronenes (Figure 3.1). In general, it was observed that increased core-size tended to enhance cohesion between the aromatic cores and hence led to an increased temperature at which the Col mesophase was stable (*i.e.* higher T_c) (Table 3.1). It should be noted that the constitution of the cores that were compared varied drastically, with a wide range of heteroatoms, sizes, symmetries and shapes. As will be seen later in this chapter, the presence and position of heteroatoms on the core does have an

appreciable effect on the self-assembly of discotic mesogens. Furthermore, we have shown in the previous chapter that both shape and symmetry have an impact on crystal-to-liquid crystal and liquid crystal-to-isotropic temperatures (see Chapter 2). As such, it is unclear to what extent the trends observed for this collection of molecules can be ascribed to size effects alone.

Figure 3.1: Previously reported molecular structures of macrocycles forming the cores of discotic materials.



Adapted from Van de Craats.⁶⁰

Table 3.1: Average phase transitions for core-size series reported by van de Craats and Warman.

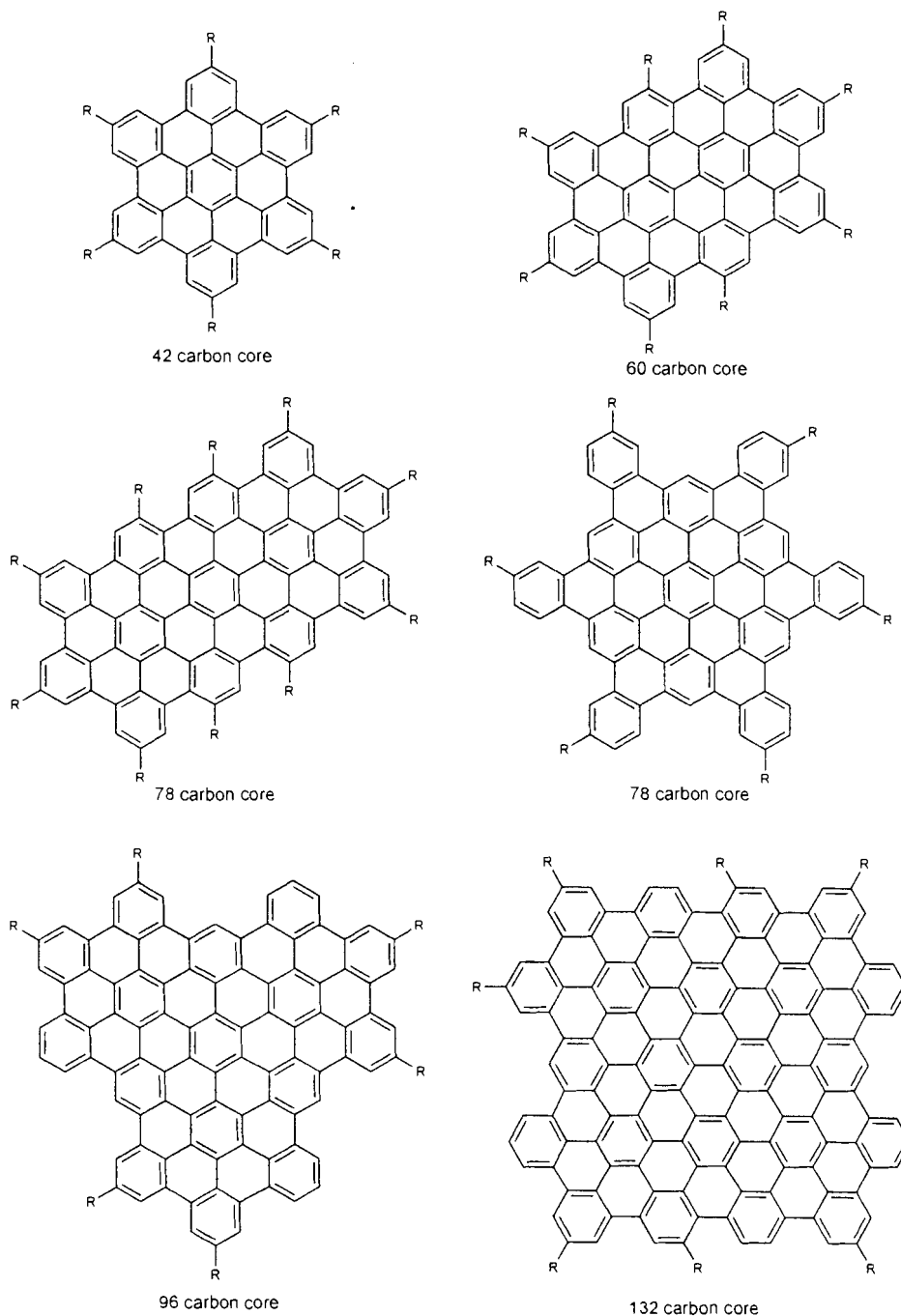
Core	Core-size [n]	Number of Compounds	Average Phase Transition Temperature [°C]	
			Cr - Col _H	Col _H - I
T	18	6	70	100
Por	24	5	96	135
Cl	29	1	113	161
Per	34	3	53	>200
Pc	40	16	97	~300
HBC	42	3	112	>400

Adapted from Van de Craats.⁶⁰ Core-size refers to the total number of C, O and N atoms in the core.

The most systematic investigation of core-size was carried out by Müllen and co-workers, who prepared a series of polycyclic aromatic hydrocarbons based on the hexabenzocoronene core that ranged in size from 42 carbons up to 132 carbons in their core (Figure 3.2).⁵⁹ These compounds showed a strong dependency of the intercolumnar packing dimensions on the aromatic core-size, the side chain length and the number of side chains. Also, increasing core-size had a large effect on whether the molecules formed a mesophase; molecules with much larger cores (>78 carbons) are non-mesogenic, regardless of the alkyl chain length substitution (Table 3.2). It should also be noted that the increase in both phase transitions is also associated with an increase in molecular symmetry (from 2 to 6 or 3 to 6 fold symmetry). The drawback of this series of compounds lies in the large step size between molecules (18-36 carbon incremental changes). The large differences between molecules in the series makes comparison between molecules difficult, as acknowledged by Müllen. Moreover,

molecular symmetry also varies with the series, further complicating interpretation of the results.

Figure 3.2: Structures of previously reported hexa-*peri*-hexabenzocoronene based disc shaped molecules.



Adapted from Müllen.⁵⁹

Table 3.2: Average phase transitions for mesogenic molecules in hexa-peri-hexabenzocoronene core series reported by Müllen and co-workers.

Core-size [n]	Number of Compounds	Average Phase Transition Temperature [°C]	
		Cr \Rightarrow Col _H	Col _H \Rightarrow I
42	9	88	380
60	2	104	>450
78	2	87	>450
96	7	Not observed	Not observed
132	2	Not observed	Not observed

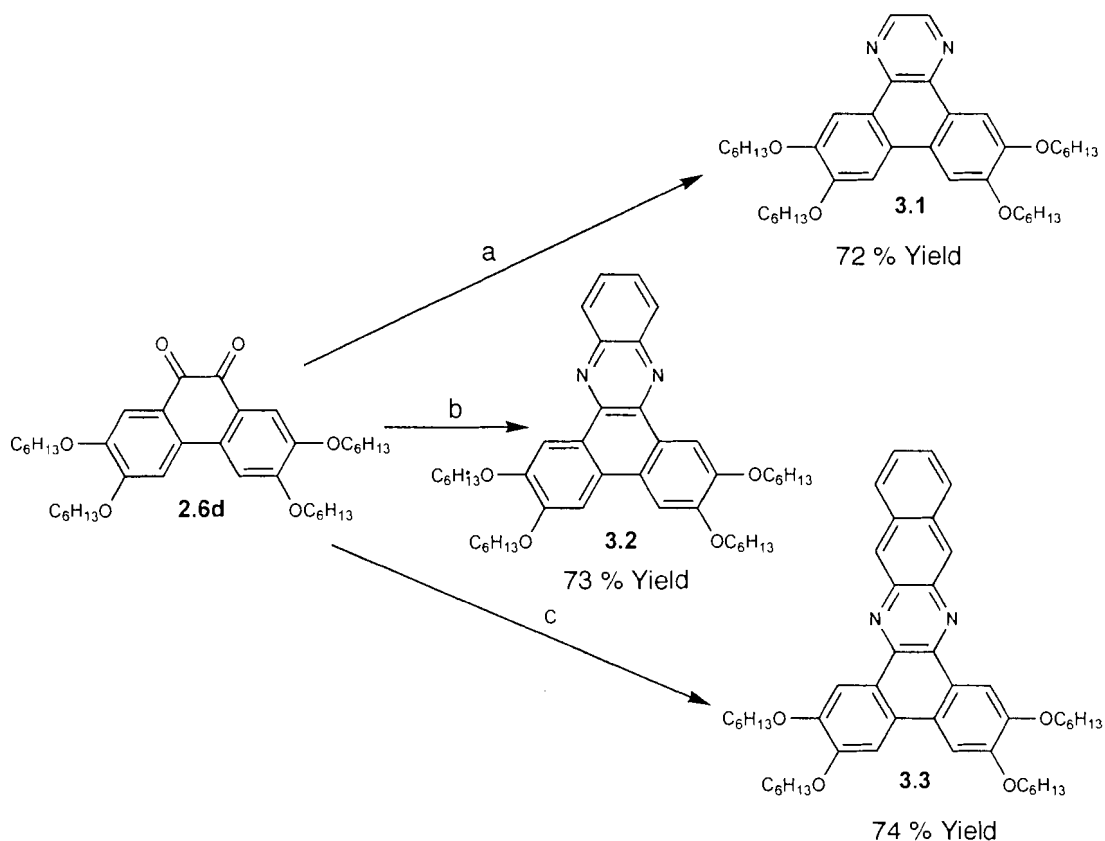
Adapted from Müllen.⁵⁹ Core-size refers to the total number of carbon in the core.

In order to investigate the effect of small changes in core-size, a series of molecules with systematically increasing core-size, composed of four, five and six rings were prepared (Scheme 3.1). These small changes, combined with keeping chain length and molecular symmetry the same should allow us to see the effect of increasing core-size. The molecules targeted could be readily prepared from the condensation of a common precursor (**2.6d**) with appropriate 1,2-diamines.

3.2.1 Core-Size Results and Discussion

Compounds **3.1**, **3.2** and **3.3**, were prepared via condensation of compound **2.6d** with 1,2-ethylenediamine, 1,2-phenylenediamine and 3,4-diaminonaphthalene on heating in acetic acid. The phase behaviour was characterized by POM and DSC and, in the case of compound **3.3**, XRD.

Scheme 3.1: Synthetic route to core-size series.



Reagents and conditions. a) 1,2-ethylenediamine, AcOH, b) 1,2-phenylenediamine, AcOH, c) 3,4-diaminonaphthalene, AcOH.

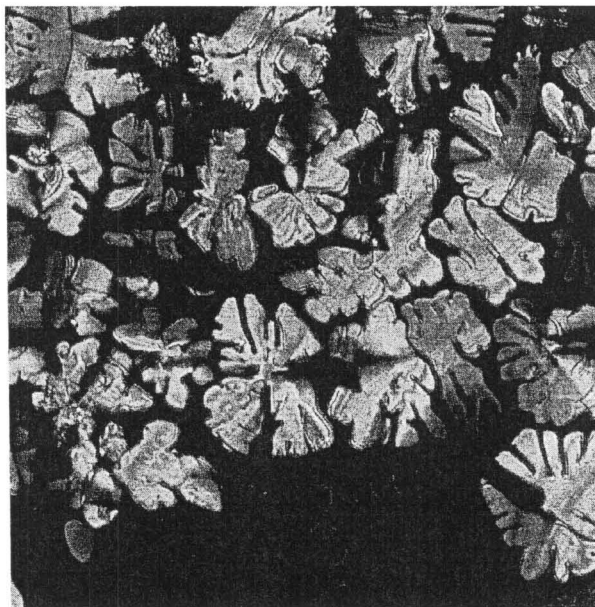
The trends in phase behaviour, as summarized below, demonstrated that even relatively small changes in the core structure can have a dramatic impact on the ability of the molecules to form liquid crystalline phases (Table 3.3). Although the two smaller members of this series, **3.1** and **3.2**, are nonmesogenic, the naphthalene derivative **3.3** was liquid crystalline over a relatively large temperature range (123-172 °C). This implies that increased core-size leads to a greater propensity to form columnar phases, which is consistent with earlier

observations that discotic mesogens with large cores tend to be liquid crystalline over broad temperature ranges.^{59,60,87,95,103,105,122-125}

Table 3.3: Phase behaviour of compounds 3.1, 3.2 and 3.3.

	Phase	$T_i/^\circ\text{C}$ ($\Delta H/\text{J g}^{-1}$)	Phase
3.1	Cr	$\xrightarrow{86.1 (1.3)}$ $\xleftarrow{65.0 (-0.9)}$	I
3.2	Cr	$\xrightarrow{170.0 (101.8)}$ $\xleftarrow{140.1 (-108.2)}$	I
3.3	Cr	$\xrightarrow{122.5 (77.7)}$ $\xleftarrow{75.6 (-65.1)}$	Col _{ho}
			$\xrightarrow{171.5 (7.4)}$ $\xleftarrow{167.6 (-6.9)}$ I
		$a = 19.3 \text{ \AA}$	

Figure 3.3: Polarized optical photomicrograph of compound (3.3) at 167 °C.



The effect of core-size on the mesogenic behaviour can be understood in terms of the interactions between neighbouring molecules within a columnar phase. Current models of π - π interactions indicate that electrostatic and

dispersion forces are the most important contributors to the overall energy of most π -stacked structures.¹²⁶⁻¹³⁸ Since dispersion forces are favoured by both increased surface area and higher polarizability, it is reasonable that larger compounds, such as compound **3.3**, show a greater tendency to π -stack and hence to assemble into columnar liquid crystalline phases.

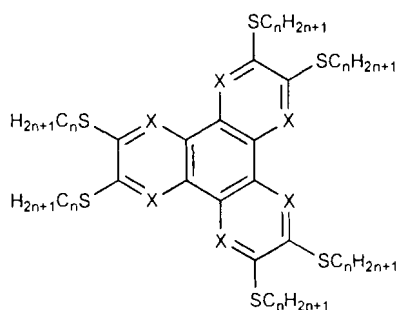
3.3 Heteroatoms in the Core

Although there is some evidence to suggest that the presence of heteroatoms can alter the strength and geometry of π -stacked dimers in solution,^{133,139-141} it is unclear how the introduction of nitrogen atoms will perturb the thermodynamic stability of extended columnar structures. This question has important implications not only for the design of new liquid crystalline materials, but also for understanding the self-assembly of π -stacked structures such as DNA and RNA, where the factors that govern base-stacking remain a matter of some debate.^{131,142-144}

There are only a few examples of molecules in which both a discotic *N*-heterocycle and the corresponding hydrocarbon have been investigated, and in all of those cases several CH groups were replaced with nitrogen atoms. In the case of the thioethers **Tha** and **Thb**, the introduction of nitrogen atoms has a deleterious effect on the phase behaviour (Table 3.4). However, the triphenylene derivatives in series **Tha** form columnar phases and members of series **Thb** are nonmesogenic. These two series have not been previously compared; the triphenylene series was reported by Praefcke and co-workers^{41,42} while the

hexaazatriphenylenes were reported by Geerts.¹¹⁵ It should be noted that the lack of liquid crystallinity for these hexaaza-compounds cannot necessarily be attributed to a destabilization of their hypothetical columnar phases. These compounds melt at temperatures higher than the clearing temperatures of the corresponding triphenylene derivatives. Thus, as Geerts and coworkers point out, the failure to observe mesophases for series **Thb** might simply be due to the greater lattice energy of their crystalline solid phases.

Table 3.4: Phase behaviour of previously reported thioethers of triphenylene and hexaazatriphenylene.



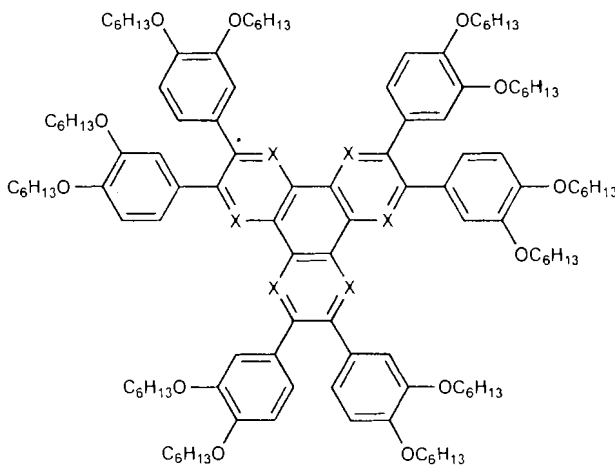
Compound	Phase	$T_i/^\circ\text{C}$	Phase
Tha6 (X=CH, n=6)	Cr	62	Col _{ho} \rightleftharpoons Col _{hd} \rightleftharpoons I
Tha8 (X=CH, n=8)	Cr	55	Col _{hd} \rightleftharpoons I
Tha10 (X=CH, n=10)	Cr	40	Col _n \rightleftharpoons I
Thb6 (X=N, n=6)	Cr	106	I
Thb8 (X=N, n=8)	Cr	93	I
Thb10 (X=N, n=10)	Cr	74	I

Tha reported previously by Praefcke.^{41,42} **Thb** reported previously by Geerts.¹¹⁵

In contrast, both the hexaphenyl-triphenylene **Tpa**¹⁰³ and the hexaphenyl-hexaazatriphenylene, **Tpb**,^{123,145} derivatives exhibit columnar phases, but the

clearing temperature of nitrogen containing **Tpb** was found to be much higher than that of **Tpa**, suggesting that the presence of the nitrogen atoms stabilizes the mesophases (Table 3.5).

Table 3.5: Phase behaviour of previously reported triphenylenes and hexaazatriphenylenes.



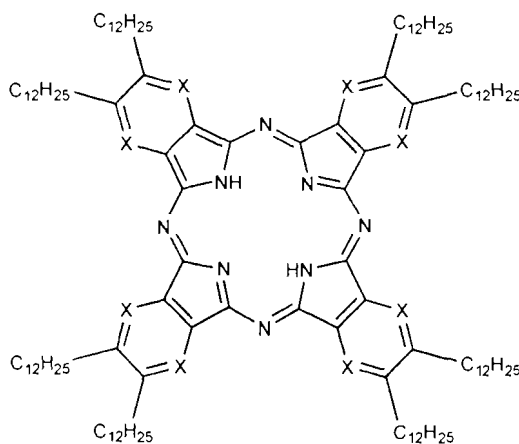
Compound		Phase	$T_i/^{\circ}\text{C}$ ($\Delta H/\text{J g}^{-1}$)	Phase
Tpa	X=CH	Cr	$\xrightleftharpoons{111}$	Col _h
			$\xrightleftharpoons{126}$	I
Tpb	X=N	Cr	$\xrightleftharpoons{65 (1.3)}$	Col _h
			$\xrightleftharpoons{135 (12.5)}$	I

Reported previously **Tpa**¹⁰³ and **Tpb**.^{123,145}

Ohta has reported that replacing the benzene rings of a peripherally substituted phthalocyanine **PcA**, with pyrazine rings to afford the tetrapyrazinophyrazine **PcB** has very little effect on the mesophase behaviour (Table 3.6).^{146,147} Although both exhibit broad mesophases, the nitrogen containing **PcB** has a slightly depressed clearing temperature relative to the

hydrocarbon analogue, indicating that the former mesophase is more stable than that of the latter.

Table 3.6: Phase behaviour of previously reported phthalocyanine and tetrapyrazinophyrazine.



Compound	Phase	$T_i, ^\circ\text{C}$	Phase
PcA X = CH	Cr	120	Col _h
		252	I
PcB X = N	Cr	118	Col _{hd}
		238	I

Previously reported by Ohta.^{146,147}

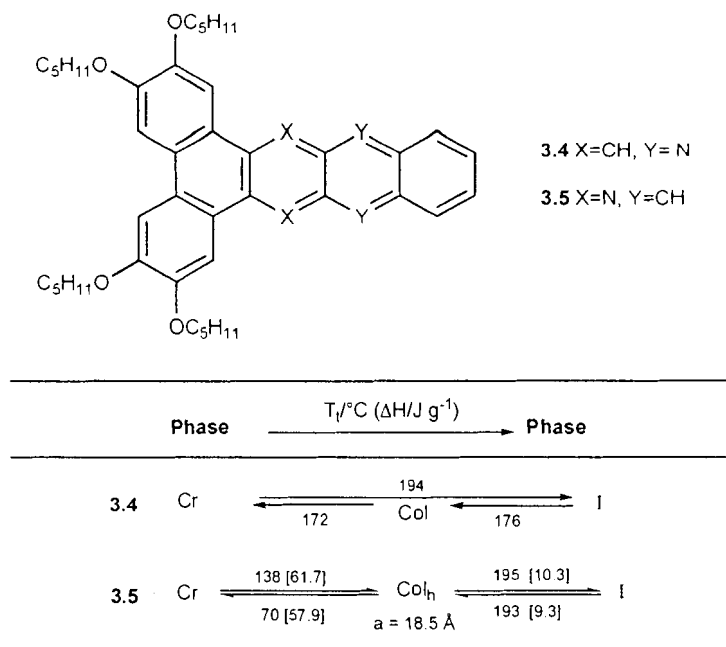
These seemingly contradictory results highlight the sensitivity of the self-assembly process to the presence and position of heteroatoms. The previous three examples also illustrate that research up to this point has focused on large changes, resulting in compounds in which 6 or 8 CH groups are replaced with nitrogen atoms. These large changes make direct comparison difficult. We have therefore undertaken further experimental studies, in which much smaller

modifications to the core are introduced in order to help elucidate the magnitude of these effects.

3.3.1 Heteroatom Results and Discussion

Kumar and co-workers have recently reported that the triphenylene derivative **3.4** cools into a narrow monotropic columnar phase between 176 °C and 172 °C.¹⁴⁸ The core of compound **3.4** is structurally similar to compound **3.3** but the nitrogen atoms are located in different positions within the molecule. This similarity provides a unique opportunity to probe the effect of nitrogen position on mesophase behaviour. However, these two compounds cannot be directly compared since the side chains are of different lengths. To this end, the tetrakis(pentyloxy) analogue of compound **2.6** was synthesized and coupled with 2,3-diaminonaphthalene to afford compound **3.5**, which is an isomer of compound **3.3** (Figure 3.4).

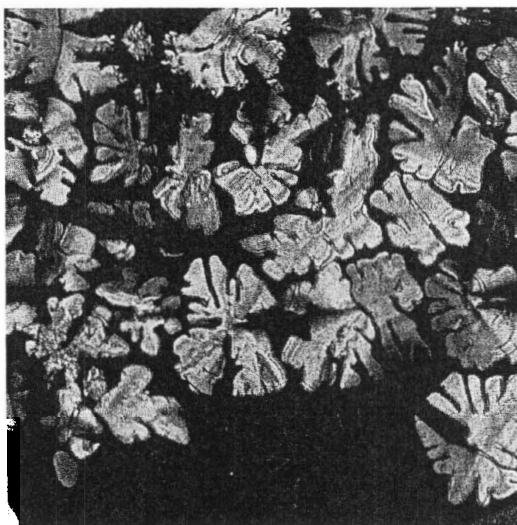
Figure 3.4: Structure and phase behaviour of compounds (3.4) and (3.5).



Compound **3.4** was reported by Kumar et al.¹⁴⁸

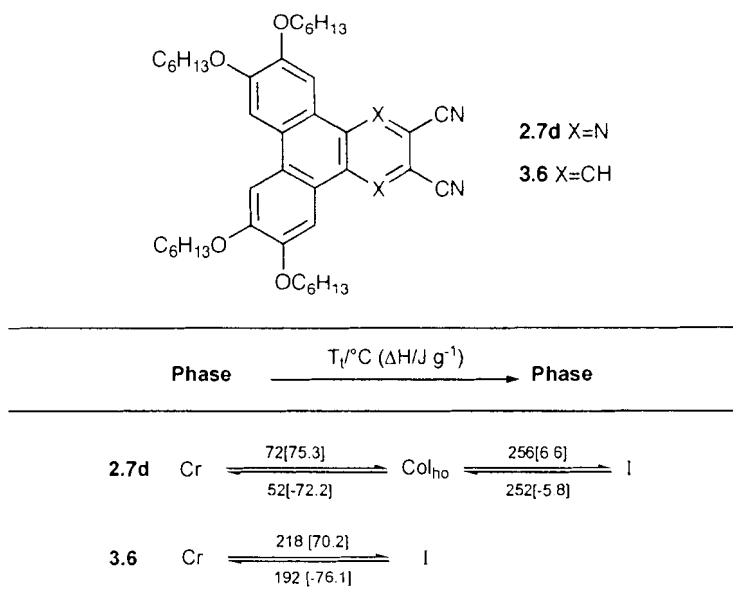
Compound **3.5** forms a broad enantiotropic mesophase between 138 °C and 195 °C which was identified as a Col_h phase on the basis of XRD and POM studies. This result suggests that there is an appreciable effect arising from changing the position of the core heteroatoms. Compound **3.4** forms only a kinetically stable monotropic phase, whereas compound **3.5** forms a thermodynamically stable enantiotropic phase that is observed on both heating and cooling. Moreover, the columnar phase of compound **3.5** persists to a considerably higher temperature than the clearing temperature of **3.4**, indicating that the mesophase of the former is much more stable.

Figure 3.5: Polarized optical micrograph of compound (3.5) at 137 °C.



In the previous chapter, it was reported that the dicyano compound **2.7d** is liquid crystalline over an extremely broad temperature range despite its relatively small core size. We were therefore interested to note that Cammidge had reported the synthesis of compound **3.6** but had not examined the mesophase behaviour.⁸⁷ In collaboration with this group, we examined the phase properties of this triphenylene, which surprisingly was found to melt directly from a crystalline solid into an isotropic liquid at 218 °C (Figure 3.6).

Figure 3.6: Structure and phase behaviour of compounds (**2.7d**) and (**3.6**).



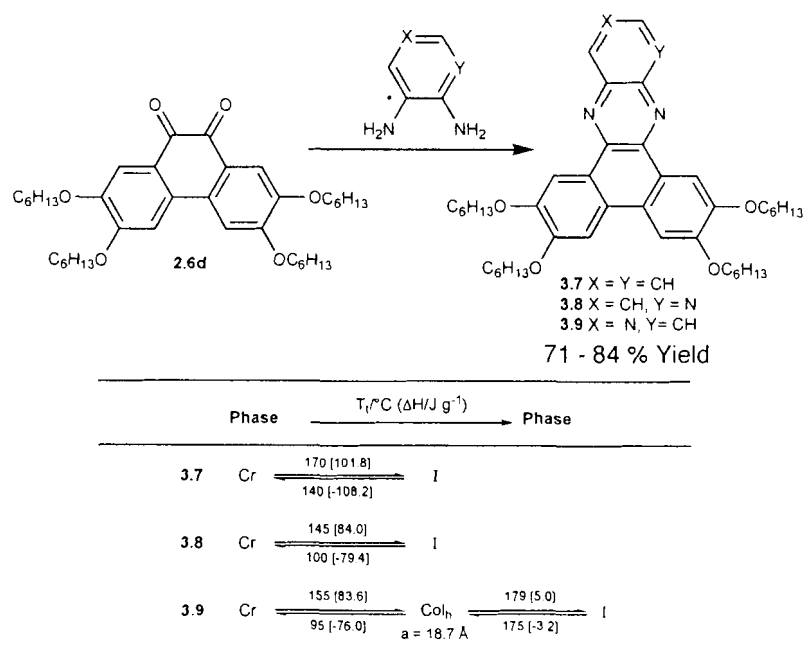
Compound **3.6** was synthesized in collaboration with Dr. Andrew Cammidge and Hemant Gopee.

The failure of this compound to form a liquid crystalline phase was unexpected, not only because of its close similarity to compound **2.7d**, but also because the introduction of strongly dipolar functional groups often favours the formation of highly stable columnar phases.^{65,149} The differences between compounds **2.7d** and **3.6** indicate that, while the presence of the cyano groups may be essential to the existence of a mesophase for **2.7d**, these groups cannot be solely responsible for the mesogenicity of this compound. The contribution of the nitrogen atoms appears to be also very important.

To further probe the extent to which heteroatoms are capable of altering liquid crystalline behaviour, we next turned to a series of disc-shaped molecules prepared by condensation of compound **2.6d** with 1,2-phenylenediamine, 2,3-diaminopyridine and 3,4-diaminopyridine (compounds **3.7**, **3.8** and **3.9**, respectively) (Figure 3.7). This series of compounds permitted us to study the

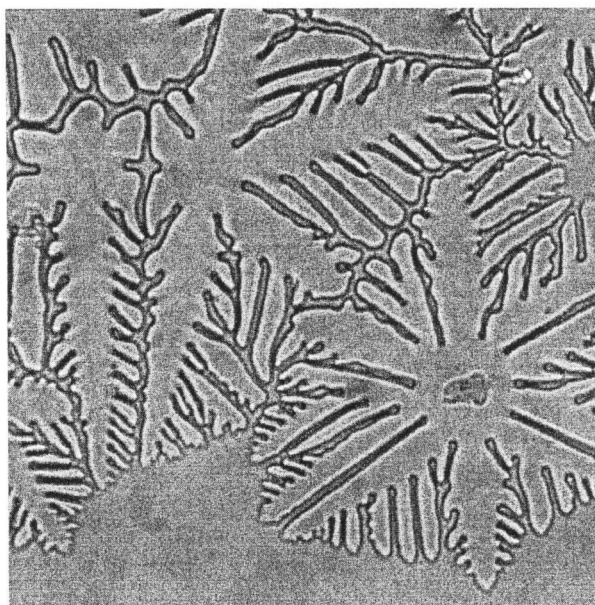
effects of introducing a single nitrogen atom into the core (i.e. compound **3.7** versus **3.8** and **3.9**) and to determine whether changing the position of this heteroatom (i.e. compound **3.8** versus **3.9**) would also appreciably alter the phase properties.

Figure 3.7: Synthesis and phase behaviour of compounds (3.7-3.9).



Neither **3.7** nor **3.8** were liquid crystalline at any temperature, but instead melted directly into isotropic liquids at 170 °C and 145 °C, respectively. In contrast, the pyridine derivative **3.9** formed a liquid crystal phase between 155 and 179 °C.

Figure 3.8: Polarized optical micrograph of compound 3.9 at 177 °C.



Examination of this phase by POM revealed the characteristic dendritic texture of a columnar phase (Figure 3.12). This assignment was confirmed by X-ray diffraction (XRD) studies, which were consistent with a columnar hexagonal phase (Col_h) having an intercolumnar spacing of 18.7 Å. The XRD of compound 3.9 showed a single peak in the low angle region that was identified as a (100) reflection. Unfortunately, since no (110) peak could be detected for compound 3.9, it was not possible to make an unambiguous assignment on the basis of the available XRD data. Many of the dendritic textures observed by POM exhibit approximately six-fold symmetry, which is consistent with a hexagonally-ordered phase.

Thus, while the introduction of a nitrogen atom *may* encourage columnar phases, its position is also an important consideration, as demonstrated by the failure the isomer of compound 3.9, compound 3.8, to exhibit any liquid crystallinity.

The ability of small perturbations in core structure to induce dramatic changes in phase behaviour likely reflects the varying strength of π - π interactions between neighbouring molecules within the columns. As already noted, both dispersion forces and electrostatic interactions are known to make significant contributions to the stability of π -stacked structures.^{130,133,134,137-139,141} However, changes in dispersion forces cannot be responsible for the observed trends in the case of heteroatom effects, since replacing a CH group with a nitrogen atom would slightly *reduce* the molecular polarizability, which would in turn decrease the strength of the dispersion forces between adjacent cores. The stronger tendency of aza-aromatic molecules to form ordered π -stacked structures therefore suggests that other types of interactions dominate in these systems. This is further supported by the observation that pairs of isomers, such as **3.8/3.9** or **3.4/3.5**, which have nearly identical polarizabilities, nonetheless exhibit very different tendencies to organize into columnar mesophases.

Electrostatic interactions between molecules within a column are expected to be strongly dependent on the distribution of positive and negative charges within the molecules' aromatic cores. The introduction of nitrogen atoms will tend to polarize the electronic distribution of the molecules, which could in turn lead to a favourable alignment of complementary charges on neighbouring molecules, hence promoting π - π interactions. This argument is also consistent with the strong observed dependence on the position of the core heteroatoms.

An additional factor that may contribute to these marked heteroatom effects is the shape of the molecules under investigation. Unlike most discotic

mesogens, which have C3-, C4- or C6-symmetric cores surrounded on all sides by flexible side chains, compounds **3.4-3.9** are low symmetry molecules with alkyl chains extending from only two of the three “edges” of the core. As a result, these molecules likely adopt an antiparallel orientation within the columns in order to assemble into hexagonally ordered phases.^{59,150} Indeed, the intercolumnar spacings obtained from XRD experiments are consistent with this model. Such a packing arrangement would impose a significant constraint on the manner in which neighbouring cores interact with one another and could explain their sensitivity to small structural changes. Moreover, the placement of heteroatoms within the core will alter its dipole moment, which is known to play an important role in the stabilization of antiferroelectrically ordered columnar phases, as will be discussed later (see Chapter 4 and 5).^{65,95,149}

3.4 Summary

The ability to make small structural changes has enabled the elucidation of the propensity of this class of discotic mesogens will form liquid crystalline phases. The effect of core-size on the mesogenic behaviour can be understood in terms of the interactions between neighbouring molecules within a columnar phase, with dispersion forces being favoured by the increased surface areas of larger core molecules.

In the case of different positioning of nitrogen atoms in the core, it is likely that electrostatic interactions have a greater role in determining whether or not the interaction between different molecules are favourable or not.

3.5 Experimental*

For general experimental see Chapter 2. All solvents employed were reagent grade. 1,2-Phenylenediamine, 3-4-diaminopyridine, 2-3-diaminopyridine, 3-4-diaminonaphthalene and 1-bromopentane were purchased from Aldrich and used without further purification.

General procedure for the synthesis of compounds **3.1-3.3**, **3.5**, **3.7-3.9**.

A solution of 2,3,6,7-tetrakis(hexyloxy)-phenanthrene-9,10-dione (80 mg, 0.13 mmol) and the appropriate 1,2-diamine (0.52 mmol) were heated at reflux in acetic acid (15 mL) for 12 hours. Upon cooling, water (150 mL) was added and the mixture extracted with CH₂Cl₂ (3 x 25 mL). The CH₂Cl₂ extracts were combined, washed with water, dried (MgSO₄), filtered, and evaporated under reduced pressure. The resultant solid was eluted through a short plug of silica with dichloromethane and then purified by column chromatography (silica gel, 1:1 CH₂Cl₂:hexanes gradient to 100% CH₂Cl₂ as eluent). The product was recrystallized from a mixture of CH₂Cl₂ and methanol to afford the dibenzo[a,c]phenazine derivative.

6,7,10,11-Tetrakis-hexyloxy-dibenzo[f,h]quinoxaline (3.1) was synthesized by the condensation of compound **2.6d** and 1,2-ethylenediamine to afford a yellow solid (72%). ¹H NMR (400 MHz) (CDCl₃) δ (ppm) 8.77 (s, 2H), 8.55 (s, 2H), 7.73 (s, 2H), 4.24-4.28 (m, 8H), 1.93-1.98 (m, ~8H), 1.35-1.60 (m,

* Compound **3.6** was synthesized in collaboration with Dr. Andrew Cammidge and Hemant Gopee.
Compounds **3.7**, **3.8** and **3.9** were characterized with the help of C. Lavigueur.

~24H), 0.91-0.95 (m, ~12H); ^{13}C NMR (125 MHz) (CDCl_3) δ (ppm) 151.1, 149.4, 141.9, 125.7, 123.5, 107.2, 105.8, 69.5, 68.9, 31.6, 29.3, 29.2, 25.7, 22.6, 14.0, 14.0; Elemental analysis: calc. (found) for $\text{C}_{40}\text{H}_{58}\text{N}_2\text{O}_4$: C, 76.15 (76.49); H, 9.27 (9.35); N, 4.44 (4.24). MALDI-TOF calc. (found): 727 (727).

2,3,6,7-Tetrakis-hexyloxy-dibenzo[a,c]phenazine (3.2). Compound **2.6d** and 1,2-phenylenediamine were condensed according to method described above to afford **3.2** as a yellow solid (73%). ^1H NMR (400 MHz) (CDCl_3) δ (ppm) 8.81 (s, 2H), 8.32 (d, 2H $J_{12} = J_{34} = 3$ Hz, $J_{23} = 7$ Hz), 7.81 (dd, 2H $J_{12} = J_{34} = 3$ Hz, $J_{13} = J_{24} = 7$ Hz), 7.75 (s, 2H), 4.26-4.39 (m, 8H), 1.94-2.02 (m, ~8H), 1.37-1.65 (m, ~24H), 0.92-0.97 (m, ~12H); ^{13}C NMR (125 MHz) (CDCl_3) δ (ppm) 152.0, 149.5, 129.3, 129.2, 128.7, 128.7, 128.7, 126.7, 108.8, 106.3, 69.6, 69.2, 31.6, 29.2, 29.2, 25.8, 25.7, 22.6, 22.6, 14.0, 14.0; Elemental analysis: calc. (found) for $\text{C}_{44}\text{H}_{60}\text{N}_2\text{O}_4$: C, 77.61 (77.56); H, 8.88 (8.86); N, 4.11 (3.94). MALDI-TOF calc. (found): 681 (682 M+1).

2,3,6,7-Tetrakis-hexyloxy-9,16-diaza-dibenzo[a,c]naphthacene (3.3)
Synthesized by the condensation of compound **2.6d** and 2,3-diaminonaphthalene, yielding a yellow solid (74%). ^1H NMR (400 MHz) (CDCl_3) δ (ppm) 8.91 (s, 2H), 8.83 (s, 2H), 8.13-8.15 (m, 2H), 7.53-7.58 (m, 4H), 4.22-4.35 (m, 8H), 1.94-2.00 (m, ~8H), 1.39-1.64 (m, ~24H), 0.93-0.98 (m, ~12H); ^{13}C NMR (125 MHz) (CDCl_3) δ (ppm) 152.0, 149.3, 143.0, 138.2, 137.8, 133.5, 128.3, 126.7, 126.0, 123.5, 109.0, 106.4, 69.5, 69.1, 31.6, 29.2, 25.8, 25.7, 22.6,

22.6, 14.0; Elemental analysis: calc. (found) for $C_{48}H_{62}N_2O_4$: C, 78.86 (78.51); H, 8.55 (8.35); N, 3.83 (3.70). MALDI-TOF calc. (found): 730 (730).

1,2-Bis-(3,4-bis-pentyloxy-phenyl)-ethane-1,2-dione

Synthesized via the alkylation of 1,2-bis(3,4-dihydroxyphenyl)ethane-1,2-dione with 1-bromopentane, according to the method described for compound **2.1c** in Chapter 2. The resultant solid was passed through a silica gel column using 1:4 ethyl acetate:hexanes as eluant. The solid was then recrystallized in $CHCl_3$ and hexanes to yield a white solid (64%). 1H NMR (400 MHz) ($CDCl_3$) δ (ppm) 7.56 (d, 2H $J = 2$ Hz), 7.43 (dd, 2H $J = 2, 8$ Hz), 6.86 (d, 2H $J = 8$ Hz), 4.02-4.07 (m, 8H), 1.93-1.98 (m, ~8H), 1.35-1.60 (m, ~16H), 0.91-0.95 (m, ~12H); ^{13}C NMR (125 MHz) ($CDCl_3$) δ (ppm) 194.0, 194.015, 155.2, 149.5, 126.4, 126.3, 126.3, 112.5, 111.8, 111.7, 69.4, 69.3, 29.0, 28.8, 28.4, 28.3, 22.7, 22.6, 14.3, 14.2; Elemental analysis: calc. (found) for $C_{34}H_{50}O_6$: C, 73.61 (73.77); H, 9.08 (9.12). MALDI-TOF calc. (found): 554 (554).

2,3,6,7-Tetrakis-pentyloxy-phenanthrene-9,10-dione

Synthesized via the oxidative cyclization of 1,2-bis-(3,4-bis-pentyloxy-phenyl)ethane-1,2-dione using VOF_3 , $BF_3 \cdot Et_2O$ in dry CH_2Cl_2 , according to the method for compound **2.6c** in Chapter 2. The resulting solid was passed through a silica gel column using 1:10 ethyl acetate:hexanes as eluant. The solid was then recrystallized in CH_2Cl_2 and hexanes to yield a red solid (92%). 1H NMR

(400 MHz) (CDCl_3) δ (ppm) 7.53 (s, 2H), 7.10 (s, 2H), 4.19 (t, 4H $J = 7$ Hz), 4.07 (t, 4H $J = 7$ Hz), 1.93-1.98 (m, ~8H), 1.35-1.60 (m, ~16H), 0.91-0.95 (m, ~12H); ^{13}C NMR (125 MHz) (CDCl_3) δ (ppm) 179.3, 155.7, 149.5, 131.3, 124.5, 113.0, 107.1, 77.5, 77.3, 77.0, 69.7, 69.3, 29.0, 28.9, 28.4, 28.362, 22.6, 14.3, 14.2; Elemental analysis: calc. (found) for $\text{C}_{34}\text{H}_{48}\text{O}_6$: C, 73.88 (73.51); H, 8.75 (8.68); MALDI-TOF calc. (found): 552 (552).

6,7,10,11-Tetrakis(hexyloxy)triphenylene-2,3-dicarbonitrile (3.6)

2,3-dibromo-6,7,10,11-tetrakis(hexyloxy)triphenylene (3.50 g, 4.45 mmol), tris(dibenzylideneacetone)dipalladium(0) (0.005 g, 4.45×10^{-5} mmol), 1,1'-bis(diphenylphosphino)ferrocene (0.006 g, 0.011 mol) were stirred in DMF at 130 °C for 30 min. $\text{Zn}(\text{CN})_2$ (0.63 g, 5.34 mmol) was added in small portions over a period of 2 h and the solution stirred at 140 °C for 48 h. The reaction mixture was then allowed to cool to room temperature and an aqueous solution of NH_4OH and NH_4Cl was added. The mixture was extracted with CH_2Cl_2 (3×100 mL) and the organic extracts were dried (MgSO_4) and concentrated *in vacuo*. The crude product was purified by column chromatography (silica, CH_2Cl_2) and recrystallisation from pentanol to give **3.6** (0.50 g, 18%) as yellow crystals. ^1H NMR (400 MHz) (CDCl_3) δ (ppm) 8.82 (s, 2 H), 7.83 (s, 2 H), 7.79 (s, 2 H), 4.22-4.30 (m, 8 H), 1.93-1.99 (m, ~8 H), 1.39-1.62 (m, ~24 H), 0.91 (t, 12 H $J = 7$ Hz); ^{13}C NMR (125 MHz) (CDCl_3) δ (ppm) 151.9, 150.1, 131.3, 129.6, 126.2, 121.1, 116.8, 110.3, 106.5, 106.3, 69.6, 31.7, 29.3, 25.8, 22.7, 14.1; Elemental analysis:

calc. (found) for $C_{44}H_{58}O_4N_2$: C, 77.57 (77.84); H, 8.67 (8.61); N, 3.93 (4.13).

FABMS m/z 678 (M^+ , 100%); Mp 218 °C.

2,3,6,7-Tetrakis-pentyloxy-9,16-diaza-dibenzo[a,b]naphthacene (3.5)

Synthesized as above, by the condensation of 2,3,6,7-tetrakis-pentyloxy-phenanthrene-9,10-dione (0.21 g, 0.38 mmol) and 2,3-diaminonaphthalene (0.30 g, 1.90 mmol), yielding a yellow solid (0.22 g, 86%). 1H NMR (400 MHz) ($CDCl_3$) δ (ppm) 8.92 (s, 2H), 8.82 (s, 2H), 8.15-8.18 (m, 2H), 7.67 (s, 2H), 7.56 (m, 2H), 4.37 (t, 4H $J = 7$ Hz), 4.28 (t, 4H $J = 7$ Hz), 1.94-2.00 (m, ~8H), 1.39-1.64 (m, ~16H), 0.93-0.98 (m, ~12H); ^{13}C NMR (125 MHz) ($CDCl_3$) δ (ppm) 128.7, 128.7, 127.2, 127.1, 126.4, 109.4, 106.8, 69.8, 69.4, 29.2, 28.6, 28.6, 22.8, 14.4, 14.4. Elemental analysis: calc. (found) for $C_{44}H_{54}N_2O_4$: C, 78.30 (78.04); H, 8.06 (8.07); N, 4.15 (4.35). MALDI-TOF calc. (found): 674 (674).

2,3,6,7-Tetrakis-hexyloxy-9,13,14-triaza-benzo[b]triphenylene (3.8)

Synthesized according to the general method described above by the condensation of compound **2.6d** and 2,3-diaminopyridine, yielding a yellow solid (71%). 1H NMR (400 MHz) ($CDCl_3$) δ (ppm) 9.26 (dd, 1H $J = 2$ Hz), 8.88 (s, 1H), 8.72-8.75 (m, 2H), 7.79 (dd, 1H $J = 4, 4$ Hz), 7.71 (d, 2H $J = 2$ Hz), 4.27-4.34 (m, 8H), 1.93-1.99 (m, ~8H), 1.39-1.61 (m, ~24H), 0.91-0.95 (m, ~12H); ^{13}C NMR (125 MHz) ($CDCl_3$) δ (ppm) 152.5, 151.8, 150.9, 148.5, 139.0, 130.1, 128.3, 127.3, 119.8, 113.5, 108.9, 106.2, 105.4, 69.6, 69.2, 31.6, 29.2, 25.7, 22.6, 13.9;

Elemental analysis: calc. (found) for $C_{43}H_{59}N_3O_4$: C, 75.73 (75.95); H, 8.72 (8.98); N, 6.16 (6.04). MALDI-TOF calc. (found): 682 (682 M+1).

2,3,6,7-Tetrakis-hexyloxy-9,12,14-triaza-benzo[*b*]triphenylene (3.9)

Synthesized according to the general method described above by the condensation of compound **2.6d** and 3,4-diaminopyridine, yielding a yellow solid (84%). 1H NMR (400 MHz) ($CDCl_3$) δ (ppm) 9.68 (s, 1H), 8.78 (d, 1H J = 5 Hz), 8.64 (d, 2H J = 7 Hz), 8.06 (d, 1H J = 6 Hz), 7.58 (s, 2H), 4.24-4.33 (m, 8H), 1.95-1.99 (m, ~8H), 1.24-1.62 (m, ~24H), 0.93-0.97 (m, ~12H); ^{13}C NMR (125 MHz) ($CDCl_3$) δ (ppm) 152.9, 152.3, 149.5, 149.3, 143.5, 127.8, 126.6, 123.0, 122.7, 109.1, 108.6, 106.1, 105.8, 69.5, 69.4, 69.1, 31.6, 29.2, 25.7, 22.6, 14.0; Elemental analysis: calc. (found) for $C_{43}H_{59}N_3O_4$: C, 75.73 (75.35); H, 8.72 (8.82); N, 6.16 (5.86). MALDI-TOF calc. (found): 681 (683 M+2).

4 SUBSTITUENT EFFECTS ON SELF-ASSEMBLY

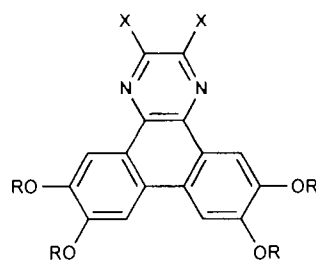
4.1 Introduction*

Despite the large number of discotic mesogens that have been prepared in the thirty years since their discovery, only a few studies have attempted to relate phase behaviour to nature of the substituent effect attached to the aromatic core.^{49,50,65,87,100,151-160} Most series of substituted discotic mesogens examined to date have been obtained by post-functionalization of an existing triphenylene core, an approach that tends to place a practical constraint on the number of compounds that can be easily prepared and that limits the scope of structure-property studies.

A comparison of the phase behaviour of compounds **2.7d** and **3.1** discussed in previous chapters revealed that the addition of two cyano groups on to the tetrahexyloxy diazatriphenylene core gave rise to a discotic molecule with a very broad liquid crystal phase (Table 4.1). The same trend was also observed with the longer chain decyloxy-derivatives (compounds **4.1** and **2.7f**).

* Portions of this chapter have been previously reported, see: a) E. J. Foster, R. B. Jones, C. Lavigueur and V. E. Williams *J. Am. Chem. Soc.*, **2006**, 128: 8569-8574 b) E. J. Foster, C. Lavigueur, Y.-K. Ke and V. E. Williams *J. Mater. Chem.*, **2005**, 15: 4062 - 4068

Table 4.1: Phase behaviour of tetraalkoxy-diazatriphenylenes.



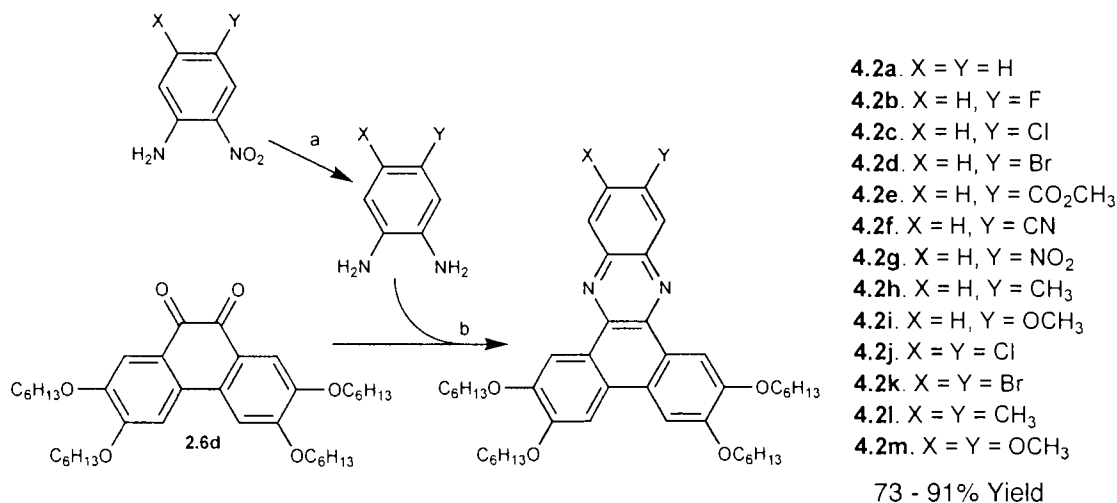
Compound		Phase	$T_i/^\circ\text{C}$	Phase
3.1	R = C ₆ H ₁₃ , X = H	Cr	86	I
4.1	R = C ₁₀ H ₂₁ , X = H	Cr	102	I
2.7d	R = C ₆ H ₁₃ , X = CN	Cr	72	Col _h $\xrightarrow{256}$ I
2.7f	R = C ₁₀ H ₂₁ , X = CN	Cr	72	Col _h $\xrightarrow{254}$ I

To further investigate the effect of substituents, a study of disc-shaped molecules derived from the coupling of a series of 1,2-diamines with 2,3,6,7-tetra(hexyloxy)phenanthrene-9,10-dione **2.6d** was undertaken. The intrinsic modularity of this synthetic approach, taken together with the large number of *ortho*-diamines available as starting materials, greatly facilitates the preparation of a broad family of potential mesogens, which should enable us to systematically probe the effects of functional groups on columnar self-assembly. Target molecules were chosen based on the availability of an appropriately substituted 1,2-phenylenediamines, which were either purchased or directly synthesized in 1-2 steps.

4.2 Synthesis

Compounds **4.2a-m** were prepared via condensation of the appropriate 1,2-diamines with compound **2.6d** on heating in acetic acid at reflux. With the exception of bromo- (**4.2d** and **4.2k**) and dimethoxy-substituted (**4.2i**) compounds, the diamines employed in this study were all either obtained commercially or prepared in one or two steps according to literature procedures (Scheme 4.1). 1,2-diamino,4,5-dimethoxybenzene was synthesized as described previously (Chapter 2).

Scheme 4.1: Synthesis of substituent series (4.2a-m) from 2,3,6,7-tetra(hexyloxy)phenanthrene-9,10-dione.

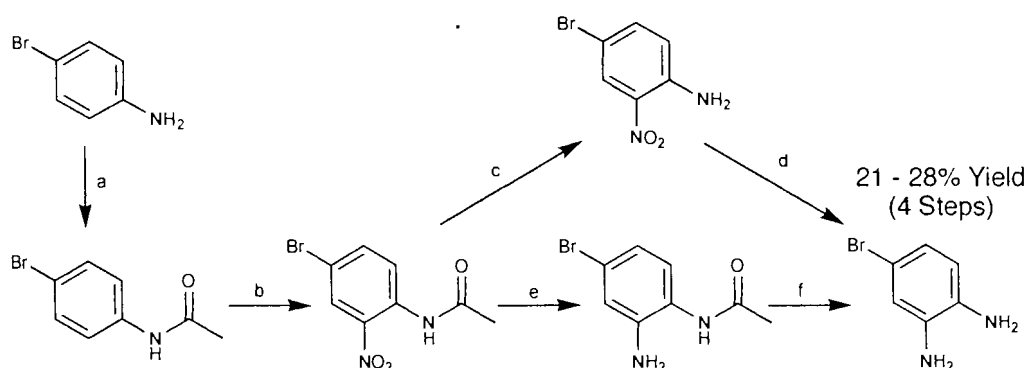


Reagents and conditions. a) N₂H₄-H₂O, Pd/C, EtOH, reflux, b) AcOH, reflux. Please note that **4.2d** was not synthesized in this manner (see text).

Synthesis of 4-bromo-1,2-diaminobenzene from 4-bromoaniline proved to be more challenging than initially envisioned. 4-Bromoaniline was first protected with an acetyl group, then nitrated in fuming nitric acid. Initial reactions showed that subsequent reduction of the nitro group using hydrazine hydrate and

palladium on carbon, either before or after the cleavage of the acetyl protecting group, led to loss of the bromine substituent. Following literature procedure for mild reduction conditions ($\text{FeCl}_3 \cdot 6\text{H}_2\text{O}$, hydrazine, MeOH),¹⁶¹ we were able to obtain the desired diamine with an average yield of 64% over 5 steps (Scheme 4.2).

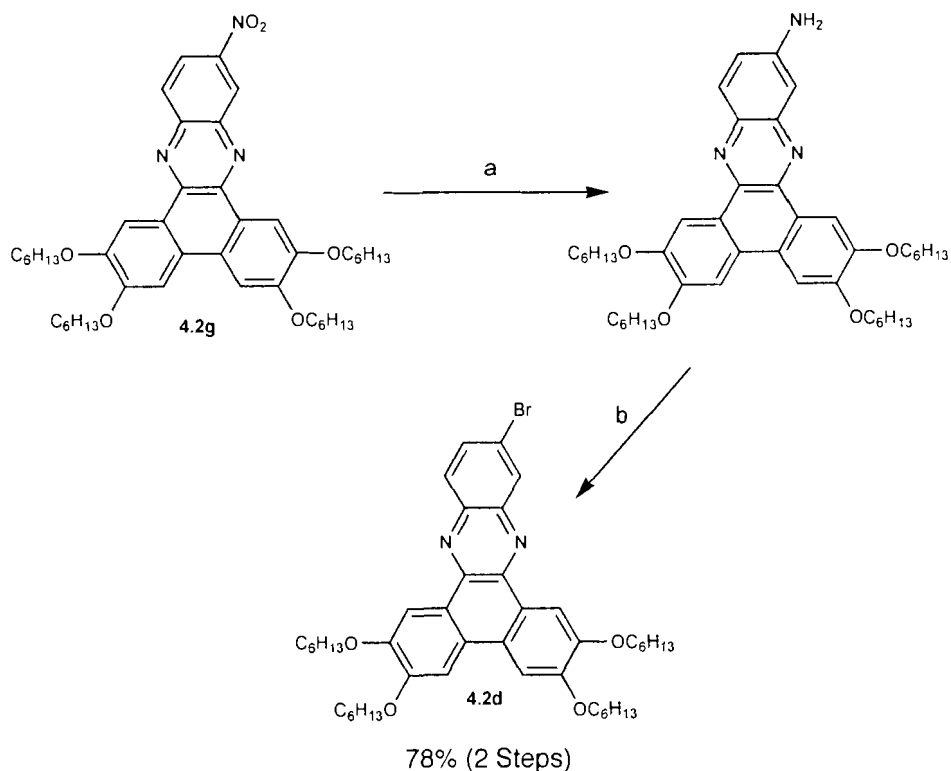
Scheme 4.2: Synthesis of 4-bromo-1,2-diaminobenzene.



Reagents and conditions. a) Ac_2O , AcOH, reflux, b) Fuming HNO_3 , c) HCl, H_2O , THF, d) $\text{N}_2\text{H}_4 \cdot \text{H}_2\text{O}$, FeCl_3 , MeOH, e) $\text{N}_2\text{H}_4 \cdot \text{H}_2\text{O}$, FeCl_3 , MeOH, f) HCl, H_2O , THF.

Unfortunately, it was found that coupling 4-bromo-1,2-diaminobenzene with compound **2.6d** under acidic conditions lead to loss of the bromine substituent and compound **4.2a** was obtained as the major product. The same result was obtained when the condensation reaction was attempted between the HCl-salt of this diamine and compound **2.6d** in ethanol in the presence of sodium acetate. This is consistent with previously reported examples of debromination in aromatic systems.¹⁶² The required brominated derivative **4.2d** was therefore synthesized instead via reduction of the nitro-derivative **4.2g** to the corresponding amine, followed by a Sandmeyer reaction to the bromine (Scheme 4.3).

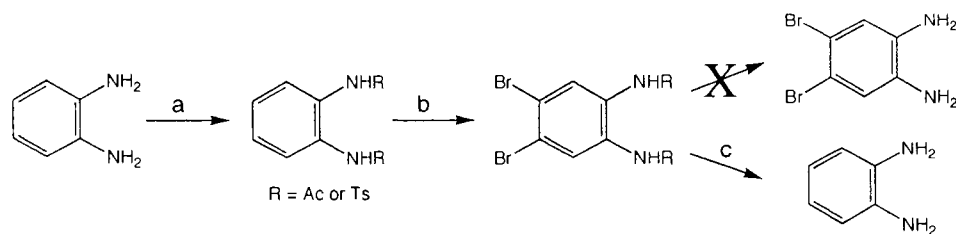
Scheme 4.3: Synthesis of compound 4.2d via a Sandmeyer reaction.



Reagents and conditions. a) N₂H₄-H₂O, Pd/C, EtOH/CH₂Cl₂, reflux, b) NaNO₂, H₂SO₄ then CuBr/HBr.

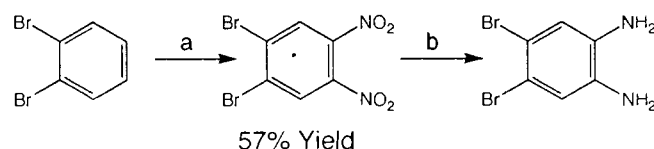
1,2-Diamino-3,4-dibromobenzene was synthesized in two steps from 1,2-dibromobenzene (Scheme 4.5). Initial reactions in which 1,2-diaminobenzene was protected with tosyl (Ts) or acetyl (Ac) groups, followed by bromination and removal of the protecting groups were not successful. Deprotection of the amines again resulted in the loss of bromine (Scheme 4.4). An alternate strategy was therefore adopted, in which 1,2-dibromobenzene was dinitrated in fuming sulphuric and nitric acid,¹⁶³ followed by reduction of the nitro groups using palladium on carbon and hydrazine hydrate to afford 1,2 diamino-4,5-dibromobenzene in 58% yield (Scheme 4.5). This product was then coupled with compound **2.6d** to give compound **4.2k**.

Scheme 4.4: Attempted synthesis of 1,2-diamino-4,5-dibromobenzene.



Reagents and conditions. a) Ac_2O or TsCl , b) Br_2 , HBr , c) H_2SO_4 .

Scheme 4.5: Synthesis of 1,2-diamino-4,5-dibromobenzene

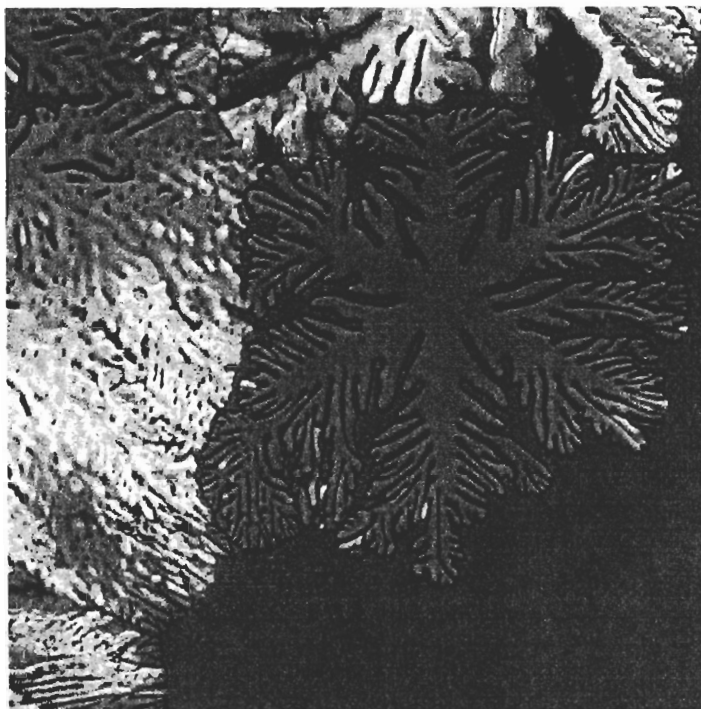


Reagents and conditions. a) fuming H_2SO_4 , fuming HNO_3 , reflux, b) $\text{N}_2\text{H}_4 \cdot \text{H}_2\text{O}$, Pd/C , EtOH , reflux.

4.3 Results

The phase behaviours of the products **4.2a-m** were examined by polarized optical microscopy (POM), differential scanning calorimetry (DSC) and variable temperature X-ray diffraction (XRD) experiments, the results of which are summarized below (Table 4.2 and Table 4.3). Compounds **4.2a**, **h**, **i**, **l**, and **m** failed to exhibit any liquid crystalline phases, but instead melted directly from crystalline solids to form isotropic liquids. The fluorinated derivative **4.2b** was not liquid crystalline on heating but forms a monotropic liquid crystal phase upon cooling from the isotropic state. On the basis of the dendritic texture observed by POM, this monotropic phase was identified as a hexagonal columnar phase (Col_h) (Figure 4.1). Unfortunately, due to the thermal instability of this phase, we were unable to confirm its identity by XRD experiments.

Figure 4.1: Polarized optical micrograph of monotropic phase of compound (4.2b) at 158 °C.



Examination of the remaining compounds by DSC revealed that each undergoes two phase transitions upon heating, which were identified by polarized optical microscopy as solid-to-liquid crystal and liquid crystal-to-isotropic liquid transitions. Samples cooled slowly into their liquid crystalline phase from the isotropic state exhibited dendritic textures when viewed by polarized optical microscopy. Representative optical micrographs are shown below (Figure 4.2). These textures are typical of columnar phases and the observation of domains with approximately six-fold symmetry suggests that these are Col_h phases. XRD experiments corroborate this assignment. Small angle X-ray diffractograms of the liquid crystalline phases of compounds **4.2f**, **4.2g** and **4.2j** each exhibited one intense peak and a second smaller peak that was indexed to the (100) and (110)

peaks of a hexagonal lattice. Each of the XRD patterns of the liquid crystalline phases **4.2c** and **4.2e** have only a single intense peak in the low of angle region that were assigned to the (100) spacings of hexagonal lattices. Broad peaks were also observed for all molecules at larger angles that correspond to distances of approximately 4.5 Å and 3.5 Å, which were attributed to the alkyl chain halo and π - π stacking distances, respectively. The presence of π - π peak in the XRD indicates that these liquid crystals are *ordered* columnar hexagonal phases (Col_{h0}).

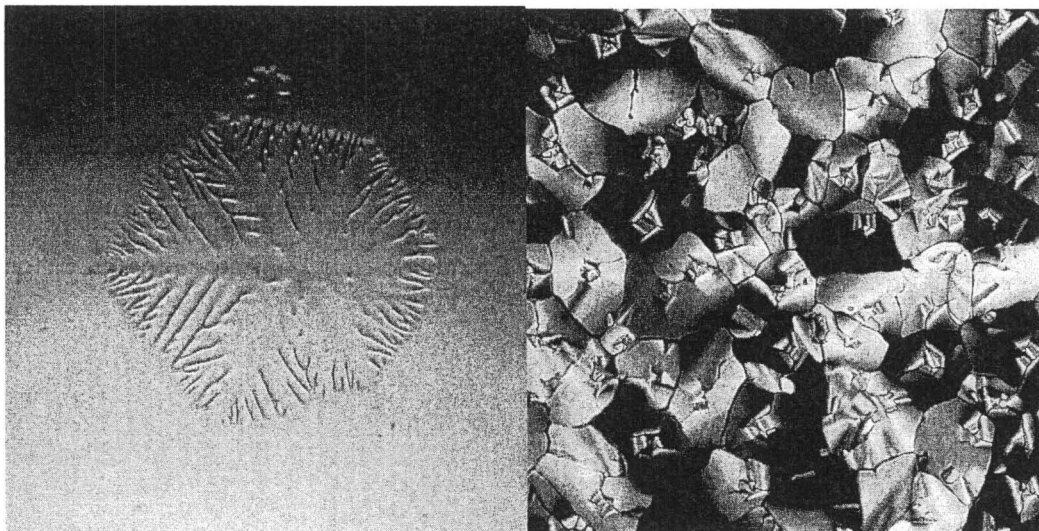
Table 4.2: Phase behaviour of compounds (4.2a-m).

Compound		Phase	$T_f/^\circ\text{C}$ ($\Delta H/\text{J g}^{-1}$)	Phase
4.2a	X = Y = H	Cr	$\xrightarrow{170.0 (101.8)}$ $\xleftarrow{140.1 (-108.2)}$	I
4.2b	X = H, Y = F	Cr	$\xrightarrow{161.3 (90.7)}$ $\xleftarrow{118.3 (-83.9)}$	Col _{ho} $\xrightarrow{154.1 (-7.6)}$ I
4.2c	X = H, Y = Cl	Cr	$\xrightarrow{137.2 (64.7)}$ $\xleftarrow{79.8 (-56.16)}$	Col _{ho} $\xrightarrow{188.4 (7.37)}$ $\xleftarrow{185.25 (-6.91)}$ I
4.2d	X = H, Y = Br	Cr ₁	$\xrightarrow{99.5 (4.0)}$	Cr ₂ $\xrightarrow{121.8 (47.5)}$ $\xleftarrow{51.3 (-23.16)}$ Col _{ho} $\xrightarrow{191.2 (5.86)}$ $\xleftarrow{186.9 (-6.42)}$ I
4.2e	X = H, Y = CO ₂ CH ₃	Cr	$\xrightarrow{111.3 (39.1)}$	Col _{ho} $\xrightarrow{200.6 (4.7)}$ $\xleftarrow{196.5 (-4.8)}$ I
4.2f	X = H, Y = CN	Cr	$\xrightarrow{101.1 (14.5)}$ $\xleftarrow{59.8 (-13.7)}$	Col _{ho} $\xrightarrow{208.2 (4.4)}$ $\xleftarrow{204.5 (-4.2)}$ I
4.2g	X = H, Y = NO ₂	Cr	$\xrightarrow{131.4 (66.5)}$ $\xleftarrow{101.59 (-53.3)}$	Col _{ho} $\xrightarrow{228.7 (7.9)}$ $\xleftarrow{226.1 (-6.6)}$ I
4.2h	X = H, Y = CH ₃	Cr	$\xrightarrow{124.5 (43.2)}$ $\xleftarrow{92.1 (-40.1)}$	I
4.2i	X = H, Y = OCH ₃	Cr	$\xrightarrow{148.5 (38.8)}$ $\xleftarrow{110.1 (-40.9)}$	I
4.2j	X = Y = Cl	Cr	$\xrightarrow{141.9 (67.4)}$ $\xleftarrow{92.9 (-68.3)}$	Col _{ho} $\xrightarrow{237.5 (9.2)}$ $\xleftarrow{234.79 (-8.3)}$ I
4.2k	X = Y = Br	Cr	$\xrightarrow{140.0 (37.8)}$ $\xleftarrow{86.1 (-41.0)}$	Col _h $\xrightarrow{225.2 (3.9)}$ $\xleftarrow{222.0 (-3.93)}$ I
4.2l	X = Y = CH ₃	Cr	$\xrightarrow{154.9 (91.6)}$ $\xleftarrow{126.5 (-95.0)}$	I
4.2m	X = Y = OCH ₃	Cr ₁	$\xrightarrow{135.8 (7.8)}$	Cr ₂ $\xrightarrow{170.5 (96.2)}$ $\xleftarrow{138.6 (-102.5)}$ I

Table 4.3: X-Ray diffraction data for liquid crystalline derivatives of (4.2).

	Temperature (°C)	d-spacing (Å)	Miller Index (<i>hkl</i>)	Phase (Lattice Const.)
4.2c	170	16.3	(100)	Col _{ho} (<i>a</i> = 18.8 Å)
		4.9	<i>alkyl halo</i>	
		3.5	π - π	
4.2e	150	17.3	(100)	Col _{ho} (<i>a</i> = 20.0 Å)
		4.3	<i>alkyl halo</i>	
		3.5	π - π	
4.2f	150	16.4	(100)	Col _{ho} (<i>a</i> = 19.0 Å)
		9.6	(110)	
		4.4	<i>alkyl halo</i>	
		3.5	π - π	
4.2g	150	16.7	(100)	Col _{ho} (<i>a</i> = 19.2 Å)
		9.3	(110)	
		4.7	<i>alkyl halo</i>	
		3.5	π - π	
4.2j	170	16.9	(100)	Col _{ho} (<i>a</i> = 19.6 Å)
		10.2	(110)	
		4.5	<i>alkyl halo</i>	
		3.5	π - π	

Figure 4.2: Polarized optical photomicrograph of compounds (4.2j) at 235°C (left) and (4.2d) at 190°C (right).



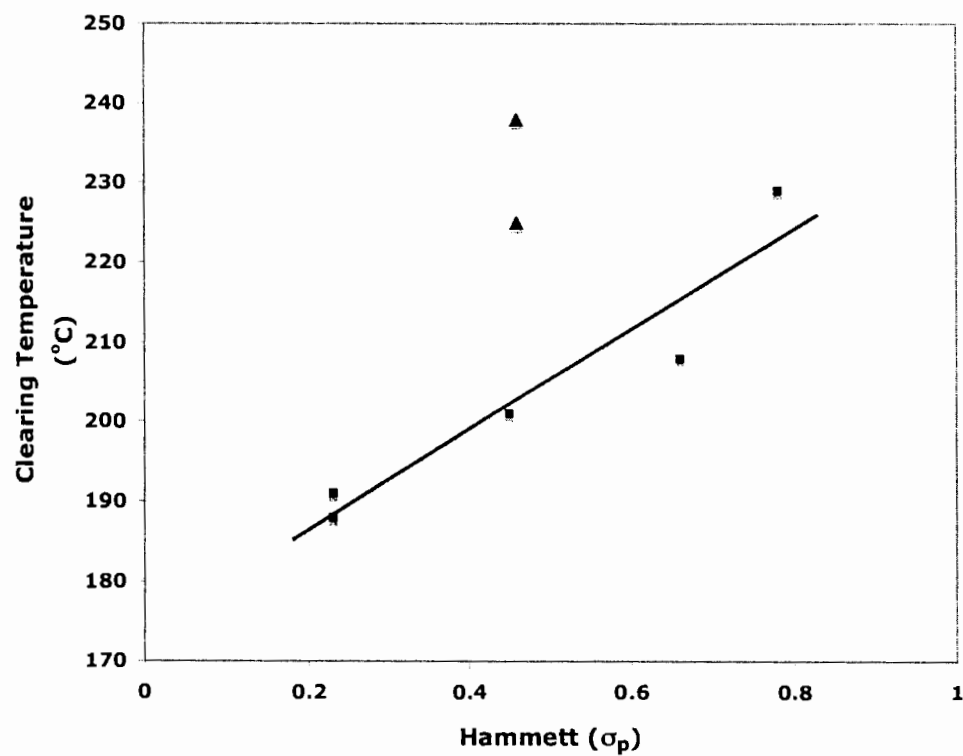
4.4 Discussion

Approximately half of the compounds in series **4.2** were found to assemble into ordered columnar hexagonal phases, while the remainder melted directly from crystalline solids into isotropic liquids. There is a striking correlation between the tendency of these molecules to form columnar phases and the electron-withdrawing or -donating ability of the functional groups attached to the core. Compounds with electron-withdrawing groups (F, Cl, Br, CO₂CH₃, CN and NO₂) all formed Col_h phases, whereas those with relatively electron-donating groups (H, CH₃ and OCH₃) were all found to be nonmesogenic. It is of note that compound **4.2b**, which bears only a weakly electron-withdrawing fluoro substituent, is unique in this series in that it forms only a metastable monotropic phase. Derivatives with more strongly electron-withdrawing groups than fluorine

all exhibit thermodynamically stable enantiotropic columnar phases, whereas more electron-rich analogues failed to form mesophases.

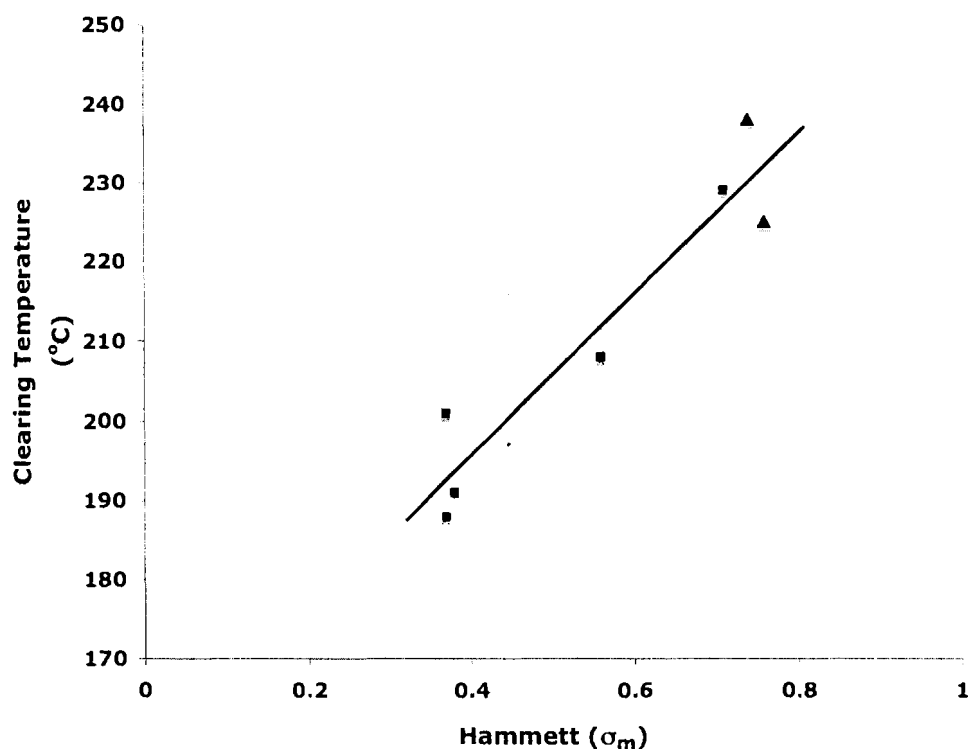
It is perhaps also notable that the nitro-derivative **4.2g**, which is the most electron-deficient mesogen in this series, also has the highest clearing temperature. A quantitative treatment of the relationship between the substituent effects and phase stability can be obtained by comparing the clearing temperatures, T_c , with Hammett parameters,¹⁶⁴ which provide a convenient measure of the withdrawing or donating ability of a functional group. Several groups have shown that σ_p parameters correlate well with the strength of arene-arene interactions in the gas phase,¹³⁸ solution^{128,129} and calamitic liquid crystalline phases.¹³⁶ A good linear correlation was obtained when the T_c of the monosubstituted mesogens **4.2c-g** were plotted versus either Hammett σ_p (Figure 4.3) or σ_m values (Figure 4.4), with R^2 values of 0.91 and 0.89, respectively (although due to the limited number of compounds in the series, these plots remain only a good estimate). This observation provides quantitative evidence that the liquid crystalline ordering is related to the electron-withdrawing character of the substituents, since a higher clearing temperature corresponds to a more thermodynamically stable phase. A similar relationship has previously been reported for the columnar phases formed by tetrahedral metallomesogens,¹⁶⁵ but to the best of our knowledge, no correlation of this type has previously been demonstrated for discotic mesogens.

Figure 4.3: Plot of Hammett σ_p versus clearing temperature (T_c).



Best-fit lines derived from linear regression on monosubstituted derivatives **4.2c-g** (squares) only; disubstituted compounds **4.2j** and **4.2k** (triangles) were excluded from this analysis (see text). Hammett values (Cl = 0.23, Br = 0.23, CN = 0.66, NO₂ = 0.78, COOCH₃ = 0.45)

Figure 4.4: Plot of Hammett σ_m versus clearing temperature (T_c).



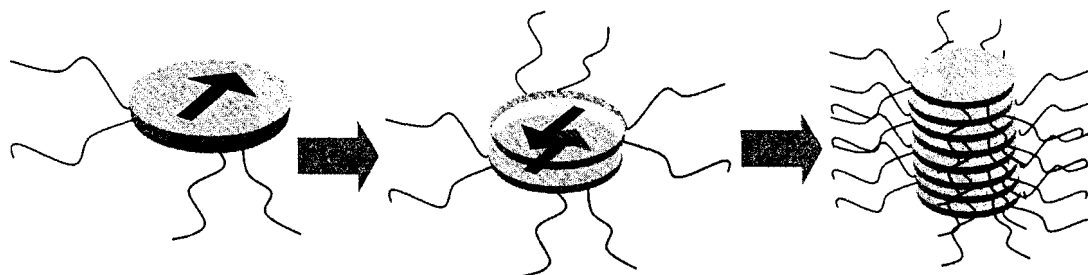
Best-fit lines derived from linear regression on monosubstituted derivatives **4.2c-g** (squares) only; disubstituted compounds **4.2j** and **4.2k** (triangles) were excluded from this analysis (see text). Hammett values (Cl = 0.37, Br = 0.38, CN = 0.56, NO₂ = 0.71, COOCH₃ = 0.37)

The correlation between clearing temperatures and Hammett parameters can be rationalized in terms of π - π interactions within the columnar phases. Cozzi and Seigel have shown that π -stacking is favoured by the addition of electron-withdrawing groups, which help to minimize the repulsive interactions between adjacent aromatic π -systems.¹²⁸⁻¹³⁰ The observation of a similar linear relationship suggests that the same mechanism is responsible for stabilizing columnar phases. The relationship between σ_m values and π -stacking is less well-established,¹⁶⁶ although these parameters do perform better than σ_p values

in at least one theoretical study of π - π interactions¹³⁸ and have been found to correlate well with the strength of cation- π interactions.¹⁶⁷

Dipole-dipole interactions may also contribute to the preferential formation of columnar phases by molecules bearing electron-withdrawing groups. The intercolumnar distances obtained by XRD studies are consistent with molecules within the columns having antiferroelectric ordering (Figure 4.5). The addition of electron-withdrawing groups should lead to an increase in the molecular dipole moment, which will favor the antiparallel orientation of adjacent molecules within the columns. Dipole-dipole interactions are also believed to play a significant role in the stabilization of mesophases formed by bent-rod¹⁶⁸⁻¹⁷⁰ and calamitic mesogens³⁹ and have been suggested as an important stabilizing feature in other dipolar discotic mesogens.^{149,160}

Figure 4.5: Schematic representation of antiferroelectric ordering in columnar phases.



Arrows represent the direction of the molecular dipole.

No significant correlation was found between the polarizabilities of the group and the clearing temperatures of the mesogenic compounds **4.2c-g**, suggesting that dispersion forces play only a secondary role in the observed trends. This conclusion is also supported by the failure of compounds **4.2h-i** and

4.2l-m to form columnar phases, despite methyl- and methoxy-substituents having comparable polarizabilities to chloro- or cyano-groups, respectively. The absence of an observed relationship between group polarizabilities and the tendency to organize into columnar phases may be due to the large size of the aromatic cores under investigation. Since functional group polarizabilities are additive,¹⁷¹ the relative contribution of the functional groups to the overall molecular polarizability will be much smaller in the present case than for simple benzene derivatives, for which there is a discernible correlation between arene-arene interactions and group polarizabilities.^{134,137,138,172} Any effects arising from the variation in dispersion forces across the series of compounds **4.2a-m** therefore may be masked by the competing electrostatic perturbations induced by the functional groups.

The dichlorinated and dibrominated derivatives **4.2j** and **4.2k** which were the only disubstituted mesogenic compounds studied, were excluded from our initial analysis of clearing temperatures. Hammett parameters for these compounds can be obtained by assuming that substituents effects are strictly additive and employing σ_p and σ_m values that are twice those used for the monosubstituted derivatives **4.2c-d**. Based on these assigned values and extrapolation from the trends obtained for the monosubstituted series, the clearing temperature of **4.2j** is predicted to be either 203 °C (σ_p) or 230 °C (σ_m), as compared to the observed value of 237.5 °C. The clearing temperature for **4.2k** is predicted to be 203 °C (σ_p) or 232 °C (σ_m), as compared to the observed value of 225.2 °C. Likewise, when the data for compound **4.2j-k** is included with

the monosubstituted derivatives **4.2c-g**, the correlation of clearing temperature with σ_p becomes dramatically worse ($R^2=0.40$) whereas the correlation with σ_m is slightly improved ($R^2=0.90$). This suggests that σ_m is a better descriptor of substituent effects in these systems than σ_p .

While the least-squares fit is better for σ_m than σ_p , it is not clear *a priori* whether a better correlation should be obtained when more symmetrical molecules such as **4.2j-k** are included alongside the lower symmetry analogues. It was shown earlier that, according to Carnelley's rule, more symmetrical molecules tend to clear at higher temperatures (Chapter 2). Consequently, we would expect that the more symmetrical mesogens **4.2j-k** to have a higher clearing temperature than predicted based on the behaviour of its lower-symmetry analogues. Such an effect could explain the discrepancy between the observed clearing temperature of **4.2j-k** and the σ_p values. This argument needs to be treated with some caution, since our studies of symmetry and shape effects mentioned earlier have invariably focused on the effects of desymmetrizing the flexible side chains (Chapter 2). Moreover, in the previous chapter it was noted that only a weak relationship between T_c and symmetry exists, and that there is a much better relationship between symmetry and T_m . Whether a similarly large symmetry or shape effect would occur in the case of groups attached to the core remains an unanswered question.

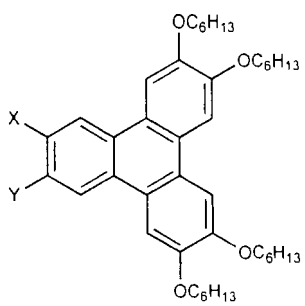
If the above explanation explains the apparent failure of σ_p values when compounds **4.2j-k** are included in the series, then the accurate prediction of this compound's transition temperature by σ_m values may be merely coincidental.

There are some reasons to distrust the reliability of σ_m values in the present context. Fluorine has a σ_m of 0.37, a value that is virtually identical to that of chlorine. On the basis of these values, compounds **4.2b** and **4.2c** are expected to have similar phase behaviour, which they clearly do not. In contrast, a fluorine substituent is only mildly electron-withdrawing according to the σ_p scale, which is consistent with compound **4.2b** forming only a monotropic phase with a relatively low clearing temperature. A similar argument can be made with respect to the methoxy-substituted derivatives **4.2i** and **4.2m**, since these groups are electron-withdrawing according to σ_m scale but electron-donating according to σ_p . The failure of these compounds to form columnar phases is therefore more consistent with σ_p than σ_m .

The observed relationship between the nature of the functional group and the mesophase stability in series of compounds **4.2a-m** prompted us to re-examine the trends obtained by other researchers working with substituted discotic mesogens. Indeed, it has been noted that electron-withdrawing groups often tend to promote the formation of columnar phases. For example, although the unsubstituted tetrakis(hexyloxy)triphenylene **THT-HH** is nonmesogenic, its bromo- and bromo-cyano-derivatives (**THT-HB**, **THT-BB** and **THT-BC**) form columnar phases (Figure 4.6).¹⁷³ Moreover, replacing a bromine atom with the more electron-withdrawing cyano group was found to cause an increase in the clearing temperature (**THT-BB** vs. **THT-BC**). Only limited conclusions can be made from such a small number of mesogenic compounds spanning a narrow range of Hammett parameters, although the series have R^2 values of 0.92 for σ_m

and 0.99 for σ_p . Somewhat surprisingly, the dicyano derivative **3.6**, does not form a liquid crystalline phase. The lack of an observed mesophase in this case may be due to the high stability of the crystalline solid phase: based on the linear fits obtained from the three mesogenic compounds, σ_m and σ_p values predict clearing temperature of 205°C and 247°C, respectively, for this compound. In this case, σ_m seems to be a better predictor of phase range, as it suggests that the liquid crystal phase would be unstable at temperatures above the melting point, whereas σ_p values predict a T_c well above the observed melting point.

Figure 4.6: Phase behaviour of previously reported 10,11-substituted 2,3,6,7-tetrahexyloxytriphenylenes.



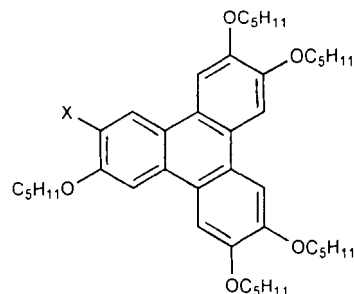
THT-HH (X = Y = H)
 THT-BH (X = H, Y = Br)
 THT-BB (X = Y = Br)
 THT-BC (X = CN, Y = Br)
3.6 (X = Y = CN)

Compound	Phase	T_f /°C	Phase
THT-HH	Cr	123	I
THT-BH	Cr	103	I
THT-BB	Cr	130	Col _h $\xrightarrow{141}$ I
THT-BC	Cr	170	Col _h $\xrightarrow{190}$ I
3.6	Cr	218	I

As reported, (THT-HH, THT-BH, THT-BB, THT-BC)¹⁷³(**3.6**) in collaboration with A. Cammidge et al. (See Chapter 3)

A more comprehensive treatment is possible with the series **PPT** (Figure 4.7).^{153,157,174} Following selective removal of the methoxy group of compound **PPT-Me**, hydrogenolysis was used to expose a β -site.^{153,175,176} These sites provide entry points for the introduction of functionality into the triphenylene through electrophilic substitution reactions. As with the **THT** series above, the parent compound (**PPT-H**) melts directly from the solid state to an isotropic liquid, whereas its substituted derivatives tend to form columnar phases. In this case, we found a weaker correlation to Hammett σ_p and σ_m parameters ($R^2=0.82$ and 0.73 , respectively), although, perhaps significantly, the linear fit improves to $R^2=0.90$ (σ_p) and 0.89 (σ_m) when the highly polarizable TMS-acetylene derivative is excluded from this analysis.

Figure 4.7: Previously reported monofunctionalized pentapentoxytriphenylene.



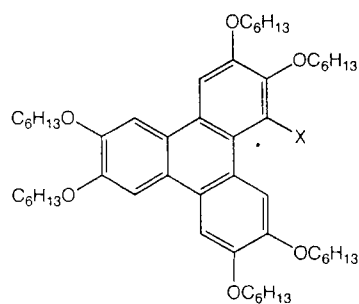
Compound		Phase	$T_i/^\circ\text{C}$	Phase
PPT-C ₅	X = OC ₅ H ₁₁	Cr	69	Col _h → I
PPT-H	X = H	Cr	86	I
PPT-Br	X = Br	Cr	-47	Col → Col _h → I
PPT-Ac	X = Ac	Cr	76	Col _h → I
PPT-CN	X = CN	Cr	51	Col → Col _h → I
PPT-TMSA	X = TMS ⁻ Acetylene	Cr	-50	Col → I

Previously reported.^{153,157,174}

For triphenylene mesogens that bear substituents at the β -positions, steric crowding tends to limit reactivity, but the systems can be partially nitrated, chlorinated or brominated at the α -position (Figure 4.8). The introduction of a nitro substituent is particularly useful since it can be readily transformed into a wide range of other substituents and many of the products show enhanced mesophase properties.^{49,50,65,155,156,158} Although the clearing points in this series show a marked dependence on the nature of the functional group, a less than straightforward relationship exists between the electronic properties of these substituents and the liquid crystal-to-isotropic transition temperatures, although nitro groups were found to increase the clearing temperature. The lack of a clear

correlation in this series is likely due to the additional complication introduced by steric effects, since the presence of functional groups at this hindered position causes large distortions of the core from planarity.

Figure 4.8: Phase behaviour of previously reported α -substituted triphenylene hexahexyl ether.



Compound		Phase	$T_I/^\circ\text{C}$	Phase
HH α -H	X = H	Cr	68	Col _h 100
HH α -NO ₂	X = NO ₂	Cr	43	Col _h 137
HH α -Cl	X = Cl	Cr	31	Col _h 96
HH α -Br	X = Br	Cr	30	Col _h 84
HH α -NH ₂	X = F	Cr	43	Col _h 124
HH α -NH ₂	X = NH ₂	Cr	54	Col _h 68
HH α -CH ₃	X = CH ₃	Cr	60	I

Adapted from Praefcke et al. and Bushby et al. ^{49,50,65,155,156,158}

4.5 Summary

We have examined a large number of disc-shaped molecules in order to elucidate how changes in the core structure alter the propensity of these compounds to self-assemble into columnar liquid crystalline phases. There is

both a qualitative relationship between the functional groups and whether a columnar phase is observed as well as a quantitative correlation of clearing temperatures of the mesogenic compounds with the electron-withdrawing ability of the substituents. This trend can most likely be explained by the changes in electrostatic interactions between molecules within the columns, which favour stacking between electron-deficient aromatic rings.

4.6 Experimental

For general experimental, see Chapter 2. All solvents employed were reagent grade. 4,5-Dichloro-1,2-phenylenediamine, 4-chloro-1,2-phenylenediamine, 4-nitro-1,2-phenylenediamine, 3,4-diaminotoluene, 1,2-ethylenediamine, naphthalene-2,3-diamine, 4,5-dimethyl-1,2-phenylenediamine, 4-fluoro-2-nitroaniline, 4-amino-3-nitrobenzotrile, and 4-methoxy-2-nitroaniline were purchased from Aldrich and used without further purification. 1,2-Dimethoxy-4,5-dinitrobenzene, prepared according to previously published methods. 4-Fluoro-1,2-phenylenediamine, 4-cyano-1,2-phenylenediamine and 4-methoxy-1,2-phenylenediamine were prepared from the appropriate 2-nitroaniline derivatives, as described below.

4-Fluoro-1,2-phenylenediamine. 4-Fluoro-2-nitroaniline (0.100 g, 0.641 mmol) was dissolved in ethanol (10 mL) and 10% palladium on activated carbon (0.050 g) was added. Hydrazine hydrate (0.16 mL, 3.2 mmol) was added dropwise and the mixture was then heated at reflux for 3 hours. The resultant solution was filtered hot through a plug of silica. This plug was washed with

ethanol (50 mL) and the solvent was evaporated under reduced pressure. The resultant solid was used immediately without further purification.

4-Cyano-1,2-phenylenediamine was synthesized from 4-amino-3-nitrobenzotrile according to the method described above. The resultant solid was used immediately without further purification.

4-Methoxy-1,2-phenylenediamine was synthesized from 4-methoxy-2-nitroaniline according to the method described above. The resultant solid was used immediately without further purification.

4,5-Dimethoxy-1,2-phenylenediamine was synthesized from 1,2-dimethoxy-4,5-dinitrobenzene according to the method described above. This compound is extremely unstable and was used immediately without further purification.

1,2-dibromo-4,5-dinitrobenzene was reduced to 4,5-Dibromo-1,2-phenylenediamine according to the method described above. This compound is extremely unstable and was used immediately without further purification.

4,5-Dibromo-1,2-phenylenediamine. 1,2-dibromobenzene (1.0 g, 4.2 mmol) was slowly added to a mixture of 25 mL fuming sulphuric acid and 25 mL fuming nitric acid. The reaction mixture was stirred at room temperature for 10 minutes then heated at reflux overnight. The hot mixture was poured over 400 mL ice and the solid product was collected by vacuum filtration to yield a 1,2-dibromo-4,5-dinitrobenzene. This material was then recrystallized twice from 95% ethanol (49% yield).

General procedure for the synthesis of compounds **4.2a-m**

A solution of 2,3,6,7-tetrakis(hexyloxy)-phenanthrene-9,10-dione (80 mg, 0.13 mmol) and the appropriate 1,2-diamine (0.52 mmol) were heated to reflux in acetic acid (15 mL) for 12 hours. Upon cooling, water (150 mL) was added and the mixture extracted with CH₂Cl₂ (3 x 25 mL). The CH₂Cl₂ extracts were combined, washed with water, dried (MgSO₄), filtered, and evaporated under reduced pressure. The resultant solid was eluted through a short plug of silica with dichloromethane, and then purified by column chromatography (silica gel, 1:1 CH₂Cl₂:hexanes gradient to 100% CH₂Cl₂ as eluent). The product was recrystallized from a mixture of CH₂Cl₂ and methanol to afford the dibenzo[a,c]phenazine derivative.

2,3,6,7-Tetrakis-hexyloxy-dibenzo[a,c]phenazine (4.2a). Compound **2.6d** and 1,2-phenylenediamine were condensed according to method described above to afford **4.2a** as a yellow solid (73%). ¹H NMR (400 MHz) (CDCl₃) δ (ppm) 8.81 (s, 2H), 8.32 (d, 2H *J* = 3, 7 Hz), 7.81 (dd, 2H *J* = 3, 7 Hz), 7.75 (s, 2H), 4.26-4.39 (m, 8H), 1.94-2.02 (m, 8H), 1.37-1.65 (m, 24H), 0.92-0.97 (m, 12H); ¹³C NMR (125 MHz) (CDCl₃) δ (ppm) 152.0, 149.5, 129.3, 129.2, 128.7, 128.7, 128.7, 126.7, 108.8, 106.3, 69.6, 69.2, 31.6, 29.2, 29.2, 25.8, 25.7, 22.6, 22.6, 14.0, 14.0; Elemental analysis (%): calc. (found) for C₄₄H₆₀N₂O₄: C, 77.61; H, 8.88; N, 4.11. Found: C, 77.56; H, 8.87; N, 3.93%. Maldi-TOF. calc. (found) 681 (682 M+1)

11-Fluoro-2,3,6,7-tetrakis-hexyloxy-dibenzo[a,c]phenazine (4.2b) 4-Fluoro-1,2-phenylenediamine was condensed with compound **2.6d** to afford a yellow solid (89%). ^1H (CDCl_3) δ (ppm) 8.75 (s, 2H); 8.37 (d, 1H J = 2Hz), 8.01 (d, 1H J = 9Hz), 7.73 (s, 2H), 7.60 (dd, 1H J = 2, 9 Hz), 4.26-4.36 (m, 8H), 1.95-1.99 (m, ~8H), 1.24-1.55 (m, ~24H), 0.92-0.95 (m, ~12H); ^{13}C NMR (400 MHz) (CDCl_3) δ (ppm) 152.2, 152.0, 149.5, 130.9, 130.8, 127.0, 126.5, 123.0, 122.7, 120.1, 111.8, 108.8, 108.6, 106.3, 106.2, 69.5, 69.2, 69.1, 31.6, 29.2, 29.2, 25.8, 25.7, 22.6, 14.0; Elemental analysis (%): calc. (found) for $\text{C}_{44}\text{H}_{59}\text{FN}_2\text{O}_4$: C, 75.61; H, 8.51; N, 4.01. Found: C, 75.39; H, 8.60; N, 4.30%. Maldi-TOF. calc. (found) 698 (698)

11-Chloro-2,3,6,7-tetrakis-hexyloxy-dibenzo[a,c]phenazine (4.2c) was synthesized by the condensation reaction of compound **2.6d** and 4-chloro-1,2-phenylenediamine, to afford a yellow solid (86%). ^1H (CDCl_3) δ (ppm) 8.24 (d, 1H J = 7 Hz), 8.31 (d, 1H J = 2 Hz), 8.75 (s, 2H), 7.73 (dd, 1H J = 2, 7Hz), 7.73 (s, 2H), 4.24-4.34 (m, 8H), 1.95-1.99 (m, 8H), 1.40-1.61 (m, 24H), 0.92-0.97 (m, 12H); ^{13}C NMR (125 MHz) (CDCl_3) δ (ppm) 151.9, 149.4, 139.7, 129.9, 126.7, 126.6, 108.6, 106.3, 106.2, 69.5, 69.1, 31.6, 29.2, 29.2, 25.7, 22.6, 14.0; Elemental analysis (%): calc. (found) for $\text{C}_{44}\text{H}_{59}\text{ClN}_2\text{O}_4$: C, 73.97; H, 8.31; N, 3.92. Found: C, 73.82; H, 8.42; N, 3.94%. Maldi-TOF. calc. (found) 714 (714)

11-Bromo-2,3,6,7-tetrakis-hexyloxy-dibenzo[a,c]phenazine (4.2d)

2,3,6,7-Tetrakis-hexyloxy-11-nitro-dibenzo[a,c]phenazine (**4.2g**) (200 mg, 0.28 mmol) and 10% palladium on carbon (100 mg) were stirred in a 1:1 mixture of ethanol and dichloromethane (20 mL). Hydrazine hydrate (0.16 ml, 3.2 mmol) was added dropwise and the mixture was then heated at reflux for 3 hours. The reaction mixture was filtered hot through a plug of silica and the plug was washed with EtOH (50 mL), CH₂Cl₂ (100 mL). Solvent was evaporated under reduced pressure, yielding 11-amino-2,3,6,7-tetrakis-hexyloxy-dibenzo[a,c]phenazine (0.17g, 85% yield), as an off-white solid. This amine was immediately dissolved in concentrated sulfuric acid (20 mL), water (20 mL) and cooled in an ice/water bath. Sodium nitrite (0.023 g, 0.33 mmol) was dissolved in water (3 mL) and added to the mixture over 10 minutes. After 20 minutes at 0 °C, the solution was poured into a mixture of CuBr (0.048 g, 0.33 mmol) and 48% aqueous HBr (20 mL) and stirred overnight at room temperature. The reaction mixture was extracted with chloroform and the solvent removed under reduced pressure. The resultant solid was eluted through a short plug of silica with dichloromethane, and then purified by column chromatography (silica gel, 20% ethyl acetate in hexanes). The product was recrystallized from a mixture of CH₂Cl₂ and methanol to afford 11-bromo-2,3,6,7-tetrakis-hexyloxy-dibenzo[a,c]phenazine (0.15 g, 78% yield), a yellow solid. ¹H (CDCl₃) δ (ppm) 8.75 (s, 2H), 8.29 (d, 1H, *J* = 2Hz), 8.25 (d, 1H *J* = 6Hz), 7.75 (dd, 1H *J* = 2, 6 Hz), 7.69 (s, 2H), 4.24-4.33 (m, 8H), 1.95-1.99 (m, ~8H), 1.40-1.61 (m, ~24H), 0.92-0.97 (m, ~12H); ¹³C NMR (125 MHz) (CDCl₃) δ (ppm) 156.3, 147.8, 135.5, 129.9, 126.7, 126.6, 108.5, 106.2, 106.1,

70.5, 70.1, 31.7, 29.2, 28.2, 25.6, 22.3, 14.0; Elemental analysis (%): calc. (found) for $C_{44}H_{59}BrN_2O_4$: C, 69.55; H, 7.83; N, 3.69% Found: C, 69.81; H, 7.72; N, 3.84%. Maldi-TOF. calc. (found) 760 (760).

2,3,6,7-Tetrakis-hexyloxy-dibenzo[a,c]phenazine-11-carbonitrile (4.2f)

4-Amino-3-nitrobenzonitrile was reduced as described above and the resultant diamine condensed with compound **2.6d** to afford an orange solid (89%). 1H NMR (400 MHz) ($CDCl_3$) δ (ppm) 8.80 (s, 2H), 8.20-8.21 (d, 1H $J = 7$ Hz), 8.10 (d, 1H $J = 2$ Hz), 7.75 (s, 2H), 7.64 (dd, 1H $J = 2, 7$ Hz), 4.24-4.32 (m, ~8H), 1.94-2.01 (m, ~8H), 1.41-1.60 (m, ~24H), 0.93-0.96 (m, ~12H), ^{13}C NMR (125 MHz) ($CDCl_3$) δ (ppm) 152.6, 152.3, 149.4, 149.3, 143.6, 143.2, 142.4, 140.0, 135.2, 130.5, 128.8, 127.3, 126.8, 122.8, 118.7, 111.6, 108.8, 108.5, 106.0, 105.8, 69.4, 69.1, 31.6, 29.2, 29.2, 25.8, 25.8, 22.6, 14.0; IR (KBr) ν_{max}/cm^{-1} : 2949, 2926, 2849, 2228, 1607, 1513, 1500, 1443, 1386, 1265, 1178, 1074, 1047, 923, 873, 826; Elemental analysis (%): calc. (found) for $C_{45}H_{59}N_3O_4$: C, 76.56; H, 8.42; N, 5.95. Found: C, 76.27; H, 8.61; N, 5.52%. Maldi-TOF. calc. (found) 706 (706).

2,3,6,7-Tetrakis-hexyloxy-11-nitro-dibenzo[a,c]phenazine (4.2g) was synthesized by the condensation reaction of **2.6d** and 4-nitro-1,2-phenylenediamine to afford a red solid (91%). 1H NMR (400 MHz) ($CDCl_3$) δ (ppm) 9.23 (d, 1H $J = 2$ Hz), 8.75 (s, 2H), 8.54 (dd, 1H $J = 2, 9$ Hz), 8.40 (d, 1H $J = 9$ Hz), 7.70 (s, 2H), 4.18-4.29 (m, 8H), 1.92-1.98 (m, ~8H), 1.43-1.61 (m, ~24H), 0.94-0.98 (m, ~12H), ^{13}C NMR (125 MHz) ($CDCl_3$) δ (ppm) 152.9, 152.4, 149.5,

149.3, 146.8, 143.5, 143.1, 139.5, 127.7, 126.8, 122.6, 122.4, 121.9, 108.5, 105.9, 105.8, 69.4, 69.2, 69.0, 31.6, 29.2, 25.8, 25.8, 22.6, 14.0; IR (KBr) $\nu_{\text{max}}/\text{cm}^{-1}$: 2953, 2929, 2859, 1607, 1520, 1460, 1389, 1339, 1268, 1178, 1071, 869, 832; Elemental analysis (%): calc. (found) for $\text{C}_{44}\text{H}_{59}\text{N}_3\text{O}_6$: C, 72.80; H, 8.19; N, 5.79. Found: C, 72.89; H, 8.40; N, 6.00%. Maldi-TOF. calc. (found) 725 (725).

2,3,6,7-Tetrakis-hexyloxy-11-methyl-dibenzo[a,c]phenazine (4.2h) was synthesized by the condensation reaction of compound **2.6d** and 3,4-diaminotoluene, to afford a yellow solid (78%). ^1H NMR (400 MHz) (CDCl_3) δ (ppm) 8.78 (d, 1H $J = 2\text{Hz}$), 8.21 (d, 1H $J = 7\text{Hz}$), 8.11 (s, 2H), 7.71 (s, 2H), 7.63 (dd, 1H $J = 2, 7\text{Hz}$), 4.25 4.36 (m, 8H), 2.66 (s, 3H), 1.93-2.01 (m, ~8H), 1.24-1.64 (m, ~24H), 0.92-0.95 (m, ~12H); ^{13}C NMR (125 MHz) (CDCl_3) δ (ppm) 151.5, 149.4, 149.3, 131.6, 128.5, 126.2, 108.5, 106.3, 69.6, 69.1, 31.6, 29.3, 29.2, 25.8, 22.6, 22.0, 14.0; Elemental analysis (%): calc. (found) for $\text{C}_{45}\text{H}_{62}\text{N}_2\text{O}_4$: C, 77.77; H, 8.99; N, 4.03. Found: C, 77.45; H, 8.99; N, 3.90%. Maldi-TOF. calc. (found) 694 (695 M+1).

2,3,6,7-Tetrakis-hexyloxy-11-methoxy-dibenzo[a,c]phenazine (4.2i) 4-Methoxy-2-nitroaniline was reduced as above and the resultant diamine condensed with compound **2.6d**, to afford a yellow solid (84%). ^1H NMR (400 MHz) (CDCl_3) δ (ppm) 8.79 (d, 1H $J = 2\text{Hz}$), 8.75 (s, 2H), 8.18 (d, 1H $J = 6\text{Hz}$), 7.59 (s, 2H), 7.46 (dd, 1H $J = 2, 6\text{Hz}$), 4.25 4.37 (m, 8H), 4.06 (s, 3H), 1.93-2.01 (m, ~8H), 1.37-1.59 (m, ~24H), 0.92-0.95 (m, ~12H); ^{13}C NMR (125 MHz)

(CDCl₃) δ (ppm) 151.3, 149.5, 149.4, 130.1, 125.7, 123.4, 108.7, 108.2, 106.5, 106.2, 69.6, 69.5, 69.2, 69.1, 55.8, 31.6, 29.6, 29.2, 25.7, 22.6, 14.0; Elemental analysis (%): calc. (found) for C₄₅H₆₂N₂O₅: C, 76.02; H, 8.79; N, 3.94. Found: C, 75.91; H, 9.15; N, 3.67%. Maldi-TOF. calc. (found) 710 (711 M+1).

11,12-Dichloro-2,3,6,7-tetrakis-hexyloxy-dibenzo[a,c]phenazine (4.2j)

was synthesized by the condensation reaction of compound **2.6d** and 4,5-dichlorobenzene-1,2-phenylenediamine, affording a yellow solid (89%). ¹H NMR (400 MHz) (CDCl₃) δ (ppm) 8.68 (s, 2H), 8.42 (s, 2H), 7.68 (s, 2H), 4.25-4.32 (m, 8H), 1.94-2.00 (m, ~8H), 1.40-1.60 (m, ~24H), 0.92-0.96 (m, ~12H); ¹³C NMR (125 MHz) (CDCl₃) δ (ppm) 152.2, 149.4, 139.9, 133.1, 129.4, 126.8, 108.6, 106.1, 69.5, 69.1, 31.6, 29.2, 29.2, 25.7, 22.6, 22.6, 14.0; Elemental analysis (%): calc. (found) for C₄₄H₅₈Cl₂N₂O₄: C, 70.48; H, 7.80; N, 3.74. Found: C, 70.70; H, 7.92; N, 3.59%. Maldi-TOF. calc. (found) 748 (748).

11,12-Dibromo-2,3,6,7-tetrakis-hexyloxy-dibenzo[a,c]phenazine (4.2k)

was synthesized by the condensation reaction of compound **2.6d** and 4,5-dibromobenzene-1,2-phenylenediamine, to afford a yellow solid (87%). ¹H NMR (400 MHz) (CDCl₃) δ (ppm) 8.69 (s, 2H), 8.41 (s, 2H), 7.65 (s, 2H), 4.24-4.33 (m, 8H), 1.94-2.00 (m, ~8H), 1.40-1.61 (m, ~24H), 0.92-0.96 (m, ~12H); ¹³C NMR (125 MHz) (CDCl₃) δ (ppm) 153.2, 150.3, 140.1, 132.1, 126.4, 120.8, 107.2, 107.1, 69.5, 69.3, 32.6, 29.1, 29.1, 25.6, 23.6, 22.8, 14.0; Elemental analysis (%):

calc. (found) for $C_{44}H_{58}Br_2N_2O_4$: C, 63.01; H, 6.97; N, 3.34% Found: C, 63.09; H, 7.01; N, 3.49%. Maldi-TOF. calc. (found) 839 (839).

2,3,6,7-Tetrakis-hexyloxy-11,12-dimethyl-dibenzo[a,c]phenazine (4.2l)

Synthesized by the condensation reaction of compound **2.6d** and 4,5-dimethyl-1,2-phenylenediamine, yielding a yellow solid (78%). 1H NMR (400 MHz) ($CDCl_3$) δ (ppm) 8.79 (s, 2H), 8.10 (s, 2H), 7.72 (s, 2H), 4.25-4.36 (m, 8H), 2.57 (s, 6H), 1.92-1.99 (m, ~8H), 1.36-1.60 (m, ~24H), 0.92-0.96 (m, ~12H); ^{13}C NMR (125 MHz) ($CDCl_3$) δ (ppm) 151.7, 149.5, 140.3, 127.4, 126.4, 108.6, 106.4, 69.6, 69.2, 31.6, 29.3, 29.2, 25.8, 25.8, 22.6, 20.5, 14.0, 14.0; Elemental analysis (%): calc. (found) for $C_{46}H_{64}N_2O_4$: C, 77.92; H, 9.10; N, 3.95. Found: C, 77.76; H, 9.08; N, 4.15%. Maldi-TOF. calc. (found) 708 (708).

2,3,6,7-Tetrakis-hexyloxy-11,12-dimethoxy-dibenzo[a,c]phenazine

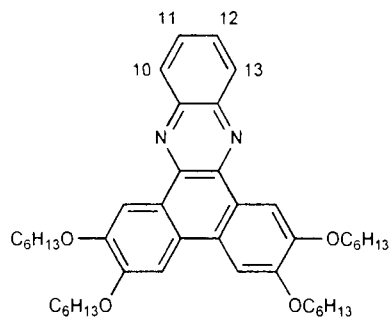
(4.2m) 1,2-Dimethoxy-4,5-dinitrobenzene was reduced as above and the resultant diamine condensed with compound **2.6d**, to afford a orange solid (85%). 1H NMR (400 MHz) ($CDCl_3$) δ (ppm) 8.71 (s, 2H), 7.70 (s, 2H), 7.53 (s, 2H), 4.24-4.35 (m, 8H), 4.13 (s, 6H), 1.92-2.01 (m, ~8H), 1.36-1.60 (m, ~24H), 0.92-0.96 (m, ~12H); ^{13}C NMR (125 MHz) ($CDCl_3$) δ (ppm) 152.0, 149.5, 129.2, 128.7, 126.7, 108.8, 106.3, 69.6, 69.2, 31.6, 29.2, 29.2, 25.7, 22.6, 14.0; Elemental analysis (%): calc. (found) for $C_{46}H_{64}N_2O_6$: C, 74.56; H, 8.71; N, 3.78. Found: C, 74.85; H, 8.96; N, 3.45%. Maldi-TOF. calc. (found) 740 (741 M+1).

5 'SIDE'-SUBSTITUENT EFFECTS ON SELF ASSEMBLY

5.1 Introduction

In the previous chapter the phase behaviour of our tetraalkoxy-[a,c]dibenzophenazine compounds, functionalized with electron-withdrawing or electron-donating groups attached at the 11 and 12 positions was discussed. Although a linear relationship existed between both σ_m and σ_p Hammett parameters, it was unclear if there was a single parameter that is better at relating electron withdrawing and donating effects and liquid crystallinity for these materials. Moreover, no research has been performed into the effect of changing the position of substituents on the core of a discotic liquid crystals. In this chapter, both of these issues are investigated by preparing derivatives of dibenzophenazine in which functional groups are placed in points other than the 11 and 12 positions.

Figure 5.1: Positions on tetraalkoxydibenzophenazine.

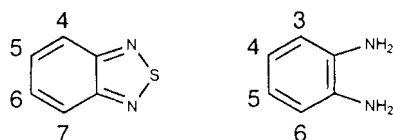


5.2 Dibrominated 2,3,6,7-Tetrakis(hexyloxy)-dibenzo[a,c]phenazine Derivatives

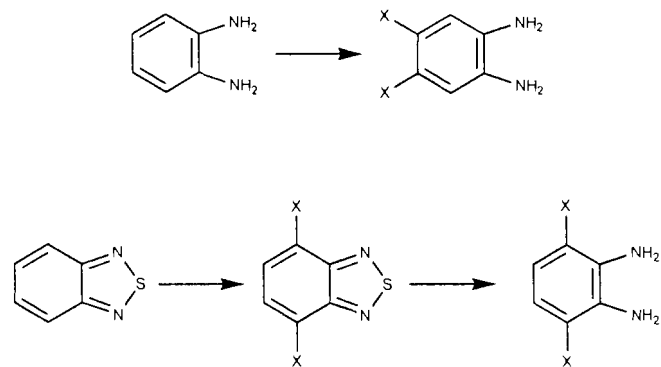
5.2.1 Synthesis of Differentially Substituted 1,2-Phenylenediamines

Although 1,2-phenylenediamines proved important intermediates in the synthesis of substituted phenazines (as shown in the previous chapters) direct functionalization is sometimes difficult and generally leads to substitution in the 4 and 5 positions (Figure 5.2). Protection of the amine by converting it into a 2,1,3-benzothiadiazole provides a useful route to functionalization at the 4 and 7 positions (Scheme 5.1).^{177,178}

Figure 5.2: Positions on 2,1,3-benzothiadiazole and 1,2-phenylenediamine.



Scheme 5.1: Routes to functionalized o-phenylenediamines.



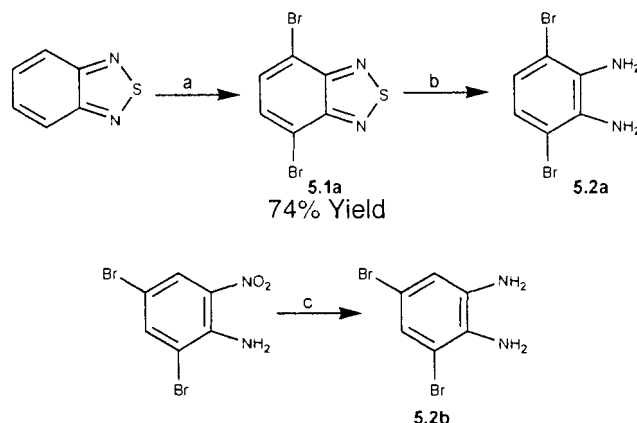
Reduction of thiadiazoles has been shown to be a viable route to o-phenylenediamines (Scheme 5.1). Several reagents have been reported for the

reduction of 2,1,3-benzothiadiazoles to 1,2-phenylenediamines, including Sn/HCl,^{179,180} SnCl₂/HCl,¹⁸¹ NaBH₄^{182,183} and Mg in methanol.¹⁸⁴

5.2.2 Synthesis of Functionalized Dibenzophenazine Derivatives

Preliminary efforts to investigate the role of functional group position focused on the synthesis of dibrominated isomers of compound **4.7k**, which was functionalized with bromines at the 11 and 12 positions. Treatment of 2,1,3-benzothiadiazole with Br₂ and HBr generated the 4,7-dibrominated derivative **5.1a** (Scheme 5.2). This compound was then treated with sodium borohydride to afford 3,6-dibromo-1,2-phenylenediamine. Commercially available 2,4-dibromo-6-nitroaniline can be readily reduced to 3,5-dibromo-1,2-phenylenediamine **5.2b**, using hydrazine and palladium on carbon. Subsequent coupling of compounds **5.2a** and **5.2b** with 2,3,6,7-tetra(hexyloxy)phenanthrene-9,10-dione **2.6d** affords compounds **5.3a-b**, which are regioisomers of compound **4.7k** (Figure 5.3).

Scheme 5.2: Synthesis of dibrominated 1,2-phenylenediamines.



Reagents and conditions. a) Br₂, HBr, b) NaBH₄, c) Pd/C, N₂H₄-H₂O, EtOH.

5.2.3 Dibrominated compounds results and discussion

The phase behaviour of the products **5.3a-b** were examined by POM and DSC and results are summarized below (Figure 5.3). Both compounds exhibited liquid crystal phases with optical textures consistent with columnar hexagonal phases (Figure 5.4). It is interesting to note that compound **5.3a**, which has bromines in the 10 and 13 positions, exhibited a much lower T_c than compound **4.2k** (Chapter 4), which has bromines at the 11 and 12 positions. This would seem to follow the reasoning that molecular dipole plays a role, with compound **5.3a** having a reduced dipole relative to compound **4.2k**, due to the placement of the bromines in the 'side' positions.

Figure 5.3: Dibrominated derivatives.

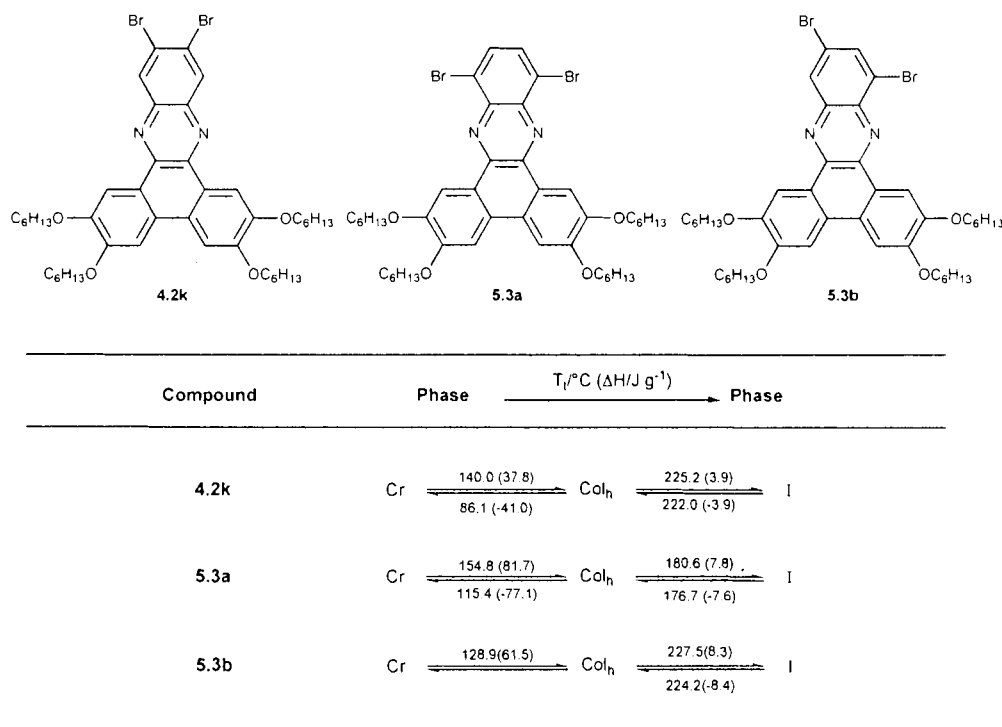
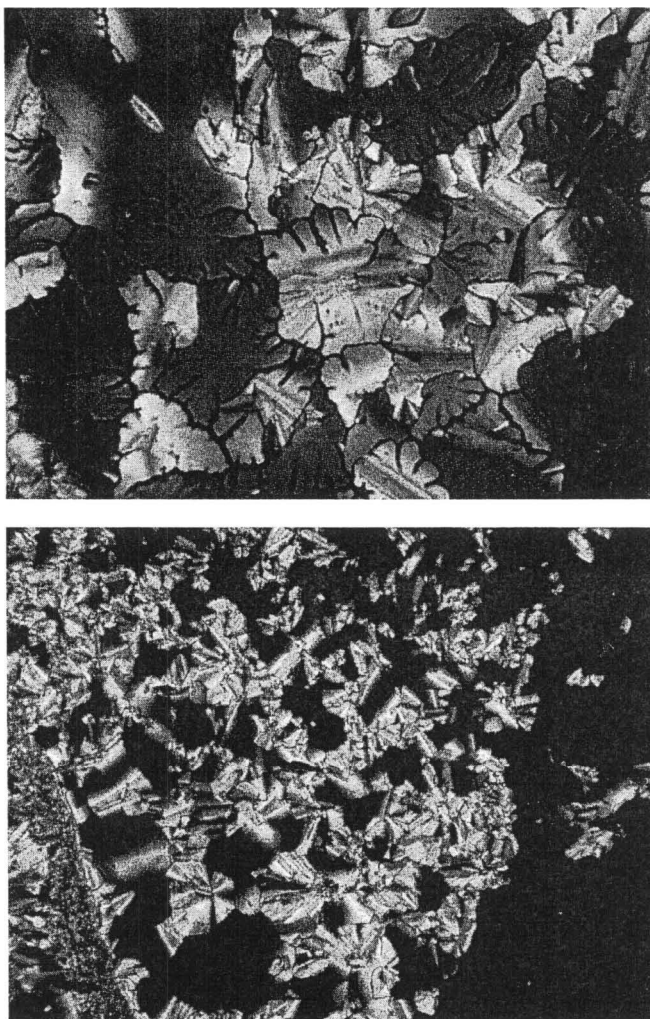


Figure 5.4: Polarized optical micrograph of compounds (5.3a) and (5.3b).



5.3a (Top) at 177°C, 5.3b (Bottom) at 226°C

Compound **5.3b** has a higher T_c than either compound **5.3a** or **4.2k**, which again indicates that the positions of the bromine substituents on the aromatic core have a large effect. However, this effect is not simply additive, as this would lead to a T_c between to that of compounds **5.3a** and **4.2k**. It is also interesting to note that this molecule has lower symmetry than **4.2k** or **5.3c**, yet has the highest T_c ; again symmetry does not appear to play a decisive role in determining the clearing temperature. The melting point of this derivative is lower than that of the

other two compounds as anticipated from Carnelley's rule. It is unclear at this time why this compound has an apparently anomalously high T_c .

Given the previous argument that molecular dipole plays a large role in phase behaviour, this molecule should have a T_c lower than **4.2k**, which is not the case. Further investigation into the effects of substituents in the 10 and 13 positions of the dibenzophenazine were therefore required.

5.3 'Side'-Substituted 2,3,6,7-Tetrakishexyloxy-dibenzo[a,c]phenazine

5.3.1 Synthesis

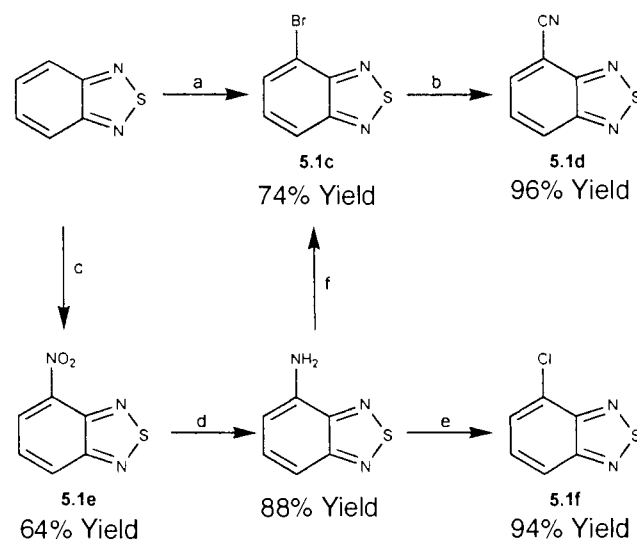
In order to create a series of compounds substituted at the 10-position of our dibenzo[a,c]phenazine core, the synthesis of the corresponding diamines was required. As already noted, 1,2-diamines protected as a thiadiazole are more activated towards substitution at the 4/7-positions and was therefore used as a key intermediate in these syntheses.

Both nitration and bromination are synthetically useful reactions for creating a series of molecules (Scheme 5.3). The mono-brominated thiadiazole derivative **5.1c** proved hard to synthesize in that the dibrominated adduct **5.1a** was also formed and these two compounds were difficult to separate. Optimized conditions were finally established, with the reaction of benzothiadiazole in dry acetonitrile, 1.0 equivalents of *N*-bromosuccinimide and 0.1 equivalents of $FeCl_3$ for 30 minutes at 30 °C, followed by column chromatography and recrystallization, which led to the isolation of the pure mono-brominated thiadiazole **5.1c** (73%).

Treatment of compound **5.1c** with one mole equivalent of copper(I)iodide and a large molar excess of copper(I)cyanide results in the nitrile **5.1d** in very good yield (96%).¹⁶³

Nitration of benzothiadiazole in 70% nitric acid affords the mononitro derivative **5.1e** (64%). Treatment of compound **5.1e** with of $\text{Fe}_2(\text{SO}_4)_3$, NH_4Cl , and zinc powder selectively reduced the nitro group to the amine.¹⁸⁵ Conversion of the amine to the diazonium salt, followed by treatment with copper(I)chloride results in 4-chloro-2,1,3-benzothiadiazole, **5.1f**. A similar route was used to prepare 4-bromo-2,1,3-benzothiadiazole **5.1c**. Although this was a longer synthesis than the direct bromination of benzothiadiazole, it did not result in the formation of dibrominated product **5.1a**.

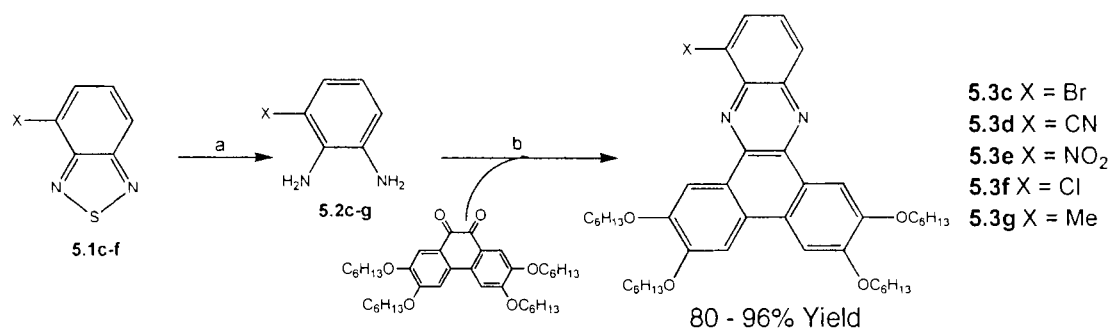
Scheme 5.3: Substitution of 2,1,3-benzothiadiazole.



Reagents and conditions. a) NBS, FeCl_3 , CH_3CN , b) i) CuCN , CuI , DMF, ii) FeCl_3 , HCl , c) HNO_3 , d) $\text{Fe}_2(\text{SO}_4)_3$, NH_4Cl , Zn , e) i) NaNO_2 , HCl , ii) CuCl , f) i) NaNO_2 , H_2SO_4 , ii) CuBr .

Attempts to reduce the 4-substituted benzothiadiazoles to 1,2-diamines with sodium borohydride were generally unsuccessful, in that only starting material resulted. Reduction of **5.1c-f** to the corresponding 1,2-phenylenediamines **5.2c-f** was accomplished using the magnesium and methanol as reported by Prashad and co-workers (Scheme 5.4).¹⁸⁴ 1,2-Diaminotoluene **5.2g** was purchased from Aldrich and used without further purification. Coupling of **5.2c-g** with 2,3,6,7-tetra(hexyloxy)phenanthrene-9,10-dione on heating in acetic acid afforded 10-substituted-2,3,6,7-tetrakis(hexyloxy)dibenzo[a,c]phenazines **5.3c-g**, in an 80% average yield over two steps.

Scheme 5.4: 10-Substituted-2,3,6,7-tetrakis(hexyloxy)dibenzo[a,c]phenazines.



Reagents and conditions. a) Mg/MeOH, b) AcOH.

5.3.2 Results

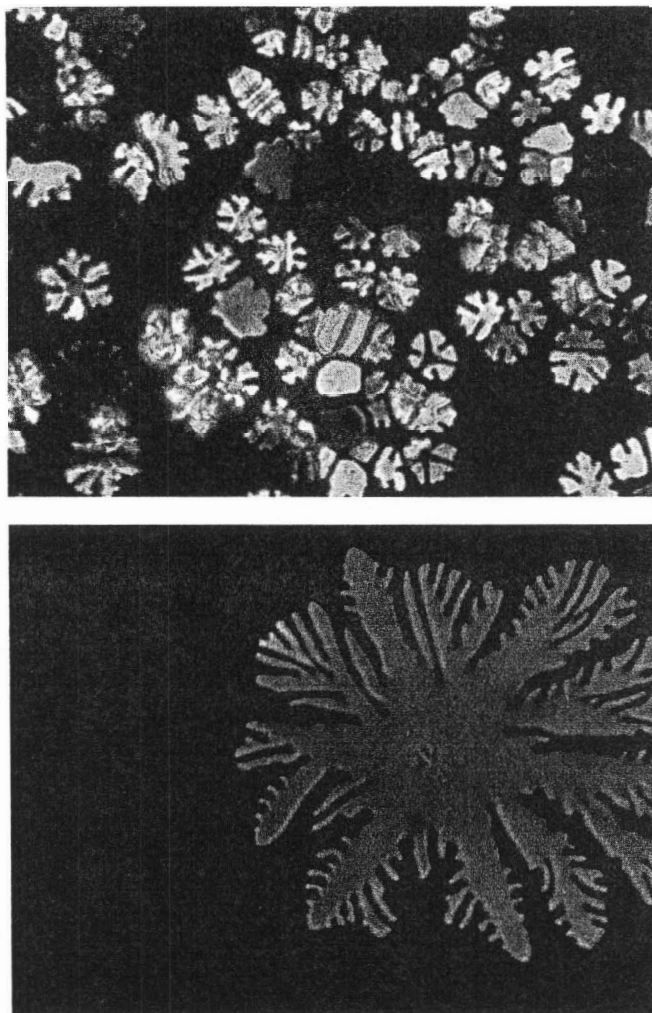
The phase behaviour of the products **5.3c-g** were examined by POM and DSC, the results of which are summarized below (Table 5.1). Compounds **5.3c-f** exhibited liquid crystal phases, while compound **5.3g** did not possess a liquid crystalline phase, but instead melted directly from a crystalline solid to an isotropic liquid at 158 °C.

Table 5.1: 10-Substituted-2,3,6,7-tetrakis(hexyloxy)dibenzo[a,c]phenazines phase behaviour.

Compound		Phase	$T_i/^\circ\text{C}$ ($\Delta H/\text{J g}^{-1}$)	Phase		
4.2a	X = H	Cr	$\xrightleftharpoons[140.1 (-108.2)]{170.0 (101.8)}$	I		
5.3c	X = Br	Cr	$\xrightleftharpoons[124.8 (-74.5)]{141.1 (90.0)}$	Col _h	$\xrightleftharpoons[137.1 (-6.9)]{166.4 (9.2)}$	I
5.3d	X = CN	Cr	$\xrightleftharpoons[102.2 (69.4)]{102.2 (69.4)}$	Col _h	$\xrightleftharpoons[161.7 (-5.3)]{172.1 (7.7)}$	I
5.3e	X = NO ₂	Cr	$\xrightleftharpoons[69.3 (-48.2)]{131.6 (42.9)}$	Col _h	$\xrightleftharpoons[168.8 (-8.1)]{173.5 (8.5)}$	I
5.3f	X = Cl	Cr	$\xrightleftharpoons[101.1 (-7.3)]{139.3 (41.1)}$	Col _h	$\xrightleftharpoons[149.2 (-6.5)]{163.1 (7.3)}$	I
5.3g	X = Me	Cr	$\xrightleftharpoons[121.1 (-79.0)]{157.5 (81.7)}$	I		

Examination of the remaining compounds by DSC revealed that each underwent two phase transitions upon heating, attributed to solid-to-liquid crystal and liquid crystal-to-isotropic liquid transitions, respectively. Samples viewed under polarized optical microscope exhibited textures typical of hexagonal columnar phase, with domains exhibiting approximately six-fold symmetry (Figure 5.5).

Figure 5.5: Polarized optical micrograph of compounds (5.3c) (top) and (5.3e) (bottom).



5.3c (Top) at 161°C, 5.3e (Bottom) at 167°C

5.3.3 Discussion

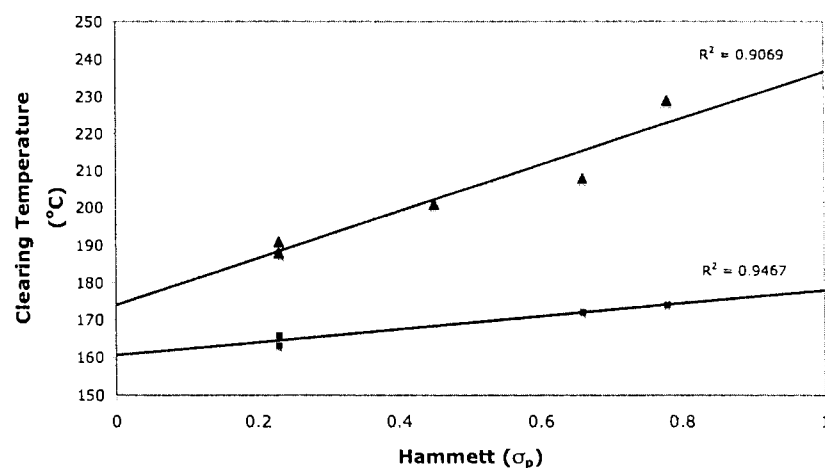
Four of the five 10-substituted compounds (**5.3c-f**) were found to form columnar hexagonal phases, while the methyl substituted derivative **5.3g** melted directly from crystalline solids into an isotropic liquid. As with the compounds **4.2a-m**, there was a correlation between the electron-withdrawing ability of the functional groups attached to the core and the tendency of these molecules to form liquid crystalline phases. Compounds with electron-withdrawing groups (Cl,

Br, CN and NO₂) formed Col_h phases, whereas those with relatively electron-donating groups (H, CH₃) were all found to be nonmesogenic.

A similar quantitative relationship as previously discussed was found between the nature of the substituents and liquid crystal phase stability when clearing temperature was plotted versus Hammett parameters (see Chapter 4 discussion). A linear correlation was observed between T_c and Hammett σ_p and σ_m values, with R² values of 0.94 and 0.87, respectively (Figure 5.6 and Figure 5.7). This observation provides further evidence that electron-withdrawing character of substituents is directly related to the stability of columnar phases.

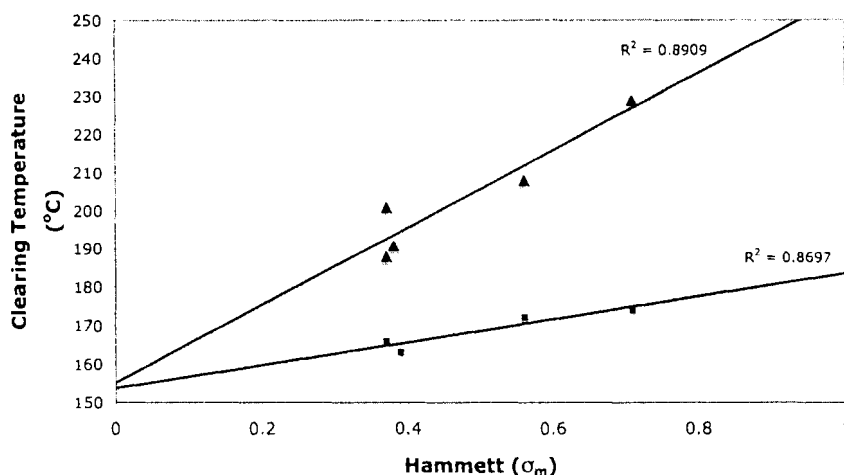
When this series was plotted on the same graph with compounds **4.2c-g** it was found that the slope of the lines for series **4.2** was much steeper than **5.2c-f**, indicating the functional groups in the 11-position raise the T_c by a greater amount than those substituted in the 10-position (Figure 5.6 and Figure 5.7).

Figure 5.6: Hammett σ_p versus clearing temperature (T_c) for compounds (5.3c-f) and (4.2c-g).



Compounds **4.2c-g** (in triangles) and compounds **5.3c-f** (in squares).

Figure 5.7: Hammett σ_m versus clearing temperature (T_c) for compounds (5.3c-f) and (4.2c-g).



Compounds **4.2c-g** (in triangles) and compounds **5.3c-f** (in squares).

It is interesting to note that if the least-squares fit for the two sets of compounds on this plot is extrapolated, they almost intersect at $\sigma_m = 0$ (Figure 5.8). 2,3,6,7-Tetrakis(hexyloxy)dibenzo[a,c]phenazine **4.2a**, wherein $X = \text{H}$, has a $\sigma_m = 0$ and is common to both series. The intersection of these two lines at $\sigma_m = 0$ therefore provides further evidence in favour of the use of σ_m values. Although the predicted clearing temperature for this compound is 154°C , it melts from a solid to an isotropic liquid at 170°C . This extrapolated line in a plot of T_c versus σ_m therefore correctly predicts that the liquid crystal phase of **4.2a** should not be observed, since it would be unstable above 170°C . In contrast to the σ_m plot, the σ_p plot versus T_c does not intersect at $\sigma_p = 0$.

The different slopes of the lines for compounds **4.2c-g** versus **5.3c-f** can be explained in terms of their component dipole moment vectors (Figure 5.8). The dipole component in the y-direction is likely the most important for the anti-

parallel alignment of molecules in the columnar phase. In the series of compounds **4.2**, the dipole in the y-direction (μ_y) component is larger than in series **5.3**. This dipole moment can be directly related to the phase stability, through the need for these molecules to adopt an anti-parallel alignment (Figure 5.9), as discussed previously (Chapter 4). The magnitude of the molecular dipole appears closely related to the propensity of disc-shaped molecules to form liquid crystalline phases.

Figure 5.8: Graphical representation of molecular dipoles for (4.2c-g) and (5.3c-g).

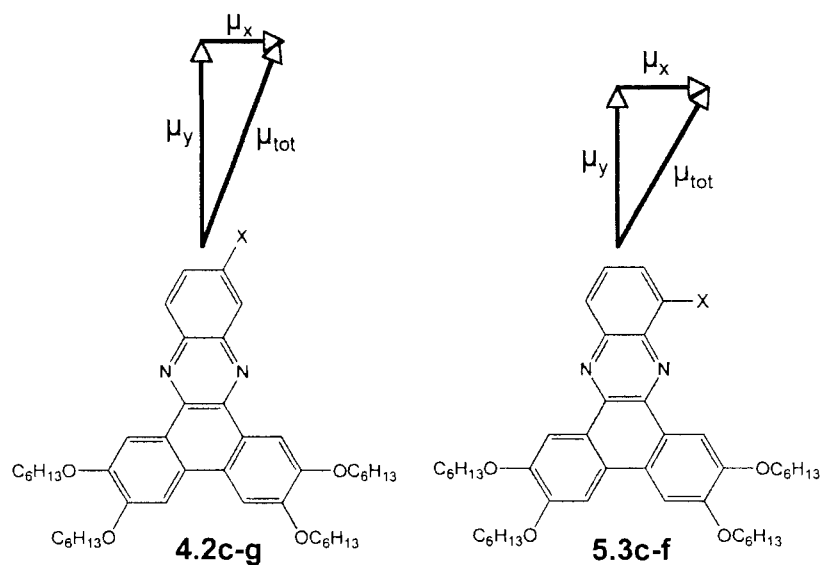
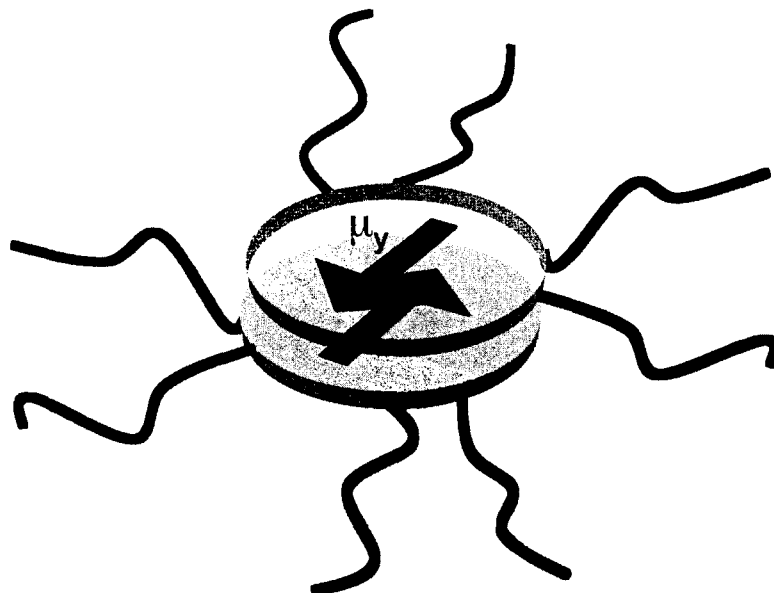


Figure 5.9: Anti-parallel alignment of adjacent molecules.



5.4 Summary

A second series of disc-shaped molecules was synthesized and characterized in order to investigate the propensity of these compounds to form liquid crystalline phases. There was again observed both a qualitative relationship between the functional groups and whether a columnar phase is observed as well as a quantitative correlation of clearing temperatures with the electron-withdrawing ability of the substituents. Significantly, the slope of the least-squares fit of clearing temperature versus Hammett parameters are smaller for series **5.3c-f** than for **4.2c-g**, indicating that there is a strong dependence of phase behaviour on functional group position.

5.5 Experimental

For general experimental, see Chapter 2. All solvents employed were reagent grade. 2,1,3-Benzothiadiazole and 2,4-dibromo-6-nitroaniline were purchased from Aldrich and used without further purification.

4,7-Dibromobenzo[c][1,2,5]thiadiazole (5.1a) To a stirring solution of 2,1,3-benzothiadiazole (0.50 g, 3.67 mmol) in 48% aqueous HBr (10 mL), bromine (0.28 mL, 5.50 mmol) was added dropwise over 10 minutes. The reaction mixture was heated to reflux for 3 hours, poured over ice and the solid collected by vacuum filtration. The solid was recrystallized in CHCl₃ and hexanes to yield a white solid (74%). ¹H NMR (500 MHz) (CDCl₃) δ (ppm) 7.74 (s, 2H); Mpt. (Lit): 187-188 (188-189)

4-Bromo-2,1,3-benzothiadiazole (5.1c) To a Schlenk flask was added 2,1,3-benzothiadiazole (0.50 g, 3.67 mmol), *N*-bromosuccinimide (0.65 g, 3.67 mmol) and iron trichloride (0.060 g, 0.37 mmol). Dry acetonitrile (10 mL) was added, and the reaction was stirred 30 minutes in a 30 °C oil bath. The reaction was poured over ice (50 mL), and the solid collected by vacuum filtration. The solid was eluted through a silica gel column (toluene:hexanes 3:2), a subsequent silica gel column (1% ethyl acetate in hexanes) followed by recrystallization in hexanes to yield **5.1c** (73%). ¹H NMR (500 MHz) (CDCl₃) δ (ppm) 7.97 (d, 1H *J* = 9 Hz). 7.845 (d, 1H *J* = 7 Hz), 7.48 (dd, 1H *J* = 7, 9Hz); Mpt. (Lit): 79-80 (79-81).
CI-MS *m/z* 214 (M⁺)

4-Cyano-2,1,3-benzothiadiazole (5.1d) To a Schlenk flask was added 4-bromo-2,1,3-benzothiadiazole **5.1c** (0.50 g, 2.30 mmol), copper(I)cyanide (0.40 g, 4.67 mmol) and copper (I) iodide (0.50 g, 2.60 mmol). Under an atmosphere of nitrogen, dry DMF (10 mL) was added, and the mixture was refluxed overnight. Upon cooling, the reaction mixture was poured into a solution of FeCl₃, HCl (10 mL), H₂O (15 mL) and then stirred overnight. The mixture was extracted with chloroform, the organic phase dried (MgSO₄) and the solvent removed under reduced pressure. The solid was eluted through a silica gel column (10% ethyl acetate in hexanes) and recrystallized from ethyl acetate and hexanes to yield a white solid (96%) ¹H NMR (500 MHz) (CDCl₃) δ (ppm) 8.70 (d, 1H *J* = 8 Hz), 8.52 (d, 1H *J* = 7 Hz), 7.83 (dd, 1H *J* = 7, 8Hz); Mpt. (Lit): 121-123 (124-125). CI-MS *m/z* 161 (M⁺)

4-Nitro-2,1,3-benzothiadiazole (5.1e) A solution of 70% nitric acid (20 mL) was cooled in an ice/water bath and 2,1,3-benzothiadiazole (3.00 g, 22 mmol) was added slowly. The reaction was allowed to warm to room temperature and the mixture was stirred for 30 minutes. The solution was poured over ice (200 mL) and the solid was collected by vacuum filtration and washed with hot hexanes to yield a yellow solid, 4-nitro-2,1,3-benzothiadiazole (64%). ¹H NMR (500 MHz) (CDCl₃) δ (ppm) 8.59 (d, 1H *J* = 7 Hz), 8.41 (d, 1H *J* = 6 Hz), 7.80 (dd, 1H *J* = 6, 7Hz); Mpt. (Lit): 105-106 (107-108). CI-MS *m/z* 181 (M⁺)

4-Amino-2,1,3-benzothiadiazole. To a solution of ethanol (5 mL) and 4-nitro-2,1,3-benzothiadiazole (0.15 g, 0.83 mmol) was added water (5 mL), $\text{Fe}_2(\text{SO}_4)_3$ (1.12 g, 2.48 mmol), NH_4Cl (0.35 g, 6.62 mmol), and zinc powder (0.16 g, 2.48 mmol). The mixture was stirred and heated to 50 °C in an oil bath for 2 hours and then filtered hot through a plug of celite. The solvent was removed under reduced pressure. Ethyl acetate (25 mL) and 25% aqueous NH_4Cl solution (50 mL) was added stirred for 10 minutes. The organic phase was separated, washed with H_2O , saturated aqueous NaHCO_3 , brine and dried over sodium sulphate. The solvent was removed under reduced pressure and the solid eluted through a short plug of silica gel (CH_2Cl_2) yielding a yellow solid (88%). The resultant solid was used immediately without further purification.

4-Chloro-2,1,3-benzothiadiazole (5.1f) 4-Amino-2,1,3-benzothiadiazole (0.42 g, 2.78 mmol) was dissolved in water (10 mL), concentrated hydrochloric acid (10 mL) and the cooled in an ice bath. Sodium nitrite (0.38 g, 5.6 mmol) was dissolved in water (3 mL) and slowly added to the reaction mixture. The reaction mixture was stirred in the ice bath for 15 minutes, then poured into a solution of copper(I)chloride (0.55 g, 5.56 mmol) in HCl (5 mL) and stirred overnight. Water (100 mL) was added and then the mixture extracted with chloroform, the organic phase dried over sodium sulphate and the solid eluted through a silica gel column (CH_2Cl_2) to yield a white solid (94%). ^1H NMR (500 MHz) (CDCl_3) δ (ppm) 7.94 (dd, 1H $J = 1, 9$ Hz), 7.64 (dd, 1H $J = 7, 1$ Hz), 7.55 (dd, 1H $J = 7, 9$ Hz); Mpt. (Lit): 79-80 (79-81). CI-MS m/z 170 (M)

3,6-Dibromo-1,2-phenylenediamine (5.2a) General procedure for reduction from Edlmann and co-workers.¹⁸⁶ To a stirred solution of ethanol (20 mL) and 4,7-dibromobenzo[*c*][1,2,5]thiadiazole (0.20 g, 0.68 mmol) was added sodium borohydride (0.52 g, 13.6 mmol). Further sodium borohydride (0.52 g, 13.64 mmol) added three times, at 2 hour intervals and the reaction mixture was stirred overnight. The solvent was removed under reduced pressure and water (100 mL) was added. The mixture was extracted with ether, the organic phase washed with brine and dried over MgSO₄. The solvent was removed under reduced pressure to yield a white solid (89%). The solid was used immediately without further purification.

3,5-Dibromo-1,2-phenylenediamine (5.2b) 2,4-Dibromo-6-nitroaniline (0.200 g, 0.676 mmol) was dissolved in ethanol (10 mL) and 10% palladium on activated carbon (0.050 g) was added. Hydrazine hydrate (0.17 mL, 3.4 mmol) was added dropwise and the mixture was then heated to reflux for 3 hours. The resultant solution was filtered hot through a plug of silica. This plug was washed with ethanol (50 mL), and the solvent evaporated under reduced pressure. The resultant solid was used immediately without further purification.

10,13-Dibromo-2,3,6,7-tetrakis(hexyloxy)dibenzo[*a,c*]phenazine (5.3a)
3,6-Dibromo-1,2-phenylenediamine was condensed with compound **2.6d** to yield

a yellow solid (84%). ^1H NMR (500 MHz) (CDCl_3) δ (ppm) 8.84 (s, 2H), 8.44 (s, 2H), 7.34 (s, 2H), 4.28-4.33 (m, 8H), 1.96-2.00 (m, ~8H), 1.24-1.54 (m, ~24H), 0.92-0.98 (m, ~12H); ^{13}C NMR (125 MHz) (CDCl_3) δ (ppm) 143.3, 133.4, 131.5, 126.4, 125.4, 124.4, 107.7, 106.3, 105.1, 73.3, 70.1, 69.4, 69.3, 68.3, 31.3, 28.7, 28.5, 26.3, 22.7, 14.0; Elemental analysis: calc. (found) for $\text{C}_{44}\text{H}_{58}\text{Br}_2\text{N}_2\text{O}_4$: C, 63.01 (63.22); H, 6.97 (7.12); N, 3.34 (3.47). MALDI-TOF calc. (found): 836 (836).

10,12-Dibromo-2,3,6,7-tetrakis(hexyloxy)dibenzo[a,c]phenazine (5.3b)

3,5-Dibromo-1,2-phenylenediamine was condensed with compound **2.6d** to yield a yellow solid (85%). ^1H NMR (500 MHz) (CDCl_3) δ (ppm) 8.74 (s, 2H), 8.44 (s, 2H), 7.80 (s, 1H), 7.39 (s, 1H), 4.27-4.23 (m, 8H), 1.98-2.01 (m, ~8H), 1.26-1.53 (m, ~24H), 0.91-0.96 (m, ~12H); ^{13}C NMR (125 MHz) (CDCl_3) δ (ppm) 143.2, 131.4, 130.5, 127.2, 125.4, 124.4, 111.2, 108.1, 107.7, 106.3, 105.1, 73.3, 71.1, 71.0, 70.1, 69.4, 69.3, 68.3, 32.5, 24.9, 24.7, 14.0; Elemental analysis: calc. (found) for $\text{C}_{44}\text{H}_{58}\text{Br}_2\text{N}_2\text{O}_4$: C, 63.01 (63.08); H, 6.97 (6.92); N, 3.34 (3.24). MALDI-TOF calc. (found): 836 (836).

10-Bromo-2,3,6,7-tetrakis(hexyloxy)dibenzo[a,c]phenazine (5.3c)

3-Bromo-1,2-phenylenediamine was condensed with compound **2.6d** to yield a yellow solid (83%). ^1H NMR (500 MHz) (CDCl_3) δ (ppm) 8.94 (s, 2H), 8.78 (s, 2H), 8.31 (d, 1H $J = 8\text{Hz}$), 8.00 (d, 1H $J = 8\text{Hz}$), 7.64-7.67 (m, 1H), 4.28-4.37 (m, 8H), 1.95-2.01 (m, ~8H), 1.24-1.56 (m, ~24H), 0.93-0.96 (m, ~12H); ^{13}C NMR

(125 MHz) (CDCl₃) δ (ppm) 156.6, 146.3, 134.5, 130.9, 126.4, 125.4, 107.9, 107.3, 107.1, 71.3, 70.2, 31.3, 28.7, 28.5, 26.3, 22.7, 14.1; Elemental analysis: calc. (found) for C₄₄H₅₉BrN₂O₄: C, 69.55 (69.75); H, 7.83 (7.79); N, 3.69 (3.67). MALDI-TOF calc. (found): 759 (760).

2,3,6,7-Tetrakis(hexyloxy)dibenzo[a,c]phenazine-10-carbonitrile

(5.3d) 2,3-Diaminobenzonitrile was condensed with compound **2.6d** to yield a yellow solid (96%). ¹H NMR (500 MHz) (CDCl₃) δ (ppm) 9.01 (s, 2H), 8.89 (s, 2H), 8.33 (d, 1H *J* = 8Hz), 8.13 (d, 1H *J* = 8Hz), 7.64-7.68 (m, 1H), 4.30-4.36 (m, 8H), 1.94-2.00 (m, ~8H), 1.23-1.56 (m, ~24H), 0.92-0.98 (m, ~12H); ¹³C NMR (125 MHz) (CDCl₃) δ (ppm) 147.3, 134.2, 133.1, 132.0, 125.7, 125.5, 115.1, 107.9, 107.3, 107.2, 106.1, 33.1 68.6, 70.3, 70.2, 70.0, 69.3, 69.3, 32.4, 32.3, 28.7, 28.4, 26.5, 22.7, 14.1; Elemental analysis: calc. (found) for C₄₅H₅₉N₃O₄: C, 76.56 (76.59); H, 8.42 (8.60); N, 5.95 (5.82). MALDI-TOF calc. (found): 706 (706).

2,3,6,7-Tetrakis(hexyloxy)-10-nitrodibenzo[a,c]phenazine (5.3e)

3-Nitro-1,2-phenylenediamine was condensed with compound **2.6d** to yield a red solid (94%). ¹H NMR (500 MHz) (CDCl₃) δ (ppm) 9.15 (s, 2H), 9.06 (s, 2H), 8.57 (d, 1H *J* = 8Hz), 8.33 (d, 1H *J* = 8Hz), 7.74-7.78 (m, 1H), 4.24-4.36 (m, 8H), 1.94-2.00 (m, ~8H), 1.23-1.56 (m, ~24H), 0.92-0.98 (m, ~12H); ¹³C NMR (125 MHz) (CDCl₃) δ (ppm) 152.2, 152.0, 149.5, 130.9, 130.8, 127.0, 126.5, 123.0, 122.7, 120.1, 111.8, 108.8, 108.6, 106.3, 106.2, 69.5, 69.2, 69.1, 31.6, 29.2, 29.2, 25.8,

25.7, 22.6, 14.0; Elemental analysis: calc. (found) for $C_{44}H_{59}N_3O_6$: C, 72.80 (72.59); H, 8.19 (8.11); N, 5.79 (5.58). MALDI-TOF calc. (found): 725 (725).

10-Chloro-2,3,6,7-tetrakis(hexyloxy)dibenzo[a,c]phenazine (5.3f) 3-Chloro-1,2-phenylenediamine was condensed with compound **2.6d** to yield a yellow solid (87%). 1H NMR (500 MHz) ($CDCl_3$) δ (ppm) 8.90 (s, 2H), 8.76 (s, 2H), 8.28 (d, 1H $J = 8$ Hz), 8.03 (d, 1H $J = 8$ Hz), 7.66-7.68 (m, 1H), 4.24-4.36 (m, 8H), 1.94-2.00 (m, ~8H), 1.23-1.56 (m, ~24H), 0.92-0.98 (m, ~12H); ^{13}C NMR (125 MHz) ($CDCl_3$) δ (ppm) 154.3, 147.3, 135.2, 131.4, 131.0, 125.4, 125.4, 107.9, 107.3, 107.2, 106.1, 33.1 70.2, 70.3, 32.4, 32.3, 28.7, 28.4, 26.5, 22.7, 14.1; Elemental analysis: calc. (found) for $C_{44}H_{59}ClN_2O_4$: C, 73.87 (73.94); H, 8.31 (8.53); N, 3.92 (4.18). MALDI-TOF calc. (found): 714 (714).

2,3,6,7-Tetrakis(hexyloxy)-10-methyldibenzo[a,c]phenazine (5.3g) Synthesized by the condensation of compound **2.6d** and 2,3-diaminotoluene to afford a yellow solid (85%). 1H NMR (500 MHz) ($CDCl_3$) δ (ppm) 8.94 (s, 2H), 8.77 (s, 2H), 8.27 (d, 1H $J = 9$ Hz), 8.04 (d, 1H $J = 9$ Hz), 7.64-7.66 (m, 1H), 4.22-4.35 (m, 8H), 3.91 (s, 3H), 1.92-1.97 (m, ~8H), 1.21-1.56 (m, ~24H), 0.92-1.00 (m, ~12H); ^{13}C NMR (125 MHz) ($CDCl_3$) δ (ppm) 155.6, 155.3, 148.2, 134.6, 131.4, 131.0, 125.4, 125.4, 108.9, 108.3, 107.1, 107.1, 33.6 70.5, 70.6, 32.5, 32.3, 28.5, 26.5, 26.4, 22.5, 14.3; Elemental analysis: calc. (found) for $C_{45}H_{62}N_2O_4$: C, 77.77 (77.69); H, 8.99 (9.11); N, 4.03 (4.09). MALDI-TOF calc. (found): 695 (695).

6 CONCLUSION AND FUTURE WORK

6.1 Conclusion

In the previous chapters, investigations into the structure-property relationships of discotic mesogens were described. Tetralkoxyphenanthrene quinone is a versatile precursor that allowed for the effects of symmetry, heteroatoms, core-size and functional groups to be probed.

Preliminary investigations into the effects of molecular symmetry by changing pendant alkoxy chain length was shown to be a viable method for modifying columnar phase behaviour. Although Carnelley's rule does not seem to apply universally to liquid crystals, the majority of compounds (80%) that were investigated did show that lowering the symmetry of the molecule lowers phase transition temperatures.

It appears that increasing the core-size of disc-shaped molecules increases the favourable dispersion forces between neighbouring molecules and increases the propensity for these molecules to form liquid crystals. Location and the number of nitrogen atoms in an aromatic core of a liquid crystal also alters the stability of columnar phases, presumably via electrostatic interactions.

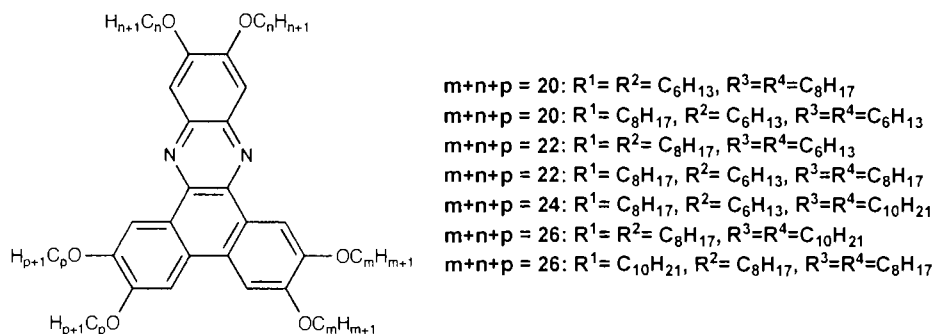
We have shown both a qualitative relationship between the nature of the functional groups and whether a columnar phase is observed as well as a quantitative correlation of clearing temperatures of the mesogenic compounds with the electron-withdrawing ability of the substituents. This trend can most

likely be explained by the changes in the electrostatic interactions between molecules within the columns which favour stacking between electron-deficient aromatic rings. This research has also shown that, like heteroatoms, functional group position is also an important factor.

6.2 Future work

The symmetry studies presented in Chapter 2 represent very preliminary efforts to understand whether Carnelly's rule applies to solid-to-liquid crystal and liquid crystal-to-isotropic transitions. More comparisons of constitutional isomers are needed before final conclusions can be drawn. The synthesis of seven more compounds to expand the hexaalkoxydibenzophenazine series can be proposed (Figure 6.1). Taken together with compounds already reported, 12 pairs of constitutional isomers of different symmetry, instead of the 5 reported in Chapter 2, will be accessible.

Figure 6.1: Hexaalkoxydibenzophenazine derivatives.

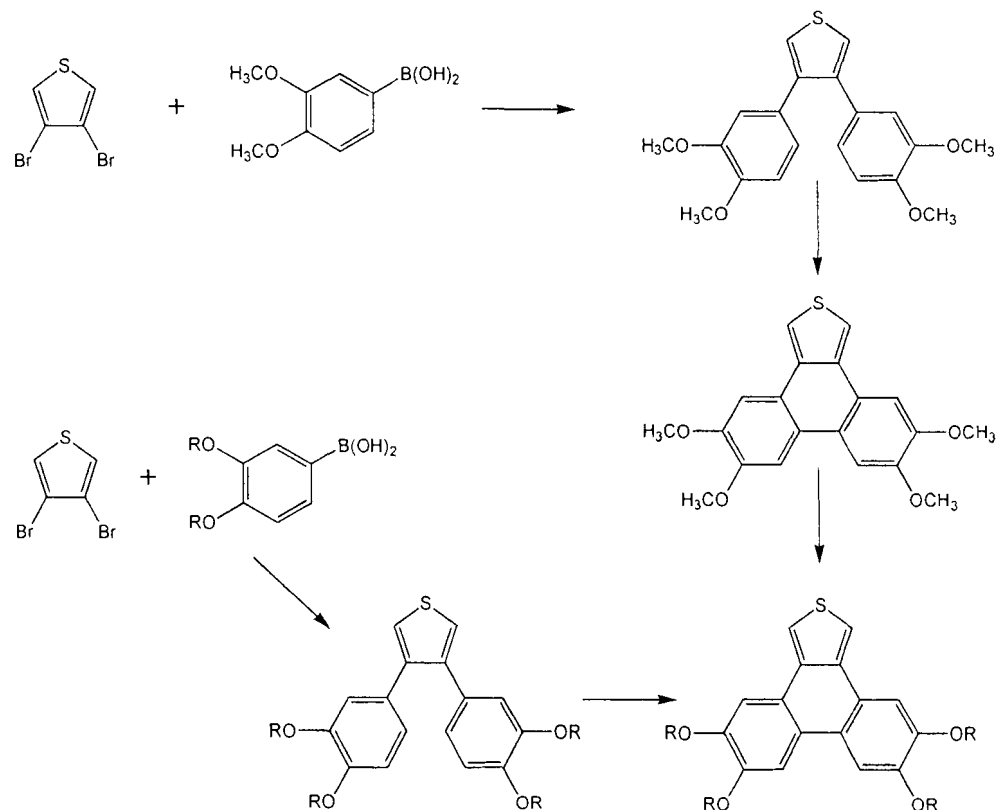


Our investigations into heteroatom effects in Chapter 3 can be extended to include heteroatoms other than nitrogen. I propose the completion of research

into two separate fused thiophene-containing cores. To the best of my knowledge, no thiophene containing discotic mesogens have been reported.

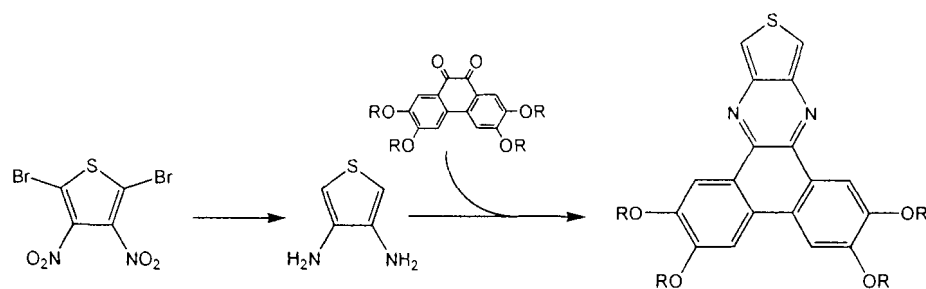
In continuation of research carried out by the Williams Research Group, use of boronic acid coupling, followed by oxidative cyclization can be used to create a series 5,6,9,10-tetrakis(alkoxy)phenanthro[9,10-c]thiophenes (Scheme 6.1). This series of compounds can be directly compared to tetraalkoxytriphenylenes and would hopefully show the effect of sulphur on π - π stacking. It should be noted that the 2,5 positions of the thiophene are very active towards polymerization and may need to be protected throughout the synthesis.

Scheme 6.1: Synthesis of sulphur containing core – type I.



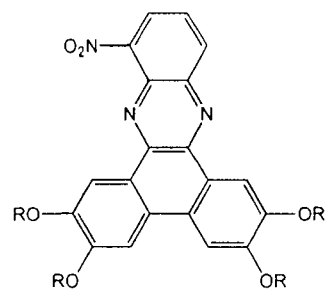
A second thiophene containing discotic mesogen could also be synthesized, from 3,4-diaminothiophene and the tetralkoxyphenanthrene quinones already at hand (**2.6a-f**) (Scheme 6.2). Nitration of commercially available 2,5-dibromothiophene in fuming nitric and sulphuric acid gives 2,5-dibromo-3,4-dinitrothiophene.¹⁸⁷ Treatment in hydrochloric acid and tin powder removes the two bromines as well as reducing the nitro groups to amines.¹⁸⁸ This 3,4-diaminothiophene could be coupled with our phenanthrene quinones to yield cores analogous to [a,c]dibenzophenazines reported in the previous chapters.

Scheme 6.2: Synthesis of sulphur containing core – type II.



It is interesting to note that compound 2,3,6,7-tetrakis(hexyloxy)-10-nitrodibenzo[a,c]phenazine **5.3e**, gels solvent at sufficiently high concentrations. This phenomenon was noticed while trying to dissolve the compound for column chromatography in 10% ethyl acetate in hexanes and has also been shown to work in a variety of solvents. Synthesis and characterization of a series of compounds containing this core structure would be interesting, to see the effect of alkyl chain length on gelation (Figure 6.2).

Figure 6.2: 2,3,6,7-Tetraalkoxy-10-nitrodibenzo[a,c]phenazines.



7 REFERENCES

- (1) Hirth, L.; Lebeurier, G.; Nicolaieff, A.; Richards, K. E. *Biophys. J.* **1980**, *32*, 460-462.
- (2) Richards, K. E.; Morel, M. C.; Nicolaieff, A.; Lebeurier, G.; Hirth, L. *Biochimie* **1975**, *57*, 749-755.
- (3) Isaacs, L. C., D.; Bowden, N.; Xia, Y.; Whitesides, G. M. *Supramolecular Technology*; Wiley: New York, 1999.
- (4) Creighton, T. E. *Biochem. J.* **1990**, *270*, 1-16.
- (5) Dagani, R. *Chem. Eng. News* **1991**, *69*, 24-25.
- (6) Deckman, H. W.; Dunsmuir, J. H.; Garoff, S.; McHenry, J. A.; Peiffer, D. *G. J. Vac. Sci. Tech. B* **1988**, *6*, 333-336.
- (7) Klug, A. *Angew. Chem., Int. Ed. in Engl.* **1983**, *22*, 565-582.
- (8) Metzger, R. M. *J. Mater. Chem.* **1999**, *9*, 2027-2036.
- (9) Metzger, R. M. *Adv. Mater. Opt. Elec.* **1998**, *8*, 229-245.
- (10) Dai, H. J.; Wong, E. W.; Lieber, C. M. *Science* **1996**, *272*, 523-526.
- (11) Craats, A. M. v. d.; Warman, J. M.; Müllen, K.; Geerts, Y.; Brand, J. D. *Adv. Mater.* **1998**, *10*, 36-38.
- (12) Niemeyer, C. M. *Angew. Chem., Int. Ed. in Engl.* **2001**, *40*, 4128-4158.
- (13) Gosele, U. *Nature* **2006**, *440*, 34-35.
- (14) Geer, D. *IEEE Pervasive Computing* **2006**, *5*, 7-11.
- (15) Lapotko, D.; Aleinikova, O.; Lukianova, E.; Shman, T.; Savitsky, V.; Oraevsky, A. *Bio. Blood And Marrow Trans.* **2006**, *12*, 104-104.
- (16) Clark, T. D.; Tien, J.; Duffy, D. C.; Paul, K. E.; Whitesides, G. M. *J. Am. Chem. Soc.* **2001**, *123*, 7677-7682.
- (17) Gracias, D. H.; Kavthekar, V.; Love, J. C.; Paul, K. E.; Whitesides, G. M. *Adv. Mater.* **2002**, *14*, 235-241.
- (18) Grzybowski, B. A.; Stone, H. A.; Whitesides, G. M. *Nature* **2000**, *405*, 1033-1036.
- (19) Srinivasan, U.; Liepmann, D.; Howe, R. T. *J. Microelect. Sys.* **2001**, *10*, 17-24.
- (20) Whitesides, G. M.; Grzybowski, B. *Science* **2002**, *295*, 2418-2421.
- (21) Cammidge, A. N.; Bushby, R. J. In *Handbook of Liquid Crystals*; Demus, D., Goodby, J., Gray, G. W., Spiess, H.-W., Vill, V., Eds.; Wiley-VCH: New York, 1998; Vol. 2B, p 693-748.
- (22) Reinitzer, F. *Annalen Der Physik* **1908**, *27*, 213-224.
- (23) Cammidge, A. N.; Bushby, R. J. In *Handbook of Liquid Crystals*; Demus, D., Goodby, J., Gray, G. W., Spiess, H.-W., Vill, V., Eds.; Wiley-VCH: New York, 1998; Vol. 2B
- (24) Rondeau, R. E.; Serve, M. P.; Steppel, R. N.; Berwick, M. A. *J. Am. Chem. Soc.* **1972**, *94*, 1096.
- (25) Chandrasekhar, S.; Sadashiva, B. K.; Suresh, K. A. *Pramana* **1977**, *9*, 471-480.
- (26) Levelut, A. *J. De Phys.* **1983**, *44*, 61-66.
- (27) Chandrasekhar, S.; Prasad, S. K. *Contemp. Phys.* **1999**, *40*, 237-245.

- (28) Freudenmann, R.; Behnisch, B.; Hanack, M. *J. Mater. Chem.* **2001**, *11*, 1618-1624.
- (29) Schmidt-Mende, L.; Fechtenkotter, A.; Müllen, K.; Moons, E.; Friend, R. H.; MacKenzie, J. D. *Science* **2001**, *293*, 1119-22.
- (30) van de Craats, A. M.; Stutzmann, N.; Bunk, O.; Nielsen, M. M.; Watson, M.; Mullen, K.; Chanzy, H. D.; Sirringhaus, H.; Friend, R. H. *Adv. Mater.* **2003**, *15*, 495-499.
- (31) Adam, D.; Closs, F.; Frey, T.; Funhoff, D.; Haarer, D.; Ringsdorf, H.; Schuhmacher, P.; Siemensmeyer, K. *Phys. Rev. Lett.* **1993**, *70*, 457-460.
- (32) Bleyl, I.; Erdelen, C.; Schmidt, H. W.; Haarer, D. *Philos. Mag. B-Phys. Condens. Matter Stat. Mech. Electron. Opt. Magn. Prop.* **1999**, *79*, 463-475.
- (33) Percec, V.; Glodde, M.; Bera, T. K.; Miura, Y.; Shiyanovskaya, I.; Singer, K. D.; Balagurusamy, V. S. K.; Heiney, P. A.; Schnell, I.; Rapp, A.; Spiess, H. W.; Hudson, S. D.; Duan, H. *Nature* **2002**, *419*, 384-387.
- (34) Shiyanovskaya, I.; Singer, K. D.; Percec, V.; Bera, T. K.; Miura, Y.; Glodde, M. *Phys. Rev. B* **2003**, *67*.
- (35) Mori, H.; Itoh, Y.; Nishiura, Y.; Nakamura, T.; Shinagawa, Y. *Jap. J. App. Phys. 1* **1997**, *36*, 143-147.
- (36) Kumar, S. *Liq. Cryst.* **2005**, *32*, 1089-1113.
- (37) Hoger, S.; Cheng, X. H.; Ramminger, A. D.; Enkelmann, V.; Rapp, A.; Mondeshki, M.; Schnell, I. *Angew. Chem., Int. Ed. in Engl.* **2005**, *44*, 2801-2805.
- (38) Boden, N.; Movaghar, B. In *Handbook of Liquid Crystals*; Demus, D., Goodby, J., Gray, G. W., Spiess, H.-W., Vill, V., Eds.; Wiley-VCH: New York, 1998; Vol. 2b, p 781-798.
- (39) Demus, D. In *Handbook of Liquid Crystals*; Demus, D., Goodby, J., Gray, G. W., Spiess, H.-W., Vill, V., Eds.; Wiley-VCH: New York, 1998; Vol. 1, p 133-187.
- (40) Destrade, C.; Tinh, N. H.; Gasparoux, H.; Malthete, J.; Levelut, A. M. *Mol. Cryst. Liq. Cryst.* **1981**, *71*, 111-135.
- (41) Gramsbergen, E. F.; Hoving, H. J.; Dejeu, W. H.; Praefcke, K.; Kohne, B. *Liq. Cryst.* **1986**, *1*, 397-400.
- (42) Kohne, B.; Poules, W.; Praefcke, K. *Chem.-Zeit.* **1984**, *108*, 113-113.
- (43) Borner, R. C.; Jackson, R. F. W. *J. Chem. Soc.-Chem. Commun.* **1994**, 845-846.
- (44) Lee, W. K.; Wintner, B. A.; Fontes, E.; Heiney, P. A.; Ohba, M.; Haseltine, J. N.; Smith, A. B. *Liq. Cryst.* **1989**, *4*, 87-102.
- (45) Destrade, C.; Tinh, N. H.; Mamlok, L.; Malthete, J. *Mol. Cryst. Liq. Cryst.* **1984**, *114*, 139-150.
- (46) Mamlok, L.; Malthete, J.; Tinh, N. H.; Destrade, C.; Levelut, A. M. *J. Phys. Lett.* **1982**, *43*, L641-L647.
- (47) Cayuela, R.; Nguyen, H. T.; Destrade, C.; Levelut, A. M. *Mol. Cryst. Liq. Cryst.* **1989**, *177*, 81-91.
- (48) Tinh, N. H.; Cayuela, R.; Destrade, C. *Mol. Cryst. Liq. Cryst.* **1985**, *122*, 141-149.

- (49) Boden, N.; Bushby, R. J.; Cammidge, A. N. *Liq. Cryst.* **1995**, *18*, 673-676.
- (50) Boden, N.; Bushby, R. J.; Cammidge, A. N.; Headdock, G. J. *Mater. Chem.* **1995**, *5*, 2275-2281.
- (51) Hanack, M.; Beck, A.; Lehmann, H. *Synth. Stutt.* **1987**, 703-705.
- (52) Guillon, D.; Weber, P.; Skoulios, A.; Piechocki, C.; Simon, J. *Mol. Cryst. Liq. Cryst.* **1985**, *130*, 223-229.
- (53) Guillon, D.; Skoulios, A.; Piechocki, C.; Simon, J.; Weber, P. *Mol. Cryst. Liq. Cryst.* **1983**, *100*, 275-284.
- (54) Piechocki, C.; Simon, J.; Skoulios, A.; Guillon, D.; Weber, P. *J. Am. Chem. Soc.* **1982**, *104*, 5245-5247.
- (55) Pisula, W.; Kastler, M.; Wasserfallen, D.; Pakula, T.; Mullen, K. *J. Am. Chem. Soc.* **2004**, *126*, 8074-8075.
- (56) Pisula, W.; Menon, A.; Stepputat, M.; Lieberwirth, I.; Kolb, U.; Tracz, A.; Siringhaus, H.; Pakula, T.; Müllen, K. *Adv. Mater.* **2005**, *17*, 684.
- (57) Pisula, W.; Tomovic, Z.; El Hamaoui, B.; Watson, M. D.; Pakula, T.; Müllen, K. *Adv. Func. Mater.* **2005**, *15*, 893-904.
- (58) Pisula, W.; Tomovic, Z.; Stepputat, M.; Kolb, U.; Pakula, T.; Müllen, K. *Chem. Mater.* **2005**, *17*, 2641-2647.
- (59) Pisula, W.; Tomovic, Z.; Simpson, C.; Kastler, M.; Pakula, T.; Müllen, K. *Chem. Mater.* **2005**, *17*, 4296-4303.
- (60) Van de Craats, A. M.; Warman, J. M. *Adv. Mater.* **2001**, *13*, 130-133.
- (61) Lau, K.; Foster, J.; Williams, V. *Chem. Commun.* **2003**, 2172-2173.
- (62) Brown, R. J. C.; Brown, R. F. C. *J. Chem. Educ.* **2000**, *77*, 724-731.
- (63) Pinal, R. *Org. Biomol. Chem.* **2004**, *2*, 2692-2699.
- (64) Allen, M. T.; Diele, S.; Harris, K. D. M.; Hegmann, T.; Kariuki, B. M.; Preece, J. A.; Tschierske, C. *J. Mater. Chem.* **2001**, *11*, 302-11.
- (65) Bushby, R. J. B., N. *J. Mater. Chem.* **2003**, *13*, 470-474.
- (66) Allen, M. T.; Harris, K. D. M.; Kariuki, B. M.; Kumari, N.; Preece, J. A.; Diele, S.; Lose, D.; Hegmann, T.; Tschierske, C. *Liq. Cryst.* **2000**, *27*, 689-692.
- (67) Kumar, S.; Manickam, M.; Varshney, S. K.; Rao, D. S. S.; Prasad, S. K. *J. Mater. Chem.* **2000**, *10*, 2483-2489.
- (68) Perez, D.; Guitian, E. *Chem. Soc. Rev.* **2004**, *33*, 274-283.
- (69) Boden, N.; Borner, R. C.; Bushby, R. J.; Cammidge, A. N.; Jesudason, M. V. *Liq. Cryst.* **1993**, *15*, 851-858.
- (70) Tinh, N. H.; Bernaud, M. C.; Sigaud, G.; Destrade, C. *Mol. Cryst. Liq. Cryst.* **1981**, *65*, 307-316.
- (71) Chapuzet, J. M.; Simonetgueguen, N.; Taillepied, I.; Simonet, J. *Tetrahedron Lett.* **1991**, *32*, 7405-7408.
- (72) Naarmann, H.; Hanack, M.; Mattmer, R. *Synth. Stutt.* **1994**, 477-478.
- (73) Cross, S. J.; Goodby, J. W.; Hall, A. W.; Hird, M.; Kelly, S. M.; Toyne, K. J.; Wu, C. *Liq. Cryst.* **1998**, *25*, 1-11.
- (74) Paraschiv, I.; Delforterie, P.; Giesbers, M.; Posthumus, M. A.; Marcelis, A. T. M.; Zuilhof, H.; Sudholter, E. J. R. *Liq. Cryst.* **2005**, *32*, 977-983.

- (75) Destrade, C.; Mondonbernaud, M. C.; Tinh, N. H. *Mol. Cryst. Liq. Cryst.* **1979**, *49*, 169-174.
- (76) Josefowicz, J. Y.; Maliszewskyj, N. C.; Idziak, S. H. J.; Heiney, P. A.; McCauley, J. P.; Smith, A. B. *Science* **1993**, *260*, 323-326.
- (77) Wenz, G. *Makromol. Chem., Rapid Commun.* **1985**, *6*, 577-584.
- (78) Maliszewskyj, N. C.; Heiney, P. A.; Blasie, J. K.; McCauley, J. P.; Smith, A. B. *Journal De Physique II* **1992**, *2*, 75-85.
- (79) Maliszewskyj, N. C.; Heiney, P. A.; Josefowicz, J. Y.; McCauley, J. P.; Smith, A. B. *Science* **1994**, *264*, 77-79.
- (80) Orthmann, E.; Wegner, G. *Angew. Chem., Int. Ed. in Engl.* **1986**, *25*, 1105-1107.
- (81) Kreuder, W.; Ringsdorf, H.; Tschirner, P. *Makr. Chem.,-Rap. Comm.* **1985**, *6*, 367-373.
- (82) Ringsdorf, H.; Schlarb, B.; Venzmer, J. *Angew. Chem., Int. Ed. in Engl.* **1988**, *27*, 113-158.
- (83) Ringsdorf, H.; Wustefeld, R. *Philosophical Transactions Of The Royal Society Of London Series A-Mathematical Physical And Engineering Sciences* **1990**, *330*, 95-108.
- (84) Mohr, B.; Wegner, G.; Ohta, K. *J. Chem. Soc., Chem. Commun.* **1995**, 995-996.
- (85) Sharma, V. B.; Jain, S. L.; Sain, B. *Tetrahedron Lett.* **2003**, *44*, 383-386.
- (86) Mohr, B.; Enkelmann, V.; Wegner, G. *J. Org. Chem.* **1994**, *59*, 635.
- (87) Cammidge, A. N.; Gopee, H. *Chem. Commun.* **2002**, 966-967.
- (88) Buck, J. I., W. *J. Am. Chem. Soc.* **1931**, 1536-1542.
- (89) Nelson, K., Robertson, J., Duvall J. *J. Am. Chem. Soc.* **1964**, 684-687.
- (90) Baskaran, S.; Das, J.; Chandrasekaran, S. *J. Org. Chem.* **1989**, *54*, 5182-5184.
- (91) McKillop, A.; Mills, L. S. *Synth. Commun.* **1987**, *17*, 647-655.
- (92) Varma, R. S.; Naicker, K. P. *Tetrahedron Lett.* **1998**, *39*, 7463-7466.
- (93) Yusubov, M. S.; Chi, K. V.; Krasnokutskaya, E. A.; Vasileva, V. P.; Filimonov, V. D. *Zh. Org. Khim.* **1995**, *31*, 1675-1678.
- (94) Chi, K. W.; Yusubov, M. S.; Filimonov, V. D. *Synth. Commun.* **1994**, *24*, 2119-2122.
- (95) Liu, C.; Fechtenkoetter, A.; Watson, M. D.; Muellen, K.; Bard, A. J. *Chem. Mater.* **2003**, *15*, 124-130.
- (96) Sakashita, H.; Nishitani, A.; Sumiya, Y.; Terauchi, H.; Ohta, K.; Yamamoto, I. *Mol. Cryst. Liq. Cryst.* **1988**, *163*, 211-219.
- (97) Ohta, K.; Hasebe, H.; Moriya, M.; Fujimoto, T.; Yamamoto, I. *Mol. Cryst. Liq. Cryst.* **1991**, *208*, 33-41.
- (98) Orito, K.; Hatakeyama, T.; Takeo, M.; Suginome, H. *Synth. Stutt* **1995**, 1273-1275.
- (99) Lee, H.-K.; Lee, H.; Chang, Y. J.; Oh, N.-K.; Zin, W.-C.; Kim, K. *Angew. Chem., Int. Ed. in Engl.* **2001**, *40*, 2669-71.
- (100) Mohr, B.; Wegner, G.; Ohta, K. *J. Chem. Soc., Chem. Commun.* **1995**, 995-996.

- (101) Ong, C. W.; Liao, S. C.; Chang, T. H.; Hsu, H. F. *Tetrahedron Lett.* **2003**, *44*, 1477-1480.
- (102) Forget, S.; Veber, M.; Strzelecka, H. *Mol. Cryst. Liq. Cryst. A* **1995**, *258-263*.
- (103) Yatabe, T.; Harbison, M. A.; Brand, J. D.; Wagner, M.; Müllen, K.; Samori, P.; Rabe, J. *J. Mater. Chem.* **2000**, *10*, 1519-1525.
- (104) Boden, N.; Bushby, R. J.; Headdock, G.; Lozman, O. R.; Wood, A. *Liquid Crystals* **2001**, *28*, 139-144.
- (105) Msayib, K.; Mahkseed, S.; McKeown, N. B. *J. Mater. Chem.* **2001**, *11*, 2784-2789.
- (106) Ong, C. W.; Liao, S. C.; Chang, T. H.; Hsu, H. F. *J. Org. Chem.* **2004**, *69*, 3181-3185.
- (107) Boden, N.; Bushby, R.; Donovan, K.; Liu, Q.; Lu, Z.; Kreouzis, T.; Wood, A. *Liq. Cryst.* **2001**, *28*, 1739-1744.
- (108) Kestemont, G.; de Halleux, V.; Lehmann, M.; Ivanov, D. A.; Watson, M.; Geerts, Y. H. *Chem. Commun.* **2001**, 2074-2075.
- (109) Lehmann, M.; Lemaur, V.; Cornil, J.; Bredas, J. L.; Goddard, S.; Grizzi, I.; Geerts, Y. *Tetrahedron* **2004**, *60*, 3283-3291.
- (110) Pieterse, K.; Lauritsen, A.; Schenning, A.; Vekemans, J.; Meijer, E. W. *Chem. Eur. J.* **2003**, 5597-5604.
- (111) Pieterse, K.; van Hal, P. A.; Kleppinger, R.; Vekemans, J.; Janssen, R. A. J.; Meijer, E. W. *Chem. Mater.* **2001**, *13*, 2675-2679.
- (112) Hoeben, F. J. M.; Jonkheijm, P.; Meijer, E. W.; Schenning, A. *Chemical Reviews* **2005**, *105*, 1491-1546.
- (113) Lehmann, M.; Kestemont, G.; Aspe, R. G.; Buess-Herman, C.; Koch, M. H. J.; Debije, M. G.; Piris, J.; de Haas, M. P.; Warman, J. M.; Watson, M. D.; Lemaur, V.; Cornil, J.; Geerts, Y. H.; Gearba, R.; Ivanov, D. A. *Chem. Eur. J.* **2005**, 3349-3362.
- (114) Lemaur, V.; Da Silva Filho, D. A.; Coropceanu, V.; Lehmann, M.; Geerts, Y.; Piris, J.; Debije, M. G.; Van de Craats, A. M.; Senthilkumar, K.; Siebbeles, L. D. A.; Warman, J. M.; Bredas, J. L.; Cornil, J. *J. Am. Chem. Soc.* **2004**, *126*, 3271-3279.
- (115) Roussel, O.; Kestemont, G.; Tant, J.; de Halleux, V.; Aspe, R. G.; Levin, J.; Remacle, A.; Gearba, I. R.; Ivanov, D.; Lehmann, M.; Geerts, Y. *Mol. Cryst. Liq. Cryst.* **2003**, *396*, 35-39.
- (116) Olivier, Y.; Lemaur, V.; Bredas, J. L.; Cornil, J. *J. Phys. Chem. A* **2006**, *110*, 6356-6364.
- (117) Schmidtke, J. P.; Friend, R. H.; Kastler, M.; Mullen, K. *J. Chem. Phys.* **2006**, *124*, 174-204.
- (118) Duzhko, V.; Semyonov, A.; Twieg, R. J.; Singer, K. D. *Phys. Rev. B* **2006**, *73*, 178-183.
- (119) Wasserfallen, D.; Kastler, M.; Pisula, W.; Hofer, W. A.; Fogel, Y.; Wang, Z. H.; Mullen, K. *J. Am. Chem. Soc.* **2006**, *128*, 1334-1339.
- (120) Bushby, R. J.; Donovan, K. J.; Kreouzis, T.; Lozman, O. R. *Opto. Elec. Rev.* **2005**, *13*, 269-279.

- (121) Kaafarani, B. R.; Kondo, T.; Yu, J. S.; Zhang, Q.; Dattilo, D.; Risko, C.; Jones, S. C.; Barlow, S.; Domercq, B.; Amy, F.; Kahn, A.; Bredas, J. L.; Kippelen, B.; Marder, S. R. *J. Am. Chem. Soc.* **2005**, *127*, 16358-16359.
- (122) Müller, G. R. J.; Meiners, C.; Enkelmann, V.; Geerts, Y.; Müllen, K. *J. Mater. Chem.* **1998**, *8*, 61-64.
- (123) Boden, N.; Bushby, R. J.; Headdock, G.; Lozman, O. R.; Wood, A. *Liq. Cryst.* **2001**, *28*, 139-144.
- (124) Herwig, P.; Kayser, C. W.; Müllen, K.; Spiess, H. W. *Adv. Mater.* **1996**, *8*, 510-513.
- (125) Makhseed, S.; Bumajdad, A.; Ghanem, B.; Msayib, K.; McKeown, N. B. *Tetrahedron Lett.* **2004**, *45*, 4865-4868.
- (126) Cockroft, S. L.; Hunter, C. A.; Lawson, K. R.; Perkins, J.; Urch, C. J. *J. Am. Chem. Soc.* **2005**, *127*, 8594-8595.
- (127) Cozzi, F.; Annunziata, R.; Benaglia, M.; Cinquini, M.; Raimondi, L.; Baldrige, K. K.; Siegel, J. S. *Org. Biomol. Chem.* **2003**, *1*, 157-162.
- (128) Cozzi, F.; Cinquini, M.; Annunziata, R.; Dwyer, T.; Siegel, J. S. *J. Am. Chem. Soc.* **1992**, *114*, 5729-5733.
- (129) Cozzi, F.; Cinquini, M.; Annunziata, R.; Siegel, J. S. *J. Am. Chem. Soc.* **1993**, *115*, 5330-5331.
- (130) Cozzi, F.; Ponzini, F.; Annunziata, R.; Cinquini, M.; Siegel, J. S. *Angew. Chem., Int. Ed. in Engl.* **1995**, *34*, 1019-1020.
- (131) Guckian, K. M.; Schweitzer, B. A.; Ren, R. X.-F.; Sheils, C. J.; Tahmassebi, D. C.; Kool, E. T. *J. Am. Chem. Soc.* **2000**, *122*, 2213-2222.
- (132) Hoeben, F. J. M.; Jonkheijm, P.; Meijer, E. W.; Schenning, A. *Chem. Rev.* **2005**, *105*, 1491-1546.
- (133) Meyer, E. A.; Castellano, R. K.; Diederich, F. *Angew. Chem., Int. Ed. in Engl.* **2003**, *42*, 1210-1250.
- (134) Sinnokrot, M. O.; Sherrill, C. D. *J. Am. Chem. Soc.* **2004**, *126*, 7690-7697.
- (135) Smith, C. E.; Smith, P. S.; Thomas, R. L.; Robins, E. G.; Collings, J. C.; Dai, C. Y.; Scott, A. J.; Borwick, S.; Batsanov, A. S.; Watt, S. W.; Clark, S. J.; Viney, C.; Howard, J. A. K.; Clegg, W.; Marder, T. B. *J. Mater. Chem.* **2004**, *14*, 413-420.
- (136) Williams, V. E.; Lemieux, R. P. *Chem. Commun.* **1996**, 2259-2260.
- (137) Williams, V. E.; Lemieux, R. P. *J. Am. Chem. Soc.* **1998**, *120*, 11311-11315.
- (138) Williams, V. E.; Lemieux, R. P.; Thatcher, G. R. J. *J. Org. Chem.* **1996**, *61*, 1927-1933.
- (139) Hunter, C. A.; Sanders, J. K. M. *J. Am. Chem. Soc.* **1990**, *112*, 5525-5534.
- (140) Janiak, C. *J. Chem. Soc., Dalton Trans.* **2000**, 3885-3896.
- (141) Hunter, C. A.; Lawson, K. R.; Perkins, J.; Urch, C. J. *J. Chem. Soc., Perkin Trans. 2* **2001**, 651-669.
- (142) Hobza, P.; Sponer, J. *J. Am. Chem. Soc.* **2002**, *124*, 11802-11808.
- (143) Hunter, C. A.; Lu, X. J. *J. Mol. Biol.* **1997**, *265*, 603-619.

- (144) Tran, F.; Alameddine, B.; Jenny, T. A.; Wesolowski, T. A. *J. Phys. Chem. A* **2004**, *108*, 9155-9160.
- (145) Arikainen, E. O.; Boden, N.; Bushby, R. J.; Lozman, O. R.; Vinter, J. G.; Wood, A. *Angew. Chem., Int. Ed. in Engl.* **2000**, *39*, 2333-2336.
- (146) Ohta, K.; Jacquemin, L.; Sirlin, C.; Bosio, L.; Simon, J. *New J. Chem.* **1988**, *12*, 751-754.
- (147) Ohta, K.; Watanabe, T.; Fujimoto, T.; Yamamoto, I. *J. Chem. Soc., Chem. Commun.* **1989**, 1611-1613.
- (148) Kumar, S.; Manickam, M. *Mol. Cryst. Liq. Cryst.* **2000**, *338*, 175.
- (149) Kishikawa, K.; Furusawa, S.; Yamaki, T.; Kohmoto, S.; Yamamoto, M.; Yamaguchi, K. *J. Am. Chem. Soc.* **2002**, *124*, 1597-1605.
- (150) Fischbach, I.; Pakula, T.; Minkin, P.; Fechtenkotter, A.; Mullen, K.; Spiess, H. W.; Saalwachter, K. *J. Phys. Chem. B* **2002**, *106*, 6408-6418.
- (151) Kumar, S. *Liq. Cryst.* **2004**, *31*, 1037-1059.
- (152) Rose, B.; Meier, H. Z. *Naturforsch. B.* **1998**, *53*, 1031-1034.
- (153) Henderson, P.; Kumar, S.; Rego, J. A.; Ringsdorf, H.; Schumacher, P. *J. Chem. Soc., Chem. Commun.* **1995**, 1059-60.
- (154) Boden, N.; Bushby, R. J.; Lu, Z. B.; Cammidge, A. N. *Liq. Cryst.* **1999**, *26*, 495-499.
- (155) Boden, N.; Bushby, R. J.; Cammidge, A. N.; Duckworth, S.; Headdock, G. *J. Mater. Chem.* **1997**, *7*, 601-605.
- (156) Praefcke, K.; Eckert, A.; Blunk, D. *Liq. Cryst.* **1997**, *22*, 113-119.
- (157) Rego, J. A.; Kumar, S.; Ringsdorf, H. *Chem. Mater.* **1996**, *8*, 1402-1408.
- (158) Boden, N.; Bushby, R. J.; Cooke, G.; Lozman, O. R.; Lu, Z. B. *J. Am. Chem. Soc.* **2001**, *123*, 7915-7916.
- (159) Babuin, J.; Foster, J.; Williams, V. E. *Tet. Lett.* **2003**, *44*, 7003-7005.
- (160) Debije, M. G.; Chen, Z. J.; Piris, J.; Neder, R. B.; Watson, M. M.; Mullen, K.; Wurthner, F. *J. Mater. Chem.* **2005**, *15*, 1270-1276.
- (161) Young, J. R.; Huang, S. X.; Walsh, T. F.; Wyvratt, M. J.; Yang, Y. T.; Yudkovitz, J. B.; Cui, J. S.; Mount, G. R.; Ren, R. N.; Wu, T. J.; Shen, X. L.; Lyons, K. A.; Mao, A. H.; Carlin, J. R.; Karanam, B. V.; Vincent, S. H.; Cheng, K.; Goulet, M. T. *Bioorg. Med. Chem. Lett.* **2002**, *12*, 827-832.
- (162) Choi, H. Y.; Chi, D. Y. *J. Am. Chem. Soc.* **2001**, *123*, 9202-9203.
- (163) Morkved, E. H.; Neset, S. M.; Bjorlo, O.; Kjoson, H.; Hvistendahl, G.; Mo, F. *Acta Chem. Scand.* **1995**, *49*, 658-662.
- (164) Hansch, C.; Leo, A.; Taft, R. W. *Chem. Rev.* **1991**, *91*, 165-195.
- (165) Chien, C. W.; Liu, K. T.; Lai, C. K. *J. Mater. Chem.* **2003**, *13*, 1588-1595.
- (166) Reek, J. N. H.; Priem, A. H.; Engelkamp, H.; Rowan, A. E.; Elemans, J. A. A. W.; Nolte, R. J. M. *J. Am. Chem. Soc.* **1997**, *119*, 9956-9964.
- (167) Mecozzi, S.; West, A. P.; Dougherty, D. A. *Proc. Natl. Acad. Sci. U. S. A.* **1996**, *93*, 10566-10571.
- (168) Kishikawa, K.; Harris, M. C.; Swager, T. M. *Chem. Mater.* **1999**, *11*, 867-871.

- (169) Levitsky, I. A.; Kishikawa, K.; Eichhorn, S. H.; Swager, T. M. *J. Am. Chem. Soc.* **2000**, *122*, 2474-2479.
- (170) Eichhorn, S. H.; Paraskos, A. J.; Kishikawa, K.; Swager, T. M. *J. Am. Chem. Soc.* **2002**, *124*, 12742-12751.
- (171) Stone, J. A. *The Theory of Intermolecular Forces*; Clarendon Press: Oxford, 1997; Vol. 32.
- (172) Sinnokrot, M. O.; Sherrill, C. D. *J. Phys. Chem. A* **2003**, *107*, 8377-8379.
- (173) Rose, B.; Meier, H. Z. *Naturforsch. B.* **1998**, *53*, 1031-1034.
- (174) Closs, F.; Haussling, L.; Henderson, P.; Ringsdorf, H.; Schuhmacher, P. *J. Chem. Soc., Perkin Trans. 1* **1995**, 829-837.
- (175) Mann, F. G.; Pragnell, M. J. *J. Chem. Soc.* **1965**, 4120-4128.
- (176) Musliner, W. J.; Gates, J. W. *J. Am. Chem. Soc.* **1966**, *88*, 4271.
- (177) Pilgram, K.; Zupan, M. *J. Org. Chem.* **1971**, *36*, 207.
- (178) Pilgram, K.; Zupan, M.; Skiles, R. *J. Heterocycl. Chem.* **1970**, *7*, 629.
- (179) Mataka, S.; Eguchi, H.; Takahashi, K.; Hatta, T.; Tashiro, M. *Bull. Chem. Soc. Jpn.* **1989**, *62*, 3127-3131.
- (180) Mataka, S.; Ikezaki, Y.; Takahashi, K.; Torii, A.; Tashiro, M. *Heterocycles* **1992**, *33*, 791-800.
- (181) Dyachenko, E. K.; Pesin, V. G.; Papirnik, M. P. *Zh. Org. Khim.* **1986**, *22*, 421-424.
- (182) Zibarev, A. V.; Miller, A. O. *J. Fluorine Chem.* **1990**, *50*, 359-363.
- (183) Mataka, S.; Takahashi, K.; Imura, T.; Tashiro, M. *J. Heterocycl. Chem.* **1982**, *19*, 1481-1488.
- (184) Prashad, M.; Liu, Y. G.; Repic, O. *Tet. Lett.* **2001**, *42*, 2277-2279.
- (185) Liu, Y. G.; Lu, Y. S.; Prashad, M.; Repic, J.; Blacklock, T. J. *Adv. Synth. Catal.* **2005**, *347*, 217-219.
- (186) Edelmann, M. J.; Raimundo, J. M.; Utesch, N. F.; Diederich, F.; Boudon, C.; Gisselbrecht, J. P.; Gross, M. *Helv. Chim. Acta* **2002**, *85*, 2195-2213.
- (187) Mazingo, R.; Harris, S. A.; Wolf, D. E.; Hoffhine, C. E.; Easton, N. R.; Folkers, K. *J. Am. Chem. Soc.* **1945**, *67*, 2092-2095.
- (188) Kenning, D. D.; Mitchell, K. A.; Calhoun, T. R.; Funfar, M. R.; Sattler, D. J.; Rasmussen, S. C. *J. Org. Chem.* **2002**, *67*, 9073-9076.